

On the Origin and Early Evolution of Terrestrial Planet Atmospheres and Meteoritic Volatiles

ROBERT O. PEPIN

School of Physics and Astronomy, University of Minnesota, Minneapolis, Minnesota 55455

Received April 17, 1989; revised February 19, 1991

A simple analytic model of mass fractionation in hydrodynamic escape is applied to the problem of the origin and evolution of terrestrial planet atmospheres and meteoritic noble gases from primordial compositions. It is shown that isotopic distributions of xenon, krypton, argon, and neon on Earth can be generated by two stages of hydrodynamic loss, first of a hydrogen-rich, isotopically solar primitive atmosphere, and then of Kr, Ar, and Ne subsequently outgassed from deep within the planet. Degassed species are also isotopically solar, and their required elemental fractionation pattern is in reasonable agreement with laboratory adsorption experiments. Models of the adsorption process suggest that they could originate from gravitationally condensed nebular noble gases adsorbed and buried in accreting protoplanetary cores. Xenon outgassing is severely restricted by isotopic considerations. This constraint mandates preferential Xe retention within the planet, and thus leads to a prediction of geochemical partitioning behavior at high pressures that defines a central experimental test of the model. On Venus, gases remaining after partial hydrodynamic escape of an isotopically solar primary atmosphere can account for the large present-day Xe, Kr, Ar, and Ne abundances. Additional contributions from planetary degassing may or may not be present. Venusian isotopic distributions are replicated to the extent they are known. Where they are not, for Kr and Xe, calculated model compositions define a second observational test. Results of extending the baseline noble gas model to include atmospheric compounds of carbon and nitrogen indicate that inventories of these elements now in surficial reservoirs on both Venus and Earth could have derived from C-N-rich veneers, accreting late in the escape epoch, that chemically resembled the contemporary enstatite chondrites.

Isotopic compositions of Ne, Ar, and Kr in the early solar nebula, in the primary atmospheres of Venus and Earth, and in planetary interiors are assumed to be similar to current estimates for the solar wind. Primordial Xe is taken to be U-Xe. The required elemental composition of atmospheric noble gases initially on Venus is solar-like for Ar : Kr : Xe ratios but is strongly depleted in Ne, suggesting that these species, and the hydrogen needed to fuel hydrodynamic escape, may have been supplied by accretion of ices carrying noble gases occluded from the nebula at low temperatures. Icy planetesimals from an outer solar system source would also have contributed to Earth. However, compared to the Venus pattern, the noble

gas abundance ratios needed in Earth's primary atmosphere are depleted, relative to Xe, in Ne, Ar, and perhaps to a lesser extent in Kr. That this fractionation of an initially Venus-like primary atmosphere could have resulted from partial atmospheric loss in a giant Moon-forming impact on Earth is plausible, but unproven.

Present-day isotopic distributions on Mars are shown to be generally compatible, as on Earth, with fractionation during sequential hydrodynamic escape of a primitive atmosphere and degassed volatiles. Anomalies in predicted vs observed isotope ratios for Martian nitrogen and neon are attributed to postescape atmospheric evolution by nonthermal loss of nitrogen to space and the addition of solar wind noble gases. Xe isotope ratios and independent estimates of bulk chemical composition, both from SNC meteorite measurements, point clearly to a carbonaceous chondrite (CI) component in the planet. Consequently much of the early Martian atmosphere is taken to originate from impact-degassing of accreted CI-like material. Later outgassing of deeply buried CI matter could have provided carbon and nitrogen to crustal reservoirs. Surface CO₂ inventories calculated from a tentative degassing model are on the order of 1 bar, equivalent to a globally distributed ~20 meter layer of carbonate rock if subsequently sequestered by chemical weathering reactions.

Hydrodynamic escape from planets in these models is driven by an initially intense, time-decaying flux of extreme ultraviolet (EUV) radiation from the young evolving sun. Chronologies for dissipation of primary atmospheres, outgassing, and other stages of atmospheric evolution are directly linked to timescales for decay of the solar EUV flux. Initial flux intensities and decay histories are inferred from the astronomical observational record of X-ray activity on solar-type pre-main-sequence and early main-sequence stars. These observations point to initial EUV fluxes a few hundred times above levels from the present sun, sufficient to satisfy escape energy demands, and evolution of terrestrial planet atmospheres by hydrodynamic escape that began at an assumed solar age of ~50 million years and ran its course within the next few hundred million years of solar system history.

A similar model is constructed for derivation of meteoritic noble gases from solar-like and nucleogenetic components carried into the accretion disk in the mantles and interiors of extrasolar grains. It is shown that transient atmospheres, outgassed from the interiors of primitive planetesimals that incorporated a population of these grains as they accumulated to sizes comparable to the largest

asteroid, could have been fractionated in a single stage of hydrodynamic blowoff into isotopic distributions that match observed compositions of Xe, Kr, Ar and Ne in surface-sited ("Q-component") meteoritic gases. Subsequent adsorption of residual atmospheric gases on planetesimal surface grains containing nucleogenetic isotopes accounts for the observed siting and for bulk isotopic compositions. Required distribution coefficients for the adsorption process in this environment can be comparable to laboratory values, alleviating a major difficulty with previous approaches. However, this model, while promising, rests on a larger number of assumptions than the planetary models and is correspondingly more speculative. © 1991 Academic Press, Inc.

I. INTRODUCTION

The sources and evolutionary histories of volatile elements in primitive meteorites and planetary atmospheres are classic unsolved problems in the planetary sciences. Signatures of origin and physical processing would be expected to survive most clearly in the chemically inert noble gases. Their record is complex, however, and not readily interpreted. Absolute abundances of noble gases in the carbonaceous chondrites and the atmospheres of Earth, Venus, and Mars display highly variable depletions with respect to solar abundances, and isotopic patterns in each of these volatile reservoirs which are generally distinct from each other and from inferred solar compositions. Historically, models of origins based on seemingly straightforward clues in one subset of this extensive data base have encountered inconsistencies in another. A celebrated example of this kind of difficulty involves neon-argon distributions. Measured $^{20}\text{Ne}/^{36}\text{Ar}$ elemental ratios are roughly the same, within a factor of two or so, on Earth, Venus, and Mars, and in bulk samples of the primitive CI carbonaceous chondrites. This approximate concordance has prompted much discussion in the modeling literature (see, for example, the review by Donahue and Pollack (1983)), usually with the view that it implies accretion of common parental material as the source of at least these two gases in inner solar system bodies. Isotope systematics, however, argue against this interpretation since the required isotopic uniformity is absent: $^{20}\text{Ne}/^{22}\text{Ne}$ on Venus is higher and $^{36}\text{Ar}/^{38}\text{Ar}$ on Mars much lower than the corresponding ratios in the other objects (Pepin 1989a, Pepin and Carr 1991).

Attempts to account for the origin of terrestrial planet atmospheres have tended in the past to focus, as in the example above, on deriving the elemental abundance patterns of atmospheric noble gases from primordial meteoritic or nebular reservoirs. One common approach has been to regard an atmosphere as a mixture of gases acquired from accretion of known (or occasionally hypothetical) volatile-rich meteoritic material or carriers of adsorbed

nebular gases. Another class of models postulates the initial presence and subsequent dissipation of gravitationally captured or impact-degassed primordial atmospheres on the planets themselves. Until recently, with a few exceptions, comparatively little attention has been paid to isotopic distributions, in particular those of the heavy species krypton and xenon, or to astrophysical environments in which evolutionary processing might plausibly have occurred.

The successes and problems of many of these "gas-poor" and "gas-rich" models are discussed by Donahue and Pollack (1983). A point to be emphasized here is that the gas-poor theories are intrinsically unable to account for the range of isotopic variability seen in planetary atmospheres. The processes of sorption and mixing invoked in these models do not fractionate isotopes, yet there is clear evidence that such fractionating mechanisms have been at work (Pepin 1989a). For this reason, gas-rich theories that assume the presence of primordial atmospheres of whatever origin on growing or fully accreted planetary bodies, or on (or in) large preplanetary planetesimals, appear fundamentally more attractive. They offer the potential for isotopic fractionation in the process(es) that subsequently dissipated these atmospheres, and the possibility that the variable distributions of noble gas abundances and isotopes seen in present-day planetary atmospheres may be understood as reflecting different degrees of processing on the individual bodies.

A new generation of evolutionary models is beginning to focus on fractionation during atmospheric escape. In the first of these, Donahue (1986) considered fractionation effects resulting from classical Jeans escape of pure, solar-composition noble gas atmospheres from large planetesimals. Their atmospheres are assumed to derive from outgassing of nebular gases previously adsorbed on the surfaces of preplanetesimal dust grains, and are subsequently fractionated to different degrees by losses that depend on the rates of planetesimal growth. These bodies later accumulate in various proportions to form the terrestrial planets and their atmospheres. Donahue's model can account reasonably well for relative Ne : Ar : Kr elemental abundances and for Ne isotopic compositions in the atmospheres of Venus, Earth, and Mars. Predicted $^{36}\text{Ar}/^{38}\text{Ar}$ ratios, however, are much lower than observed, and variations in Kr and Xe elemental and isotopic compositions in different planetary reservoirs cannot be explained since Jeans escape of these heavy species from the parent planetesimals is essentially nil.

These problems are proving to be more tractable in the context of a related thermal loss mechanism, hydrodynamic escape (Zahnle and Kasting 1986, Zahnle *et al.* 1990a, Sasaki and Nakazawa 1986, 1988, Pepin 1986, 1987, 1989a,b, 1990b, Hunten *et al.* 1987, 1988, 1989). Here atmospheric loss is assumed to occur from much larger bodies, partially or fully accreted planets. In this process

hydrogen-rich primordial atmospheres are assumed to be heated at high altitudes, after the nebula has dissipated, by intense far-ultraviolet radiation from the young sun. Under these conditions hydrogen escape fluxes can be large enough to exert upward drag forces on heavier atmospheric constituents sufficient to lift them out of the atmosphere, at rates that depend on their mole fractions and masses (Zahnle and Kasting 1986, Hunten *et al.* 1987). Lighter species are entrained and lost with the outflowing hydrogen more readily than heavier ones, leading to mass fractionation of the residual atmosphere. Hydrogen escape fluxes high enough to sweep out and fractionate atmospheric species as massive as Xe require energy inputs roughly two to three orders of magnitude greater than presently supplied to planetary exospheres by solar extreme ultraviolet (EUV) radiation—implying large but, as discussed later, not unreasonable enhancements of surface activity on the early sun. Hydrodynamic escape is particularly attractive for its ability to generate, in an astrophysically plausible environment, large isotopic fractionations of the type displayed by terrestrial xenon with respect to solar Xe—first observed and attributed to an (unknown) fractionation process almost 30 years ago (Krummenacher *et al.* 1962)—and by Xe in the atmosphere of Mars relative to Xe in primitive meteorites (Swindle *et al.* 1986).

The potential power of the hydrodynamic loss mechanism, given adequate supplies of hydrogen and energy, to replicate observed isotopic distributions is well illustrated by Hunten *et al.*'s (1987) applications of the process to several specific cases, including the derivation of terrestrial Xe from solar Xe; by Sasaki and Nakazawa's (1986, 1988) independent treatment of the terrestrial Xe problem; and by Zahnle *et al.*'s (1990a) consideration of Ne and Ar compositions on Earth and Mars. The next step in assessing its more general viability as an actual instrument of volatile evolution is to examine the consequences of hydrodynamic escape for the full range of elemental and isotopic mass distributions found in contemporary planetary atmospheres and volatile-rich meteorites, and to explore the astrophysical and planetary conditions under which the process could reconcile this data base. A first attempt to construct such a synthesis is presented in this paper.

II. ASSUMPTIONS AND OVERVIEW

II.A. Assumptions

The model developed in the following chapters rests on three basic postulates: (1) Noble gases in terrestrial planet atmospheres and primitive meteorites, excluding contributions from radioactive decay and the solar wind, derived from one or both of two primordial sources: "local" volatiles in the gas phase of the local protosolar nebula,

and "exotic" volatiles sequestered in interstellar grains carried into the nebula from presolar molecular cloud environments. (2) Present-day mass distributions of these volatiles evolved from primordial source compositions through fractionation by either or both of two primary processes: gas adsorption and fixation on accreting solid matter or on nebular dust grains, fractionating elements but not isotopes; and hydrodynamic escape of atmospheres from the partially or fully assembled planets and from meteorite parent bodies, fractionating both elements and isotopes. (3) Planetary conditions for hydrodynamic escape were established when primary (primordial) atmospheres rich in hydrogen or water accumulated around the growing terrestrial planets and were exposed, following dissipation of the accretion disk, to intense far-ultraviolet solar radiation that declined in strength with time.

More specific assumptions are made within the context of the three general postulates. A number of these, discussed more fully in Section IV, relate to the data base applied to the model. Gases trapped in the glassy phase of one of the SNC meteorites are considered to be an unfractionated sample of the contemporary atmosphere of Mars. Noble gas isotopic compositions in the "local" primordial nebular reservoir are taken to be those of the solar wind for neon, argon, and krypton. The validity of this assumption cannot be proven, nor are these compositions themselves precisely known as yet, particularly for argon and krypton. A quasitheoretical composition ("U-Xe"), derived from analysis of meteoritic and terrestrial data but only marginally observed directly in meteorites, is assumed for primitive xenon. The uncertainties attendant on the use of all these estimates for isotopic distributions are, however, ameliorated to some extent by the ability of the model to accommodate a comparatively broad range of initial compositions. That the model is robust in this sense is demonstrated explicitly for krypton in Section V.B. The one essential model constraint on primordial isotope patterns is that they be similar to or isotopically lighter than their present-day derivatives in atmospheres and meteorites.

Serious attempts to derive the compositions of the contemporary atmospheres on Earth and Mars from primitive nebular, planetesimal, or planetary source reservoirs have had to confront, in one way or another, the apparent decoupling of the evolutionary histories of krypton and xenon (see Pepin 1989a). This implies separate provenances for the two species. In the present model Xe is considered to be a fractionated relict of the primary atmosphere, and Kr and the lighter noble gases the products of planetary outgassing. This effective isolation of the heaviest gas from lighter species follows naturally from the processes intrinsic to the model, in all respects but one. Isotope mixing systematics impose a strict upper limit on the allowed level of "contamination" of residual primary Xe by later degassing from the interior. This limit

falls well below the amount of Xe that ordinarily would be expected to accompany the outgassed Kr. Therefore, the model's most crucial assumption is that the bulk of this Xe has been retained in the bodies of the planets. Xe is known to metallize somewhat above 1 megabar (Goettel *et al.* 1989), and so could have partitioned into metal phases deep in the Earth. But Mars is the more critical case, since interior pressures are, and always were, well below 1 megabar. There are theoretical suggestions, discussed in Section VII.A, that Xe may display siderophilic behavior in the submegabar range, but as yet no experimental studies at the relevant Martian pressures of a few hundred kilobars.

The model postulates the existence of a potent energy source for driving hydrodynamic escape and the raw material—large amounts of atmospheric hydrogen—needed to implement it on planets. A likely inference from the astronomical observations reviewed below in Section III.B.3 is that an adequate supply of energy, in the form of a strongly enhanced flux of EUV radiation from the young sun, was indeed present in the early solar system. However, this radiation must also have been able to penetrate the midplane to planetary distances, which could not have happened as long as gas and dust opacities remained high (Prinn and Fegley 1989). The interval needed for sufficient dissipation of nebular gas and decay of collisionally generated dust densities in the inner solar system is taken, more or less arbitrarily, to be 50 myr. By this time Earth-, Venus-, and Mars-like bodies in the “standard model” of planetary accretion had respectively grown to 97%, 96%, and 92% of their final masses, and the chances of later giant impacts, which probably would have derailed their atmospheres from the evolutionary tracks modeled here in unknown ways, were diminishing (Wetherill 1986, 1990a). Model results are not particularly sensitive to this choice of initial time t_0 for the beginning of hydrodynamic escape. Calculations of final compositional states are independent of this parameter, evolutionary timescales increase or decrease only additively with changes in initial time, and EUV energy requirements remain plausible for $t_0 \leq 120$ myr or so (Section VI.A).

The assumption that massive hydrogen-rich primordial atmospheres were present at this time on the terrestrial planets is more conjectural. Although they are a natural consequence of accretion of Earth and Venus to roughly their final masses in the presence of nebular gas (e.g., Hayashi *et al.* 1979, 1985), gravitational capture of such atmospheres requires either planetary accretional time scales an order of magnitude shorter than current estimates of $\sim 10^8$ yr (Wetherill 1986, 1990a), or survival of the nebular gas phase well beyond the observationally inferred maximum lifetimes ($\sim 10^7$ yr) of fine circumstellar dust (Strom *et al.* 1989a,b, 1991). Addition of water amounting to a few weight-percent or less of planetary

masses by accretion of icy planetesimals could also have supplied the required hydrogen. At the moment water accretion seems the more likely of these two potential sources (Sections VI.D.1,2), but much more work on modeling the probable fluxes of comets and other outer-system objects into terrestrial planet space during the first $\sim 10^8$ yr of solar system history is needed to judge whether it is plausible.

It is important to emphasize that hydrodynamic escape and fractionation of planetary atmospheres *would* have occurred if these conditions for energy source, midplane transparency, and hydrogen supply were even partially met. Consequently the process is intrinsically interesting—and perhaps crucially important—for atmospheric evolution in the context of current observations and ideas about the astrophysical environment of the early solar system. The general rationale for modeling it is therefore firm, despite the likelihood that some of the assumptions in this particular model will later prove to be wrong.

II.B. Overview of the Model

A detailed qualitative description of an earlier but generally similar version of this model has been published elsewhere (Pepin 1989b). This and the preceding section briefly outline that report, with comments in areas where it differs from the current approach to the problem. One important change is that in the earlier version some of the numerical estimates given for initial times t_0 , “crossover” masses m_c^0 , and specific timescales for various stages of atmospheric evolution were derived using power-law expressions for solar EUV flux history. The model presented here, however, utilizes an analytically simpler exponential formulation that fits the observational data at least as well (Section III.B.3) but for which the assumptions and numerical results are somewhat different. So these estimates in Pepin (1989b), while still valid for the flux histories described there, do not apply exactly to the present one.

During its first ~ 50 myr of growth to nearly final mass, each planet is assumed to acquire two spatially separated noble gas reservoirs of solar isotopic composition. The first of these, incorporated deep in planetary interiors, was the source for species later outgassed to the surface. The second was a surficial reservoir, contained in a hydrogen-rich primary atmosphere coaccreting with the planet. It was earlier thought that the interior component could have originated from nebular gases by adsorption on preplanetary dust grains, and the primary atmosphere by gravitational capture (Pepin 1989b); at present adsorption on accumulating protoplanetary cores (Section VII.D.2) and accretion of icy planetesimals (Section VI.D.2) appear more likely. When gas and dust opacities became low enough (by assumption at $t_0 = 50$ myr) for midplane

penetration of solar EUV radiation to planetary distances, intense heating by EUV absorption at high altitudes began to drive hydrodynamic escape of primary atmospheres.

II.B.1. Earth (Section V.B.1)

Atmospheric loss, and concomitant elemental and isotopic fractionation of residual atmospheric species, continued for $t > t_0$ until EUV heating declined to a level where the Xe isotopes could no longer be lifted out of the atmosphere by the drag forces exerted on them by the weakening hydrogen escape flux. At this point the non-radiogenic Xe inventory was frozen at its present-day terrestrial abundance and isotopic composition, while escape of constituents lighter than Xe continued. By the time of planetary outgassing, presumably triggered by later stages of differentiation, these lighter species from the primary atmosphere had been depleted to levels well below their contemporary atmospheric abundances. Kr, Ar, and Ne degassed from the interior—accompanied by little if any degassed Xe, in what was noted above to be the central assumption of the model—then entered the atmosphere and were mass-fractionated by continuing hydrodynamic escape to isotopic compositions identical or close to their present-day values. The source reservoir of outgassed noble gases must have been elementally fractionated with respect to solar composition if their relative abundances are to match those in the Earth's atmosphere. The required elemental composition is in reasonable agreement with fractionation patterns produced in laboratory adsorption experiments.

II.B.2. Venus (Section V.B.2)

Current data on abundances and isotopic compositions of minor atmospheric constituents on Venus are uncertain—but not to the point of preventing diagnostic comparisons with the other planets. The atmosphere is clearly much richer than Earth's in noble gases, for ^{36}Ar by a factor of ~ 70 . There is a pronounced solar-like signature in the elemental Xe/Kr and Ar/Kr ratios and in the Ne isotopes, and nominally in Ar as well although measurement errors are large. These clues suggest that the noble gas inventories on Venus are dominated by abundant, lightly fractionated remnants of its primary atmosphere. A straightforward model of hydrodynamic escape of an atmosphere that originally was isotopically solar and, except for Ne, elementally near-solar in composition fits the limited data we have very well. Contributions by planetary degassing, say at the level experienced by Earth, would constitute only minor fractions of the total noble gas inventories and are not discernable. However, this simple view of Venus' atmospheric evolution does require a much lower initial Ne abundance, by a factor of ~ 100 , than would have been present in an atmosphere of purely

solar elemental composition. It is partly for this reason that origin of the primary atmosphere from accretion of icy planetesimals carrying noble gases occluded from the nebula at low temperatures, a process likely to discriminate against Ne, seems more attractive at present than gravitational capture of ambient nebular gases directly by the planet.

II.B.3. Mars (Section V.B.3)

An evolution very similar to Earth's, of primary atmospheric and degassed secondary noble gases to present-day compositions by hydrodynamic escape, is indicted for Mars, although derived timescales for outgassing are somewhat longer. The calculated elemental fractionation pattern of degassed solar-like Kr, Ne, and Ar is essentially identical to that deduced for Earth. Retention of Xe within the planet is again required. However, there are two noteworthy differences. The SNC-derived isotopic composition of contemporary Martian atmospheric Xe (Swindle *et al.* 1986) points to a primordial atmosphere in which Xe was not isotopically solar, as on Earth, but instead resembled that found in the CI carbonaceous chondrites. This observation implies a major CI-like accretional component in Mars, a view independently supported by geochemical models of the planet's bulk composition (Dreibus and Wänke 1985, 1987, 1989). The second difference is the inability of the basic escape model to replicate simultaneously the isotopic compositions of present-day Ar and Ne; any simple escape episode that generates the unusually low $^{36}\text{Ar}/^{38}\text{Ar}$ ratio shown in Fig. 3 overfractionates $^{20}\text{Ne}/^{22}\text{Ne}$. This apparent anomaly could be a consequence of the unique compositional sensitivity of Ne in the tenuous Martian atmosphere to postescape addition of solar wind gases, by either direct capture or accretion of solar-wind-rich interplanetary dust, over geologic time.

II.B.4. Planetary Carbon and Nitrogen (Section V.C)

The planetary model outlined above does not address the evolutionary histories of carbon dioxide and nitrogen. One or the other of these two constituents dominates in all three present-day atmospheres. Among several possibilities for the origin of the carbon and nitrogen now present in crustal and atmospheric reservoirs on Earth and Venus is one that can be explored by a straightforward extension of the baseline noble gas model—that they were supplied by a late-accreting veneer of C- and N-rich matter toward the end of hydrodynamic escape. The present-day elemental and isotopic distributions of C, N, and the noble gases on the two planets set constraints on the abundances and compositions that all of these elements may have in candidate source materials for the veneer. Among extant meteoritic classes, these chemical constraints are remarkably well met by the enstatite (E) chondrites, and only by

them. Inclusion in the baseline model of an E-chondrite veneer, accreted more or less simultaneously by the two planets at a time when waning hydrodynamic escape was just capable of fractionating isotopically light E-chondrite nitrogen to its observed composition in Earth's atmosphere, yields satisfactory matches to planetary C/N ratios and isotopic compositions without seriously perturbing the noble gas histories outlined above. To match estimates of the absolute atmospheric and crustal abundances of C and N requires accretion of relatively modest amounts of veneering material: a total of about 3/4 of a lunar mass, with ~75% of this on Venus. The steep falloff with heliocentric distance suggests an inner solar system provenance for the veneering material. It may or may not have contributed to Mars. As noted above, there are geochemical arguments for a large, CI-like Martian accretional component. This type of material would comprise an independent and potent source of both carbon and nitrogen. A minor variant of the baseline model, in which a small fraction of the initial CI volatile inventory is degassed from the planetary interior along with the noble gases, suggests that abundances of C and N emplaced on the surface of Mars could have been considerably greater than current atmospheric inventories. These excesses imply significant sinks, presumably later sequestering of CO₂ in carbonate rock and losses of N to space.

II.B.5. Meteoritic Noble Gases (Section V.D)

Isotopic distributions of noble gases in meteorites differ in several respects from both primordial solar and present-day planetary compositions. Carbonaceous chondrite gases were included above as one component of the initial volatile system on Mars without addressing the question of how they themselves might have evolved, prior to planetary accretion, from the primary "local" and "exotic" solar-system gas reservoirs postulated at the beginning of this chapter. Hydrodynamic escape, operating in an environment quite different from the planetary cases, appears to be a promising way to generate the required fractionations. The model developed in this paper assumes the accumulation of a CI parent planetesimal, in this example to about four times the mass of Ceres, in a cold enough ambient environment to permit incorporation of thermally unprocessed or lightly processed extrasolar grains carrying adsorbed solar-like gases in grain-mantle ices, and presolar "exotic" gases in grain interiors. Grain-mantle volatiles are assumed to mobilize in higher temperature regions within the planetesimal, and episodically outgas to the cold surface where species of lower volatility condense. The resulting gaseous atmosphere, containing noble gases and a dominant light carrier gas, is transient, i.e., unstable against hydrodynamic blowoff. This type of hydrodynamic escape can be described by a simple

analytic formalism. With the assumption that the atmospheric noble gases were initially isotopically solar but elementally depleted in Ne, the model leads to a residual planetesimal atmosphere in which Xe, Kr, Ar and Ne are fractionated to isotopic compositions in close agreement with the surface-sited "Q"-component in carbonaceous chondrites. Subsequent adsorption on planetesimal surface grains containing "exotic" nucleogenetic components replicates the bulk composition of CI noble gases.

III. PROCESSES

III.A. Adsorptive Fractionation

Laboratory studies have shown that noble gases exposed to particular kinds of finely divided solid materials are adsorbed on or within the surfaces of individual grains. Adsorption is most efficient for various forms of carbon, where it appears to reflect intrinsic structural properties (Frick *et al.* 1979, Niemeyer and Marti 1981, Wacker *et al.* 1985, Zadnik *et al.* 1985, Wacker and Anders 1986, Wacker 1989), but has also been experimentally demonstrated for other minerals (Yang *et al.* 1982, Yang and Anders 1982a,b) and for polymineralic meteorite powder (Fanale and Cannon 1972). Moreover, the process occurs naturally in sedimentary materials (Canalas *et al.* 1968, Fanale and Cannon 1971, Phinney 1972, Podosek *et al.* 1980, 1981, Bernatowicz *et al.* 1984). Adsorbed gases on these substrates generally display fractionation patterns, relative to ambient gas-phase abundances, in which heavier species are enriched. For the most part the fractionations are remarkably uniform, considering the wide range of experimental and natural conditions under which they are produced, and are primarily elemental. Although occasional isotopic effects have been reported in natural samples (Phinney 1972), they are not observed in equilibrium adsorption in the laboratory (Bernatowicz and Podosek 1986). Isotopic fractionation does however occur in experimental environments involving ion implantation from plasmas rather than simple adsorption of neutral gases (Frick *et al.* 1979, Dziczkaniec *et al.* 1981, Bernatowicz and Fahey 1986, Bernatowicz and Hagee 1987).

The noteworthy characteristic of this adsorptive fractionation process is that it can generate, from ambient gases of solar composition, relative elemental abundances that qualitatively resemble the mass distributions of noble gases in meteorites and planetary atmospheres (see Fig. 6 below). This similarity suggests that adsorption of solar gases on nebular dust may have played an important role in establishing these patterns. Although it cannot by itself satisfy certain isotopic constraints (Pepin 1989a), and laboratory estimates of single-stage gas/solid partition coefficients are generally low, adsorptive fractionation is assumed in the model discussed here to be a fundamental

process, occurring on dust grains in the early solar nebula and in reservoirs derived from it.

III.B. Hydrodynamic Escape

III.B.1. Theory

A simple analytic theory of mass fractionation in hydrodynamic escape of gases from planetary atmospheres has been developed by Hunten *et al.* (1987). A brief synopsis of the formalism is given here. Hunten *et al.* considered an atmosphere consisting primarily of a light gaseous species of mass m_1 and column density N_1 particles per centimeter squared, containing minor amounts of heavier constituents of masses m_2 and inventories N_2 . Energy input at high altitudes, in their model by absorption of solar EUV radiation, drives thermal loss of the light constituent with escape flux F_1 particles per centimeter squared per second. The escaping gas exerts upward drag forces on heavier species. For a given F_1 the upward drag is sufficient to lift all species with masses m_2 less than a critical mass m_c out of the atmosphere. The escape fluxes of these species depend on their mole fractions in the atmosphere and on their masses. The critical or ‘‘crossover’’ mass m_c , defined as the smallest mass m_2 for which the escape flux of constituent 2 is zero, is given by

$$m_c = m_1 + \frac{kTF_1}{bgX_1}, \quad (1)$$

where b is the diffusion parameter (product of diffusion coefficient and total number density) for constituent 2 in constituent 1, X_1 is the mole fraction of the major constituent, and g is the gravitational acceleration.

If solar EUV output declines with time over the $\approx 10^6$ - to 10^9 -year period of interest for the early history of planetary atmospheres, as seems likely for the young sun (Zahnle and Walker 1982, Walter *et al.* 1988, Feigelson and Kriss 1989, Walter and Barry 1990), the principal source of upper atmospheric heating likewise diminishes. Consequently $F_1(t) = F_1^0 f(t)$, where $f(t)$ is some decreasing function of time and F_1^0 represents the escape flux of constituent 1 at some initial time t_0 . The corresponding initial crossover mass from Eq. (1) is then

$$m_c^0 = m_1 + \frac{kTF_1^0}{bgX_1}, \quad \text{and} \quad F_1^0 = \left(\frac{gX_1}{kT} \right) b(m_c^0 - m_1). \quad (2)$$

Under these conditions the expression for the time rate of change of N_2 , the atmospheric inventory of constituent 2, is

$$\frac{dN_2}{N_2} = - \frac{F_1^0}{N_1} \left[f(t) - \frac{m_2 - m_1}{m_c^0 - m_1} \right] dt \quad (3)$$

for any $m_2 < m_c$, if X_1 , the mole fraction of constituent 1, is assumed to remain constant near unity throughout the escape process.

The model described in this paper is applied to planetary atmospheres rich in hydrogen, under one of two different sets of escape conditions. In the first we assume an environment in which the full complements of minor species N_2 are initially in the atmosphere, but hydrogen is replenished from some source at roughly its rate of escape so that the atmospheric inventory N_1 is approximately constant throughout the escape episode. The evolution of N_2 from initial time t_0 to time t_2 when escape of m_2 ceases is then given in this ‘‘constant inventory’’ model by integration of Eq. (3) from t_0 to t_2 with constant N_1 , yielding

$$\frac{N_2}{N_2^0} = \exp \left[- \frac{F_1^0}{N_1} \int f(t) dt + \frac{F_1^0}{N_1} \left[\frac{m_2 - m_1}{m_c^0 - m_1} \right] (t_2 - t_0) \right], \quad (4)$$

where N_2^0 is the initial inventory of constituent 2. From Eq. (3), termination of N_2 loss ($dN_2/N_2 = 0$) at t_2 occurs when

$$f(t_2) = \frac{m_2 - m_1}{m_c^0 - m_1}, \quad (5)$$

which yields t_2 given a functional form for $f(t)$. Over the time interval $t_2 - t_0$, the crossover mass decreases from m_c^0 to m_2 as the hydrogen escape flux declines from F_1^0 . All atmospheric species of mass less than m_c^0 are depleted during the escape episode.

As an alternative to the constant hydrogen inventory model, suppose that all of the hydrogen is initially in the atmosphere along with the minor species. With no replenishment, N_1 in this ‘‘Rayleigh fractionation’’ model declines with time along with N_2 ; $dN_1/dt = -F_1 = -F_1^0 f(t)$, and with $N_1/N_1^0 \equiv g(t)$ Eq. (3) becomes

$$\frac{dN_2}{N_2} = \frac{dg(t)}{g(t)} + \frac{F_1^0}{N_1^0} \left[\frac{m_2 - m_1}{m_c^0 - m_1} \right] \frac{dt}{g(t)}, \quad (6)$$

where $g(t) = 1 - (F_1^0/N_1^0) \int f(t) dt$ integrated from t_0 to t .

III.B.2. Energy-Limited Escape Flux

The energy required for escape of m_1 from its local gravitational field, at radial distance $r \geq r_s$ from a body of mass M and radius r_s , is Gm_1M/r ergs per particle. If the global mean solar EUV input is ϕ ergs $\text{cm}^{-2} \text{sec}^{-1}$, the energy-limited escape flux is

$$F_1 = \frac{r\phi\varepsilon}{Gm_1M} \text{ particles cm}^{-2} \text{ sec}^{-1}, \quad (7)$$

where ε is the fraction of incident EUV flux converted to the thermal escape energy of m_1 . In what follows ϕ is conveniently expressed in terms of the current mean EUV flux at Earth $\phi_{\oplus}(t_p)$, heliocentric distance R , and the ratio Φ_{EUV} of the flux at past time t to that at present time t_p . We define $\phi(R, t_p) \equiv (R_{\oplus}/R)^2 \phi_{\oplus}(t_p)$ and $\Phi_{\text{EUV}}(t) \equiv \phi(R, t)/\phi(R, t_p)$, yielding $\phi(R, t) = \phi_{\oplus}(t_p) \Phi_{\text{EUV}}(t)$. Substituting this into Eq. (7) and Eq. (7) into Eq. (1), with $g = GM/r^2$ and M expressed in terms of r_s and density ρ , yields

$$m_c - m_1 = \left(\frac{3}{4\pi G\rho} \right)^2 \left(\frac{1}{r_s} \right)^3 \left(\frac{R_{\oplus}}{R} \right)^2 \left(\frac{kT}{X_1} \right) \left(\frac{\phi_{\oplus}(t_p)\varepsilon}{bm_1} \right) \left(\frac{r}{r_s} \right)^3 \Phi_{\text{EUV}}(t), \quad (8)$$

relating crossover mass to the EUV flux irradiating a planetary object at heliocentric distance R .

III.B.3. History of the Solar EUV Flux

Our only information on what $\Phi_{\text{EUV}}(t)$ might have been in the early solar system comes from astronomical observations of radiation from young solar-type stars at various stages of pre- and early-main-sequence evolution (Canuto *et al.* 1982, Zahnle and Walker 1982, Simon *et al.* 1985, Walter *et al.* 1988, Strom *et al.* 1988, Feigelson and Kriss 1989, Walter and Barry 1990). Since early solar EUV radiation could not have penetrated a full gaseous nebula to planetary distances, the applicable time dependence of stellar activity in the present model is that following dissipation of the dense accretion disks surrounding the classical T-Tauri stars (CTTS). Transition from a CTTS to a “weak-lined” (WTTS; Strom *et al.* 1989a) or “naked” (NTTS; Walter 1986) T-Tauri star by disk loss can apparently occur at stellar ages ranging from $\sim 2 \times 10^5$ to $\sim 10^7$ years, and both coronal and chromospheric activity on the WTTS appear to be roughly constant, within a factor of ~ 3 , over this age range and beyond to $\sim 2\text{--}5 \times 10^7$ years (Walter *et al.* 1988, Strom *et al.* 1988, Walter and Barry 1990).

Interstellar extinction of EUV radiation from this ensemble of young solar-like stars requires estimation of $\Phi_{\text{EUV}}(t)$ from measurements at other wavelengths. Among present observational data, soft ($\sim 3\text{--}60 \text{ \AA}$) X-ray fluxes are most likely to be representative of at least the short-wavelength coronal component ($\lambda < 700 \text{ \AA}$) of the EUV spectrum. The combined Walter *et al.* (1988) and Simon *et al.* (1985) data base on X-ray activity ($\text{ergs cm}^{-2} \text{ sec}^{-1}$ of stellar surface), converted to total X-ray luminosity L_X in ergs per second since this is the appropriate quantity for calculation of planetary irradiation fluxes, has been discussed by Pepin (1989b). Figure 1, a plot of estimated

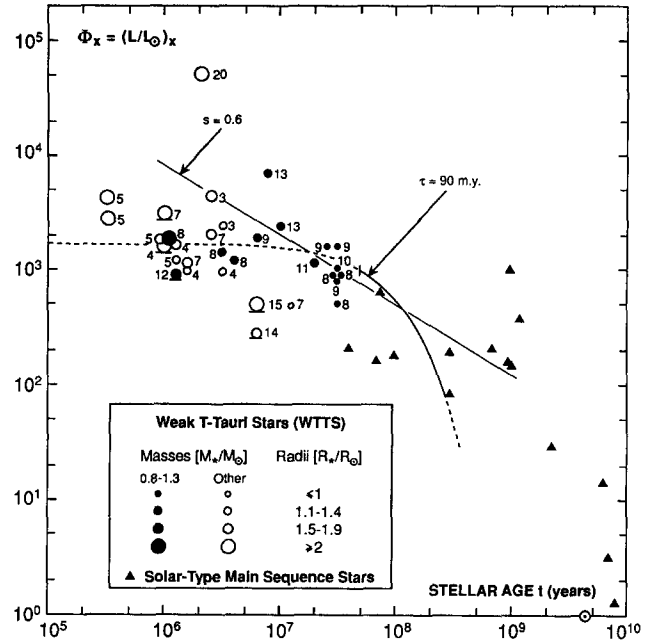


FIG. 1. Observed X-ray luminosities L_X relative to the present sun vs stellar ages for “weak-lined” T-Tauri stars and solar-type main sequence stars (after Pepin 1989b). All WTTS data from Water *et al.* (1988), MSS data from Simon *et al.* (1985) and Walter and Barry (1990). Numbers adjacent to the plotted WTTS points are stellar mass estimates in tenths of a solar mass. Underlining identifies measurements that yielded only lower limits on luminosity. In the present model both soft X-ray (Φ_X) and EUV (Φ_{EUV}) luminosity enhancements are taken to decline exponentially with a mean decay time $\tau = 90$ myr over the period of interest for planetary atmospheric evolution (indicated by the solid portion of the plotted curve). A $\Phi_X \propto (1/t)^{0.6}$ power law decay (Feigelson and Kriss 1989) is shown for comparison.

stellar age vs $\Phi_X(t) = (L(t)/L_{\odot})_X$ where L_{\odot} is the X-ray luminosity of the contemporary sun, is an updated version of Pepin’s (1989b) Fig. 1(b) in which Simon *et al.*’s (1985) main sequence star (MSS) data have been replotted against Walter and Barry’s (1990) more recent estimates of their ages. It is clear that both the WTTS and MSS scatter considerably from a single functional dependence of Φ_X on stellar age. However, most of the MSS data for t between ~ 50 and 500 myr do indicate a decline in Φ_X by a factor of ~ 5 from WTTS levels at ~ 20 myr.

To illustrate the hydrodynamic escape model discussed here, Φ_X is assumed to decline exponentially with time. The exponential plotted in Fig. 1, chosen as one possible example of the dependence of Φ_X on t for the young sun, is $\Phi_X = 1700 \exp[-(t - t_r)/\tau]$ with time in years, where $t_r = 10^5$ years and the mean decay time τ is taken to be 90 myr (up from 60 myr in Pepin 1989b). The period of hydrodynamic loss of planetary atmospheres, beginning by assumption at $t_0 = 50$ myr and terminating at $t_f \leq 400$ myr, is indicated by the solid portion of the curve. Note that at 50 myr, $\Phi_X^0 \cong 1000$. This level of enhancement

over present-day solar radiation applies strictly only to soft X-ray and short-wavelength EUV radiation from the stellar corona. Current data on radiation longward of the EUV, from transition regions and upper chromospheres of the WTTS and solar-type MSS where additional components of the $\lambda < 1025 \text{ \AA}$ EUV radiation also originate, indicate smaller increases (Simon *et al.* 1985, Walter *et al.* 1988, Pepin 1989b). Thus we would expect the total EUV enhancement at 50 myr to have been somewhat less than 1000.

There is no consensus on the mean decay time chosen above (Walter *et al.* (1988) and Walter and Barry (1990) adopt a much larger value in attempting to fit the entire Fig. 1 data field from 10^5 to 10^{10} years), nor on the assumption of exponential decline for L_X . Feigelson and Kriss (1989), for example, suggest that a power law of the form $L_X \propto t^{-s}$ with $s \cong 0.6-0.7$ may hold over the broad stellar age range from $\sim 10^6$ to 10^{10} years. The solid line in Fig. 1 is a plot of the power law $\Phi_X = 3 \times 10^4 (t/t_r)^{-0.6}$ constrained to pass through the cluster of $\sim 1 M_\odot$ WTTS points near 30 myr. Its fit to the scattered data does not appear to be convincingly worse than the exponential function over the times of interest for planetary atmospheres. Although they are not pursued in this paper, models of hydrodynamic escape analogous to those described here for exponential flux decay have been constructed for power law dependence with a comparable exponent ($s = 5/6$; see Pepin 1989b). Results are similar enough to indicate that the particular mathematical form of the decay in stellar flux through the period of atmospheric evolution is not centrally important. The crucial requirement is simply for flux decline, by roughly the factor suggested by present astronomical data.

III.B.4. Numerical Estimates and Operational Equations

Values of T , b , g , ρ and r_s used in this paper for Earth, Venus, and Mars are set out in Table I. Values of the diffusion parameters b at the indicated temperatures were calculated from Zahnle and Kasting's (1986) expressions for diffusion of Ne, Ar, Kr, Xe, N_2 , and CO_2 in H_2 as functions of T . Effects on model results of choosing much higher (and perhaps more realistic) atmospheric temperatures are shown later to be minor (Section VII.B). With $X_1 = 1$ and $r/r_s = \beta$, Eqs. (2) and (8) yield

$$F_1^0 = \mathbf{A}b(m_c^0 - m_1) \text{ particles cm}^{-2} \text{ sec}^{-1} \quad (9)$$

$$\text{and} \quad m_c - m_1 = \mathbf{B} \left(\frac{\phi_\oplus(t_p)\varepsilon}{bm_1} \right) \beta^3 \Phi_{\text{EUV}} \text{ amu} \quad (10)$$

at time t , where $\Phi_{\text{EUV}} = \eta \exp[-(t - t_r)/\tau]$ with $\tau = 90$ myr if we assume that Φ_X and Φ_{EUV} decay together. (Here and in all other equations involving b and m_c^0 , it should

TABLE I
Temperatures T , Diffusion Parameters b for Diffusion in H_2 (Mason and Marrero 1970, Zahnle and Kasting 1986), Surface Gravitational Accelerations g , Body Densities and Radii ρ and r_s , and Equation Constants \mathbf{A} , \mathbf{B} , and \mathbf{C} Used to Calculate Fractionations in Hydrodynamic Escape from Various Bodies

	T (K)	$b(\text{Xe})$	$b(\text{Kr})$	$b(\text{CO}_2)$ (units of $10^{18} \text{ cm}^{-1} \text{ sec}^{-1}$)	$b(\text{Ar})$	$b(\text{N}_2)$	$b(\text{Ne})$
Planets							
Venus	320	16.3	18.4	17.4	21.3	20.1	29.7
Earth	270	14.4	16.3	15.3	18.8	17.6	26.1
Mars	200	11.7	12.9	12.2	14.9	14.1	21.0
Planetesimal							
	80 ^a	1.40	1.71	2.36	2.24	2.88	4.01
		g (cm sec^{-2})	ρ (g cm^{-3})	r_s (cm)	\mathbf{A}^b	\mathbf{B}^c	\mathbf{C}^d
Planets							
Venus	890	5.269	6.050(8)	3.346(-08)	6.388(19)	1.056	
Earth	978	5.517	6.378(8)	4.357(-08)	2.194(19)	1.375	
Mars	371	3.945	3.397(8)	2.231(-08)	9.056(19)	0.704	
Planetesimal ^e							
$8 \times 10^{24} \text{ g}$	65.5	2.6	9.02(7)	8.86(-09)	1.28(21)	0.280	

Note. Powers of ten multipliers in parentheses.

^a Diffusion parameters b for diffusion in O (Zahnle and Kasting 1986). Values of b for diffusion in CH_4 should be similar.

^b $\mathbf{A} = 1.66 \times 10^{-24} (gX_1/kT)$.

^c $\mathbf{B} = (1.66 \times 10^{-24})^{-2} (3/4\pi G\rho)^2 (1/r_s)^3 (R_\oplus/R)^2 (kT/X_1)$.

^d $\mathbf{C} = 3.156 \times 10^7 \mathbf{A}$.

^e Planetesimal at $R = 3 \text{ AU}$; for other R , multiply \mathbf{B} by $(3/R)^2$. X_1 taken to be 0.9, $T = 80 \text{ K}$.

be understood that for a given value of m_c^0 for a particular species (e.g., Xe), the value of b from Table I is that corresponding to the same species). Expressions for \mathbf{A} (bracketed term in Eq. (2) for F_1^0) and \mathbf{B} (first four bracketed terms in Eq. (8)) and their calculated values for each planet are given in Table I, for m_c and m_1 in amu, $\phi_\oplus(t_p)$ in $\text{ergs cm}^{-2} \text{ sec}^{-1}$, b in $\text{cm}^{-1} \text{ sec}^{-1}$, and t_0 in years. With $m_c = m_c^0$ (determined from the model) at initial time t_0 , Φ_{EUV}^0 from Eq. (10) is

$$\Phi_{\text{EUV}}^0 = \frac{m_1(m_c^0 - m_1)}{(\mathbf{B}/b)\phi_\oplus(t_p)\varepsilon\beta^3} = \eta \exp[-(t_0 - t_r)/\tau]. \quad (11)$$

This expression defines the EUV energy demand of the escape model, to be compared later in Section VI.A with the values of η and $\Phi_X^0 \cong 1000$ estimated above from the observational X-ray data.

Constant inventory model. We may write $f(t) = F_1/F_1^0 = \Phi_{\text{EUV}}/\Phi_{\text{EUV}}^0 = \exp[-(t - t_0)/\tau]$ in Eq. (4). Then with

N_1 constant, Eq. (4) is readily integrated to

$$\ln \frac{N_2}{N_2^0} = -\alpha \left[\frac{m_c^0 - m_2}{m_c^0 - m_1} \right] - \alpha \left[\frac{m_2 - m_1}{m_c^0 - m_1} \right] \ln \left[\frac{m_2 - m_1}{m_c^0 - m_1} \right] \quad (12)$$

for the time evolution of N_2 , where the dimensionless parameter $\alpha \equiv F_1^0 \tau / N_1$. From Eq. (5),

$$f(t_2) = \frac{m_2 - m_1}{m_c^0 - m_1} = \exp[-(t_2 - t_0)/\tau] \quad \text{and} \\ t_2 - t_0 = -\tau \ln \left[\frac{m_2 - m_1}{m_c^0 - m_1} \right], \quad (13)$$

where t_2 is the time when loss of m_2 ceases. Fractional depletions at $t = t_2$ of species with masses $m_2' < m_2$ are found by replacing m_2 with m_2' in Eq. (12) (but *not* in Eqs. (13)). The (constant) hydrogen inventory $N_1 = F_1^0 \tau / \alpha$ is given by

$$N_1 = \frac{Cb(m_c^0 - m_1)\tau}{\alpha} \text{ particles cm}^{-2}. \quad (14)$$

Values of C are tabulated in Table I. The integrated hydrogen loss ΔN_1 during an escape episode extending from t_0 to t_2 , in units of the constant hydrogen inventory, is

$$\frac{\Delta N_1}{N_1} = \frac{1}{N_1} \int F_1(t) dt = \alpha \left[\frac{m_c^0 - m_2}{m_c^0 - m_1} \right]. \quad (15)$$

Rayleigh fractionation model. With $f(t) = \exp[-(t - t_0)/\tau]$, Eq. (6) is directly integrable. The solution, with $\alpha_0 \equiv F_1^0 \tau / N_1^0$, is

$$\ln \frac{N_2}{N_2^0} = \ln \frac{N_1}{N_1^0} + \frac{\alpha_0}{1 - \alpha_0} \left[\frac{m_2 - m_1}{m_c^0 - m_1} \right] \ln \left[\frac{N_1 m_c^0 - m_1}{N_1^0 m_2 - m_1} \right], \quad (16)$$

where

$$\frac{N_1}{N_1^0} = 1 - \alpha_0 + \alpha_0 \frac{m_2 - m_1}{m_c^0 - m_1} \quad (17)$$

and $t_2 - t_0$ is given by Eq. (13) above. As before, fractional depletions at $t = t_2$ of species with masses $m_2' < m_2$ are calculated from Eq. (16) with m_2' replacing m_2 . The Rayleigh analog of Eq. (14) is

$$N_1^0 = \frac{Cb(m_c^0 - m_1)\tau}{\alpha_0} \text{ particles cm}^{-2}, \quad (18)$$

where N_1^0 is the initial hydrogen inventory. Equation (15) for loss of the major species is replaced by

$$\frac{\Delta N_1}{N_1^0} = 1 - \frac{N_1}{N_1^0} \quad (19)$$

in units of the initial inventory, with N_1/N_1^0 given by Eq. (17).

IV. DATA

Noble gases and other species of high volatility were largely lost from the early planetary system when solid matter separated from the gas phase of the solar accretion disk and the disk's gaseous component later dissipated. Planetary atmospheres, meteorites, comets, and of course the sun are the principal surviving volatile reservoirs. "Solar" or "Solar System" abundances of the elements based on data from the sun's photosphere, the solar wind, meteorites (for nonvolatile species), and galactic sources represent our best estimates for the composition of the primordial solar nebula. As shown in Fig. 2, noble gases in primitive meteorites and the atmospheres of the terrestrial planets are grossly depleted relative to these estimates, by factors ranging from 4–9 orders of magnitude for xenon to 9–13 orders of magnitude for neon. There are no data as yet for comets. Carbon and nitrogen are relatively more

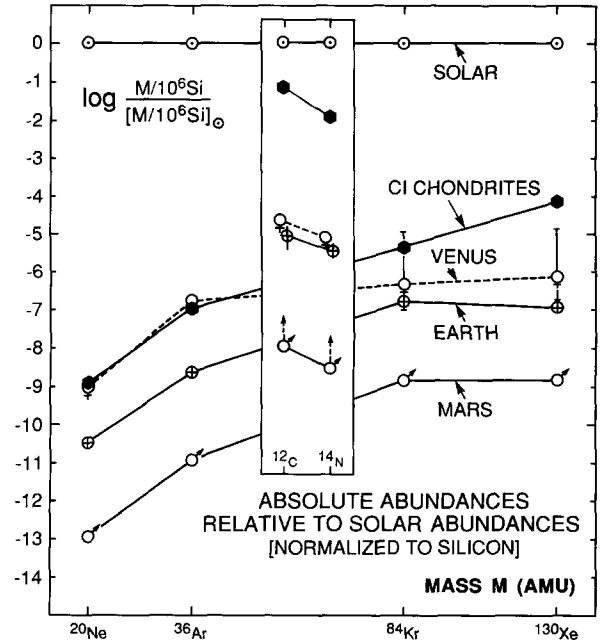


FIG. 2. Absolute noble gas, carbon and nitrogen abundances in planetary atmospheres (atoms per 10^6 planetary Si atoms) and in CI meteorites with respect to the corresponding solar ratios. "Atmospheric" abundances of terrestrial C and N are summed estimates for all crustal reservoirs from Walker (1977).

TABLE II
Abundances of Hydrogen, Carbon, Nitrogen, and Noble Gases in Solar System Matter (in g/g-Solar Composition), Two Classes of Volatile-Rich Meteorites (in g/g-Meteorite), and Terrestrial Planet Atmospheres and Known Crustal Reservoirs (in g/g-Planet)

	^{130}Xe	^{84}Kr	$^{12}\text{C}^{16}\text{O}_2$	^{36}Ar	$^{14}\text{N}_2$	^{20}Ne	^{12}C	$^1\text{H}_2$								
Solar																
Cameron (1982)	9.43	(-10)	5.73	(-08)	1.42	(-02)	9.33	(-05)	9.39	(-04)	1.34	(-03)	3.87	(-03)	7.72	(-01)
Anders and Ebihara (1982)	6.71	(-10)	5.94	(-08)	1.44	(-02)	8.61	(-05)	9.44	(-04)	1.77	(-03)	3.93	(-03)	7.43	(-01)
Average	8.07 ± 1.36	(-10)	5.84 ± 0.11	(-08)	1.43 ± 0.01	(-02)	8.97 ± 0.36	(-05)	9.42 ± 0.03	(-04)	1.56 ± 0.22	(-03)	3.90 ± 0.03	(-03)	7.58 ± 0.15	(-01)
Meteorites																
CI chondrites ^a	7.0 ± 1.9	(-12)	3.57 ± 0.15	(-11)	1.36 ± 0.26	(-01)	1.25 ± 0.10	(-09)	1.51 ± 0.31	(-03)	2.89 ± 0.77	(-10) ^b	3.70 ± 0.70	(-02)	6.68 ± 0.83	(-03)
E chondrites																
South Oman ^c	2.78 ± 0.28	(-12)	6.39 ± 0.64	(-11)	5.54	(-03)	1.22 ± 0.12	(-08)	5.0 ± 2.8	(-04)	1.98 ± 0.20	(-11)	1.51	(-03)		
Range ^d	1.05-27.8	(-13)	5.35-639	(-13)	5.54-25.7	(-03)	1.47-1220	(-11)	1.33-9.46	(-04)	-0-6.80	(-11)	1.51-7.00	(-03)		
Average ^e	4.1 ± 2.9	(-13)	3.0 ± 2.7	(-12)	1.54 ± 0.59	(-02)	3.3 ± 2.8	(-10)	5.0 ± 2.4	(-04)	2.0 ± 2.0	(-11)	4.2 ± 1.6	(-03)		
Planets																
Venus ^f	$8.9^{+2.5/-6.8}$	(-14)	$4.7^{+0.6/-3.4}$	(-12)	9.55 ± 0.16	(-05)	2.51 ± 0.97	(-09)	2.20 ± 0.50	(-06)	2.9 ± 1.3	(-10)	2.60 ± 0.04	(-05)		
Earth ^g	1.40 ± 0.02	(-14)	1.66 ± 0.02	(-12)	$3.7^{+2.5/-2.2}$	(-05)	3.45 ± 0.01	(-11)	$9.1^{+5.4/-2.4}$	(-07)	1.00 ± 0.01	(-11)	$1.0^{+0.7/-0.6}$	(-05)	3.10	(-05)
Mars ^h	2.08 ± 0.41	(-16)	1.76 ± 0.28	(-14)	4.08 ± 0.73	(-08)	2.16 ± 0.55	(-13)	7.3 ± 1.9	(-10)	4.38 ± 0.74	(-14)	1.11 ± 0.20	(-08)		

Note. Powers of ten multipliers in parentheses.

^a Mazor *et al.* (1970) for noble gases; Kerridge (1985) for hydrogen, carbon, and nitrogen.

^b $(^{20}\text{Ne})_0 = 4.1 \pm 1.1$ (-11) (Wieler *et al.* 1989).

^c Crabb and Anders (1981) for noble gases; Grady *et al.* (1986) for carbon and nitrogen.

^d References in *c* plus Kung and Clayton (1978) for nitrogen.

^e Excluding South Oman.

^f Von Zahn *et al.* (1983) for carbon, nitrogen, neon, and argon; Donahue and Pollack (1983) for krypton; Donahue (1986) for xenon.

^g Rubey (1951) for hydrogen (from H_2O); Walker (1977) for carbon and nitrogen (carbon uncertainties include the lower estimate of Rubey (1951) and the higher estimate of McElroy *et al.* (1977); nitrogen uncertainties include the higher estimate of Donahue and Pollack (1983), and the atmospheric inventory of 6.7 (-07) g/g-Earth as a lower limit).

^h Owen *et al.* (1977) Viking data for carbon and nitrogen; Hunten *et al.* (1987) and references therein for SNC noble gas data.

abundant, particularly in the meteorites. In addition to large and variable elemental depletions, each of these contemporary volatile reservoirs displays its own set of isotopic signatures.

IV.A. Solar

IV.A.1. Elemental Abundances

Separate compilations of Solar System nuclidic abundances from Cameron (1982) and Anders and Ebihara (1982) are given in Table II, here converted to units of grams per gram of solar-composition matter. Average values, with uncertainties that represent only the differences between the two estimates, are also tabulated and are used throughout this paper. Changes from the Anders and Ebihara (1982) abundances in the more recent Anders and Grevesse (1989) compilation are <10% for the noble gases and <30% for carbon and nitrogen and are unimportant for the present study.

Helium abundances are not listed in Table II. Helium is only weakly bound gravitationally and escapes thermally from the atmospheres of the terrestrial planets. The helium contents and compositions of these atmospheres are thus of little relevance as signatures of their origin and early evolution, and are omitted from consideration in this model. However, one should note that an isotopically solar-like helium component does exist in the Earth's interior and in meteorites, and the question of its origin—perhaps by adsorption (Sections V.B.4, VII.D), or by some other process—is of considerable importance.

IV.A.2. Isotopic Compositions

Relative isotopic abundances of elements now in the sun, and those once extant in the early solar nebula, are not subject to direct measurement. Isotope ratios that can arguably be taken to represent these compositions for the noble gases are set out in Table III. Neon and krypton are straightforward in that they reflect the best available data on isotopic compositions in the solar wind. The principal uncertainty for these elements, beyond that imposed by analytic errors, is the general question of whether the wind is an accurate sample of the solar composition and, by extension, that of the early nebula. Estimates of solar argon and, in particular, xenon compositions chosen for this model are less firm: the former involves a slight extrapolation of the current solar wind data base, and the latter other assumptions that may be reasonable but are model-dependent. There are two widely divergent schools of thought concerning the isotope ratios of carbon and nitrogen in the ancient sun and solar nebula.

The neon isotope ratio $^{20}\text{Ne}/^{22}\text{Ne}$ in various solar system reservoirs is shown in the left panel of Fig. 3. Sample identifications and references are given in the legend and caption. Several isotopically distinct neon components in carbonaceous chondrites, indicated by the filled symbols and discussed in Section IV.B below, are evident. Measurements in samples dominated by solar wind neon (1-7 in Fig. 3) are tightly grouped between $^{20}\text{Ne}/^{22}\text{Ne} \cong 13-14$. The solar ratio of 13.7 assumed here (Table III) is identical to that found in samples of the contemporary wind directly

TABLE III
Isotopic Compositions of Carbon, Nitrogen, and Noble Gases in Solar-Composition Matter, Volatile-Rich Meteorites, and Terrestrial Planet Atmospheres and Known Crustal Reservoirs

Argon, neon, nitrogen, and carbon									
	$\frac{^{36}\text{Ar}}{^{38}\text{Ar}}$	$\frac{^{20}\text{Ne}}{^{22}\text{Ne}}$	$\frac{^{21}\text{Ne}}{^{22}\text{Ne}}$ ($\times 10^{-2}$)	$\frac{^{15}\text{N}^{14}\text{N}}{^{14}\text{N}_2}$ ($\times 10^{-3}$)	$\delta^{15}\text{N}_{\text{AIR}}$ (‰)	$\frac{^{13}\text{C}^{16}\text{O}_2}{^{12}\text{C}^{16}\text{O}_2}$ ($\times 10^{-4}$)	$\delta^{13}\text{C}_{\text{PDB}}$ (‰)		
Assumed solar ^a	5.8	13.7	3.27 ± 0.05	?	?	?	?		
CI chondrites ^b	5.30 ± 0.05 ^c	8.9 ± 1.3 ^c	? ^c	7.662 ± 0.081	42 ± 11	111.21 ± 0.28	-10.3 ± 2.5		
E chondrites ^d	5.46 ± 0.04	7.4 ± 1.2	?	7.118 ± 0.088	-32 ± 12	111.43 ± 0.89	-8.4 ± 7.9		
Venus ^e	5.56 ± 0.62	11.8 ± 0.7	?	7.3 ± 1.5	~0 ± 200	112 ± 2	-3 ± 18		
Earth ^f	5.320 ± 0.002	9.800 ± 0.080	2.899 ± 0.025	7.353 ± 0.008	=0	111.65 ± 0.15	-6.4 ± 1.3		
Mars ^g	4.1 ± 0.2	10.1 ± 0.7	?	11.9 ± 1.2	620 ± 160	<118	<50		
Krypton									
	⁷⁸ Kr	⁸⁰ Kr	⁸² Kr	⁸³ Kr	⁸⁴ Kr	⁸⁶ Kr			
Assumed solar (Kr-1)	0.6359	4.075	20.501	20.276	=100	30.115			
Assumed solar (Kr-2)	0.6470	4.124	20.629	20.340	=100	29.915			
CI chondrites ^h	0.5962 ± 0.0046	3.919 ± 0.030	20.149 ± 0.080	20.141 ± 0.080	=100	30.950 ± 0.077			
E chondrite (S. Oman) ⁱ	0.634 ± 0.016	4.05 ± 0.03	20.45 ± 0.09	20.27 ± 0.07	=100	30.73 ± 0.17			
Earth atmosphere ^j	0.6087 ± 0.0020	3.960 ± 0.002	20.217 ± 0.021	20.136 ± 0.021	=100	30.524 ± 0.025			
Mars atmosphere ^k	0.637 ± 0.036	=4.09	20.54 ± 0.20	20.34 ± 0.18	=100	30.06 ± 0.27			
Xenon									
	¹²⁴ Xe	¹²⁶ Xe	¹²⁸ Xe	¹²⁹ Xe	¹³⁰ Xe	¹³¹ Xe	¹³² Xe	¹³⁴ Xe	¹³⁶ Xe
Assumed solar (U-Xe) ^l	2.947	2.541	50.873	628.7	=100	499.58	604.79	212.88	166.34
CI chondrites ^l	2.851 ± 0.051	2.512 ± 0.040	50.73 ± 0.38	635.8 ^m -670.8	=100	504.3 ± 2.8	615.0 ± 2.7	235.9 ± 1.3	198.8 ± 1.2
H-xenon ^l	0	0	0	0	0	7.3 ± 5.2	24.9 ± 1.8	71.23 ± 0.78	=100
E chondrite (S. Oman) ⁱ	2.97 ± 0.10	2.620 ± 0.086	51.12 ± 0.58	827.8 ± 7.0	=100	503.4 ± 3.7	606.4 ± 3.7	228.1 ± 2.1	187.4 ± 1.7
Contemporary Earth atmosphere ^j	2.337 ± 0.007	2.180 ± 0.011	47.146 ± 0.047	649.58 ± 0.58	=100	521.27 ± 0.59	660.68 ± 0.53	256.28 ± 0.37	217.63 ± 0.22
Nonradiogenic Earth atmosphere ^j	2.337 ± 0.007	2.180 ± 0.011	47.146 ± 0.047	605.3 ± 2.9	=100	518.73 ± 0.71	651.8 ± 1.3	247.0 ± 1.3	207.5 ± 1.3
Mars atmosphere ⁿ	2.45 ± 0.24	2.12 ± 0.23	47.67 ± 1.03	1640.0 ± 8.0	=100	514.7 ± 3.7	646.0 ± 8.8	258.7 ± 2.4	229.4 ± 2.4

Note. Units are parts per thousand (‰) deviations from the indicated standard compositions for $\delta^{15}\text{N}_{\text{AIR}}$ and $\delta^{13}\text{C}_{\text{PDB}}$, and atom/atom for isotope ratios.

^a Bochsler and Geiss (1977), Benkert *et al.* (1988) for Ne; see Section IV.A.2 for Ar.

^b Kerridge (1985) for C, N; Mazor *et al.* (1970) for Ne, Ar.

^c Q-component: $(^{36}\text{Ar}/^{38}\text{Ar})_Q = 5.32 \pm 0.02$; $(^{20}\text{Ne}/^{22}\text{Ne})_Q = 10.75 \pm 0.15$; $(^{21}\text{Ne}/^{22}\text{Ne})_Q \leq 0.0300 \pm 0.0006$ (Wieler *et al.*, 1990a,b).

^d Grady *et al.* (1986) for C and N; Deines and Wickman (1985) for C; Kung and Clayton (1978) for N; Crabb and Anders (1981) for Ne and Ar (South Oman only).

^e Von Zahn *et al.* (1983) for C and N; Donahue (1986) for Ne and Ar.

^f Schwarcz *et al.* (1969) for C; Junk and Svec (1958) for N; Eberhardt *et al.* (1965) for Ne; Nier (1950) for Ar.

^g Nier and McElroy (1977) for C and N; Wiens *et al.* (1986) for Ne and Ar.

^h Eugster *et al.* (1967).

ⁱ Crabb and Anders (1981); nonradiogenic 129/130 assumed = 6.287 (U-Xe).

^j Basford *et al.* (1973).

^k Becker and Pepin (1984a), Swindle *et al.* (1986).

^l Pepin and Phinney (1978).

^m Range from Mazor *et al.* (1970).

ⁿ Swindle *et al.* (1986).

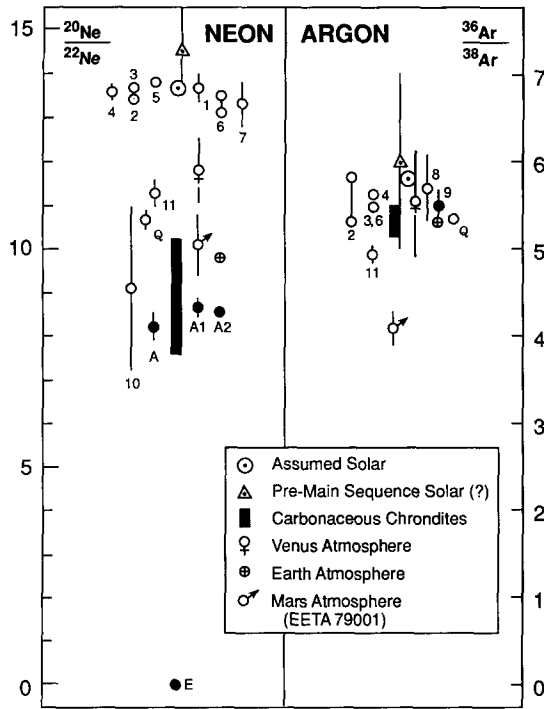


FIG. 3. Nonspallogenic neon and argon isotope ratios in solar system volatile reservoirs. Numbered and lettered data points from (1) solar wind composition foils (Bochsler and Geiss 1977); (2) Weston meteorite metal (Becker *et al.* 1986a,b, Becker and Pepin 1991); (3) minerals from lunar soil 71501 and lunar breccia 79035 (Benkert *et al.* 1988); (4) lunar soil 67701 (Frick and Pepin 1981, Frick *et al.*, 1988); (5) Pantar meteorite metal (Hintenberger *et al.* 1965, Wänke 1965); (6) ilmenites from lunar soil 71501 (Frick *et al.* 1988) and lunar breccia 79035 (Becker and Pepin 1989); (7) Washington County meteorite metal (Becker and Pepin 1984b); (8) Pantar meteorite (Signer and Suess 1963); (9) Mokoia meteorite (Mazor *et al.* 1970); (10) solar flares (Mewaldt *et al.* 1984); (11) solar energetic particles (Wieler *et al.* 1986, Benkert *et al.* 1988); (A) Ne-A (Pepin 1967); (A1,A2) Ne-Al,A2 (Alaerts *et al.* 1980); (E) Ne-E (Jungck and Eberhardt 1979); (Q) Q-component Ne and Ar (Wieler *et al.* 1990a,b). For references to all other plotted data, see Table III or text.

collected in foils deployed and irradiated on the lunar surface (measurement 1).

Measurements of Solar System $^{36}\text{Ar}/^{38}\text{Ar}$ ratios are summarized in the right panel of Fig. 3, along with an estimate by Black (1971, 1972) for the premain-sequence solar wind. The composition of solar wind argon was not well defined in the lunar foil experiments. Current efforts to determine it are utilizing delicate experimental techniques for extracting and analyzing gases from the outer few hundred angstroms—the solar wind “implantation zone”—of lunar and meteoritic regolith grains. Results from the two laboratories presently pursuing this investigation are shown in Fig. 3, and plotted on an expanded scale in Fig. 4. The solar $^{36}\text{Ar}/^{38}\text{Ar}$ ratio is taken to be 5.8, a value that allows the escape model discussed here to be expressed in its simplest and most consistent form. This

choice is not in disagreement with the highest measurement, but it is important to point out that this value (upper #2 in Fig. 4, where the other No. 2 points represent compositions obtained on progressively deeper oxidations of the Weston metal grains) could be fractionated in favor of the lighter isotope (Becker and Pepin 1991). The average ratio from Fig. 4 is $\sim 5.6 \pm 0.1$, and so the choice of a somewhat higher solar value involves an assumption that the Fig. 4 data do not quite represent pure solar-wind Ar, but are still contaminated to varying degrees by spallogenic or solar-energetic-particle (Benkert *et al.* 1988) argon components with lower $^{36}\text{Ar}/^{38}\text{Ar}$.

Current data on the isotopic composition of *unfractionated* solar wind krypton are shown in Fig. 5, where $^{84}\text{Kr}/^{86}\text{Kr}$ ratios are plotted as parts per thousand (‰) deviations from terrestrial ratios. The composition of carbonaceous chondrite Kr is shown for comparison. Although the data base for krypton compositions in solar-wind-rich samples, and in particular in lunar regolith materials, is relatively large, this one is sparse because most such measurements are on bulk samples in which isotope ratios have been fractionated by diffusive losses of implanted volatile species (Basford *et al.* 1973, Bogard *et al.* 1974, Frick *et al.* 1988). Reported solar-wind compositions derived from such samples, such as SUCOR (Podosek *et al.* 1971) and BEOC 12001 (Eberhardt *et al.* 1972), therefore do *not* represent the primary wind—they are isotopically much too heavy. Data in Fig. 5 are from samples in which isotopic alterations by diffusion or spallation are judged to be minor. (Of these, South Oman is

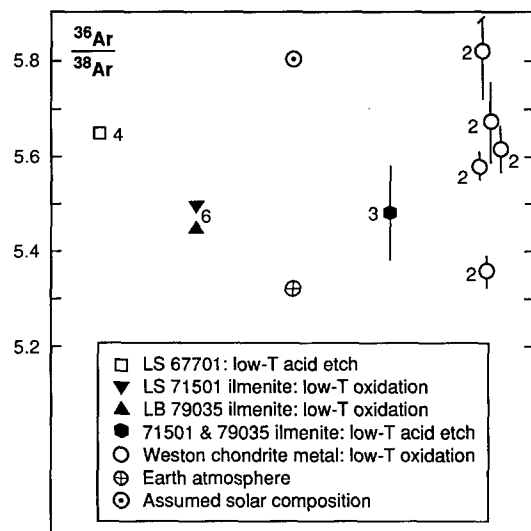


FIG. 4. Recent experimental estimates using acid-etch and oxidation techniques of the isotopic composition of solar wind argon, shown in Fig. 3 and plotted here on an expanded scale. Numbers identify references given in the Fig. 3 caption. “LS” and “LB” respectively denote lunar soil and lunar breccia samples.

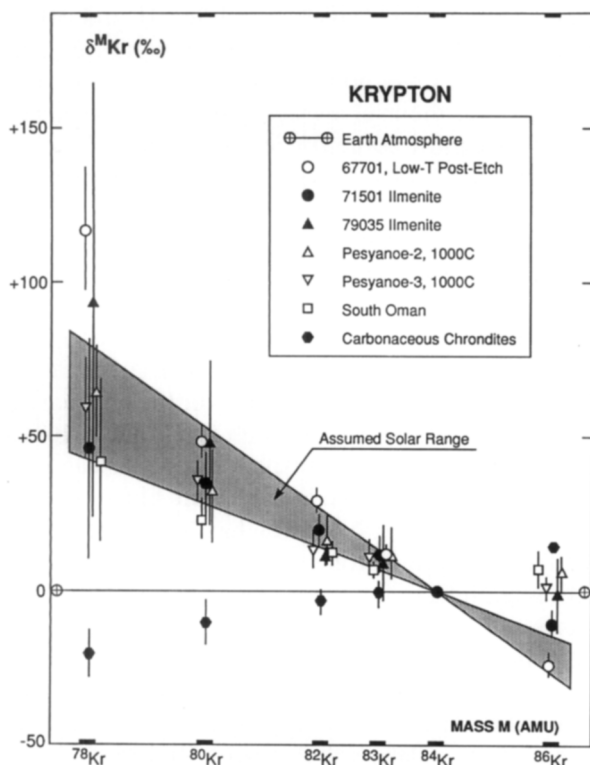


FIG. 5. Current estimate from measured isotope data of the probable compositional range for unfractionated solar krypton (shaded area). All isotopically light compositions are from solar-wind-rich samples except for South Oman (see text, Section IV.A.2). The fractionated carbonaceous chondrite pattern is shown for comparison. The ordinate δ -unit is defined for Kr isotopes as $\delta^M \text{Kr} = 1000 \{ [(^M \text{Kr}/^{84} \text{Kr})_{\text{sample}} / (^M \text{Kr}/^{84} \text{Kr})_{\text{Earth}}] - 1 \}$ in permil (‰) and is similarly defined for other species in all tables and figures where it occurs. Data sources are Frick and Pepin (1981) and Frick *et al.* (1988) for 67701; Frick *et al.* (1988) for 71501 ilmenite; Becker and Pepin (1989) for 79035 ilmenite; and Marti (1980) for Pesyanoe-2 and -3. Earth, South Oman, and carbonaceous chondrite references in Table III.

particularly interesting in that there is no evidence for solar wind irradiation (Crabb and Anders 1981); Kr and other noble gases in this E-chondrite may reflect direct adsorption from an ambient gas phase.) The isotopic pattern suggests relatively smooth mass fractionation relationships between solar, terrestrial, and meteoritic Kr. Deviations at ^{86}Kr are not understood, but may be due to an “exotic” contribution at this isotope associated with a nucleogenetic Xe component (Section V.D.1). Data scatter is relatively large, and the actual solar composition is correspondingly uncertain although it probably lies somewhere within the shaded area of Fig. 5. For this reason two different estimates for solar Kr, one (Kr-1) corresponding to the lower boundary of the shaded area and the other (Kr-2) roughly bisecting it, are tabulated in Table III and separately utilized in the following applications of the escape model.

Derivation of the isotopic composition of solar wind xenon from lunar and meteoritic samples is severely impeded by this same problem of diffusive fractionation, and in addition by the pervasive presence in such materials of fission and/or exotic nucleogenetic components at the heavy isotopes (Frick *et al.* 1988). For both these reasons, the “solar” composition extracted by Pepin and Phinney (1978) from a multicomponent analysis of Xe in bulk lunar samples now appears to be isotopically too heavy.

There is an alternate approach to estimating the isotopic composition of nebular xenon that does not involve solar wind data. Krummenacher *et al.* (1962) first pointed out that the light isotope abundance patterns in terrestrial and meteoritic xenon are fully consistent with generation of one from the other by mass fractionation. This kind of relationship was shown by Pepin and Phinney (1978) to be in accord with all Xe isotope abundances if two conditions were met: (1) the parent reservoir from which Xe on the early Earth derived was free of the nucleogenetic heavy-isotope component present in the carbonaceous chondrites; and (2) contemporary terrestrial Xe contains radiogenic contributions, produced by ^{129}I and ^{244}Pu decay in the Earth and outgassed to the atmosphere following the fractionating separation of nonradiogenic terrestrial Xe from its parent reservoir. The required parental composition—named “U-Xe”—calculated by Pepin and Phinney falls on isotopic correlations defined by carbonaceous chondrite data, and so could still be extant as one component of meteoritic Xe. A small amount of Xe with distinctive heavy-isotope ratios close to the predicted U-Xe composition was later found in the CM chondrite Murray (Niemeyer and Zaiowski 1980). On a number of grounds, U-Xe is an attractive choice for the primordial nebula. It appears to be genetically related to both terrestrial and meteoritic Xe. It is isotopically somewhat lighter than Pepin and Phinney’s lunar-derived solar wind Xe composition, an expected consequence of the diffusive fractionation effects and extraneous heavy isotope contributions, noted above, that perturb isotopic records in most bulk samples of solar-wind-rich materials. Therefore the U-Xe composition, given in Table III, is assumed here to represent solar (nebular) Xe. Its relationships to the ancient nonradiogenic terrestrial composition and to meteoritic Xe are shown later in Figs. 9 and 12.

Extensive data exist for solar wind C and N isotopes in lunar samples, with strong evidence for secular variation of N composition, but there is no consensus on what these may signify for the isotopic compositions of these elements in the young sun or solar nebula. Estimates for the value of $\delta^{15}\text{N}$ that might have pertained in the protosolar nebula range from near -200% or lower in the ancient sun (Kerridge 1980, 1982, Clayton and Thiemens 1980, Ray and Heymann 1980) to about $+120\%$ (Geiss and Bochsler 1982).

IV.A.3. Summary

The solar elemental and isotopic data set out in Tables II and III are of widely different types and are drawn from a variety of sources. Cameron's (1982) neon abundance is from solar cosmic ray data; the Anders–Ebihara (1982) value is a compromise between solar wind measurements and estimates from galactic stellar and molecular cloud observations. Argon, krypton, and xenon abundances are interpolated, using nucleosynthetic criteria, from neighboring element abundances in unfractionated (CI) meteorites. Carbon and nitrogen estimates are from solar spectroscopic observations. Neon, argon, and krypton isotope ratios are based on measurements of solar wind, either directly implanted in collector foils or extracted from irradiated dust grains in the lunar regolith and in meteorites. The assumed xenon composition is derived from a model-dependent analysis of meteoritic and terrestrial data.

The extent to which this hybrid data base actually represents the primordial solar nebula is an open issue. It is reasonable to suppose that the compositions of the sun and the early nebula are closely related, but the unresolved question for the solar wind data is that of fractionation of the wind with respect to solar photospheric abundances by the processes supplying gases to the corona (Geiss 1982, Geiss and Bochsler 1985, Bochsler *et al.* 1986, von Steiger and Geiss 1989). There is evidence that observed interelement fractionations arising from variations in first ionization potential (FIP) are not serious for the high-FIP suite of elements considered here (von Steiger and Geiss 1989), but there are also observations that point to element-specific isotope fractionation in solar particle emission. One celebrated example is the large and unexplained discrepancy in the isotopic compositions of Ne measured in the solar wind and in solar flares (Mewaldt *et al.* 1984), shown in the left panel of Fig. 3 by comparison of the wind (1–7) and flare (10) data points. Taken at face value, this must mean that either the wind or the flare isotopes are fractionated with respect to the true solar ratio.

IV.B. Meteorites

Volatile-rich meteorites contain a rich and intriguing assortment of distinct noble gas, carbon, and nitrogen components of both extrasolar and "local" (i.e., nebular) origin, associated with a variety of carrier phases (see Anders 1987, 1988 for recent reviews). In considering planetary volatiles, however, we are most interested in the possibility that entire meteorite parent bodies accreted by planets were important sources of primordial atmospheric gases. Therefore, on the assumption that present and past populations of these objects were chemically similar, the relevant data for the origin of planetary atmospheres are the average bulk meteoritic inventories and

isotopic compositions given in Tables II and III. This consideration of meteoritic contributions to planets avoids the question of how, when, and from what sources the meteorites themselves acquired their gaseous elements. This central issue for investigations of the origin and evolution of Solar System volatiles in general is addressed in Section V.D.

Elemental and isotopic data for both the CI carbonaceous chondrites and the enstatite chondrites are listed in Tables II and III; references are noted in the tables. In contrast to the relatively constant elemental abundances in CI chondrites, the E chondrites span a broad range. Both this range and the specific data for the unusual South Oman member of the class (Crabb and Anders 1981) are given in Table II. The corresponding noble gas isotope ratios in Table III are from South Oman alone, where the nonspallogenic $^{20}\text{Ne}/^{22}\text{Ne}$ ratio has been crudely estimated from a three-isotope correlation plot of the Crabb and Anders Ne data for South Oman and several other E chondrites.

Elemental abundance ratios for meteoritic noble gases, calculated from the Table II data, are plotted normalized to solar ratios in Fig. 6. To include all classes of volatile-rich chondrites, relative abundances for CM, CV3, CV4, and CO3 carbonaceous chondrites (Mazor *et al.* 1970, Srinivasan *et al.* 1977, Alaerts *et al.* 1979, Matsuda *et al.* 1980) are also shown. The first three are indistinguishable from the CI distribution on this scale, and the CO3s fall within the E-chondrite range. The general pattern of progressively greater relative depletion with decreasing mass for Ar/Kr and Ne/Kr suggests varying degrees of mass-dependent fractionation of solar-composition noble gases. (It is important to note that this monotonic pattern with respect to mass does *not* hold for carbon and nitrogen: abundances of these elements, relative to ^{84}Kr as in Fig. 6, range from about $3\times$ solar for atmospheric nitrogen on Mars to $20,000\times$ solar for carbon in an average E chondrite). Similar fractionation patterns have been generated in experimental investigations of noble gas adsorption, discussed above in Section III.A. Most elemental abundance ratios of gases adsorbed on various substrates in the laboratory, when plotted with respect to ambient gas-phase compositions, fall within the darker shaded area of Fig. 6 (Fanale and Cannon 1972, Frick *et al.* 1979, Niemeyer and Marti 1981, Yang *et al.* 1982, Yang and Anders 1982a,b). The smaller and even reversed fractionations shown by the lighter shading are generated by physical adsorption and solution of noble gases in carbon black (Wacker and Anders 1986, Wacker 1989).

Relevant meteoritic isotope data for Ne, Ar, and Kr are plotted in Figs. 3 and 5. Note in particular the comparatively wide range of $^{20}\text{Ne}/^{22}\text{Ne}$ ratios found in bulk carbonaceous chondrites, indicated in the left panel of Fig. 3 together with the compositions of several individual

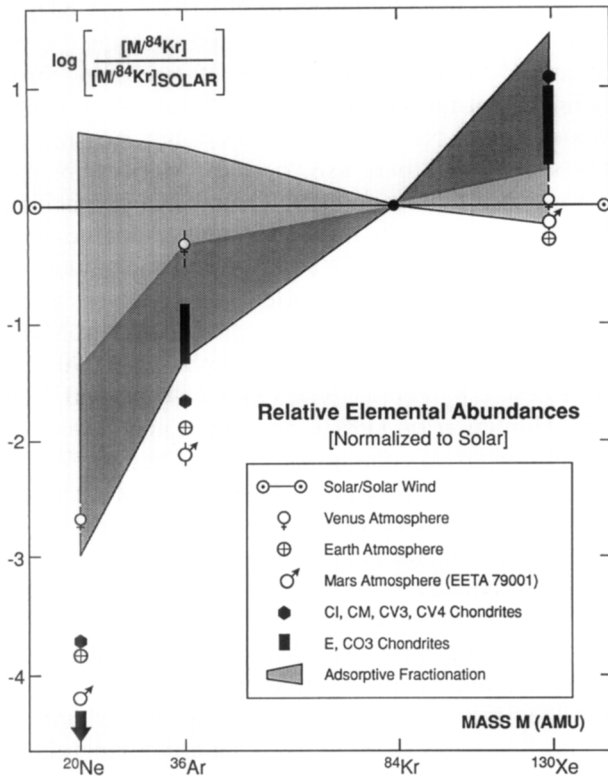


FIG. 6. Noble gas $M/^{84}\text{Kr}$ abundance ratios in terrestrial planet atmospheres and volatile-rich meteorites, plotted with respect to solar relative abundances and compared to the range of elemental fractionations (with respect to ambient gas-phase abundance ratios) determined from laboratory adsorptive experiments and from analyses of natural sedimentary materials. These fractionations generally fall in the darker shaded area of the figure, except for a number of measurements on carbon black (Wacker and Anders 1986, Wacker 1989) displaying the smaller or reversed patterns within the lighter shading. Data from Table II, and from references given in the text for CM, CV3, CV4, and CO3 chondrites (Section IV.B) and for laboratory and sedimentary adsorption studies (Section III.A).

components (E, A, and Q) that contribute to neon in these meteorites. Of these, E and A are entirely or largely of exotic origin, synthesized in galactic nucleosynthetic environments and transported into the primitive solar system in presolar carbonaceous dust grains which still survive in these meteorites (see Anders 1987, 1988). Q-Ne, however, appears to derive from the local nebula: this component, along with most of the meteoritic inventories of Ar, Kr, and Xe, is sited on grain surfaces—or more precisely in sites from which gases are readily released by acid oxidation (Alaerts *et al.* 1979, Wieler *et al.* 1989, 1990a,b)—as might be expected for species adsorbed from an ambient gas phase. Compositional characteristics of Q-component noble gases are given in footnotes to Tables II and III, and are discussed in Section V.D.2.

IV.C. Planetary Atmospheres

The planetary data compilations set out in Tables II and III, and plotted for absolute abundances in Fig. 2, refer entirely to *atmospheric* inventories except for terrestrial carbon and nitrogen. A relevant question is whether volatiles once in these atmospheres have been extracted by physical or chemical partitioning into surface materials, and perhaps later sequestered in planetary interiors by crustal cycling. Given the thermal and geologic state of Venus, the answer for that planet is likely to be no (Kaula 1990). On Earth, the hydrosphere, biosphere, and sedimentary column are important subsidiary reservoirs for some atmophilic species. They contain fractions of total “atmospheric” inventories that range from probably minor for the nonradiogenic noble gases—including Xe (Bernatowicz *et al.* 1984, 1985)—to perhaps significant for N to dominant for C and H. To the extent that there has been a net transport of volatiles into the upper terrestrial mantle by subduction of sediments over geologic time, the inventory estimates in Table II based on summation over all these “accessible” reservoirs are lower limits. For Mars, theoretical and experimental estimates of the carrying capacity of the cold megaregolith for H_2O and CO_2 are such that, for these species at least, the observable Martian volatile reservoirs (atmosphere, ice caps, and layered deposits) are likely to contain only small fractions of total inventories (Fanale 1976, Fanale and Jakosky 1982, Fanale *et al.* 1982, 1991). In addition, the Martian volatile system is open to loss of molecular species, including N_2 , to space. Over the history of the planet, nonthermal escape of at least a few times the present atmospheric nitrogen inventory is required to account for the present-day enrichment in $^{15}\text{N}/^{14}\text{N}$ (McElroy *et al.* 1977, Yung *et al.* 1977). Martian C and N abundances in Fig. 2 are therefore indicated as lower limits.

IV.C.1. Venus

Data from *in situ* compositional measurements of the Venus atmosphere by mass spectrometers and gas chromatographs on U.S. and Soviet spacecraft have been comprehensively reviewed and assessed by von Zahn *et al.* (1983). Abundances of C, N, ^{20}Ne , and ^{36}Ar in Table II were calculated from the recommended mixing ratios given in their Table II. There is a profound difference of interpretation in the literature concerning the Kr and Xe concentrations measured by Pioneer Venus and by Venera 11 and 12. The von Zahn *et al.* review traces the derivation of the disparate ^{84}Kr mixing ratios from the two sets of instrumental data—their estimate of 0.4 ppm from Venera, based on analysis by Istomin *et al.* (1980), vs 0.025 ppm from Donahue *et al.*'s (1981) refinement of Pioneer Venus data—and sets out the authors' arguments

in favor of the former. The contrary case is made by Donahue *et al.* (1981), and their lower value is chosen for Table II—in particular because severe terrestrial Kr contamination of the Venera 11 and 12 measurements is now thought to be likely, and Venera 13 and 14 data are in better agreement with the Pioneer Venus results (T. Donahue, personal communication).

Venusian Xe estimates are certainly in no better shape—von Zahn *et al.* (1983) suggest that it might not have been detected at all. However, the Pioneer Venus ^{132}Xe mixing ratio, reported as an upper limit of 10 ppb by Donahue and Pollack (1983), was further refined by Donahue (1986), where $^{84}\text{Kr}/^{132}\text{Xe}$ is given as 13.5 ± 3.5 , implying a ^{132}Xe mixing ratio of about 1.9 ppb. This value has been used together with an assumed $^{130}\text{Xe}/^{132}\text{Xe}$ isotope ratio of 0.164 to calculate the ^{130}Xe abundance in Table II. Kr and Xe concentrations adopted here thus consistently reflect the views of Donahue and his co-workers. They define the strikingly solar-like Ar : Kr : Xe distribution shown in Figs. 2 and 6.

Ne and Ar isotopic data also suggest a solar affinity for noble gases on Venus, but are too uncertain to establish it rigorously. The $^{20}\text{Ne}/^{22}\text{Ne}$ ratio from Pioneer Venus was originally reported to be 14.3 ± 4.1 (Hoffman *et al.* 1980). The Table III value of 11.8 ± 0.7 is from a later compilation by Donahue (1986), and as shown in Fig. 3 is significantly higher than the terrestrial and CI ratios. Thus there appears to be a solar signature in Venusian Ne. It would seem, from the nominally high Pioneer Venus $^{36}\text{Ar}/^{38}\text{Ar}$ ratio of 5.56 ± 0.62 given in Table III (Hoffman *et al.* 1980, Donahue 1986) and plotted in Fig. 3, that this could also be the case for Ar, though the uncertainty is large. There are no quantitative data on Kr and Xe compositions.

IV.C.2. Earth

The well known elemental and isotopic abundances of noble gases in the Earth's atmosphere are listed in Tables II and III and plotted in part in Figs. 2, 3, 4, and 6. The isotopic composition of nonradiogenic terrestrial Xe calculated by Pepin and Phinney (1978) is included in Table III. The abundances of nitrogen and carbon in Table II are Walker's (1977) estimates; indicated uncertainties are discussed in the footnote. Terrestrial atmospheric nitrogen, with $^{14}\text{N}/^{15}\text{N} = 272$, is the standard reference gas for nitrogen isotopic measurements. The $^{12}\text{C}/^{13}\text{C}$ ratio in the PDB (PeeDee belemnite) standard for $\delta^{13}\text{C}$ measurements is 88.99. The $\delta^{13}\text{C}_{\text{PDB}}$ value in Table III refers to integrated carbon from all reservoirs.

IV.C.3. Mars

Mass spectrometric data on the composition of the Martian atmosphere from instruments on the Viking space-

craft were reported by Owen *et al.* (1977) and Nier and McElroy (1977). Uncertainties in mixing ratios for ^{20}Ne , ^{84}Kr , and ^{132}Xe are about a factor of 3. Except for one very important ratio ($^{129}\text{Xe}/^{132}\text{Xe} = 2.5 \pm 70\%$), isotopic compositions of Ne, Kr, and Xe were not measured.

The second data base used here for Mars atmospheric composition is that from the SNC meteorites, specifically from analyses of gases trapped in glassy nodules in the antarctic shergottite EETA 79001. The geochemical case for the origin of the SNC meteorites on Mars, and for trapping of an unfractionated sample of ambient Martian atmosphere in shock-generated melt phases of 79001, has been reviewed by Pepin (1985, 1987), Dreibus and Wänke (1985), Hunten *et al.* (1987), and Pepin and Carr (1991). Detailed numerical comparisons of Viking and 79001 determinations for CO_2 , N_2 , and the noble gases are given in the last two of these reports. All abundances and isotopic compositions common to the two data sets agree within their respective uncertainties. The generally more precise noble gas measurements from 79001 yield most of the isotopic ratios missing from Viking. Abundances of the two major atmospheric constituents, CO_2 and N_2 , were determined more accurately by Viking; uncertainties in ^{36}Ar and ^{40}Ar from 79001 and Viking are comparable.

The selected Viking-EETA 79001 data base for the Martian atmosphere is given in Tables II and III. Absolute abundances are shown in Fig. 2, the noble gas elemental composition normalized to solar ratios in Fig. 6, and noble gas isotopic compositions in Figs. 3, 7, and 8. The $^{20}\text{Ne}/^{22}\text{Ne}$ ratio of 10.1 ± 0.7 in Table III is not particularly well established. It is a compromise between different results in two laboratories: 10.6 ± 0.6 from Swindle *et al.* (1986) and 9.6 ± 0.6 from Wiens *et al.* (1986). Pending resolution of the interlaboratory discrepancy, the average of the two measurements, with an appropriate uncertainty attached, will have to serve.

The $^{36}\text{Ar}/^{38}\text{Ar}$ ratio of 4.1 ± 0.2 from EETA 79001 (Table III) is seen in Fig. 3 to be uniquely low among all known nonspallogenic Ar compositions in solar system reservoirs. It is important to note in this regard that the Mars atmosphere ratio of $5.3 \pm 10\%$ —nominally close to the terrestrial value—reported by Owen *et al.* (1977) is erroneous; Viking measurements indicate only a possible range from about 4 to 7 (Owen 1986).

The Kr composition, from concordant 79001 measurements in two laboratories, is clearly isotopically light relative to the terrestrial and meteoritic compositions with which it is compared in Fig. 7, despite a large uncertainty at ^{78}Kr and significant interference from neutron capture in ^{79}Br at ^{80}Kr . In fact, Martian Kr appears to be compositionally similar to the rough lower bound on solar Kr (cf. Figs. 5 and 7). The Xe composition, plotted relative to CI Xe in Fig. 8, is reasonably well determined except at

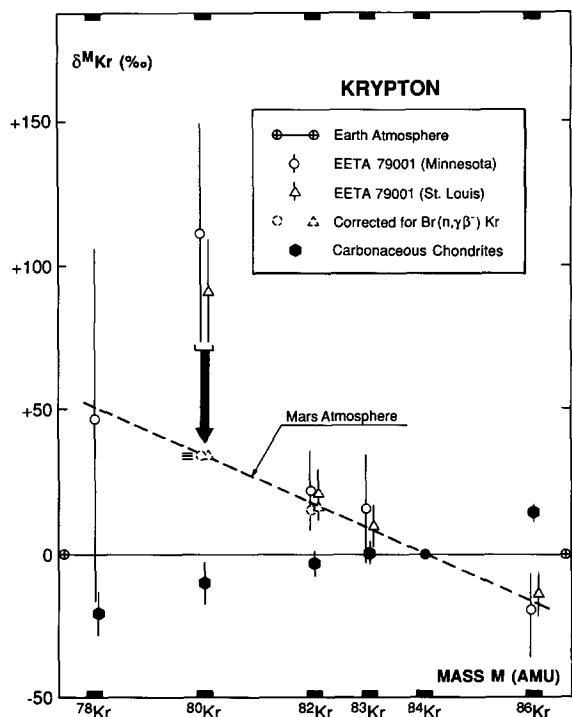


FIG. 7. The isotopic composition of krypton in the SNC meteorite EETA 79001, assumed to represent the Martian atmosphere, plotted relative to terrestrial isotope ratios and compared to the CI spectrum. Minnesota analysis from Becker and Pepin (1984a), St. Louis analysis from Swindle *et al.* (1986), other data from Table III. The measured compositions at ^{80}Kr have been corrected (downward arrow) for a presumed contribution from cosmic-ray-neutron capture in $^{79,81}\text{Br}$, by assuming that without this component the $^{80}\text{Kr}/^{84}\text{Kr}$ ratio would lie on the regression line defined by the remaining isotopes. The much smaller correction required for ^{82}Kr is also shown.

the lightest isotopes. The strong implication of a mass fractionation relationship between CI and Martian Xe in Fig. 8 and the solar-like pattern displayed by Kr in Fig. 7 are particularly important clues to the origin and evolution of these two species on Mars (Section V.B.3).

V. APPLICATIONS

In the first parts of this section the analytic expressions for hydrodynamic escape and fractionation developed in Section III.B are utilized, together with the elemental and isotopic abundance data in Section IV, to model numerically the planetary noble gas histories outlined in Section II.B. This baseline model is then extended to include one possible scenario for the origin of carbon and nitrogen in atmospheric and crustal reservoirs. A final section addresses the issue of noble gas mass distributions in meteoritic carrier phases.

V.A. Construction of the Model

V.A.1. Components

The baseline model requires two—and only two—primordial noble gas components on each of the three planets, one residing in a primary atmosphere and the other in the planet’s interior. On Earth and Venus, both the atmospheric (A) and interior (I) reservoirs are assumed to contain isotopically solar noble gases. The atmospheric component on Mars is dominated by gases with CI isotopic compositions; the interior component is again taken to be isotopically solar. Relative *elemental* abundances in the solar-composition atmospheric and interior reservoirs are not initially specified to be solar; instead they are treated as free variables in the model, and assume whatever values are needed to exactly replicate present-day planetary abundances. The atmospheric component on Mars, however, is taken to be both isotopically *and* elementally similar to CI noble gases, and therefore characterized by the CI relative abundance pattern given in Table II.

V.A.2. Notation

The notations A_S and A_{CI} respectively designate isotopically solar and CI-like primary atmospheric components.

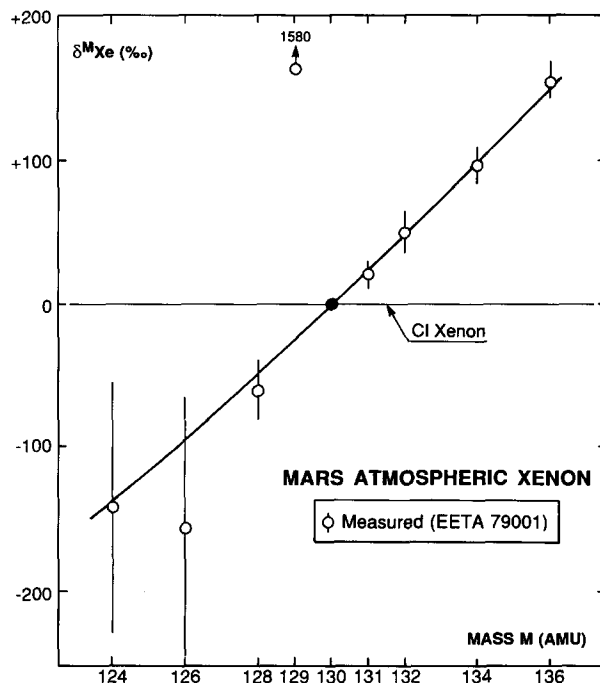


FIG. 8. Xenon isotopic composition measured by Swindle *et al.* (1986) in the SNC meteorite EETA 79001 and assumed to represent the Martian atmosphere, plotted relative to the CI-Xe isotope ratios in Table III. The plotted curve represents the compositional match generated by the Mars I and II models (Table IV).

Gases from interior (I) reservoirs, all of solar isotopic composition, are transported to atmospheres by planetary outgassing and are termed OG_I components. The initial concentration of any isotope M in an atmosphere, *prior* to its depletion by hydrodynamic escape, is denoted by $C_M^i(A_S)$ or $C_M^i(A_{Cl})$ (in g/g-planet) for gases originally residing in the primary atmosphere, and by $C_M^i(OG_I)$ (in g/g-planet) for species contributed by outgassing. The initial *ratio* of a second isotope M' to isotope M in either of these reservoirs, given by $C_{M'}/C_M^i$, is written as $C_{M'/M}^i$.

The decline in abundance of an isotope M of mass m_2 from its initial concentration C_M^i during atmospheric escape is described by Eq. (12) or Eqs. (16) and (17) in Section III.B.4, with C_M/C_M^i replacing N_2/N_2^0 . We represent this hydrodynamic escape fractionation (HEF) of M by the fractionation factor \mathbf{f}_M , where $\mathbf{f}_M = N_2/N_2^0 \equiv C_M/C_M^i$ and is written as $\mathbf{f}_M(A)$ or $\mathbf{f}_M(OG)$ for loss of atmospheric or outgassed species, respectively. Fractionation of an isotopic ratio M'/M is given by $(C_{M'}/C_M)/(C_{M'}/C_M^i)$, which may be written as $(C_{M'}/C_{M'}^i)/(C_M/C_M^i)$. This is just $\mathbf{f}_{M'}/\mathbf{f}_M$, or $\mathbf{f}_{M'/M}(A)$ and $\mathbf{f}_{M'/M}(OG)$ in shorthand notation.

V.A.3. Formalism

A simple formalism is used to apply the baseline noble gas model through two stages of atmospheric evolution characterized by a declining solar EUV flux and therefore by decreasing crossover masses for hydrodynamic escape (Eq. (10)). Stage 1 involves loss and fractionation of only the primary atmosphere. It begins at initial time t_0 when the crossover mass m_c for a particular species is m_c^0 , and ends at some later time t_{fA} when the crossover mass has declined to a value $m_c = m_c^{fA}$. Stage 2, beginning when the planet outgasses at time $t_{og} \geq t_{fA}$ and a corresponding crossover mass m_c^{og} , and terminating at a final time t_f and crossover mass m_c^f , includes both escape of the freshly degassed interior component and continuing loss of the remnants of the primary atmospheric component still remaining in the atmosphere at t_{og} .

We designate the final residual concentrations of noble gases surviving at t_f by $C_M^f(X)$, and isotopic ratios by $C_{M'/M}^f(X)$, with X denoting their A_S , A_{Cl} , or OG_I sources. Then from the definitions above, with $\mathbf{f}_M(A)$ and $\mathbf{f}_M(OG)$ representing HEF from t_0 to t_{fA} and from t_{og} to t_f respectively, the formal expressions for $C_M^f(X)$ (in g/g-planet) are

$$C_M^f(A_S) = \mathbf{f}_M(OG)[\mathbf{f}_M(A)[C_M^i(A_S)]] \quad (20)$$

or

$$C_M^f(A_{Cl}) = \mathbf{f}_M(OG)[\mathbf{f}_M(A)[C_M^i(A_{Cl})]] \quad (21)$$

and

$$C_M^f(OG_I) = \mathbf{f}_M(OG)[C_M^i(OG_I)]. \quad (22)$$

The sum of $C_M^f(X)$ from all contributing sources constitutes the present-day planetary abundances of species M . Similarly, isotopic ratios $C_{M'/M}^f(X)$ at t_f are given by

$$C_{M'/M}^f(A_S) = \mathbf{f}_{M'/M}(OG)[\mathbf{f}_{M'/M}(A)[C_{M'/M}^i(A_S)]] \quad (23)$$

or

$$C_{M'/M}^f(A_{Cl}) = \mathbf{f}_{M'/M}(OG)[\mathbf{f}_{M'/M}(A)[C_{M'/M}^i(A_{Cl})]] \quad (24)$$

and

$$C_{M'/M}^f(OG_I) = \mathbf{f}_{M'/M}(OG)[C_{M'/M}^i(OG_I)]. \quad (25)$$

and present-day isotopic compositions are the abundance-weighted sums of these individual contributions. The hydrodynamic escape fractionation factors \mathbf{f}_M and $\mathbf{f}_{M'/M}$ in Eqs. (20)–(25) may be thought of mathematically as operators on C_M^i and $C_{M'/M}^i$ that generate final atmospheric abundances C_M^f and isotope ratios $C_{M'/M}^f$ from each contributing source.

The objectives of the following numerical calculations are to determine values for the various free parameters in the model (discussed in the next section) that lead to best agreement between calculated and observed—or inferred—noble gas inventories on each terrestrial planet, and to assess the plausibility of these values. Calculations were set up as follows. The central equations for elemental and isotopic evolution are Eqs. (20)–(25) above, together with Eq. (12) (constant inventory models) or Eqs. (16) and (17) (Rayleigh fractionation models) for the fractionation factors \mathbf{f}_M and $\mathbf{f}_{M'}$. Including carbon and nitrogen as well as Xe, Kr, Ar, and Ne, there are six concentrations C_M^f and 18 isotope ratios $C_{M'/M}^f$ of interest, and thus six separate versions of Eq. (20) (or (21)) and Eq. (22), and 18 separate versions of Eq. (23) (or (24)) and Eq. (25). These 48 individual equations were written out in spreadsheet format, with the 24 equations pertaining to the first evolutionary stage (fractionation of the primary atmosphere) and the 24 pertaining to the second (fractionation of both outgassed species and primary atmosphere gases still remaining at t_{og}) interlinked in the following two ways. First, concentrations C_M and isotope ratios $C_{M'/M}$ in the remnant primary atmosphere at t_{fA} were redefined as initial values for input into the second stage equations at t_{og} . Second, the sums of final noble gas concentrations $C_M^f(A_S)$ or $C_M^f(A_{Cl})$ deriving from stage 1 and $C_M^f(OG_I)$ from stage 2 were constrained to equal the present-day planetary abundances of ^{130}Xe , ^{84}Kr , ^{36}Ar , and ^{20}Ne listed in Table II.

V.A.4. Variables and Procedure

Equation (12) (or (16, 17)) for \mathbf{f}_M and $\mathbf{f}_{M'/M}$ contains the parameters m_1 , m_2 , m_c , and α (or α_0), and Eqs. (20)–(25) the additional initial abundances and isotope ratios $C_M^i(A_S)$ or $C_M^i(A_{CI})$, $C_M^i(OG_I)$, $C_{M'/M}^i(A_S)$ or $C_{M'/M}^i(A_{CI})$, and $C_{M'/M}^i(OG_I)$. Of these parameters in the operational equations for elemental and isotopic evolution, m_2 represents the mass of the isotope M under consideration and has a defined value. The choice of molecular hydrogen as the light constituent sets $m_1 = 2$ amu. Initial noble gas isotope ratios $C_{M'/M}^i$ are taken to be either solar, for the A_S and OG_I components, or CI composition for the A_{CI} component.

Values for initial elemental abundances C_M^i are constrained in various ways by the requirement that the sum of final abundances C_M^f from all contributing sources must equal observed planetary inventories. The elemental concentrations $C_M^i(OG_I)$ of the outgassed component are completely fixed by this stipulation for Ne, Ar, and Kr (by assumption, no Xe is degassed), and so they are products of the model rather than input parameters. Since without degassed Xe the A_S or A_{CI} component is the only contributor to planetary Xe, the value of $C_{130}^i(A_S)$ or $C_{130}^i(A_{CI})$ is similarly fixed, and therefore so are the remaining values of $C_M^i(A_{CI})$ —for Kr, Ar, and Ne—by the assumption of CI elemental composition for A_{CI} noble gases. However, we will *not* assume that the elemental composition of the A_S component in the primary atmosphere is necessarily solar, and so here the ratios of Kr, Ar, and Ne abundances to that of Xe are taken to be free variables.

The remaining parameters are also free variables: crossover masses m_c , which appear in various equations as m_c^0 , m_c^{fA} , m_c^{og} , or m_c^f as defined in Section 3 above; and α (or α_0) for both stage 1 ($\alpha(A)$) and stage 2 ($\alpha(OG)$). It is important to note that any particular m_c may be freely chosen for just one of the noble gases. Once this selection is made, say for Xe, values for the remaining gases are specified by Eq. (10) and their differing diffusion parameters b (Table I). The dimensionless parameters $\alpha(A) \equiv F_1^0\tau/N_1$ (or $\alpha_0(A) \equiv F_1^0\tau/N_1^0$) and $\alpha(OG) \equiv F_1^{og}\tau/N_1$ (or $\alpha_0(OG) \equiv F_1^{og}\tau/N_1^{og}$) involve the mean decay time τ of the solar EUV flux, which for illustration is taken to be 90 myr (Section III.B.3). A selected value for a crossover mass m_c stipulates a corresponding value for the hydrogen escape flux F_1 via Eq. (9). Thus the only independently free variable in α is the atmospheric molecular hydrogen inventory N_1 , and the effect of a choice for α or α_0 in either evolutionary stage is to fix the inventory for that stage, either at a constant value N_1 throughout the stage for constant inventory models, or at its beginning— N_1^0 at t_0 or N_1^{og} at t_{og} —for Rayleigh models.

Of these two possibilities—constant inventory or Ray-

leigh distillation—for the temporal behavior of atmospheric hydrogen during the course of an evolutionary stage, the Rayleigh model seems more straightforward on geochemical grounds. Conditions for maintaining exactly constant hydrogen inventories over long periods of time would be difficult to realize in a natural planetary environment. In principle, chemical buffering at the surface (e.g., $H_2 + FeO \rightleftharpoons H_2O + Fe$) could have resulted in uniform atmospheric H_2 column densities if timescales for hydrogen escape were longer than those for equilibration of the buffering reaction, if temperatures were constant and water were degassed from the interior at just the rate needed to maintain a constant H_2O pressure as H_2 was lost to space, and if metallic Fe were continuously available. In fact, it seems much more likely that constant inventory models represent highly idealized approximations of more realistic situations where hydrogen pressures varied both up and down in the short term with fluctuations in buffering conditions, but on average were roughly constant over the escape episode. Simple Rayleigh escape of an initial hydrogen inventory, without replenishment, is less demanding in that it does not require the surface buffering needed to maintain constant H_2 column densities (although it does require rapid chemical reduction of H_2O to H_2 if water was the principal hydrogen source). For this reason Rayleigh distillation, described by Eqs. (16) and (17), is the preferred choice. It is used throughout this paper in all but one case: stage I evolution of the primary atmosphere on Earth (Section V.B.1 below), where the constant inventory model yields a much more acceptable fit to the isotopic composition of nonradiogenic terrestrial Xe in Table III.

In summary, in applying the model specified above to a particular planet, one may choose either constant inventory or Rayleigh fractionation, and arbitrary values for the following free parameters: (1) the relative elemental composition of the A_S component in the primary atmosphere; (2) $\alpha(A)$, and the beginning and ending crossover masses m_c^0 and m_c^{fA} , for stage 1; and (3) $\alpha(OG)$, and the beginning and ending crossover masses m_c^{og} and m_c^f , for stage 2. Values for all these free variables are determined by the criterion of best calculated matches to the isotopic compositions of the noble gases currently present in planetary atmospheres. The utility of arranging and interlinking the separate evolutionary equations for each isotope in a spreadsheet format is that the effects of change in any single variable on final calculated compositions are readily and rapidly apparent. This allows efficient feedback to final variable selection in what is essentially a trial-and-error fitting process. Condensed versions of the spreadsheet outputs for the planetary models discussed below, together with values for all of the fixed and free parameters, are given in Tables AI–AVI.

The plausibility of the particular parameter choices that

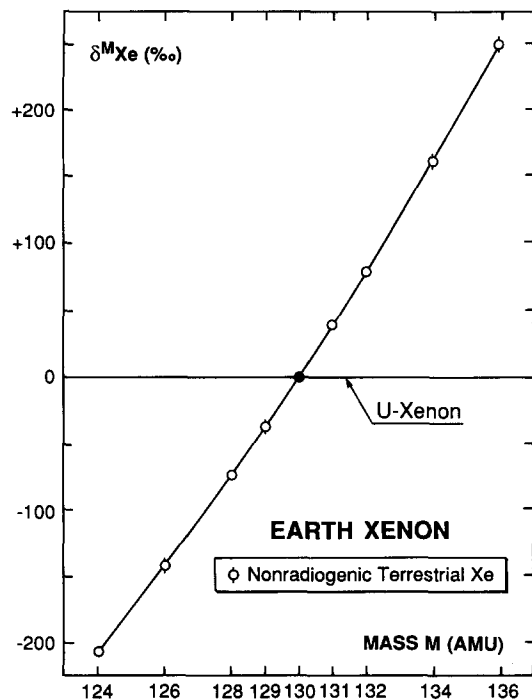


FIG. 9. The isotopic composition of nonradiogenic terrestrial xenon, plotted relative to U–Xe isotope ratios. Data from Table III. The essentially exact match to the terrestrial composition indicated by the plotted curve is yielded by the pure U–Xe progenitor assumed in the Earth I model; Earth II model results fall within the indicated error bars (Table IV).

lead to acceptable fits to the mass distributions of noble gases in planetary atmospheres must ultimately be assessed on other grounds. Among these are the implications of parameter values for the masses and possible sources of hydrogen in primary atmospheres, the present oxidation states of the planets if most or all of the required hydrogen was supplied as water and later reduced to H₂, and absolute timescales for planetary differentiation and outgassing. These issues are considered later in Section VI.

V.B. Planetary Model I: Noble Gases on Earth, Venus, and Mars

The following three sections outline how this baseline Model I is applied to noble gas distributions on the terrestrial planets. Results are briefly noted, and are discussed in detail in Section V.B.4.

V.B.1. Earth

Stage 1. With the constant inventory model, an exact match to the terrestrial isotopic spectrum for nonradiogenic Xe, given by the solid curve in Fig. 9, is uniquely

obtained for $m_c^0(\text{Xe}) = 343$ amu, any $m_c^{fA}(\text{Xe}) < 124$ amu, and $\alpha(A) = 13.133$. As noted above, Rayleigh escape of the primary atmosphere is *not* an acceptable choice here because the derived Rayleigh fractionation factors $f_{M/130}(A)$ cannot fractionate the solar Xe (U–Xe) isotopic composition into the nonradiogenic terrestrial distribution given in Table III. The resulting composition is isotopically too heavy for any choice of (m_c^0, α) parameters. (However it is important to note that this exclusion depends sensitively on the accuracy of Pepin and Phinney’s (1978) nonradiogenic Xe composition.)

It is not surprising that HEF is able to generate the precise fit shown in Fig. 9. In deducing the U–Xe composition, Pepin and Phinney (1978) *assumed* that U–Xe and nonradiogenic terrestrial Xe were related by a fractionating process. They were ignorant of what the process might have been and the environment in which it could have operated, and so for illustration utilized both diffusion and Jeans escape—which gave nearly identical results—in their derivation. To first approximation, most fractionating mechanisms, including HEF, yield about the same fractionation factors when applied to fit across a limited (i.e., isotopic) mass range. Therefore the significance of the present result is not that the match in Fig. 9 is so good, but that it can be generated by a straightforward physical process operating in a realistic astrophysical environment.

Stage 2. Since the Xe fit in Fig. 9 was obtained for $m_c^{fA}(\text{Xe}) < 124$ amu, the mass of the lightest Xe isotope, the Xe inventory is now frozen and can no longer be influenced by escape. However it *can* be modified by mixing with subsequently degassed solar-composition Xe, which is why Xe from the interior reservoir is required to remain in the planet. The extent to which this restriction can be relaxed is considered later in Section VII.A.

We now ask whether stage 2 fractionation of outgassed species and residual gases from the primary atmosphere can replicate the terrestrial compositions of Kr, Ar, and Ne. Because the composition of solar Kr is not well known (Fig. 5), a further question involves the ability of the model to accommodate a range of possible initial Kr compositions. Available free parameters for stage 2 evolution are the Kr/Xe, Ar/Xe, and Ne/Xe elemental ratios in the initial A_S component, and $\alpha_0(\text{OG})$, m_c^{og} and m_c^f .

For a given solar Kr composition, it turns out that the model is capable of delivering fits to observed compositions for all three gases with just one set of values for the six variables. Adopted parameter values and partial results are set out in Table AI. Moreover, a spread of Kr compositions, from the lower boundary to approximately the middle of the shaded area in Fig. 5 (respectively Solar Kr-1 and Solar Kr-2 in Table III), can be accommodated by relatively small changes in the six-variable set with no

deterioration in the precision of the fits. Equally good matches can also be generated using the isotopically lighter compositions occupying the upper part of the uncertainty field in Fig. 5, but they require Kr/Xe ratios in A_S that appear unlikely in that they exceed the solar ratio (see Section V.B.4 below for discussion of the full elemental composition of the A_S component).

This stage 2 model for Earth is the Rayleigh model described by Eqs. (16) and (17), chosen for reasons given above. However, the alternative choice of constant inventory yields very similar results. It is interesting that the hydrogen inventory $N_1^{H_2}$ at the beginning of stage 2, derived from the selected value of $\alpha_0(OG)$, exceeds the constant inventory N_1 calculated from $\alpha(A)$ in stage 1 (Section VI.C.1, Fig. 19). This implies degassing of additional H_2 at t_{og} , accompanying and perhaps carrying the outgassed noble gases. The transition from a constant inventory stage 1 to Rayleigh loss in stage 2 further suggests that planetary conditions supporting a roughly constant atmospheric hydrogen pressure during dissipation of most of the primary atmosphere could have been disrupted by the outgassing process itself.

V.B.2. Venus

It is not obvious, from comparison of the volatile mass distributions on Earth and Venus given in Tables II and III, that these two atmospheres are end products of similar evolutionary processes acting on similar primordial volatile sources. Absolute abundances on Venus exceed those on Earth by a factor >70 for ^{36}Ar , but only by factors of $\sim 3-6$ for Kr and Xe. Consequently, as noted earlier, there is a pronounced solar-like signature in the relative Ar:Kr:Xe abundances shown in Fig. 6. This similarity does *not* extend to Ne: the $^{20}Ne/^{36}Ar$ ratio is low, coincidentally (Section I; Pepin 1989a) close to the terrestrial value. Venusian $^{20}Ne/^{22}Ne$, however, is significantly higher—i.e., more solar-like—than on Earth. The nominal value of the rather uncertain $^{36}Ar/^{38}Ar$ ratio from Pioneer Venus is also higher.

Volatile compositions on Venus are not known precisely enough, if at all, to allow application of the model to Venus in the same way it is developed for Earth. Isotopic constraints on parameter definition are much more poorly defined and for the heavy noble gases are missing entirely (Section IV.C.1). In this situation we cannot follow the procedure used for stage 1 on Earth of determining ab initio the m_c^0 , m_c^{fA} , and $\alpha(A)$ parameter set from fits to xenon isotopic data. However, certain key results from the Earth model should apply approximately to Venus as well, and this input together with the information we do have allows construction of at least a preliminary model for volatile evolution. One such result is that evolution of the terrestrial atmosphere took place in stages spanning

tens to hundreds of million years (Section VI.B, Table VI). On these long timescales it seems reasonable to suppose that clearing of the nebula, and initiation at t_0 of atmospheric loss by EUV-driven hydrodynamic escape, occurred essentially simultaneously on all the terrestrial planets. If identical planetary values of t_0 are assumed, then from Eq. (10), taking the product of the efficiency ε of EUV energy deposition and the ratio β of escape level to planetary radius to be the same for both planets, the Venus/Earth ratio of $m_c^0 - m_1$ is just $(B/b)_{Venus}/(B/b)_{Earth}$. From Table I data, and with $m_c^0(Xe)$ on Earth = 343 amu from Section 1 above, $m_c^0(Xe)$ for Venus is 879 amu.

Stage 1. The largely solar-like elemental and isotopic abundance patterns on Venus are considered here to be important clues to the origin of atmospheric noble gases. Such signatures strongly suggest, in the context of the present model, that these are residual gases left on the planet after partial hydrodynamic escape of a primary atmosphere initially characterized by solar isotopic compositions, and solar or near-solar Ar:Kr:Xe elemental ratios. The specific hypothesis that essentially *all* of the inventories of nonradiogenic noble gases now on Venus originated in this way provides the basis for the present model. Rayleigh loss of the primary atmosphere is assumed—in contrast to stage 1 on Earth, this mode of H_2 escape is not incompatible with anything we currently know about noble gas compositions on Venus.

In the absence of xenon isotopic data, values for the six-parameter set describing atmospheric loss and fractionation were determined by fitting to the rather uncertain data we do have on hand. The specific criterion, simultaneous match to the measured $^{36}Ar/^{38}Ar$ and $^{20}Ne/^{22}Ne$ isotopic ratios, is met well within their errors (Table AIII). As anticipated, the elemental abundance pattern required for the A_S component is indistinguishable from solar for Ar:Kr:Xe, but is much depleted in Ne (see Section V.B.4 below). Of the remaining variables, m_c^0 is fixed by the Earth value as discussed above, $\alpha_0(A) = 1.018$, and terminal crossover masses m_c^{fA} for Xe, Kr, Ar, and Ne are each below the masses of their lightest isotopes. All noble gas inventories (except He) are thus frozen, and escape of the still rather large hydrogen inventory remaining at t_{fA} (Section VI.C.1) could continue indefinitely, to exhaustion, without affecting them.

Stage 2. There is no discernible evidence that outgassing played a major role in establishing present-day noble gas inventories. Stage 1 loss of the primary atmosphere, governed by the parameters above, generates *by itself* approximate matches to observed compositions. Thus, in contrast to the case for Earth, the presence of an outgassed component on Venus is not required. This is not to say that the planet could not have degassed at some time during or after this stage of atmospheric evolution.

But even if it did, say in comparable amounts per gram-planet as on Earth ($C_M^i(\text{OG}_i)$ in Table AI), outgassed species would comprise at most <35%, <3%, and <15% of the present atmospheric Kr, Ar, and Ne inventories, respectively, and proportionally less if outgassing occurred during stage 1 when all of these species were more abundant on Venus than they now are. Contributions of this order to gases derived from the primary atmosphere cannot be isolated in the model, given present uncertainties in the Venus data base.

V.B.3. Mars

Relative to Earth, atmospheric abundances of noble gases on Mars are depleted by even larger factors than Venus is enriched. The SNC meteorites (Section IV.C.3) provide relatively precise data on the compositions of "contemporary" noble gases. Their isotopic patterns are puzzling in that they seem to display contradictory signatures of origin. Xenon superficially resembles terrestrial Xe, and the krypton composition appears close to solar (cf. Figs. 5 and 7). At the same time the uniquely low $^{36}\text{Ar}/^{38}\text{Ar}$ ratio is as far from solar as one sees in any nonspallogenic Solar System reservoir, and $^{20}\text{Ne}/^{22}\text{Ne}$ is Earth-like (Fig. 3).

The crucial diagnostic clue to the origin of Martian Xe comes from Swindle *et al.*'s (1986) experimental study of noble gases in the SNC meteorites. They pointed out that the isotopic composition of Xe trapped in the glassy phases of EETA 79001 is just that of mass-fractionated carbonaceous chondrite xenon, for every isotope but radiogenic ^{129}Xe —a relationship that had been missed entirely in Becker and Pepin's (1984a) earlier analysis. The basis for Swindle *et al.*'s interpretation was the smooth fractionation pattern displayed in Fig. 8, where their data are plotted relative to CI chondrite Xe. This observation strongly implies that the primary atmosphere on Mars was dominated by CI-Xe, and that view is adopted here by taking the initial A component to be A_{CI} (Eqs. (21) and (24)), characterized by the elemental and isotopic compositions of carbonaceous chondrite noble gases.

Stage 1. The xenon isotopic data in Table III and Fig. 8 are not precise enough to define a meaningful initial crossover mass $m_c^0(\text{Xe})$ for Mars by isotopic fitting, and so it is taken to be that calculated from the corresponding value for Earth using Eq. (10) (an assumption, also made earlier for Venus, that presumes a more-or-less simultaneous decline in midplane EUV opacity at t_0 throughout terrestrial planet space). Then for $m_c^0(\text{Xe}) = 343$ amu on Earth, $m_c^0(\text{Xe})$ on Mars is 1734 amu, and after choosing a Rayleigh loss model, only m_c^{fA} , the crossover mass at the end of stage 1, and $\alpha_0(\text{A})$ remain as free variables for stage 1 evolution.

Despite this restriction, it turns out that the values of

these two parameters that generate fits to the present-day composition of atmospheric Xe on Mars are not uniquely defined. The number of [$\alpha_0(\text{A}), m_c^{\text{fA}}(\text{Xe})$] variable combinations which can replicate the composition is unbounded, with each pair of values corresponding to a different initial Xe concentration $C_{130}^i(A_{\text{CI}})$. To illustrate this model for Mars, however, we can use an estimate from an independent source for what $C_{130}^i(A_{\text{CI}})$ might have been. Dreibus and Wänke's (1985, 1987, 1989) geochemical model of Mars' bulk composition calls for an ~40% mass fraction of volatile-rich, oxidized (CI-like) material in the planet. If we assume for the moment that this component contained CI noble gases at abundance levels found in extant meteorites of this type, and further assume complete impact-degassing of this material during accretion, and retention of the degassed noble gases in a coaccreting primary atmosphere prior to t_0 , then $C_{130}^i(A_{\text{CI}})$ would have been ~40% of the CI Xe abundance in Table III, or $\sim 2.8 \times 10^{-12}$ g/g-Mars. This value, together with $\alpha_0(\text{A}) = 1.384$, $m_c^0(\text{Xe}) = 1734$ amu as calculated above, and $m_c^{\text{fA}}(\text{Xe}) = 483$ amu (Table AIV), generates the isotopic fit shown by the solid curve in Fig. 8. Note that the fractionation factor $f_{130}(\text{A})$ in Table AIV is very small, reflecting the fact that a severe depletion of this large an initial Xe abundance by hydrodynamic escape is required to match the presently low Martian inventory. Note also that $m_c^{\text{fA}}(\text{Xe})$ is >136 amu, so stage 1 atmospheric loss in this Rayleigh model must be throttled, by H_2 exhaustion or increase in atmospheric molecular weight (Section VI.C.1), while the crossover is still above the Xe mass region; escape evolution then ceases until t_{og} , when outgassed hydrogen fuels a second episode of Rayleigh loss. Values of $m_c^{\text{fA}}(\text{Xe})$ below Xe (<124 amu) result in underfractionation of the Xe isotopes. The physical reason, from examination of Eq. (3), is that as N_1 becomes small near the end of the escape episode, the mixing ratios of minor constituents and thus their rate of evolution increases. If Xe is still escaping when N_1 is low—i.e., if m_c exceeds 136 amu—it is sufficiently fractionated, otherwise not. (It is interesting that this restriction does not apply in constant inventory models that generate similar isotopic matches.)

Stage 2. As on Earth, outgassing of an isotopically solar OG_1 component is needed to account for present-day Kr, Ar, and Ne inventories. An interesting difference is that atmospheric Kr (Fig. 7) is isotopically indistinguishable, within error, from the lower bound on solar Kr composition in Fig. 5 (Kr-1 in Table III). A choice of Kr-1 for solar Kr therefore implies that degassed Kr was *not* subsequently fractionated by hydrodynamic escape, which in turn indicates that outgassing occurred after the crossover mass had declined below the mass region spanned by the Kr isotopes. This restricts $m_c^{\text{og}}(\text{Kr})$ to <78 amu. (The

situation when the isotopically lighter Kr-2 composition is selected to represent solar Kr is considered later, in Section V.C.3). An additional difference from stage 2 on Earth and Venus, and a further restriction on degrees of freedom in matching observed Ar and Ne compositions, is that the elemental ratios Kr/Xe, Ar/Xe, and Ne/Xe in the primary atmosphere A_{CI} component are known, and so all of the remaining $C_M^i(A_{CI})$ abundances are fixed by the choice of $C_{130}^i(A_{CI})$ in stage 1 and are not free variables.

A stage 2 Rayleigh model for Mars, with these $C_M^i(A_{CI})$ values and $\alpha_0(OG) = 3.530$, $m_c^{og}(Ar) = 55$ amu, and $m_c^f(Ar) = 40$ amu, yields an exact match to Ar composition (Table AIV). Here again the three free parameter values are not unique; identical results are obtained over a range of m_c^{og} crossover masses falling between Kr and Ar, with correspondingly different α_0 and m_c^f . However, all parameter choices capable of strongly fractionating degassed solar Ar to the uniquely low $^{36}Ar/^{38}Ar$ ratio of ~ 4.1 recorded in the SNC meteorites simultaneously overfractionate degassed Ne, to a final $^{20}Ne/^{22}Ne$ ratio significantly ($>2\sigma$) below the average SNC value.

One rather attractive possibility, discussed below in Section V.B.4, is that this Ne anomaly could signal the presence of a solar wind component added to the planet over the >4 -byr period following the end of hydrodynamic escape. The effects of such a component, in the context of the current model, may be explored by invoking a third, post- t_f stage of Martian atmospheric evolution during which unfractionated solar wind is added in the amount necessary to elevate the low $^{20}Ne/^{22}Ne$ ratio generated by HEF to its present value. In this case the initial elemental and isotopic abundances in the solar wind component, denoted by $C_M^i(SW)$ and $C_{M'/M}^i(SW)$ in Table AIV, are unaltered by HEF and thus are identical to the final inventories $C_M^f(SW)$ and $C_{M'/M}^f(SW)$. All elemental and isotopic compositions are assumed to be given by the solar data in Tables II and III. If we now require that the sum of all contributions to ^{20}Ne from the A_{CI} , OG_I , and SW components be equal to its present abundance on Mars, and further that the final planetary $^{20}Ne/^{22}Ne$ ratio be the SNC value of 10.1, an integrated stage 2–stage 3 model yields a mixing ratio of SW Ne in Martian Ne of ~ 0.44 (Table AIV). Solar wind contributions to all other species are too small to sensibly affect their final concentrations and compositions generated by HEF, a consequence of the very high abundance of Ne relative to heavier gases in the unfractionated wind.

V.B.4. Discussion of Model I Results

Planetary isotopic compositions generated by the baseline noble gas models (Earth I, Venus I, and Mars I) are given in part in the spreadsheet Tables AI, AIII, and AIV, and completely in Table IV. Results in the spreadsheet

tables assume the solar Kr-1 ratios in Table III; Table IV includes the final compositions yielded by solar Kr-2 as well, with slightly different choices for the free model variables. The specific isotope ratios in Table III for both these possible solar Kr compositions within the Fig. 5 uncertainty field were chosen on the criterion of exact replication of the terrestrial Kr composition by the Earth I models. Both yield agreement within error with Kr on Mars, except perhaps at ^{80}Kr —but here the “measured” value is poorly known because of the large neutron-capture correction at this isotope indicated in Fig. 7.

Neon and argon. Calculated isotope ratios are compared with present-day planetary compositions in Fig. 10. Observed Ne and Ar compositions are well reproduced by the basic Model I (open circles), except for $^{20}Ne/^{22}Ne$ on Mars where addition of the postescape solar wind component (“+SW”) postulated above is needed to raise the clearly low “HE” value generated by hydrodynamic escape to the average SNC ratio.

The two most obvious ways in which Mars could have collected such a component are by accretion of solar-wind-rich interplanetary dust particles (IDPs) or by direct

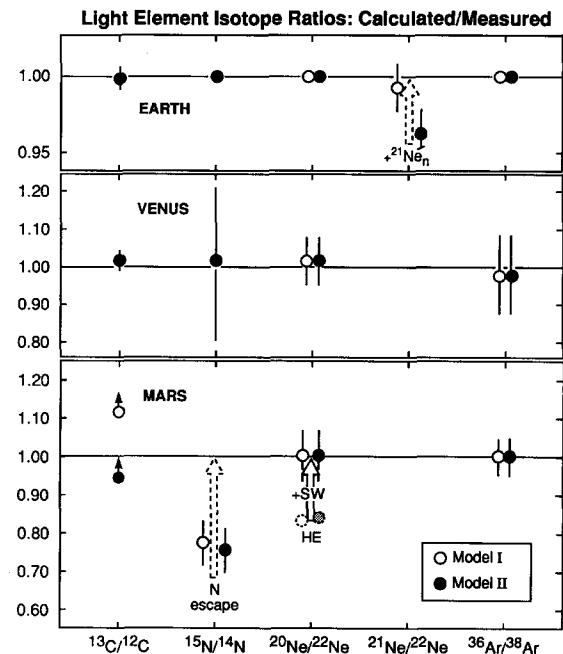


FIG. 10. Comparison of measured neon, argon, carbon, and nitrogen isotopic compositions on Earth, Venus, and Mars with those calculated from Models I and II. Filled and open symbols respectively designate results without (Model I) and with (Model II) late-stage accretion of a C–N-rich veneer. Solid symbols (dotted for $^{20}Ne/^{22}Ne$ on Mars) represent atmospheric compositions left on the planets at the end of hydrodynamic escape. Upward arrows indicate how some of these residual isotope ratios might later have evolved on Earth or Mars by postescape degassing of nuclear $^{21}Ne_n$ (Section V.B.4), nonthermal nitrogen escape (Section V.C.4), and capture of solar wind gases (Section V.B.4).

TABLE IV
Computed Model Isotopic Compositions in Planetary Atmospheres and Meteorites

Argon, neon, nitrogen, and carbon ^a								
Model	$\frac{^{36}\text{Ar}}{^{38}\text{Ar}}$	$\frac{^{20}\text{Ne}}{^{22}\text{Ne}}$	$\frac{^{21}\text{Ne}}{^{22}\text{Ne}}$ ($\times 10^{-2}$)	$\frac{^{15}\text{N}^{14}\text{N}}{^{14}\text{N}_2}$ ($\times 10^{-3}$)	$\delta^{15}\text{N}_{\text{AIR}}$ (‰)	$\frac{^{13}\text{C}^{16}\text{O}_2}{^{12}\text{C}^{16}\text{O}_2}$ ($\times 10^{-4}$)	$\delta^{13}\text{C}_{\text{PDB}}$ (‰)	
Venus I			3.06 ± 0.05	—	—	—	—	
Venus II	5.43	11.96	3.06 ± 0.05	7.40 ± 0.09	+6 ± 12	113.3 ± 0.9	+8.1 ± 8.0	
	5.43	11.94						
Earth I			2.878 ± 0.044	—	—	—	—	
Earth Ib ^b		9.800	2.782 ± 0.043	—	—	—	—	
Earth II	5.320	9.800	2.789 ± 0.043	7.353	≡0	111.43 ± 0.89	-8.4 ± 7.9	
	5.320	9.800						
Mars I			2.790–2.821	9.286–9.009	—	—	—	
Mars Ia ^c	4.10	10.10	2.792–2.802	9.218–8.969	—	—	—	
Mars II	4.10	10.10	2.790–2.821	8.992 ^d	+223	111.2 ^d	-10.3	
	4.10	10.10						
CI chondrites (Q–Ar, Q–Ne)	5.34–5.31	10.75	2.90 ± 0.04	—	—	—	—	
Krypton ^a								
Model	^{78}Kr	^{80}Kr	^{82}Kr	^{83}Kr	^{84}Kr	^{86}Kr		
Venus I	0.5896–0.5999	3.877–3.924	20.006–20.131	20.031–20.095	≡100	30.839–30.634		
Venus II	0.5924–0.6027	3.890–3.936	20.037–20.163	20.048–20.111	≡100	30.791–30.587		
Earth I	0.6087	3.960	20.217	20.136	≡100	30.524		
Earth Ib ^b	0.6088	3.959	20.212	20.133	≡100	30.542		
Earth II	0.6087	3.960	20.217	20.136	≡100	30.527		
Mars I,II	0.6328–0.6391	4.061–4.091	20.467–20.549	20.260–20.304	≡100	30.177–30.074		
Mars Ia ^c	0.6303–0.6397	4.050–4.092	20.438–20.550	20.245–20.302	≡100	30.221–30.053		
CI chondrites (Q–Kr)	0.5980–0.6007	3.915–3.928	20.104–20.143	20.081–20.101	≡100	30.684–30.610		
Nonradiogenic xenon ^a (Relative to $^{130}\text{Xe} \equiv 100$)								
Model	^{124}Xe	^{126}Xe	^{128}Xe	^{129}Xe	^{131}Xe	^{132}Xe	^{134}Xe	^{136}Xe
Venus I	2.819	2.468	50.14	624.2	503.2	613.5	219.0	173.5
Venus II	2.837	2.480	50.25	624.8 ^e	502.8	612.3	218.7	173.3
Earth I, Ib ^b	2.337	2.180	47.146	605.3	518.72	651.8	247.0	207.5
Earth II	2.334	2.184	47.168	605.4 ^e	518.76	651.3	247.2	207.7
Mars I,II	2.479	2.288	48.42	614.2 ^f	516.2	644.4	258.9	228.7
Mars Ia ^c	2.456	2.272	48.24	613.0 ^f	516.8	646.0	258.8	228.1
CI chondrites								
Q–Xe:	2.863–2.833	2.493–2.476	50.40–50.23	625.8–624.7 ^e	501.9–502.7	610.3–612.4	216.7–218.2	170.8–172.5
Q–Xe + H–Xe:	2.863–2.833	2.493–2.476	50.40–50.23	625.8–624.7 ^e	503.9–504.6	617.1–618.8	236.2–236.5	≡198.2

Note. Single entries denote identical values for both compositions unless otherwise noted.

^a If two values are listed, the first assumes initial Kr composition = solar Kr-1, and the second assumes initial Kr = solar Kr-2 (Table III).

^b Variant of the baseline Earth I model in which escape temperature is assumed to be 3000 K (Section VII.B).

^c Variant of the baseline Mars I model in which a Venus-like "solar" A_S component is included in the primary atmosphere (Section V.B.4).

^d Initial Kr composition = solar Kr-2.

^e Assuming nonradiogenic $(^{129}\text{Xe}/^{130}\text{Xe})_E = (^{129}\text{Xe}/^{130}\text{Xe})_U = 6.287$ (Table III).

^f Assuming nonradiogenic $(^{129}\text{Xe}/^{130}\text{Xe})_{\text{CI}} = (^{129}\text{Xe}/^{130}\text{Xe})_U = 6.287$ (Table III).

interception of the wind by the planet. Source strengths needed to supply the required amount of Ne over geologic time are not unreasonably large for either of these. "Chondritic" IDPs collected in the terrestrial stratosphere contain $\approx 4 \times 10^{-7}$ g/g of ^{20}Ne and display a solar-like light noble gas abundance pattern (Hudson *et al.* 1981). Accretion of only about 20 g/cm²-planet of IDP material this heavily loaded with solar Ne would supply the inferred Martian $C_{20}^i(\text{SW})$ inventory of $\approx 1.9 \times 10^{-14}$ g/g-planet (Table AIV), assuming efficient outgassing of dust to the atmosphere during infall or in subsequent surface cratering and weathering. This accumulation over 4 byr implies an average IDP mass flux of $\approx 10^4$ tons/yr to Mars, just about equal to estimates for the contemporary IDP flux to Earth (Brownlee 1985) and so a factor of a few larger than one would expect on the smaller Mars today. It seems reasonable to suppose that very early fluxes were higher.

Direct capture of the solar wind itself might also have contributed to the Martian Ne inventory. About 0.2 g/sec of ^{20}Ne is presently incident on the cross-sectional area of Mars, calculated from a mean proton flux of 3.9×10^8 cm⁻²sec⁻¹ at 1 AU (Feldman *et al.* 1977) and the Table II solar composition. The 4 byr fluence at the present flux is thus $\approx 6 \times 10^{16}$ g ^{20}Ne , and so the average capture efficiency that would have supplied *all* of $C_{20}^i(\text{SW})$ is only around 0.02%—possibly an upper limit since there is some lunar evidence, reviewed by Pepin (1980), for a more intense wind in the past. Direct wind interception by Earth and Venus over 4 byr with the same low capture efficiency (ignoring the further reduction by magnetospheric shielding on Earth) would contribute only negligibly to their much larger Ne inventories. A similar statement holds for the IDP source.

Turning to another result in Fig. 10, the approximate agreement of derived and measured $^{21}\text{Ne}/^{22}\text{Ne}$ on Earth is significant in that this ratio is a "free-floater" in the model—it was not explicitly considered in deriving parameter values for best fits to isotopic data. This concordance is interesting in another respect as well. Substantial amounts of ^{21}Ne have been produced in the Earth's crust and mantle over geologic time by nuclear effects, primarily $^{18}\text{O}(\alpha, n)^{21}\text{Ne}$ reactions induced by uranium- and thorium-derived α -particles (Wetherill 1954), with much of it generated early in terrestrial history because of the strong dependence of its production rate on the abundance of relatively short-lived ^{235}U (Kyser and Rison 1982). The $^{21}\text{Ne}/^{22}\text{Ne}$ ratio in Earth's atmosphere is sensitive to addition of this nuclear $^{21}\text{Ne}_n$ component by outgassing because of the low atmospheric abundance of this isotope. Rison (1980) has calculated that $\sim 3.6\%$ of the current terrestrial ^{21}Ne inventory derives from crustal degassing of $^{21}\text{Ne}_n$, or perhaps more—up to $\sim 12\%$ —if mantle outgassing was substantially involved (see also Heymann *et*

al. 1976, Ozima and Podosek 1983, pp. 130–131). But it would appear, *if* Model I is taken to be a valid description of the evolution of terrestrial Ne to its present composition, that the early atmospheric ^{21}Ne abundance established by HEF has not been significantly augmented by $^{21}\text{Ne}_n$ outgassing during postescape geologic history. Note, however, that both Model II (see Sections V.C.1,4) in Fig. 10 and variants of Model I in which some Xe is outgassed (Earth Ia, Section VII.A) or escape occurs at high temperature (Earth Ib, Section VII.B) *do* require such augmentations of ^{21}Ne , and by amounts very similar to Rison's (1980) estimate.

Krypton and xenon. Model I results are shown in Figs. 11 and 12. Both solar Kr-1 and Kr-2 are fractionated into contemporary terrestrial Kr, to which the other compositions in Fig. 11 are referenced. As noted in the preceding section, Mars Kr falls very close to the Kr-1 composition along the lower boundary of the solar field (and within error of Kr-2, which lies approximately along the dashed

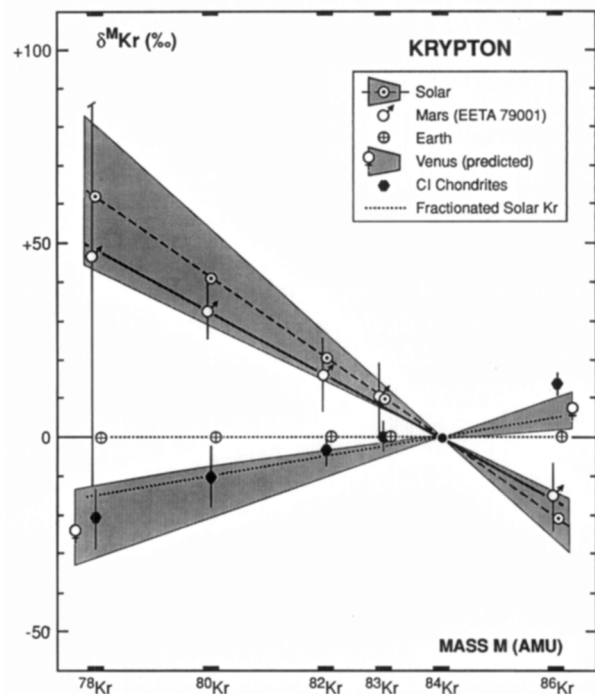


FIG. 11. Matches to measured Kr isotope ratios on Earth and in the CI chondrites (dotted lines) generated by solar Kr fractionation in planetary Model I and the CI carrier model (Section V.D.4). All δ -values calculated with respect to terrestrial ratios. The upper shaded region is the uncertainty field for solar Kr shown in Fig. 5; the solar Kr-1 composition lies along its lower boundary, and solar Kr-2 along the dashed line (Table III). The lower shaded region represents the predicted Model I compositional range for present-day Venus Kr, bounded below by fractionated solar Kr-1 and above by fractionated Kr-2. Calculated terrestrial and CI compositions (dotted lines) assume solar Kr-1, but are similar for Kr-2 and for Models I and II (Table IV). Martian Kr falls within the solar field and is considered to be unfractionated by hydrodynamic loss.

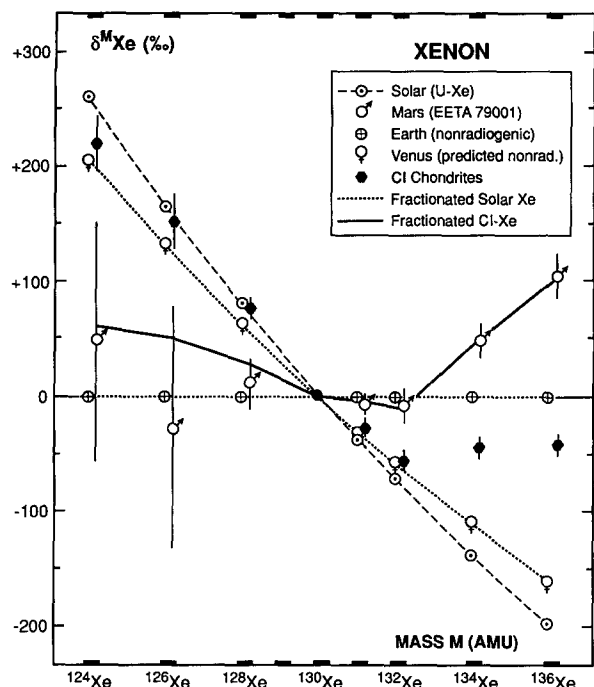


FIG. 12. Matches to nonradiogenic Xe isotope ratios on Earth (dotted line) and Mars (solid line) generated respectively by fractionation of solar Xe and CI-Xe in planetary Models I and II. There are no comparison data for Venus: the dotted curve represents the predicted nonradiogenic Xe composition. All δ -values calculated with respect to terrestrial ratios.

bisector of this field); thus no fractionation by escape is required. The lower shaded area, bounded below by Kr-1 and above by Kr-2 fractionations, contains the range of predicted compositions for Venus. They resemble CI-Kr. Estimates of Kr isotope mixing ratios from Pioneer Venus data (Donahue *et al.* 1981, von Zahn *et al.* 1983) are too imprecise for meaningful comparison.

Solar Xe (U-Xe) in Fig. 12 is fractionated into Pepin and Phinney's (1978) nonradiogenic terrestrial Xe, which here is taken to be the reference composition. The solid line shows the fit of fractionated CI-Xe to Mars Xe; it is equivalent, with a different normalization, to the solid curve fit in Fig. 8. In this representation the distinction between the Earth and Mars Xe compositions is evident: although within error of terrestrial isotope ratios at ^{124}Xe – ^{132}Xe , there are significant departures for Mars at ^{134}Xe , ^{136}Xe .

The predicted nonradiogenic Venus composition in Fig. 12, a mildly fractionated derivative of solar Xe, resembles Venus Kr in Fig. 11 in that it falls close to the plotted CI composition (absent the nucleogenetic heavy isotope contributions to CI-Xe discussed later in Section V.D.1). If both Earth and Venus accreted from compositionally similar materials, as tacitly assumed in the present model, contemporary heavy-isotope ratios could be elevated

above these calculated values by postescape outgassing of uranium or transuranium decay products from the planetary crust. However, they could well be enhanced to a lesser degree than on Earth (cf. contemporary and nonradiogenic terrestrial Xe compositions in Table III) because of dilution by the higher nonradiogenic Xe inventory on Venus.

There is no observational information on present-day Venusian Xe isotope distributions. Accurate measurement of the Venus pattern would provide a powerful discriminator between two contrasting models for the origin of planetary Xe—that presented here where Xe evolution is driven by a process operating on the planets themselves, and one originally suggested by Ozima and Nakazawa (1980) and recently redeveloped and extended by Zahnle *et al.* (1990b), in which nebular Xe is fractionated into the terrestrial composition by gravitational isotopic separation in porous planetesimals that are later accreted by the terrestrial planets. This source is supposed by Zahnle *et al.* (1990b) to supply isotopically identical, terrestrial-like Xe to Earth, Mars, and Venus. The fact that Earth and Mars are characterized by significantly *different* heavy isotope ratios, as shown in Fig. 12, casts considerable doubt on this hypothesis. However, an isotopic analysis of Xe on Venus, where the Xe compositions predicted by the two models are even more discrepant, should rule definitively between them—or create problems for both.

Relative elemental abundances in the primary atmosphere and outgassed components. Recall from Sections V.B.1 and 2 above that the Kr/Xe, Ar/Xe, and Ne/Xe elemental ratios in the initial A_5 component on Earth and Venus were taken to be free modeling variables. The choices for A_5 elemental compositions (Tables AI, AIII) which led to the best-fit isotopic results discussed above are plotted in Fig. 13a, normalized to the solar composition. In addition, the absolute concentrations of Kr, Ar, and Ne in the outgassed OG_1 components on Earth and Mars were fixed internally by the requirement that the model replicate observed planetary noble gas abundances. Solar-normalized elemental abundance ratios calculated from these derived OG_1 concentrations (Tables AI, AIV) are shown by the solid line and associated data points in Fig. 13b.

The required A_5 composition in Fig. 13a for the primary atmosphere on Venus is essentially solar within its (considerable) uncertainties, with the conspicuous exception of the ~ 100 -fold Ne depletion. Compared to the Venus pattern, the initial A_5 compositional range shown for Earth displays clear evidence of mass-dependent losses of light species, either just of Ar and Ne with the choice of Kr-2 to represent solar Kr (short-dashed lower boundary) or, with Kr-1, of all three lighter gases relative to Xe (long-dashed upper boundary). In both cases the plotted Ar/Kr and Ne/Kr ratios are approximate upper limits;

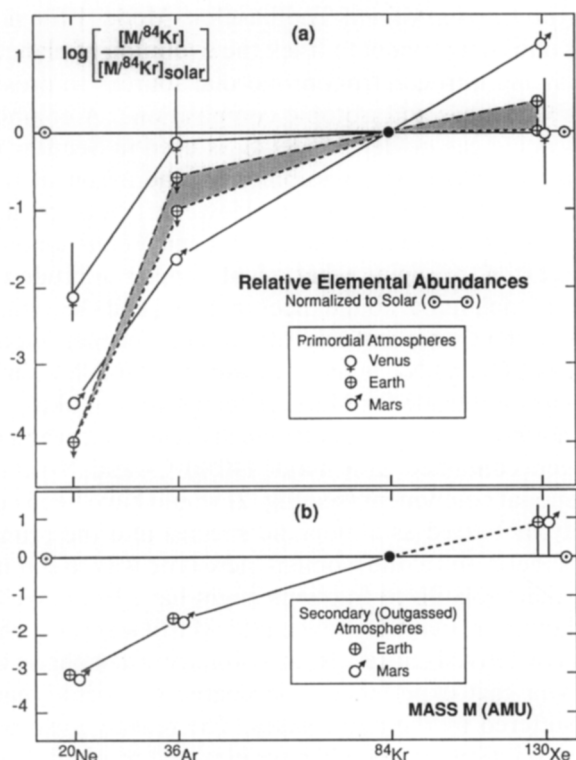


FIG. 13. Solar-normalized noble gas elemental compositions of (a) primary (primordial) atmospheres on Venus and Earth, and (b) secondary (outgassed) atmospheres on Earth and Mars, required in Models I and II to match present-day elemental and isotopic abundances. The CI composition adopted for Mars' primary atmosphere is also shown in (a). By assumption, Xe is not outgassed: the Xe/Kr enhancement of $\approx 8 \pm 7$ plotted in (b) and assumed to characterize the interior sources of degassed species on Earth and Mars is the average Kr/Xe fractionation obtained in laboratory adsorption experiments (Section III.A, Fig. 18).

any lower values will serve, including zero (which was in fact assumed, instead of the very low upper limit in Fig. 13a, for $C_{20}(A_S)$ in Table AI). The primary A_{CI} composition assumed for Mars, specified by observed CI elemental ratios and therefore not a free parameter in the Mars model, is also shown in Fig. 13a.

The issue raised by Fig. 13a is how these rather different noble gas distributions in the initial atmospheres of the three planets might have originated. The question of origin of primary atmospheres is discussed in Sections VI.D.1,2 in the context of possible sources for initial planetary hydrogen inventories, and reasons are given there for preferring accretion of icy planetesimals rather than gravitational capture of nebular gases. Adopting this hypothesis, and considering first only Venus and Earth, let us suppose that such planetesimals also carried noble gases, incorporated into ices by low-temperature adsorption or clathration of ambient solar-composition gases, in the relative proportions characterizing the A_S component on Venus. In this view the pronounced Ne deficit is qualita-

tively reasonable, since the very low temperatures (< 25 K) necessary for efficient trapping in amorphous water ice (Bar-Nun *et al.* 1985) might not have been reached in regions where these bodies formed, and clathration sharply discriminates against Ne (Lunine and Stevenson 1985). One may speculate, in the current absence of relevant laboratory data, that the heavier noble gases could have physically adsorbed on amorphous ices in roughly their gas-phase (solar) relative abundances. It is important to note, however, that this kind of relatively unfractionated occlusion does not appear to occur in clathration. Trapped Ar : Kr : Xe ratios in clathrate structures are distinctly nonsolar in Lunine and Stevenson's (1985) thermodynamic modeling calculations.

A clear consequence of assuming an outer solar system, icy planetesimal source for primary noble gases on Venus is that its accretion could not have been restricted just to Venus. Earth too would have acquired a Venus-like primary atmosphere, and so the central issue for these two planets is the evolution of Earth's noble gases, prior to our assumed t_0 at ~ 50 myr, into the different compositional pattern shown in Fig. 13a. One possibility is a mass-dependent episode of atmospheric escape during and following a giant Moon-forming impact. It is plausible, perhaps probable, that a preexisting terrestrial atmosphere would have been at least partly lost as a result of collision of a very large body with Earth (Cameron 1983, Cameron and Benz 1988, Benz and Cameron 1991), and that surviving residues would be fractionated (Hunten *et al.* 1989, Benz and Cameron 1991). This could be qualitatively consistent with the requirement here for significant, perhaps total, loss of Ne and Ar relative to heavier species, but with comparatively less or no depletion of Kr relative to Xe.

There remains the problem of unavoidable planetesimal contributions of A_S noble gases to the primary atmosphere on Mars, where both present-day Xe composition and geochemical modeling point to domination by CI rather than solar Xe. It turns out, however, that an initial Martian atmosphere containing an appropriate mixture of the A_{CI} and A_S components is still characterized by a high CI/solar mixing ratio for Xe, and serves equally well for isotopic matching. A variant of the basic Mars I model (Mars Ia), in which A_S noble gases with identical elemental ratios *and* the same absolute abundances (in g/g-planet) as those derived for Venus are simply added to the original A_{CI} component in Mars' primary atmosphere, yields comparable—or, for Xe, even somewhat better—fits to all present-day isotopic distributions. There are no additional free parameters in this version of Mars I. Isotopic compositions from the Mars Ia model are included in Table IV, and spreadsheet results are set out in Table AV.

Turning to the compositions of outgassed components plotted in Fig. 13b, we see that Ar/Kr and Ne/Kr ratios

calculated from the required $C_M^i(OG_1)$ concentrations in Tables AI and AIV are essentially identical for Earth and Mars. A common process is thus indicated for the origin of source reservoirs in the interiors of these two planets—and by extension in Venus as well, although there its expression by outgassing is not presently evident. Moreover the similarity of the fractionation pattern in Fig. 13b to the lower boundary of the laboratory data field in Fig. 6 points to adsorption of solar gases as a plausible mechanism. Two models for incorporating gases into growing planets, by adsorption on preplanetary nebular dust or on protoplanetary cores, are considered in Section VII.D. The protoplanetary core approach appears to be more in accord with current laboratory estimates of gas/solid distribution coefficients, and also fits comfortably into the most recent version of the standard model for planetary accumulation (Wetherill 1990a,b).

Terrestrial degassing of primordial helium and neon. It seems unlikely that the contents of interior reservoirs would have been totally outgassed over geologic time on any planet. Residual gases from this source, still migrating upward from deep within the Earth, provide a natural explanation for the presence of isotopically near-solar Ne in a few mantle-derived samples (Honda *et al.* 1987, Ozima and Zashu 1987, Sarda *et al.* 1988), and logically for the celebrated solar-like He component as well, which coexists with nonatmospheric Ne in samples from several different mantle provenances (Honda *et al.* 1991, and references therein). Since laboratory partition coefficient data for this lightest noble gas do not exist, the plausibility of an adsorbed He source for this latter component cannot yet be assessed in any rigorous way—although Wacker (1989) points out that the high trapping efficiencies observed for Ne in laboratory adsorption on carbon imply similar behavior for He as well.

One would expect this primordial He and Ne component to be accompanied by smaller amounts of isotopically solar Ar and Kr from the interior reservoir, and perhaps by a trace of solar Xe as well although most of the associated Xe is assumed to be locked up deep in the planet. These heavier species have not been seen, and will be formidably difficult to resolve from the proportionately much larger background components of essentially atmospheric Ar, Kr, and Xe in the upper mantle. The point of view taken in the present model is that these background gases have probably been recycled into the mantle by subduction of crustal sedimentary volatiles. If this is the case, the existence, in particular, of isotopically atmospheric mantle Xe does not necessarily imply that atmospheric Xe is a product of degassing from an interior reservoir to the surface (Ozima and Igarashi 1989)—which, in this model, it is not. The mantle could equally well have been contaminated by transport *from* the surface.

Carbon and nitrogen. The baseline Model I for noble gases does not attempt to track the evolution of planetary carbon and nitrogen from primordial sources to present-day abundances and isotopic compositions. A combined C–N–noble gas model, Model II, is used in Section V.C below to explore one possibility for the origin of these species on Earth and Venus. However, both of these elements are included in the Earth I and Venus I models, to the extent of seeing what might happen to crude estimates of their initial abundances in the A_5 and OG_1 components *if* they were entirely atmophilic and participated fully, as CO_2 and N_2 , in hydrodynamic escape. No similar estimates are made for Mars. It seems very unlikely that the enormous amounts of chemically reactive carbon and nitrogen contained in a major (40%) C- and N-rich CI accretional component (see Fig. 2) would have been completely mobilized as atmophilic species into the primary atmosphere, and at the moment there is no way to estimate what their volatilized fractions might have been. We can say, however, that CO_2 now on the Martian surface could *not* have derived entirely from a primary atmospheric CO_2 reservoir that experienced the degree of hydrodynamic loss suffered by the noble gases. The reason is isotopic: escape fractionation would have elevated residual $^{13}C/^{12}C$ to 0.0131 from its CI value of 0.0111 (Table AIV), well above the observational limit of <0.0118 (Nier and McElroy 1977).

In Model I, for illustration, the ratios of C (as CO_2) and N (as N_2) to Kr in the Venus primary atmosphere are taken to be solar, and thus similar to Ar/Kr in Fig. 13a. On Earth the Ar/Kr fractionation to ~ 0.25 of solar (for Kr-1) is assumed for both ratios. We find that subsequent hydrodynamic escape reduces these particular estimates of initial atmospheric abundances to $\sim 1\%$ or less of present N_2 and CO_2 inventories on Venus (Table AIII) and to much lower fractions on Earth. Outgassing from the adsorbed interior reservoir on Earth (and perhaps on Venus as well) would probably not have added very much more. In the absence of laboratory adsorption data for N_2 and CO (the likely molecular form of nebular carbon), we take CO/Kr and N_2 /Kr fractionation in the Earth's interior reservoir, relative to solar ratios, to be similar to the factor of ~ 50 depletion for Ar/Kr indicated in Fig. 13b. Then even with the assumption that carbon and nitrogen species degassed as efficiently as the inert gases, there are still shortfalls of several orders of magnitude on Earth (Table AI), and similar outgassing on Venus does little to make up the discrepancies there. To account for contemporary terrestrial inventories by outgassing from adsorbed reservoirs would require sorption affinities for C- and N-bearing species that are many orders of magnitude above those for the noble gases (e.g., $\approx 10^4$ times larger for N_2 than for ^{36}Ar). The extensive literature on removal of gases, including noble gases and carbon and nitrogen compounds, from vacuum systems by adsorption on a wide

variety of substrates does not support differences of this order, at least not under the conditions of pressure, temperature, and time pertaining to laboratory environments and experiments (Dushman 1962).

Inheritance of carbon and nitrogen from the source of the primary atmospheres on Earth and Venus could have been much larger if the assumption that source ratios of C and N to noble gases were solar, or that these species were entirely atmophilic, is wrong. For example, as discussed later in Section VI.D.2, a chemically Halley-like icy planetesimal source for enough water to supply the hydrogen needed to fuel hydrodynamic escape on Venus would also have contributed more than enough C and N to account for present-day atmospheric CO₂ and N₂ abundances, whether or not C- and N-bearing species were later depleted in the escape episode.

An alternative possibility, independent of whatever supplied the water, is accretion and degassing of nonicy solid materials containing C- and N-rich chemical phases. The nebular origins and natures of these phases have been discussed by Prinn and Fegley (1989). They could have accreted either homogeneously—implying their presence in relatively fixed proportions in the planetesimals that comprised the bulk of the planet—or heterogeneously, which we take here to designate late contributions of C–N-rich bodies to form a surface veneer after most of the planet had accumulated from a chemically distinct (C–N-poor) planetesimal population.

Some homogeneous accretion of such carrier materials is probably necessary to account for the carbon content of the bulk Earth. But a number of geochemical and geophysical arguments can be made for origin of *surficial* carbon and nitrogen on Earth and Venus by infall from a common, chemically uniform planetesimal source late in their accumulation histories. These two species in the Venus atmosphere and in integrated crustal reservoirs on Earth are characterized by indistinguishable elemental abundance ratios, and apparently isotope ratios as well to the extent this comparison can be made with the currently poorly known Venus data (Tables II,III). Absolute abundances are also roughly comparable, but appear to be somewhat larger on Venus by factors of ~2–3 (although one should note the relatively large uncertainties for the terrestrial data listed in Table II). Emplacement of such similar inventories in the two surface reservoirs by outgassing of homogeneously accreted C–N-rich materials would plausibly imply equally similar magmatic and tectonic histories on both planets, contrary to observational evidence and theoretical arguments that they have been notably different, and in ways that should have reduced Venus's degassing efficiency relative to Earth's over geologic time, not enhanced it (e.g., Kaula 1990). Direct surface deposition of C and N by late-stage heterogeneous accretion seems a more likely or at least a credible alterna-

tive to derivation from an interior source. This is the rationale for extending the noble gas evolutionary model to include veneer-derived carbon and nitrogen in the following section.

V.C. Planetary Model II: Combined Noble Gas–Carbon–Nitrogen Models

A central aspect of atmospheric evolution following t_0 concerns the inventories of carbon and nitrogen currently present in surface reservoirs on Earth and Venus. It is clear from the absolute abundance data shown in Fig. 2 that they are significantly less depleted relative to solar abundances than are the noble gases and, as noted earlier, one or the other is presently the major atmospheric constituent on the two planets. In this section the basic HEF model is extended as outlined in Section II.B.4 to include these two elements, and used together with relevant abundance and isotopic data to assess the proposition that carbon and nitrogen in the atmospheres and associated crustal reservoirs of Earth and Venus were contributed primarily by late-accreting veneers with volatile contents resembling those in present-day enstatite chondrites. The principal result of the model calculations is that this hypothesis does indeed lead to acceptable matches to observed elemental and isotopic distributions. This veneer is assumed not to contribute significantly to Mars. In Section V.C.3 below a Mars II model very similar to the baseline Mars I is utilized to explore one of the ways in which C and N in the Martian atmosphere and crustal reservoirs might have derived from an abundant CI accretional component in the planet.

To be attractive in the context of the HEF model, a candidate veneer source for surficial carbon and nitrogen on Earth and Venus must satisfy several criteria which taken together rather rigidly constrain its nature. (1) Hydrodynamic losses of veneer-supplied C and N, to the extent they occurred, would have involved escape of volatile, atmophilic molecules: CO₂ or CO or CH₄, and N₂ or NH₃. If losses were minor, or if nitrogen escaped in a comparable or lighter mass form than carbon, the N/C ratio in the veneer material must have been similar to or higher than present ratios in planetary surface reservoirs, since escape preferentially depletes lighter species. Only loss as CH₄ and N₂ would require a lower N/C. (2) By the same argument, but now referred to isotope ratios independent of molecular forms, and therefore much more powerful, ¹³C/¹²C and ¹⁵N/¹⁴N in the veneer material must have been comparable to or lower than the corresponding planetary isotope ratios. (3) Noble gases contributed by the veneer must combine with those from the A_S and OG_I sources in Model I to produce acceptable matches to present-day isotopic compositions. This requirement effectively sets upper limits on veneer ratios of noble gases

to C and N. (4) To qualify as a veneer, C and N contents must have been high enough to supply atmospheric and crustal inventories by addition of material comprising relatively small fractions of total planetary masses. (5) Accretion of this material by Venus and Earth (as seen below, in amounts about $3\times$ larger on Venus), but not substantially on Mars, requires an inner Solar System provenance.

We are not forced to invoke, in an ad hoc way, a vanished or unsampled planetesimal population with these properties as the veneer source. The five criteria are all satisfied, or could be satisfied, by material that in composition and suggested origin strikingly resembles present-day enstatite chondrites. The E chondrites are unique in this respect. The four carbonaceous chondrite classes fail one or more of the geochemical-isotopic constraints. $^{15}\text{N}/^{14}\text{N}$ in the CIs and CMs is significantly above the terrestrial ratio (Kerridge 1985). Xe/C is too high and N/C probably too low in the CIs and CMs, and even more so in the CVs and COs (Mazor *et al.* 1970) although these latter two classes do contain isotopically light N (Kerridge 1985). Moreover residence near the sun for a carbonaceous chondrite population is most unlikely, considering their low inferred formation and storage temperatures. An inner solar system provenance for the enstatite chondrites is debatable, but has been suggested on cosmochemical (Kallemeyn and Wasson 1986) and oxygen isotopic (Clayton *et al.* 1984) grounds, and there are chemical hints in lunar samples that E-like material may have been an important projectile component in early lunar bombardment (Gros *et al.* 1976).

V.C.1. Earth

A veneer component is integrated quantitatively into the baseline Model I in the following way. Average $\delta^{15}\text{N}$ in the E chondrites is -32% (Table III). Residual $^{15}\text{N}/^{14}\text{N}$ now in the Earth's atmosphere, with $\delta^{15}\text{N} \equiv 0\%$, must therefore reflect elevation of the E chondrite $^{15}\text{N}/^{14}\text{N}$ ratio by the isotopic fractionation factor $f_{29/28} = 1.033$ during hydrodynamic loss of N_2 degassed by impact from the veneer material. Thus the veneer must have accreted and degassed at a time t_v in the hydrodynamic escape episode such that the ratio was fractionated by this factor as the crossover mass for N_2 declined from $m_c^v(\text{N}_2)$, its value at veneer accretion, to $m_c^f(\text{N}_2)$. Time t_v turns out to occur fairly late in the episode, during stage 2 escape of the outgassed (OG_1) noble gas component in Model I (Section V.B.1). The stage 2 atmospheric hydrogen inventory in Model II, initially N_1^{og} at t_{og} , is assumed to decline monotonically as in Model I since there is no chemical reason to expect a major gain of H_2 or H_2O as a direct result of E chondrite-like veneer accretion at t_v . Thus HEF evolution of veneer volatiles in Model II is entirely governed by

whatever values for the $\alpha_0(\text{OG})$, m_c^{og} and m_c^f parameters, plus the additional free variable m_c^v , are chosen for best fits to observed isotopic compositions.

Formally, we may write

$$C_M^f(V) = f_M(V)[C_M^i(V)] \quad (22')$$

and
$$C_{M'/M}^f(V) = f_{M'/M}(V)[C_{M'/M}^i(V)] \quad (25')$$

as Model II addenda to the Model I Eqs. (20)–(22) and (23)–(25) given in Section V.A.3. Elemental ratios in the $C_M^i(V)$ veneer component are taken to be those characterizing the average E chondrite composition given in Table II (excluding the anomalous South Oman individual). However, noble gas isotope ratios are most accurately determined for South Oman and are utilized here along with measurements in several laboratories for isotopic compositions of E chondrite C and N (Table III) to represent $C_{M'/M}^i(V)$. Thus, compared to Model I, we have added just two free variables to accommodate a veneer in Model II, and both apply specifically only to the evolution of veneer volatiles: the crossover mass at accretion (m_c^v), and the initial absolute concentration of one accreted species, say carbon as CO_2 ($C_{44}^i(V)$).

Best-fit values for $f_M(V)$ and $f_{M'/M}(V)$ in Eqs. (22') and (25'), calculated from Eqs. (16) and (17) for those veneer species light enough to escape at a crossover mass of m_c^v (for those that do not, both values are $\equiv 1$), were determined in the following way. Fractionation of a species over a particular interval of crossover mass decline, say from m_c^{og} to m_c^f , must equal the product of fractionations incurred over subdivisions of that interval, here from m_c^{og} to m_c^v and from m_c^v to m_c^f . Then for any veneer species, $f_M(V)[m_c^v \rightarrow m_c^f] = f_M(V)[m_c^{\text{og}} \rightarrow m_c^f]/f_M(V)[m_c^{\text{og}} \rightarrow m_c^v]$, with equivalent expressions for the isotopic fractionation factors $f_{M'/M}(V)[m_c^v \rightarrow m_c^f]$. An additional 24 evolutionary equations for veneer isotopes, incorporating these expressions for $f_M(V)$ and $f_{M'/M}(V)$, were added to the 48 in the Model I spreadsheets (Section V.A.3) to construct Model II.

As in Model I, a best-fit set of values for all stage 1 and stage 2 free parameters was then determined by trial-and-error matching to terrestrial noble gas, carbon, and nitrogen inventories. The crossover mass $m_c^v(\text{N}_2)$ was chosen to be the value (32 amu) that exactly reproduced the $^{15}\text{N}/^{14}\text{N}$ ratio in the terrestrial atmosphere; it is low enough that, of all the veneer volatiles, only N and Ne could escape after accretion. Model I estimates for initial C and N abundances in the A_5 and OG_1 components, discussed above in the final part of Section V.B.4, were again used. It was necessary, for these two elements, to drop the restriction that the sum of contributions from all sources must reproduce observed terrestrial abundances, since here there were no free variables left to implement it.

Model II results are set out in Table AII, and in Table IV for choices of both the Kr-1 and the Kr-2 solar compositions. They are discussed in Section V.C.4 below.

V.C.2. Venus

Model II for Venus was constructed in the same way as Earth II from Earth I, except that here veneer addition occurs late in stage I (there is no stage 2) and so the relevant parameters for Eqs. (16) and (17) are $\alpha_0(A)$, m_c^0 and m_c^A . As in Model I (Section V.B.2), m_c^0 for Venus II was calculated from m_c^0 for Earth II assuming simultaneous nebular clearing; with $m_c^0(\text{Xe}) = 208$ amu on Earth from Table AII, Eq. (10) yields $m_c^0(\text{Xe}) = 532$ amu on Venus. C/Kr and N/Kr ratios in the primary atmosphere were taken to be solar, as in Venus I (Section V.B.4). The E chondrite composition assumed for veneering material on Earth must obviously apply as well to a Venus veneer from the same source. Measurement of Venusian $\delta^{15}\text{N}$ (and $\delta^{13}\text{C}$) is too imprecise to independently define a chronology (m_c^v and t_v) for veneer accretion in the same way as for Earth. However, it is probably a reasonable assumption that the population of veneer planetesimals, perhaps generated by collisional disruption of large E chondrite-like parent bodies in the inner solar system, would have been swept up roughly synchronously by both planets. Simultaneous accretion, and the crossover mass $m_c^v(\text{N}_2) = 32$ amu for Earth, fixes $m_c^v(\text{N}_2)$ on Venus at 78.4 amu from Eq. (10). This is marginally high enough for Kr escape ($m_c^v(\text{Kr}) = 85.4$ amu), and certainly allows loss of veneer carbon as CO_2 or any lighter molecular species. For illustration of effects on residual $\delta^{13}\text{C}$, carbon is assumed to escape as CO_2 . (Other, perhaps more likely alternatives exist, ranging from virtually no loss if refractory E chondrite graphitic carbon (Grady *et al.* 1986) was retained in nonvolatile form, to greater loss as CO or CH_4 in this reducing environment. Depletion by CO_2 escape falls between these two possibilities).

With these specifications, the only additional degree of freedom left for the Venus II veneer is the absolute accreted abundance $C_M^i(V)$ of one of its constituents. Results of the matching exercise are given in the lower part of Table AIII and in Table IV.

V.C.3. Mars

The Martian volatile system is open to loss of molecular constituents such as nitrogen by nonthermal escape to space. Moreover, carbon dioxide and water are very likely sequestered in the cold megaregolith, in amounts which are unknown but may well be large compared to contemporary atmosphere-polar cap abundances (Fanale *et al.* 1991). Therefore, we cannot assume that present-day atmospheric inventories of these species represent the

abundances—and, at least for nitrogen, the isotopic composition—originally generated on the planet by early accretional and evolutionary processes.

As pointed out previously, the bulk chemical composition of Mars and the isotopic composition of present-day Martian Xe, both deduced from the SNC meteorites, point to CI material in the planet. Carbonaceous chondrites are rich in carbon and nitrogen as well as noble gases (Fig. 2); the average ^{12}C (as CO_2) and ^{14}N to ^{84}Kr ratios in CI material are 3.8×10^9 g/g and 4.2×10^7 g/g, respectively, from Table II. One would thus expect this material to be a powerful source of planetary carbon and nitrogen. Abundances greatly in excess of those now seen in observable surface reservoirs could have subsequently degassed from the unknown fractions of these two elements that were retained in the planet during accretion of the CI component—i.e., that were not mobilized as atmophilic compounds into the primary atmosphere and later lost in hydrodynamic escape. Therefore, with such a source available, Model II for Mars does not assume an E chondrite-like veneer, but instead explores one restricted and very tentative scenario for the origin of surface carbon and nitrogen by outgassing.

Mars II is essentially just a specific version of Mars I which adopts Kr-2 as the composition of solar Kr, and assumes that Kr-2 really is isotopically lighter than Martian Kr despite the uncertainty overlap of the two compositions (e.g., see Fig. 11). The veneer discussed above is presumed to have contributed C and N to Earth (and Venus), and so the Earth II value of $m_c^0(\text{Xe}) = 208$ amu (Table AII) is used to fix $m_c^0(\text{Xe}) = 1048$ amu for Mars II from Eq. (10). The assumed isotopic discrepancy between solar Kr-2 and Martian Kr is resolved by postulating degassing of just enough CI-Kr, as an OG_{CI} component, to yield the observed Martian ratios by isotopic mixing with the solar-composition $\text{OG}_{\text{I}}\text{-Kr}$. The elemental and isotopic composition for all other species in the OG_{CI} component, including C and N, are fixed by the data in Tables II and III for the CI meteorites. This additional outgassed component formally requires two more equations in the set given in Section V.A.3, identical to Eqs. (22) and (25) with OG_{CI} replacing OG_{I} , and adds one more free variable, $C_{84}^i(\text{OG}_{\text{I}})$, to those in Mars I. Evolutionary stages and fitting procedures are otherwise the same as for Mars I (Section V.B.3).

Mars II involves an argument within the error bars of current isotopic data and a number of other assumptions, and is therefore more an illustrative example of what might have happened than a defensible model of what did happen. Nevertheless the results, given in Tables AVI and IV and discussed in Section V.C.4 below, are of some interest. They indicate, for example, that outgassing of a CI component carrying only a trace of Kr ($\sim 10^{-4}$ of that originally acquired by the planet if the 40% of CI-like

material proposed by Dreibus and Wänke (1985, 1987, 1989) contained a full complement of CI volatiles) would still have provided more than two orders of magnitude more surface carbon than is currently present in the Martian atmosphere.

V.C.4. Discussion of Model II Results

Neon, argon, and krypton. Isotope ratios derived from Model II differ little, if at all, from Model I results except for $^{21}\text{Ne}/^{22}\text{Ne}$ (Fig. 10), where the $\sim 2.7\%$ (with Kr-2) to $\sim 3.8\%$ (with Kr-1) depression of the calculated/measured ratio suggests postescape augmentation by degassing of $^{21}\text{Ne}_n$ from the terrestrial crust (Section V.B.4) in approximately the amount proposed by Rison (1980). The ^{20}Ne mixing ratio of the SW and OG_I components required to match atmospheric $^{20}\text{Ne}/^{22}\text{Ne}$ on Mars is almost identical (cf. Tables AVI and AIV). Model II krypton compositions on Earth and Mars are indistinguishable from the Model I compositions plotted in Fig. 11; predicted Kr on Venus is isotopically slightly lighter (Table IV) and even more similar to CI-Kr.

Nonradiogenic xenon. The relatively small ($\sim 6\%$) but isotopically distinct E-Xe component, supplied to the Earth's surface by the Model II veneer after the end of stage I Xe evolution, is accommodated by a somewhat greater fractionation, compared to Earth I, of residual solar Xe. Later isotopic mixing of these two Xe components reproduces the nonradiogenic terrestrial composition to well within its error bars (Table IV). It is this required stage I "overfractionation" of primary Xe that forces the changes in the $\alpha(A)$ and m_c^0 parameters from Model I to II (cf. Tables AI and AII). Contemporary Martian Xe is well matched—but again only by presuming that degassed components, here including both OG_I and OG_{CI} , carry little if any Xe to the surface. The predicted composition of nonradiogenic Xe on Venus is very similar in the two models. In general, the Fig. 12 compositions derived from Model I can be taken, at that scale of resolution, to apply to Model II as well.

Radiogenic ^{129}Xe on Earth. To this point radiogenic ^{129}Xe has not been considered in any of these calculations. The relatively large abundances of radiogenic ^{129}Xe from extinct ^{129}I decay in most of the present-day E chondrites could pose a problem for the veneer hypothesis. From the present ^{130}Xe inventory on Earth (Table II) and values for $^{129}\text{Xe}/^{130}\text{Xe}$ in the contemporary and nonradiogenic atmospheres (Table III), the atmospheric $^{129}\text{Xe}_{\text{rad}}$ abundance is $\equiv (6.496 - 6.053)(1.4 \times 10^{-14}) = 6.2 \times 10^{-15}$ g/g-planet. The veneer mass accreted by Earth is readily calculated by dividing $C_M^i(V)$ for any veneer species in Table AII (e.g., $C_{44}^i(V) = 3.38 \times 10^{-5}$ g/g-Earth) by its corresponding average concentration in the E chondrites (e.g., 1.54×10^{-2} g/g-veneer for C as CO_2), yielding

2.2×10^{-3} g-veneer/g-Earth. Veneer concentrations of $^{129}\text{Xe}_{\text{rad}}$ must therefore have been limited to $\leq 2.8 \times 10^{-12}$ g/g-veneer. However, the average $^{129}\text{Xe}_{\text{rad}}$ abundance in E chondrites, from data by Crabb and Anders (1981), is $\sim 8.3 \times 10^{-12}$ g/g, about $3 \times$ higher; only 2 of 17 individuals (Bethune I and Atlanta) contain $< 2.8 \times 10^{-12}$ g/g. If a veneer resembling enstatite chondrites was in fact involved, its radiogenic ^{129}Xe content must have been significantly lower than the average in the contemporary meteorite population. Even then, most if not all of the current atmospheric inventory of $^{129}\text{Xe}_{\text{rad}}$ could have been supplied in this way. If it was, it is unrelated to decay of ^{129}I in the Earth unless accretion was early enough for the veneer material itself to have carried live ^{129}I . This is not the case in the present model: Earth II veneer accretion occurred at $t_v \cong 205$ myr (Section VI.B.2, Table VI), about 12 half-lives of ^{129}I .

Isotopic composition of interior xenon in Mars. As pointed out above, the present model requires that outgassing of Xe to the Martian atmosphere from interior sources of both the OG_I and the OG_{CI} components was largely suppressed. The same stipulation is made for Earth, but in the smaller Mars it sets more stringent upper limits on the hydrostatic pressures at which Xe must partition into solid phases if this central assumption is to be valid (Section VII.A). Some of this sequestered Xe, originally sited in the deep interior, could since have migrated upward in the mantle and into magma source reservoirs for the SNC meteorites. If so, it could comprise the nonatmospheric "second component" of Martian Xe identified by Ott and Begemann (1985) and Ott (1988) in the SNCs and represented in purest form in Chassigny. Thus it is of interest to compare the isotopic composition of retained interior Xe predicted by the Mars II model to that found in Chassigny. The $C_{84}^i(\text{OG}_{CI})$ value of 1.56×10^{-15} g/g in Table AVI yields an associated CI-Xe concentration of 3.1×10^{-16} g/g from the CI Xe/Kr ratio in Table II. An equivalent derivation of associated I-Xe from $C_{84}^i(\text{OG}_I) = 1.56 \times 10^{-14}$ g/g runs into the problem that the Xe/Kr ratio in the interior reservoir for the OG_I component is unknown. On the assumption that it was populated by adsorption (Section VII.D), we may estimate Xe/Kr from the grand average (a factor $\approx 8 \pm 7$ above the solar ratio) of the laboratory measurements plotted in Fig. 6. This yields concentrations of isotopically solar I-Xe ranging from ≈ 2.2 to 32×10^{-16} g/g. Both of these "missing" Xe components were presumably partitioned at high pressures into solid phases, and migrated into magma chambers by upward magmatic or solid-state convective transport of these phases. A mixture of the two at these relative concentration levels generates the shaded compositional field plotted relative to CI-Xe in Fig. 14, where the upper boundary corresponds to an approximately solar $(\text{Xe}/\text{Kr})_I$

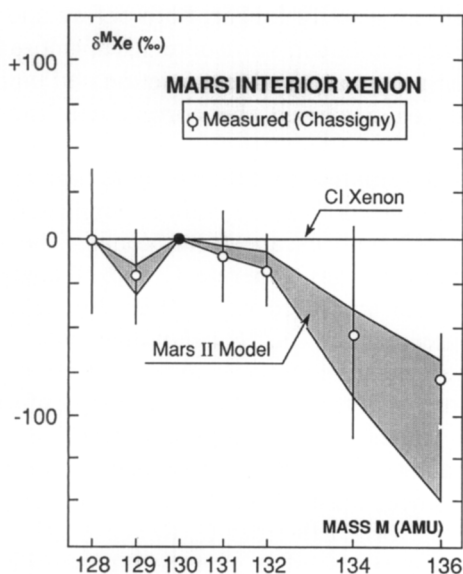


FIG. 14. The compositional range for xenon retained in the interior of Mars (shaded area), calculated from the Mars II model (Section V.C.4) and compared to the spallation-corrected composition found in the SNC meteorite Chassigny by Ott and Begemann (1985) and Ott (1988). The common CI normalization here and in Fig. 8 allows direct comparison of the two isotopically distinct Martian volatile reservoirs.

ratio and the lower boundary to $15 \times$ solar. The spallation-corrected Chassigny spectrum in Fig. 14, calculated from data given by Ott (1988), tends to follow the trend of the derived compositions reasonably well. Note in particular the apparent depression of both calculated and measured $^{129}\text{Xe}/^{130}\text{Xe}$ ratios ($\delta^{129}\text{Xe}$) below the CI value (here taken to be 6.53, an average for the CIs from Mazor *et al.*'s (1970) compilation).

Radiogenic ^{129}Xe on Mars. Comparison of Figs. 8 and 14 illustrates the distinct differences between atmospheric and interior Xe compositions on Mars. The most striking of these is the very large enhancement of $\delta^{129}\text{Xe}$ in the atmosphere relative to that in the planet itself. Derivation of atmospheric Xe by simple outgassing of the interior reservoir is thus forbidden. The reason is straightforward. If the present atmosphere had separated from the mantle at a time when mantle ^{129}I was still extant, subsequent production of radiogenic ^{129}Xe would have elevated interior $^{129}\text{Xe}/^{130}\text{Xe}$ above the atmospheric ratio. Alternatively if outgassing occurred later, after disappearance of live ^{129}I , $\delta^{129}\text{Xe}$ would now be the same in both reservoirs. Both predictions are clearly contrary to observation. Ott and Begemann (1985) and Ott (1988) identified this problem, and concluded that the atmosphere must either have originated from a veneer, independent of the interior, or received its radiogenic ^{129}Xe by preferential degassing of

this species relative to nonradiogenic isotopes. Becker and Pepin (1986) and Dreibus and Wänke (1987), in considering the latter possibility, pointed out that geochemical concentration of live ^{129}I in the planetary crust, followed by release of daughter ^{129}Xe after partial loss of primordial atmospheric Xe from the planet, would have led to enhancement of atmospheric $\delta^{129}\text{Xe}$. Becker and Pepin (1986) also noted that a similar early crustal concentration of ^{40}K could account for evidence that the $^{40}\text{Ar}/^{36}\text{Ar}$ ratio is also higher in the atmosphere than in the interior (Bogard and Johnson 1983, Swindle *et al.* 1986, Wiens *et al.* 1986, Ott 1988, Wiens 1988). A recent model by Musselwhite *et al.* (1991) addresses the issues of surface concentration of ^{129}I on Mars, and the separation of nonradiogenic Xe from radiogenic ^{129}Xe that ultimately led to strong atmospheric enhancement of $^{129}\text{Xe}/^{130}\text{Xe}$, in a novel and interesting way. Their mechanisms involve early surficial concentration of iodine by preferential solution of degassed I into standing water which is then hydrothermally incorporated into the upper crust, simultaneous loss of degassed nonradiogenic Xe by atmospheric impact erosion, and later outgassing of daughter ^{129}Xe from the crustal I reservoir. This approach is very similar in concept, if not in processes, to that suggested by the present model.

The escape model discussed here provides a natural physical context both for generating high surface concentrations of volatile I and K (and other halogens and alkali metals as well) and for fractionating their daughter products with respect to nonradiogenic noble gases. One would expect such species, one of which was live ^{129}I , to degas efficiently from impacting CI material along with the noble gases during planetary growth, and to continually mobilize and recycle between the surface and the atmosphere in the accretional thermal environment. Residues remaining in the interior would be expected also to migrate upward into the crust, along with other incompatible elements, as the planet differentiated during accretion. Much of their total planetary abundances would then be concentrated on or near the surface when hydrodynamic loss began at t_0 . Some of these volatile species would subsequently have escaped—and been isotopically fractionated in the process. But fractional losses should generally have been smaller than for noble gases of comparable mass since their atmospheric inventories, unlike those of purely atmophilic species, would have been limited by temperature-dependent partitioning between vapor and surface condensates or compounds (or, as suggested by Musselwhite *et al.* (1991), by solution into surface water—if it existed).

The proportion of each such species that was sequestered against escape clearly depends on its volatility in the ambient thermal regime. Dreibus and Wänke (1987)

note that large losses of CI-derived iodine and other halogens are necessary to account for their estimated abundances on Mars today. It seems likely that whatever part of the planetary iodine inventory was in the form of very volatile I_2 or HI would have been in the atmosphere at t_0 and subsequently mostly lost, about as efficiently as Xe if present as HI, somewhat less so as I_2 . Although the actual analytic calculation can be complicated, it is possible to estimate that significant enrichment of residual atmospheric ^{129}Xe from decay of gaseous ^{129}I could have taken place *while* the primary atmosphere was escaping if the time for escape was comparable to or longer than the 17 myr ^{129}I half-life—as it is in the present Mars models (Section VI.B, Table VI). ^{129}Xe would have been further enriched during the escape period if the condensed part of the iodine inventory released radiogenic Xe as it was generated. Later, after the end of escape, degassing of Xe retained in the condensed phase plus that subsequently produced by all remaining ^{129}I would have added still more ^{129}Xe , now to an atmosphere severely depleted in nonradiogenic isotopes. With reasonable estimates for the initial ^{129}I inventory, the sum of these radiogenic contributions appears adequate to elevate $^{129}\text{Xe}/^{130}\text{Xe}$ from its low ratio in the primary atmosphere to its contemporary value in the remnant of that atmosphere. The similar distribution of radiogenic ^{40}Ar between the atmosphere and the mantle of Mars inferred from SNC data may likewise be due to release from ^{40}K concentrated in surface materials by these same processes.

Carbon and nitrogen. A crossover mass $m_c^v(\text{N}_2) = 32$ amu at the time of veneer accretion on Earth, in combination with the other parameter values given in Table AII, results in fractionation of the CI nitrogen composition into exact agreement with atmospheric $\delta^{15}\text{N}$. With this initial crossover mass, veneer-derived carbon cannot escape as CO_2 . Assuming also that it was not lost as CO or CH_4 (although some escape in either form is isotopically permissible), the calculated $\delta^{13}\text{C}$ for Earth in Table IV is just the unfractionated average E chondrite value of $-8.4 \pm 7.9\text{‰}$ —not very diagnostic because of the large range but certainly consistent with the terrestrial composition of $\delta^{13}\text{C} = -6.4 \pm 1.3\text{‰}$ (Fig. 10). The amounts of C and N contributed by the veneer mass of 2.2×10^{-3} g/g-Earth calculated above, after minor hydrodynamic loss of N_2 , replicate Walker's (1977) estimates for C and N abundances in surficial terrestrial reservoirs to within $<10\%$ (but note from Table II that these are very uncertain).

It is important to point out that this specific value of m_c^v , and the corresponding time t_v given by Eq. (13) (Section VI.B.2), does not necessarily imply a sharp chronology of veneer accretion. The flux of impacting planetesimals could have been distributed in time over a span of

several million years or longer, both before and after t_v , as long as the resulting mixture of relatively more fractionated (added prior to t_v) and less fractionated (added later than t_v) nitrogen carried the correct net fractionation factor.

With the assumption that the absolute time t_v of accretion was the same as on Earth, veneer-supplied C (as CO_2) and N (as N_2) both escape from Venus. The resulting isotopic fractionations generate C and N compositions consistent with measured ratios (Fig. 10), although the nominal agreement at $^{15}\text{N}/^{14}\text{N}$ is not diagnostic in view of the $\pm 200\text{‰}$ measurement uncertainty. Calculated isotopic compositions of both elements are not very different from terrestrial values—not a surprising result considering their common source and rather similar fractionation factors. The veneer mass of 8.2×10^{-3} g-veneer/g-Venus, calculated as for Earth from $C_{44}^i(\text{V})$ or $C_{28}^i(\text{V})$ in Table AIII and the corresponding average E chondrite concentrations in Table II, yields amounts of C and N on Venus, after hydrodynamic losses, that fall within $\leq 5\%$ of observed atmospheric abundances.

For Mars, we must assume that most of the CO_2 associated with the OG_{CI} component was chemically intercepted while migrating to the surface, delaying its actual outgassing to the atmosphere until after the end of hydrodynamic escape at t_f (or at least until the CO_2 crossover mass had fallen below 44 amu). This delay is mandated by isotopic considerations. Earlier release to the atmosphere, say contemporaneous with the degassing of Kr, the lighter noble gases, and nitrogen at t_{og} , would have resulted in partial hydrodynamic loss of CO_2 and violation of a carbon isotope constraint. Viking measurements indicate that $\delta^{13}\text{C}$ in present-day atmospheric CO_2 is less (probably much less) than $+50\text{‰}$ (Nier and McElroy 1977). Although, like nitrogen, fast carbon atoms have also escaped to space over Martian history, it seems clear that these losses, unlike those for nitrogen, comprised such a small fraction of the total (exchangeable) CO_2 inventory that net isotopic evolution of $^{13}\text{C}/^{12}\text{C}$ has been negligible (McElroy *et al.* 1977, Fanale *et al.* 1982). Thus $\delta^{13}\text{C} < +50\text{‰}$ is a likely measure of carbon composition at t_f . Had most or all of the available CO_2 entered the atmosphere during the outgassing episode at t_{og} , about 40% would have survived until t_f (Table AVI, footnote *c*), still up to $\sim 60\times$ the present inventory. But a large fractionation of the carbon isotopes would have occurred during escape. The calculated value for $f_{45/44}(\text{OG})$ given in the footnote yields $\delta^{13}\text{C} \cong +135\text{‰}$ at t_f , far above the measured upper limit. With no escape fractionation the carbon composition given by Mars II is just the CI value of $\delta^{13}\text{C} = -10.3 \pm 2.5\text{‰}$, well below this limit (Fig. 10).

Unlike carbon, volatile nitrogen from the OG_{CI} component is assumed to enter the atmosphere at t_{og} and escape as N_2 along with the lighter noble gases. Subsequent frac-

tionation to an isotopically heavier composition, as for escaping Ne and Ar (Section V.B.3), is severe. Nevertheless it is clear from Fig. 10 that the measured $^{15}\text{N}/^{14}\text{N}$ ratio on Mars is even heavier, by $>300\%$, than that derived from Mars II. The measured value, however, refers to the *present-day* atmosphere, whereas the model calculations describe inventories on Mars at a time >4 billion years ago. Therefore this discrepancy is interpreted as reflecting isotopic evolution over the postescape history of the planet, by nonthermal isotope-dependent escape of atmospheric nitrogen to space (Nier and McElroy 1977, McElroy *et al.* 1977, Yung *et al.* 1977). (For illustration the C and N compositions given by the Mars I model are also plotted in Fig. 10. $\delta^{13}\text{C}$ violates the carbon isotopic constraint, and $\delta^{15}\text{N}$ is again low. But note that neither of these deserves much attention, since without the degassed CI component there are enormous shortfalls in computed planetary abundances (Table AIV).)

Calculated CO_2 and N_2 inventories on Mars at the end of hydrodynamic loss (Table AVI) exceed those in the present atmosphere by factors of ~ 145 and ~ 7 , respectively. This amount of CO_2 , equivalent to a pressure of ~ 1 bar, is significantly larger than the likely adsorptive capacity of the Martian megaregolith but could be stored as carbonate rock (Fanale *et al.* 1982, 1991). The N_2 excess is close to the minimum loss factor of ~ 7 required by McElroy *et al.* (1977) to account for the present-day enrichment of atmospheric ^{15}N . However, McElroy *et al.* assumed that the initial $^{15}\text{N}/^{14}\text{N}$ ratio was terrestrial, and therefore that the isotopic enrichment factor in nonthermal escape was 1.62 since $\delta^{15}\text{N}$ is about $+620\%$ in the contemporary atmosphere (Table III). In the Mars II model this is not the case: N_2 degassing at t_{og} would have been depleted by a factor of ~ 13 , leaving a residual inventory at t_f in which $\delta^{15}\text{N}$ was about $+220\%$ (Table IV). The initial isotope ratio relative to terrestrial at t_f was thus already 22% higher, implying subsequent enrichment in the nonthermal escape process by a factor of ~ 1.3 . This requires loss of only about twice the present nitrogen inventory (Y. Yung, personal communication). The calculated N_2 abundance at t_f can satisfy this demand, and also permits some storage of outgassed nitrogen on Mars in nonvolatile nitrogen compounds or as adsorbed N_2 in the regolith.

Measured C/N ratios in CI and E chondrites, on Earth and Venus, and in the atmosphere of Mars, are all identical within a factor of ~ 2 (Table II; Pepin and Carr 1991). In the present model, as noted above, about the same values would be expected for Earth and Venus: the postulated source was the same, and subsequent fractionations of the ratio not very different. But the apparent agreement for Mars, based on data from the one currently observable surface reservoir, appears to be purely coincidental and thus misleading in its implication of a common source

for carbon and nitrogen on all three planets. A similar coincidence haunts interpretation of planetary and meteoritic $^{20}\text{Ne}/^{36}\text{Ar}$ ratios (Section I). The model results above suggest that Martian C/N in present-day atmospheric *plus* regolith reservoirs is on the order of $30\times$ higher than the atmospheric ratio.

Required veneer masses. The E-chondrite mass fraction on Earth, 2.2×10^{-3} g/g-planet, is equivalent to an accreted layer ~ 9 km deep (assuming a density of 3 g cm^{-3}), presumably now thoroughly mixed into the upper mantle by impact and subsequent crustal cycling. The mass fraction collected by Venus, 8.2×10^{-3} g/g-planet, would have added ~ 29 km of material. Both contributions are small enough to be appropriately called “veneers.” The total absolute mass on both planets is $\sim 3/4$ of a lunar mass, with $\sim 75\%$ of this on Venus and 25% on Earth. This Venus/Earth accreted mass ratio of ~ 3 may be compared to Hartmann’s (1976) estimate of ~ 1.6 for a planetesimal source near Venus’s orbit, and to Wetherill’s (1988) calculation of the provenances of planet-forming planetesimals, where in the example shown in his Fig. 6 the Venus/Earth ratio of mass accreted from within 0.7 AU is ~ 5 . The absence or near absence of this material on Mars seems plausible in view of the inference drawn from the high Venus/Earth ratio that it derived from a source deep within the inner solar system, perhaps from a leftover population of Wetherill’s (1988) “Vulcanoid” contributors to Mercury.

Finally, it is interesting to consider the extent to which the Moon, assuming that it then existed with its present mass, might now display the chemical signature of such a bombardment. Hartmann (1976) estimates that the mass ratio of impactors deposited on Moon relative to Earth from an inner solar system source would have been $\sim 5.5 \times 10^{-2}$, here yielding $\sim 10^{-2}$ g-veener/g-Moon or ~ 6 km of material impacting the lunar surface. Completely retained and thoroughly mixed by infall into, say, a 100-km deep magma ocean, its mixing ratio with indigenous material would be $\approx 5\%$. Alternatively, much of the projectile material expanding outward from impact sites might have escaped to space from this small body (H. J. Melosh, personal communication).

V.D. Noble Gases in Meteoritic Carrier Phases

In the previous sections carbonaceous and enstatite chondrites were assumed to contribute to planetary volatile inventories without considering how the meteoritic noble gas compositions themselves could have been generated from more fundamental components. This question is addressed here, by showing that CI elemental and isotopic distributions could have evolved from primary solar and extrasolar compositions through the sequential action of hydrodynamic escape and adsorptive fractionation, and

by considering a parent-body regime in which these processes might have occurred. E chondrite distributions are not discussed, but can be generated by the same processes operating in similar environments. A brief summary of the present model has appeared in abstract form (Pepin 1990b).

The simple analytic formalism used throughout this paper was developed by Hunten *et al.* (1987) to describe hydrodynamic escape of volatile species from planetary bodies with spherically symmetric atmospheres in which diffusion and outflowing gas drag are the controlling processes and escape is driven by energy input at high altitudes. The physical contexts for the evolutionary models of terrestrial planet atmospheres in Sections V.A–C are in reasonable accord with these stipulations. We will assume that analogous conditions existed on meteorite parent bodies. But one should keep in mind that the evolutionary histories of volatiles in meteoritic carrier grains could have been governed by processes of fractionating gas loss in quite different nebular environments, where assumptions underlying the present hydrodynamic escape formalism are problematic or invalid. Examples might include regimes of erosion from the inner edge or bounding surfaces of a turbulent accretion disk (Wood and Morfill 1988, Boss *et al.* 1989), with material loss driven by energy deposition from massive solar wind impact shocks or from solar ultraviolet radiation scattered onto the plane of the disk from above. Models of this kind are not explored here.

V.D.1. Components and Notation

From the postulates in Section II.A the two basic noble gas constituents of the primitive nebula were a “local” isotopically solar gas-phase component (here termed the S-component), and “exotic” nucleosynthetic species (the N-component) carried in extrasolar dust surviving from stellar nuclear processing environments. Contemporary meteoritic noble gas distributions in the model discussed below are proposed to derive from these initial components by adsorption of escape-fractionated S-gases on surfaces of N-bearing dust grains. The meteorite versions of Eqs. (20)–(25) for planetary atmosphere evolution in Section V.A.3 are therefore

$$C_M^f(S,N) = k_M[f_M(S)[P_M^i(S)]] + C_M^i(N) \quad (26)$$

$$\text{and } C_{M'/M}^f(S,N) = f_{M'/M}(S)[P_{M'/M}^i(S)] + C_{M'/M}^i(N). \quad (27)$$

Here $C_M^f(S,N)$ and $C_{M'/M}^f(S,N)$ respectively represent final calculated abundances (in g/g-meteorite of species M) and isotopic ratios M'/M deriving from combinations of local (S) and nucleogenetic (N) sources, and so are defined much as they were earlier. In the same sense, $C_M^i(N)$ and

$C_{M'/M}^i(N)$ are initial concentrations and compositions in N-bearing materials. Note, however, that $P_M^i(S)$ and $P_{M'/M}^i(S)$, denoting initial gas-phase partial pressures (in atmospheres) and isotope ratios, have replaced the concentrations and compositions previously represented in Eqs. (20)–(25) by C_M^i and $C_{M'/M}^i$. This is because we will be dealing here with final abundances adsorbed from a gas phase and thus governed by the gas/solid adsorptive distribution coefficient k_M , defined as grams of adsorbed species M per gram material per atmosphere partial pressure of M in the ambient gas phase (gM/g-atm). No $k_{M'/M}$ factor appears in Eq. (27), since isotopic fractionation is assumed not to occur in adsorption (Bernatowicz and Podosek 1986) and therefore $k_{M'/M} \equiv 1$. As before, f_M and $f_{M'/M}$ are the dimensionless fractionation factors—here the ratio of final to initial partial pressures and isotope ratios—generated in hydrodynamic escape. (It should be borne in mind that Eq. (27) is just a shorthand way of writing $C_{M'}^f(S,N)/C_M^f(S,N)$, and so the indicated isotopic addition is schematic; actual summation requires the magnitudes of the two terms to be weighted by the abundance of the reference isotope in each of them.)

The model is applied to meteoritic noble gas distributions in just the way it was to planetary atmospheres, by first seeking conditions for escape-fractionation such that Eq. (27) generates observed isotopic compositions. Using xenon as an example, the objective for Earth was to reproduce the composition of nonradiogenic terrestrial Xe. There the differences between the nonradiogenic and contemporary terrestrial Xe compositions in Table III were attributed to postescape outgassing of radiogenic daughter products $C_M^i(N)$ from ^{129}I and ^{244}Pu decay, as discussed in Section IV.A.2. The situation for meteorites differs only in that the isotopes $C_M^i(N)$ are considered to be *already present* in meteoritic carrier grains at the time when isotopes from the local gas phase were adsorbed on grain surfaces. Here $C_M^i(N)$ includes ^{129}I or its daughter ^{129}Xe , and H–Xe, an extrasolar nucleogenetic component (Pepin and Phinney 1978) contributing to the heavy meteoritic isotopes $^{131}\text{–}^{136}\text{Xe}$. Therefore, the objective for meteorites is to find an escape process which generates appropriate values of $f_{M'/M}(S)$ in a plausible astrophysical environment.

V.D.2. The Carbonaceous Chondrite Data Base

The composition of total Xe in CI chondrites from Table III is plotted in Fig. 12, normalized to the nonradiogenic terrestrial isotope ratios. The important feature of the Fig. 12 isotope pattern for the present discussion is the close match of the CI–Xe composition to solar Xe (U–Xe) at the light-shielded isotopes $^{124}\text{–}^{130}\text{Xe}$ where meteoritic contributions from H–Xe are absent. This implies that the bulk CI–Xe composition can be interpreted as originating

from the adsorption of unfractionated or lightly fractionated solar Xe on carrier grains containing the radiogenic and nucleogenic $C_M^i(N)$ components. (We will see later, in Fig. 16, that H–Xe addition to such a solar-derived component does in fact replicate the bulk CI composition in Fig. 12 at $^{131-136}\text{Xe}$.)

This apparent absence of significant escape fractionation does not extend to krypton. The relevant isotopic compositions are plotted in Fig. 11. A relatively severe fractionation of solar Kr is clearly required to generate the CI–Kr pattern. (It is interesting to note, in Fig. 5, that the E chondrite (South Oman) Kr isotope ratios fall along the lower boundary of the likely compositional field for solar Kr, and so, given present uncertainties, may be considered to be fractionated only slightly if at all. Although not pursued here, an escape model for the E chondrites, in contrast to the CI model, could therefore involve an initial crossover mass $m_c^0(\text{Kr})$ lying below the Kr mass range.)

The central modeling question for the CIs is whether the substantial isotopic differences between CI and solar Kr, Ar, and Ne can be understood in the context of an escape episode which only mildly fractionates solar Xe. And there is a further stipulation. Just as for Xe, one would expect to see evidence, in the meteoritic noble gas carriers, of a superposition of escape-fractionated solar gases adsorbed from the local environment onto grains containing nucleogenic or radiogenic $C_M^i(N)$ nuclides such as H–Kr, ^{40}Ar , Ne–A, and Ne–E (Section IV.B). Such evidence exists: the adsorbed gases are logically identified with the meteoritic Q-component, which appears to be sited on or near grain surfaces. A viable escape model must therefore be able to generate the observed isotopic characteristics of the Q-component.

The Q-component. Except for the H–Xe and radiogenic contributions to $^{131-136}\text{Xe}$ and ^{129}Xe , a component at ^{86}Kr which is probably associated with H–Xe, and ^{40}Ar from decay of ^{40}K , and Q-component comprises virtually all of the total inventories of Xe, Kr, and Ar in the carbonaceous carrier phase of the CI meteorites (Lewis *et al.* 1975, 1979, Alaerts *et al.* 1980, Wieler *et al.* 1989). Not so with Ne: here the Q–Ne inventory amounts to only a fraction of the total ^{20}Ne , first inferred by difference in oxidation experiments to be about 15% (Alaerts *et al.* 1980), or $^{20}\text{Ne}_Q \cong 4.2 \pm 1.7 \times 10^{-11}$ g/g-meteorite from the average CI ^{20}Ne content in Table II. This estimate was later confirmed by a direct measurement of Q-gases released in acid etching, which yielded $^{20}\text{Ne}_Q = 4.1 \pm 1.1 \times 10^{-11}$ g/g-meteorite (Wieler *et al.* 1989). Earlier estimates of Q–Ne composition were $[^{20}\text{Ne}/^{22}\text{Ne}]_Q = 10.3 \pm 0.4$ (Alaerts *et al.* 1980) and 10.1 ± 0.2 (Schelhaas *et al.* 1985); the direct and precise Wieler *et al.* (1989) experiment gave 10.65 ± 0.15 (and $[^{21}\text{Ne}/^{22}\text{Ne}]_Q \leq 0.0316$). The most recent

acid etch measurements (Wieler *et al.* 1990a,b) yield $[^{20}\text{Ne}/^{22}\text{Ne}]_Q = 10.75 \pm 0.15$ and $[^{21}\text{Ne}/^{22}\text{Ne}]_Q \leq 0.0300 \pm 0.0006$. These Wieler *et al.* (1989, 1990a,b) values for Q–Ne abundance and composition are adopted here, along with their Q–Ar ratio of $[^{36}\text{Ar}/^{38}\text{Ar}]_Q = 5.32 \pm 0.02$ (which is not distinguishable from the Table III average of 5.30 ± 0.05 in bulk CI meteorites, consistent with $\text{Ar}_Q \cong \text{total Ar}$). The central test for derivation of the Q-component from local (S-component) sources by a fractionation–adsorption mechanism is the extent to which escape-fractionated solar gases are able to fit the CI–Xe and CI–Kr isotopic compositions discussed above, and these isotope ratios for Q–Ar and Q–Ne.

V.D.3. Astrophysical and Geological Settings

As was the case for volatile evolution on Earth, Venus, and Mars, we need credible models of the astrophysical, chemical, and geologic conditions governing the escape process in order to make this test. However, assumptions about where, when, and how conditions for generation of observed volatile distributions may have developed are more speculative for meteorites than for planets. Open issues include the question of whether escape from meteorite parent bodies was involved, and if so the sizes and locations of these objects, the source and composition of their atmospheres, and the identity of the dominant atmospheric constituent (i.e., hydrogen or some heavier species); the timing of parent body accretion and evolution with respect to nebular dissipation and the accumulation of planets; and the energetics of the process and the nature and role, if any, of external energy sources such as the early sun. All these uncertainties unquestionably afford a wide latitude for modeling. Even so, it is interesting that a simple and robust model which accounts very well for Q-component isotopic distributions can be developed within them. In the approach discussed here, we assume a representative CI-carrier parent body at ≈ 3 AU, and suppose that the requisite fractionations were generated by hydrodynamic loss of an atmosphere containing isotopically solar noble gases. Two conjectures for the origin of such an atmosphere are considered: gravitational condensation of ambient nebular gases if the solar accretion disk was still present, or degassing from the body's interior.

Nebular capture. The temperature T_n and pressure p_n of an existing nebula at this heliocentric distance may be estimated, from Beckwith *et al.*'s (1990) observational survey of circumstellar disks (see Section VII.D.2), to have been ≈ 80 K and $\approx 3 \times 10^{-8}$ atm, respectively. It is readily shown, using the analytic expressions for gravitational atmospheric capture developed in Section VII.D.2, that condensation of surrounding gases to high enough surface pressures will not occur at these ambient condi-

tions unless the mass of the embedded body appreciably exceeds a lunar mass. The minor enhancements of nebular noble gas partial pressures on the surfaces of smaller objects cannot generate the high abundances observed in carrier grains of the CI Q-component by adsorption at plausible values of k_M . Moreover such atmospheres on bodies of any size are stable against loss until the back-pressure of the nebula is removed, and so escape and fractionation could only occur, and only once, during atmospheric blowoff at the time of nebular gas phase dissipation (Hunten 1979). Since we are interested here in considering much smaller parent bodies, on the order of 0.1 lunar mass or less and thus roughly comparable to present asteroidal masses, and do not wish to assume as necessities either the presence of nebular gases or single episodes of escape, we turn to the alternative of outgassed atmospheres.

Outgassing. Processing of CI-type noble gases on small parent bodies might be possible in a planetesimal environment similar to that considered by Donahue (1986). His model involves fractionation of pure, solar-composition noble gas atmospheres by Jeans escape from planetesimals in the $\sim 10^{24}$ – 10^{26} g mass range. Too small for effective gravitational gas capture from the nebula, these bodies are assumed to acquire their atmospheres by outgassing of noble gases adsorbed on accreted dust grains (Section VII.D.1). Donahue showed that if early accretional growth were rapid enough—from $<10^{24}$ g to $\sim 5 \times 10^{24}$ g in $\sim 30,000$ yr at $T \approx 160$ K, comparable to the timescales yielded by the Greenberg *et al.* (1978) collisional evolution models for growth to the $\sim 10^{24}$ g mass range—neither outgassed Ne nor any heavier species would be thermally lost from planetesimal atmospheres during this interval. Escape and fractionation of Ne and Ar occur in planetesimals that happen to grow much more slowly from this mass range to $\sim 10^{26}$ g, but not in objects that continue to accrete quickly. Mixtures of these two planetesimal types, with their noble gases still in the gas phase, then accumulate to form the terrestrial planets and their atmospheres. Problems with this approach to the origin of planetary noble gas distributions, specifically in accounting for atmospheric $^{36}\text{Ar}/^{38}\text{Ar}$ ratios and planet-to-planet variations in Kr and Xe elemental and isotopic compositions, were noted in Section I. In its present form Donahue's model does not address the origin of elemental and isotopic distributions of noble gases in meteorites. But perhaps it could, with modifications in the presumed source of degassed volatiles and their mode of escape from the planetesimal.

It seems rather unlikely, from current laboratory data, that any substantial amounts of volatiles were adsorbed on naked silicate or carbonaceous dust grains in the nebula prior to their accumulation into planetesimals (Section

VII.D.1). However the carbonaceous chondrites contain abundant water as well as noble gases, suggesting parent-body incorporation of icy matter that could have been markedly rich in occluded noble gases. At distances of ~ 3 AU or beyond and temperatures of ≈ 80 K, locally accreting material could have included relatively unaltered extrasolar grains from the parent molecular cloud. Let us suppose for this discussion that some small fraction of icy grain mantles acquired in the cloud environment still survived under these and earlier (infall) thermal conditions, and that the remnant ices contained Xe, Kr, and Ar—and possibly some Ne if cloud temperatures were low enough—condensed from ambient cloud gases (Greenberg 1978, 1982, Huss 1987, Huss and Alexander 1987). With the assumption that the gas-phase composition of the cloud was similar to that of the solar nebula, partial pressures may be estimated from average solar abundances (Table II) and the following speciation: all carbon as CO, half the balance of the oxygen (O minus C) as H_2O and the other half as Si, Mg, and Fe oxides (Prinn and Fegley 1989), hydrogen not in water as H_2 , nitrogen as N_2 , and all other species in elemental form. The mean molecular weight μ of this gas phase is 2.30 amu. Calculated partial pressures $P_M^i(S)$ of the noble gases and nitrogen for a total pressure p_n are given in Table V. With half the O not in CO available for H_2O , its partial pressure would be $\sim 2.6 \times 10^{-4} p_n$, and the ambient number densities of noble gases relative to water follow from the $P_M^i(S)$ values in Table V (e.g., $\sim 5.5 \times 10^{-8}$ for $^{130}\text{Xe}/\text{H}_2\text{O}$). At cloud temperatures of ~ 10 – 25 K these species would probably have condensed on mantle ices in proportions roughly similar to their ambient relative abundances, except perhaps for Ne where temperatures of <25 K are required for trapping in amorphous water ice (Bar-Nun *et al.* 1985).

Infrared spectroscopic observations suggest that a typical grain in a dense interstellar cloud consists of a 0.05- to 0.10- μm diameter refractory silicate-carbon core surrounded by an icy mantle of thickness comparable to the core radius (Allamandola 1984, Allamandola and Sandford 1988). About 45 wt% of the mantle, on average, is estimated to be water ice (Tielens and Allamandola 1987a,b), so water comprises $\approx \frac{1}{3}$ of the total grain mass. Therefore the noble gas inventories in a pristine grain could be very high, exceeding CI carrier concentrations—which are $\sim 12.5 \times$ higher than bulk meteorite concentrations (Lewis *et al.* 1979)—by ~ 1500 -fold for Xe and by larger factors for Kr and Ar. However, one would expect only small fractions of these initial inventories to survive shock during grain infall from cloud to accretion disk, residence for some period in the nebula, and accretional warming during planetesimal formation, all of which would promote evaporation and loss of volatile icy mantle constituents (Tielens and Allamandola 1987a).

In planetesimals accreting in part from this kind of

TABLE V
CI Meteorite Model Data, Assuming Initial Kr Composition = Solar Kr-1 (Table III)

	Mass M (amu)					Isotopes M'/M					
	130 (Xe)	84 (Kr)	36 (Ar)	28 (N ₂)	20 (Ne)	$\frac{124\text{Xe}}{130\text{Xe}}$	$\frac{78\text{Kr}}{84\text{Kr}}$	$\frac{36\text{Ar}}{38\text{Ar}}$	$\frac{15\text{N}^{14}\text{N}}{14\text{N}_2}$	$\frac{20\text{Ne}}{22\text{Ne}}$	$\frac{21\text{Ne}}{22\text{Ne}}$
	Partial pressures										
$P_M^i(S), P_{M'/M}^i(S)$ (nebula) ^a	1.43 $p_n(-11)$	1.60 $p_n(-09)$	5.72 $p_n(-06)$	7.75 $p_n(-05)$	1.76 $p_n(-04)$	2.947(-2)	6.359(-3)	5.8	?	13.7	3.27
$P_M^i(OG), P_{M'/M}^i(OG)$ (planetesimal surface) ^b	5.42(-34) $F_1^0 M_p^{1/3} \tau$	3.91(-32) $F_1^0 M_p^{1/3} \tau$	4.60(-29) $F_1^0 M_p^{1/3} \tau$	—	7.76(-30) $F_1^0 M_p^{1/3} \tau$	2.947(-2)	6.359(-3)	5.8	?	13.7	3.27
	Hydrodynamic escape fractionation factors										
$f_{M'/M}(OG)_R, f_{M'/M}(OG)_R^c$	8.047(-01)	6.697(-01)	3.190(-01)	2.438(-01)	1.384(-01)	0.97145	0.94031	0.92138	1.07443	0.78467	0.88
	Initial atmospheric partial pressures ($F_1^0 = 2.96 \times 10^{12} \text{ cm}^{-2} \text{ sec}^{-1}, M_p = 8 \times 10^{24} \text{ g}, \tau = 10^4 \text{ years}$)										
$P_M^i(OG), P_{M'/M}^i(OG)$ ^b	3.21(-09)	2.31(-07)	2.72(-04)	—	4.59(-05)	2.947(-2)	6.359(-3)	5.8	?	13.7	3.27
	Residual atmospheric partial pressures										
$P_M^i(RA), P_{M'/M}^i(RA)$ ^d	2.58(-09)	1.55(-07)	8.69(-05)	—	6.36(-06)	2.863(-2)	5.980(-3)	5.34	—	10.75	2.90
	Required partition coefficients for adsorption on planetesimal surface dust										
Required k_M ($k_{M'/M} = 1$) ^e	3.39(-02)	2.88(-03)	1.80(-04)	—	8.0(-05)	1	1	1	1	1	1
$C_M^f, C_{M'/M}^f$ (Q-gases, calculated) ^f	8.75(-11)	4.46(-10)	1.56(-08)	—	5.1(-10)	2.863(-2)	5.980(-3)	5.34	—	10.75	2.90
$C_M^g, C_{M'/M}^g$ (Q-gases, CI carrier phase) ^g	8.75(-11)	4.46(-10)	1.56(-08)	1.89(-02)	5.1(-10)	2.851(-2)	5.962(-3)	5.32	7.662(-3)	10.75	≤ 3.00
	Required partition coefficients for adsorption on nebular dust ($p_n = 4 \times 10^{-7} \text{ atm}$)										
Required k_M ($k_{M'/M} = 1$) ^h	1.53(+07)	6.97(+05)	6.82(+03)	6.10(+08)	7.24(+00)	1	1	1	1	1	1
$C_M^f, C_{M'/M}^f$ (Q-gases, calculated) ^f	8.75(-11)	4.46(-10)	1.56(-08)	1.89(-02)	5.1(-10)	2.947(-2)	6.359(-3)	5.8	—	13.7	3.27

Note. Subscript "R" designates Rayleigh escape. Powers of ten multipliers in parentheses.

p_n = total nebular pressure. $P_M^i(S)$ in atm for p_n in atm, $P_{M'/M}^i(S)$ in atom/atom.

$P_M^i(OG)$ in atmospheres for initial methane flux F_1^0 in No./cm²-sec, planetesimal mass M_p in grams, flux decay constant τ in years; $P_{M'/M}^i(OG)$ in atom/atom.

$\alpha_0(OG) = 1.00000, m_1 = 16. (m_2^0, m_2^f) = 255.0, 36.4 (Xe); 210.6, 32.6 (Kr); 165.0, 28.7 (Ar); 137.2, 26.3 (N_2); 104.5, 23.5 (Ne).$

$P_M^i(RA) = f_M P_M^i(OG), P_{M'/M}^i(RA) = f_{M'/M} P_{M'/M}^i(OG). P_M^i(RA)$ in atm, $P_{M'/M}^i(RA)$ in atom/atom.

Required $k_M = C_M^f[\text{Q-gases, CI carrier phase}]/P_M^i(RA)$. Units are g/g-meteorite/atm for k_M .

Units are g/g-meteorite for C_M^f , atom/atom for $C_{M'/M}^f$.

Tables II, III. Bulk CI noble gas abundances (Table II) multiplied by a factor 12.5 to reflect concentrations in CI carrier (residue) material (Lewis *et al.* 1979). A similar enhancement is assumed for the carrier phase. Average CI abundances and isotope ratios (Table III) assumed to represent CI_Q except for ²⁰Ne_Q (Table II, footnote b) and (³⁶Ar/³⁸Ar)_Q, (²⁰Ne/²²Ne)_Q, (²¹Ne/²²Ne)_Q (Table III, footnote c).

Required $k_M = C_M^f(\text{Q-gases, CI carrier phase})/P_M^i(S)$. Units are g/g-meteorite/atm for k_M .

source material, gravitational or radionuclide heating would liberate and drive volatiles from surviving grain mantles toward the surface of the body. A crucial difference between this and Donahue's (1986) model is the possible presence here of a large inventory of a light carrier gas that potentially could assist atmospheric blowoff of all the noble gases. In the planetary models discussed in Sections V.A–C this major atmospheric constituent was hydrogen, but the H₂ content of grain mantle ices is probably low (Tielens and Allamandola 1987a,b) and in this environment there is no obvious way to make it by photolysis or chemical reduction of water at the surface. Water itself is a candidate. However, at temperatures of ≈80 K (or even up to, say, double this if accretional heating (Section VII.D.2) was very substantial), outgassing H₂O would freeze in a layer of ice near the surface. Water vapor could still enter the atmosphere from the ice by sublimation or impact heating, but its steady-state vapor pressure would be much too low for it to comprise the initial light constituent abundance N_1^{og} needed for hydrodynamic escape (here and below, the superscript "og" is used to denote initial abundances, fluxes, and crossover masses at the time t_{og} of atmospheric outgassing). The ice layer would be thick—for the 8×10^{24} -g planetesimal chosen below to illustrate this model, on the order of 850 m for each 0.1 wt% of water mobilized to the surface and frozen. Subsurface circulation of liquid water could occur below this, consistent with mineralogic and chemical evidence for aqueous alteration in the CI and CM chondrites (Fredriksson and Kerridge 1988 and references therein).

From thermodynamic considerations, an attractive possibility for a light, relatively noncondensable, and abundant outgassed species is methane. Methane contents of grain mantle ices appear to be low to nil (Tielens and Allamandola 1987a). But at $T \cong 400\text{--}600^\circ\text{C}$ in the planetesimal interior—temperatures that do not seem too high for small bodies at early evolutionary stages, given the existence of basaltic meteorites and spectroscopic evidence for differentiated asteroids such as Vesta—the reaction $\text{C}[\text{graphite}] + 2\text{H}_2\text{O}[\text{gas}] + 2\text{Fe}[\text{metal}] \rightarrow \text{CH}_4[\text{gas}] + 2\text{FeO}[\text{in olivine}]$ is potentially important (Holloway 1988a,b). The first two reactants are certainly abundant in mantled interstellar grains. While there is no direct evidence for metallic iron (Allamandola, personal communication; Tielens and Allamandola 1987b), the small amount needed (probably ≤ 1 wt%—see below) could have been present in other accretional components. In what follows we will assume for illustration that an outgassed methane-rich atmosphere containing noble gases from grain mantle ices represents a possible initial state of volatile evolution on a meteorite parent planetesimal, and see where this takes us. Ambient nebular gases are not required to supply such an atmosphere. Whether they were present or absent, and what the absolute timing

of CI noble gas evolution relative to nebular clearing at t_0 might have been, are open questions.

V.D.4. An Escape–Adsorption Model for CI Noble Gases

To be useful, a planetesimal evolutionary model must have the same analytic capabilities as the planetary models (Sections V.A–C) for numerical calculation of fractionation factors over a range of free parameters in the escape equations. Thus both the escape mode of the abundant constituent N_1 —by Rayleigh distillation or at constant inventory—and the time dependence of the methane escape flux $F_1(t)$ must be specified. Of the two escape modes, Rayleigh loss is much more consistent with the presumed geologic and thermal character of the planetesimal environment. A thick ice layer in the shallow subsurface, inhibiting continuous outgassing, could have been penetrated by a large impact crater or an episode of "hot-spot" volcanism driven by the internal energy source. Interior gases would then vent to the atmosphere until the fissure cooled and resealed. Conditions for Rayleigh fractionation would be met as long as the duration of venting was relatively short compared to the timescale for subsequent atmospheric evolution—implying transient volcanism (i.e., rapid thermal evolution) or cratering events that were rare at the scale needed to penetrate the ice layer. Conditions leading to an approximately constant methane inventory appear considerably less probable. Maintenance of atmospheric CH₄ pressure by any kind of chemical buffering would be kinetically inhibited at low surface temperatures. Absent such a surface–atmosphere feedback, methane from the interior would have had to outgas through the ice barrier at a rate coincidentally equal to its escape flux from the top of the atmosphere.

The escape flux $F_1 = F_1^{\text{og}}f(t)$ must decline with time to produce the observed isotopic compositions in meteoritic noble gases by HEF of a degassed, isotopically solar parent reservoir. Flux decline was also required for the planetary models; there it was assumed to track the decay of the early solar EUV flux. But one cannot assume that solar EUV radiation necessarily played any role whatsoever in driving the evolution of these planetesimal atmospheres. Timescales for accumulation of bodies to the size range considered here could be rapid (Greenberg *et al.* 1978, Wetherill 1990a,b), although the physical mechanisms acting in the early stages of the process are uncertain (Weidenschilling 1988). Thus it is not unlikely that outgassing and loss of transient atmospheres occurred before the nebula dissipated or when postdissipation dust levels were still high, and the median plane was therefore opaque to solar EUV transmission. The energy input needed to drive escape from small bodies needed not have been large (see below). Potential sources include thermal equilibration of escaping gases with the local radiant energy

field, maintaining temperatures against the cooling effects of expansion, or heating from below by a planetesimal surface warmed to somewhat above ambient temperatures by release of accretional energy.

The physically most straightforward analytic description of atmospheric loss in the planetesimal model is one in which the escape flux is taken to be source-limited, rather than energy-limited as assumed in the planetary models. For a time-invariant atmospheric temperature this implies $F_1 \propto N_1$. With $1/\tau$ as the proportionality constant, $F_1 \equiv -dN_1/dt = N_1/\tau$, and $f(t) = F_1/F_1^{\text{og}} = \exp[-(t - t_{\text{og}})/\tau]$, so flux and inventory both decay with the same (exponential) time dependence. The parameter $\alpha_0(\text{OG}) \equiv F_1^{\text{og}}\tau/N_1^{\text{og}}$ is unity. The corresponding solution of Eq. (6), or of Eqs. (16) and (17) when $\alpha_0 \rightarrow 1$, is given by the simple expressions

$$\ln \frac{N_2}{N_2^{\text{og}}} = \ln \frac{N_1}{N_1^{\text{og}}} + \left[\frac{m_2 - m_1}{m_c^{\text{og}} - m_1} \right] \left[\frac{N_1^{\text{og}}}{N_1} - 1 \right] \quad (28)$$

and

$$\frac{N_1}{N_1^{\text{og}}} = \exp[-(t_2 - t_{\text{og}})/\tau] = \left[\frac{m_2 - m_1}{m_c^{\text{og}} - m_1} \right], \quad (29)$$

where “og” designates initial values at time t_{og} when escape of the planetesimal atmosphere begins. Equations (28) and (29) are utilized to calculate the fractionation factors \mathbf{f}_M and $\mathbf{f}_{M'/M}$ appearing in the evolutionary Eqs. (26) and (27), which for the Q-component alone may now be expressed as

$$C_M^i(Q) = \mathbf{k}_M[\mathbf{f}_M(\text{OG})[P_M^i(\text{OG})]] \quad (26')$$

and

$$C_{M'/M}^i(Q) = \mathbf{f}_{M'/M}(\text{OG})[P_{M'/M}^i(\text{OG})], \quad (27')$$

where “S” throughout Eqs. (26) and (27) has been replaced by “OG” to reflect the fact that we are dealing with an outgassed atmospheric component—which, however, is still assumed to be isotopically solar in accord with the hypothesis for its origin discussed above—and the grain-sited nucleogenetic contributions $C_M^i(N)$ deleted since they are assumed not to be in the gas phase.

Isotopic matching. Initial isotope ratios $P_{M'/M}^i(\text{OG})$ in Eq. (27') are solar (Table III); as in the planetary cases, solar Kr compositions are allowed to range from Kr-1 to Kr-2 within the Fig. 5 uncertainty field. So the only free variables available for isotopic fitting occur in calculating best-fit values of $\mathbf{f}_{M'/M}(\text{OG})$ from Eqs. (28) and (29). With $\alpha_0(\text{OG}) \equiv 1$, $m_1 = 16$ amu for methane as the light constituent, and using the values of b in Table I for diffusion in

O (Zahnle and Kasting 1986) as estimates for diffusion in CH_4 , there are just two of these: the initial (m_c^{og}) and final (m_c^f) crossover masses for one noble gas.

Despite this severe limitation on degrees of modeling freedom, Eq. (27'), for a one-stage episode of hydrodynamic loss described by a single pair of these two parameters for each choice of solar Kr composition, yields a notable result: agreement with observed Q-component isotopic distributions, within or very close to current measurement uncertainties, for most isotopes of all noble gases from Xe to Ne. Free and fixed parameter values for the Kr-1 case are listed in Table V (for Kr-2, $m_c^{\text{og}}(\text{Xe}) = 425$ amu and $m_c^f(\text{Xe}) = 37.1$ amu), and complete isotopic results for both Kr-1 and Kr-2 in Table IV. Noble gas isotopic evolutions from solar to Q-like compositions by escape fractionation are plotted in Figs. 15 and 16, where the shaded regions represent the spread in best-fit ratios derived for the two solar Kr compositions.

The calculated matches to Wieler *et al.*'s (1990a,b) measured $[^{20}\text{Ne}/^{22}\text{Ne}]_Q$ and $[^{36}\text{Ar}/^{38}\text{Ar}]_Q$ isotope ratios are quite good (Fig. 15). Their upper limit for $[^{21}\text{Ne}/$

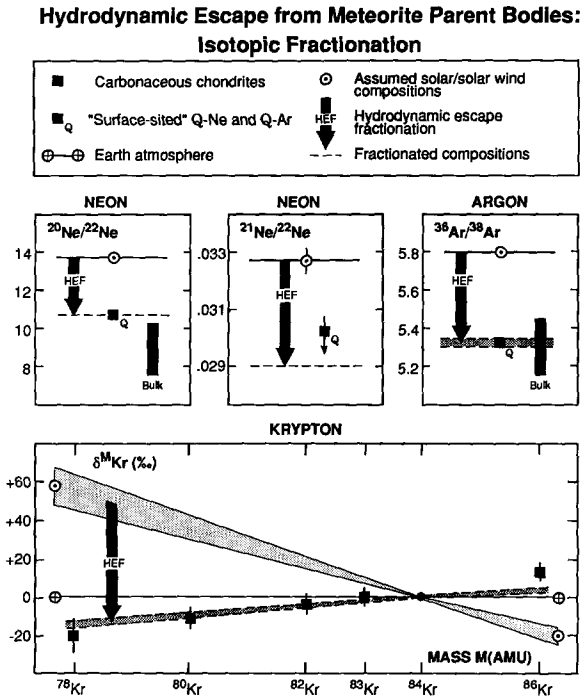


FIG. 15. Calculated isotopic compositions of Ne, Ar, and Kr (dashed lines) generated by hydrodynamic loss of a transient, isotopically solar atmosphere from a parent planetesimal for the Q-component carrier phase (Section V.D.4), compared to measured Q-Ne and Q-Ar isotope ratios, Ne and Ar isotopic ranges in bulk CI chondrites, and average chondritic Kr composition. Kr δ -values are referenced to terrestrial Kr, and the shaded ranges for solar and fractionated Kr are bounded by the Kr-1 and Kr-2 compositions. All data and references are listed in Tables III and IV.

Hydrodynamic Escape from Meteorite Parent Bodies: Isotopic Fractionation

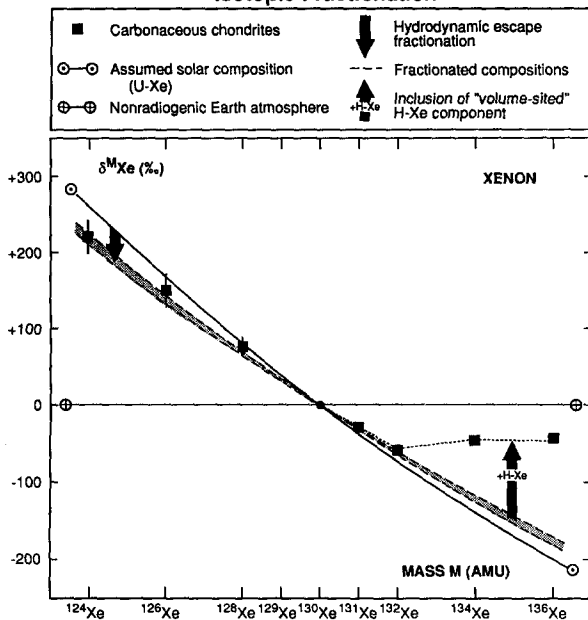


FIG. 16. As in Fig. 15, for Xe. The shaded range for fractionated Xe is again bounded by the two different assumptions for the composition of solar Kr. The indicated model fits to the heavy isotopes $^{131-136}\text{Xe}$ (dotted line) assume superposition of nucleogenetic H-Xe on the lightly fractionated solar Xe. A similar addition of monoisotopic ^{129}Xe from ^{129}I decay elevates measured $^{129}\text{Xe}/^{130}\text{Xe}$ (Table III CI data) above the calculated nonradiogenic composition shown here.

$^{22}\text{Ne}]_Q$ —the lowest (most spallation-free) values observed in their experiments (Wieler *et al.* 1990a)—is $\sim 3\%$ ($\sim 1.7\sigma$) above the calculated ratio of 2.90×10^{-2} . This discrepancy may not be particularly serious in view of the uncertainty in the initial solar ratio (Table III), and the possibility that the measurement includes some spallogenic ^{21}Ne (although contamination from this source is thought (R. Wieler, personal communication) to be very small if not completely absent).

The nucleogenetic component $C_M^i(N)$ at $^{131-136}\text{Xe}$ is H-Xe (Table III), sited within the carrier grains on which Q-Xe is adsorbed. Addition of this component (Eq. (27)) to the lightly fractionated solar composition comprising Q-Xe is seen in Fig. 16 to closely reproduce the measured bulk CI pattern. Deviations of observed and computed compositions at ^{86}Kr (Fig. 15) and ^{129}Xe (Table III) are respectively attributed to contributions from a nucleogenetic H- ^{86}Kr component associated with H-Xe, and decay of grain-sited ^{129}I . It must be noted, however, that the predicted Q-Xe (i.e., H-Xe-free) heavy isotope ratios $^{134,136}\text{Xe}/^{130}\text{Xe}$ in the shaded band in Fig. 16 have not been seen in experimental attempts to isolate and measure Q-Xe directly. Wieler *et al.*'s (1990a,b) estimates of the Q-Xe ratios at these isotopes from etching experiments

are only slightly lower than the plotted bulk ratios. Moreover, in their opinion, the presence of this H-Xe-like component (which they tentatively attribute to U- and Pu-derived fission Xe) is intrinsic to surface-sited Q-Xe, and not merely a contaminant released by overetching into H-carrier grains or otherwise an artifact of their experimental protocol. This observation may not necessarily pose a problem for the present model if these observed enhancements above the derived Q-composition at the heaviest isotopes really are due to gas-phase mixing with fission Xe from an external source, as suggested by Wieler *et al.* (1990b), and not to H-Xe degassed from carrier grain interiors and mixed with Q-Xe prior to adsorption on grain surfaces. The problem with this latter possibility is that it would then be necessary to account for the facts that (1) nucleogenetic components do exist in grain interiors, and (2) this kind of gas-phase homogenization apparently did not occur for Ne, since the Q and bulk $^{20}\text{Ne}/^{22}\text{Ne}$ ratios in Fig. 15 are different.

Relative elemental abundances. The evolution of relative noble gas abundances from their initial atmospheric composition to the observed Q-component pattern in CI carrier grains is tracked in Fig. 17, where all elemental ratios are normalized to solar. It is likely that an initial composition established by low-temperature occlusion in ices was depleted in Ne relative to solar ratios (Section V.D.3 above), and in fact could have resembled the composition of the primordial A_5 component on Venus, shown in Fig. 13a and also suggested to derive from a similar, icy planetesimal source (Section VI.D.2). Therefore, for illustration, the initial elemental composition of the out-gassed atmosphere is taken to be Venus-like. The final, observed Q-pattern is generated in two sequential stages: relative fractionation f_M/f_{84} of this initial composition during hydrodynamic loss, calculated from Table V values and represented by the unlabeled arrows in Fig. 17, followed by adsorptive fractionation ("AF" arrows) as residual atmospheric gases adsorbed on grain surfaces. The shaded region of Fig. 17 is just the laboratory data field from Fig. 6, but here normalized to the escape-fractionated compositions at the heads of the unlabeled arrows rather than to solar ratios. The AF arrows lie within this field, and so the relative adsorptive fractionations required to replicate the observed Q-pattern are consistent with laboratory measurements.

Absolute elemental abundances. Isotopic compositions of Q-component noble gases in the CI chondrites are non-solar, and their elemental abundances are large. These two characteristics of Q-gases have historically posed awkward problems for an earlier hypothesis for their origin—that they were adsorbed from the nebula itself onto nebular dust grains that were subsequently incorporated into meteorites. The basis for this proposition rested on

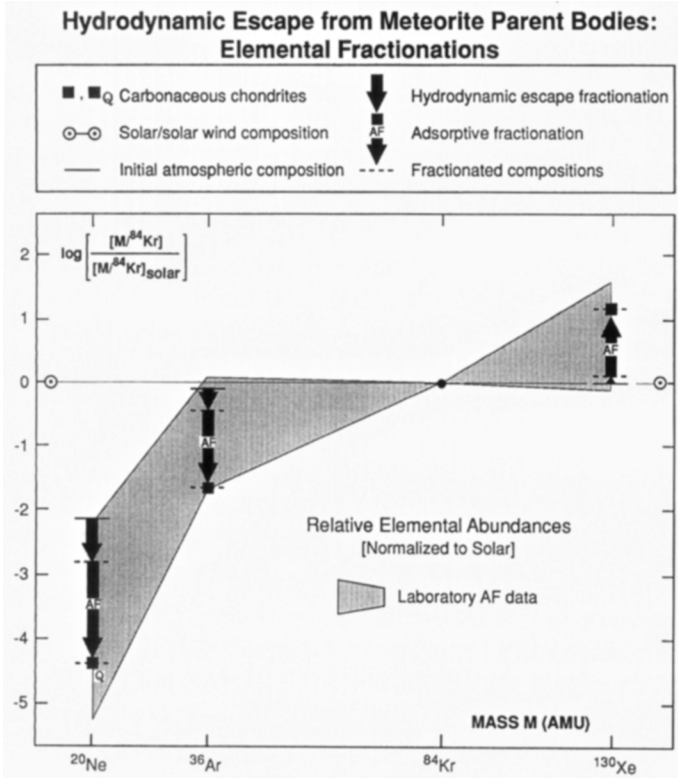


FIG. 17. Elemental noble gas fractionations in the escape-adsorption model for the Q-component carrier phase. Sequential fractionations by hydrodynamic escape (solid arrows) and adsorption ("AF" arrows) generate observed relative abundances. The shaded area is the Fig. 6 data field from experimental adsorption studies, here replotted with respect to the elemental ratios at the tips of the solid arrows since the ambient atmospheric composition from which adsorption occurs is that following hydrodynamic escape. All plotted ratios are normalized to the solar elemental composition.

the observation, illustrated in Fig. 6, that the relative abundance patterns in chondrites and in many laboratory adsorptive fractionation experiments display similar trends with mass.

Both problems are evident in the Table V listing of calculated $C_{M'/M}^f(Q)$ and k_M values for adsorption of the Q-component on nebular CI carrier grains at ~ 3 AU, utilizing a model-derived pressure at this heliocentric distance (Wood and Morfill 1988) of $p_n \approx 4 \times 10^{-7}$ atm, which yields corresponding partial pressures $P_{M'/M}^i(S)$ of nebular noble gases from the first line of Table V. First, ambient nebular gases are isotopically unfractionated in adsorption, and since there is no escape fractionation, $f_{M'/M}(S) \equiv 1$ and predicted Q-component isotopic compositions are therefore solar, in conflict with the observation that they are not. Second, at reasonable nebular pressures the distribution coefficients k_M required to match observed CI carrier abundances, calculated from Eq. (26') with $f_M \equiv 1$ and plotted in Fig. 18, are very much larger—by ~ 5 to 13 orders of magnitude for k_{130} —than

those yielded by current laboratory measurements. The highest experimental k_{130} , from data set (a), is still too low for the CI carrier by a factor $> 10^5$. One point of view could be that this distribution coefficient problem is simply an artifact of laboratory experiments that fail to replicate the conditions of time and grain growth under which gas trapping actually took place. Reservations about the degree to which a laboratory regime can represent time-dependent conditions and processes in the actual nebula are well-founded. The principal difficulty with arguments along this line, however, lies in the first point: they cannot account for the fact that Q-component isotopic compositions are nonsolar.

An alternative view, adopted here, is that the low values of k_M measured in the laboratory are at least roughly applicable to the natural regime. The large Q-carrier gas abundances then require that adsorption occurred in an environment where noble gas partial pressures were many orders of magnitude higher than in the open nebula. Nonsolar isotope ratios further require that these ambient gases be isotopically fractionated prior to adsorption. It

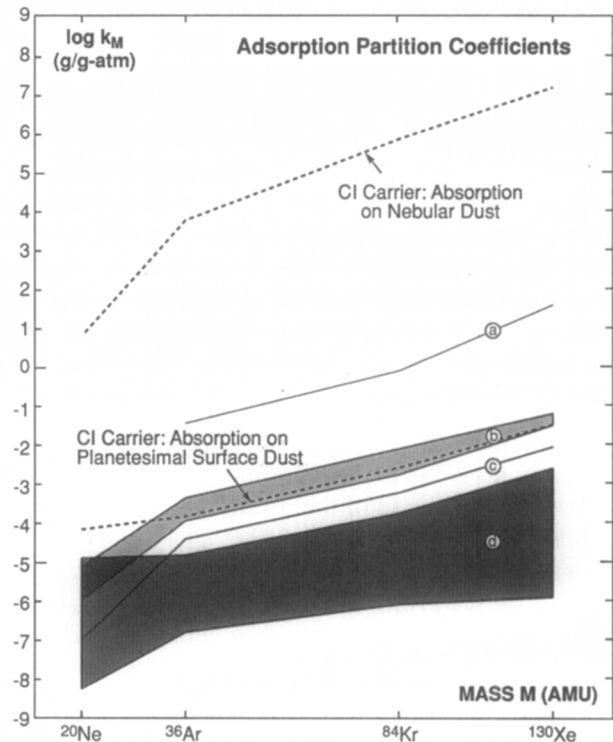


FIG. 18. Required gas \rightarrow solid partition coefficients k_M for adsorption of Q-component noble gas species M on CI carrier grains in the nebula, and on parent-body surface grains in the planetesimal model. Ranges of distribution coefficient values obtained in laboratory adsorption on a variety of substrates are plotted for comparison. Experimental data field (a) from Fanale and Cannon (1972); (b) from Niemyer and Marti (1981); (c) from Frick *et al.* (1979); and (d) from Yang *et al.* (1982), Yang and Anders (1982a,b), Wacker *et al.* (1985), Wacker and Anders (1986), and Wacker (1989).

appears from Figs. 15–17 that the planetesimal blowoff model can accommodate the isotopic demands, and yields realistic values of k_M/k_{84} for the fractionation of relative elemental abundances. In what follows we argue, with some additional assumptions, that this environment could account for high absolute abundances as well.

Using $\alpha_0(\text{OG}) \equiv F_1^{\text{og}}\tau/N_1^{\text{og}} \equiv 1$, and substituting a best-fit parameter value m_c^{og} from Table V together with planetesimal data from Table I into Eq. (9) for F_1^{og} , the initial methane inventory in the outgassed planetesimal atmosphere is found to be $N_1^{\text{og}} = F_1^{\text{og}}\tau = 2.96 \times 10^{12} \tau$. The initial noble gas loading of this atmosphere is not known ab initio; for illustration of roughly maximum loading a molar mixing ratio of 0.1 (see below) for the sum of all noble gas abundances has been used in calculating N_1^{og} , yielding a mole fraction of the principal constituent still near unity at $X_1 = 0.9$. With the assumption above of a Venus-like elemental composition, initial inventories N_M^{og} and surface partial pressures $P_M^i(\text{OG})$ for each of the noble gases can now be calculated for the Q-carrier parent body. Expressions for $P_M^i(\text{OG})$ are given in Table V as functions of F_1^{og} in $\text{No. cm}^{-2} \text{ sec}^{-1}$, τ in years, and the planetesimal mass M_p in grams.

As a specific numerical example, we take $M_p = 8 \times 10^{24} \text{ g}$ (about $4 \times$ the mass of Ceres) with a density of 2.6 g cm^{-3} (in the CI–CM chondrite range). It remains to estimate the mean flux decay time τ . Here we utilize Hunten's (1979) treatment of a polytropic approximation due to Gross (1974), in which the surface outflow velocity v_0 of a gravitationally unbound atmosphere from a body may be expressed in terms of the physical characteristics of the body and its atmosphere, a polytropic index α , and an energy input rate. The energy flux required to drive a methane escape flux of $2.96 \times 10^{12} \text{ cm}^{-2} \text{ sec}^{-1}$ out of the potential well of the planetesimal described above is $\sim 0.5 \text{ ergs cm}^{-2} \text{ sec}^{-1}$. With this and a ratio of specific heats γ anywhere between ~ 1.35 and 1.67 , simultaneous solution of Hunten's (1979) Eqs. (17)¹ and (18) (requiring $\alpha = 1.062$) and substitution of the resulting v_0 into his Eq. (19) yields $\tau \approx 10^4$ years.

This τ and the F_1^{og} and M_p values given above yield an initial Xe partial pressure on the CI body of $P_{130}^i(\text{OG}) = 3.4 \times 10^{-9} \text{ atm}$ (which in the open nebula would require $p_n \approx 240 \text{ atm}$). The partial pressure of Xe after escape is $P_{130}^i(\text{RA}) = f_{130} P_{130}^i(\text{OG})$, where "RA" denotes residual atmosphere, and from $k_M = C_M^f(\text{CI}_Q)/P_{130}^i(\text{RA})$ and Table V data the required value of k_{130} for subsequent adsorption is 3.2×10^{-2} , more than eight orders of magnitude lower than for adsorption in the nebula. Distribution coefficients for adsorption on planetesimal surface dust, calculated in this way for all the noble gases, are listed in Table V and plotted in Fig. 18, where they fall amid the laboratory

data fields and show mass dependences that are generally congruent with experimental patterns.

For the one case in Fig. 18 that does appear somewhat anomalous—the high value of k_{20} relative to k_{36} —it is interesting to note that the k_{20}/k_{36} ratio of ~ 0.5 is not greatly below the average of ~ 1.4 (2.6 in their units) measured by Wacker and Anders (1986) and Wacker (1989) for adsorption on carbon black. Wacker and Anders (1986) considered this value "much too large" to be compatible with planetary and meteoritic data. In the present model, however, the perspective is different: a large k_{20} is *required* because of the sharp Ne depletion assumed in the initial atmosphere from which Q–Ne derived.

Mass balances. The planetesimal model, given its assumptions, appears capable of reproducing the isotopic and elemental mass distributions of noble gases observed in the CI carrier phase. The next question is whether the amounts of initial and end-product volatiles in the model are reasonable, in terms of demands on their assumed sources and the quantities of CI carrier materials produced. These mass balance considerations are illustrated for the $M_p = 8 \times 10^{24} \text{ g}$ planetesimal, which with $\rho = 2.6$ has a radius of about 900 km (Table I).

With $\tau = 10^4 \text{ yr}$ and $X_1 = 0.9$, the initial atmospheric inventory of outgassed CH_4 is $N_1^{\text{og}} = F_1^{\text{og}}\tau = 9.3 \times 10^{23} \text{ particles cm}^{-2}$ ($\sim 1.6 \text{ mbar}$) or $\sim 2 \times 10^{-8} \text{ moles/g-planetesimal}$. To produce this by Holloway's (1988a,b) reaction (Section V.D.3 above) in the interior would require only about 0.2 ppm graphite, 0.7 ppm water, and 2 ppm metallic iron in the planetesimal as a whole. Concentrations of all three reactants would still be $\leq 2\text{--}3 \text{ wt\%}$ even if heating to the required temperatures of $400\text{--}600^\circ\text{C}$ was confined to the inner 1% of the body's mass and the outgassing efficiency was only 1%. Water requirements at this low level leave much room for the massive losses of grain mantle ices that would be expected during grain infall shock heating, preaccumulation residence in the accretion disk, and degassing and loss from impacting materials during planetesimal accumulation.

The mole fraction of noble gases outgassed to the planetesimal atmosphere was taken for illustration to be 0.1, with the balance methane. The distribution coefficients calculated above depend critically on this initial mixing ratio, since k_M values scale inversely with atmospheric abundances and would be much higher if the noble gases were merely trace constituents. Only one possibly relevant estimate of its assumed value comes to mind. For a Venus-like elemental composition, a 0.1 mole fraction translates to an initial atmospheric ^{130}Xe inventory $N_{130}^{\text{og}} = 2.3 \times 10^{17} \text{ atoms cm}^{-2}$ and a $^{130}\text{Xe}/\text{CH}_4$ ratio of 2.5×10^{-7} by number. Because two water molecules are consumed for each methane molecule generated in Holloway's reaction, the implied $^{130}\text{Xe}/\text{H}_2\text{O}$ ratio in the source

¹ There is a typographical error in Hunten's (1979) Eq. (17): the exponent written as $(-5-3\alpha)/(\alpha-1)$ should be $(5-3\alpha)/(2(\alpha-1))$.

is $\sim 10^{-7}$ if xenon and methane degassed with the same efficiency, remarkably close to the estimate in Section V.D.3 of $\sim 5 \times 10^{-8}$ for this ratio in the molecular cloud gas phase and in grain mantles. So this calculation, while naive, does suggest that noble gas mole fractions on the order of ≈ 0.1 might have been reached.

It is useful to apply the same reasoning to other grain mantle constituents that could have been outgassed to the planetesimal atmosphere. According to Tielens and Allamandola (1987a) the major molecular composition of a typical icy grain mantle is water/methanol/ammonia/carbon monoxide $\cong 1/0.66/0.05/0.05$. Methanol and ammonia would have been miscible in mobilized liquid water and frozen with it near the planetesimal subsurface, but the CO component could have been swept into the atmosphere along with the methane. The CO/CH₄ ratio, however, would be about 0.1, too small to substantially increase the mean atmospheric molecular weight.

It is clear that the estimates above yield lower limits to the degassed atmospheric inventories of noble gases and CO, since it is assumed that they derived only from a core reservoir in which water was chemically destroyed and methane generated. The planetesimal mantle above this volatile-rich core may well have been depleted in these species, since the increasing impact energies of accreting material, although small (on the order of ≥ 10 cal/g for $M_p \geq 10^{23}$ g and infall at escape velocity), could still have mobilized highly volatile noncondensable gases from grain ices and promoted their loss from the small growing body. But if some of these gases survived in the overlying mantle and upwardly migrating volatiles entrained and swept them out, methane could easily have become only a minor component of the planetesimal atmosphere. In this case blowoff could still have occurred, but more energy would have been needed to implement the escape since the major outflowing constituent, say CO, was more massive.

The mass of Q-carrier material produced could be relatively high. The available atmospheric column density of ¹³⁰Xe following escape is $f_{130} N_{130}^{\%} \cong 1.9 \times 10^{17}$ atoms cm⁻². If totally absorbed on regolith grains this would generate carrier abundances in a surface layer ~ 2 km deep, assuming a carrier density of 2.2 g cm⁻³. After dilution by a factor of ~ 12.5 with gas-poor phases, the maximum "CI-chondrite" yield would be roughly 25 km or about 7% of the planetesimal mass. Multiple outgassing-blowoff-adsorption episodes, occurring as the body accumulated and fresh material buried previously-loaded carrier grains, could have significantly increased this yield.

V.D.5. Adsorption, Fixation, and Comparison with Observed Distributions

The reasonably good replication of isotopic and elemental abundances in CI carrier grains discussed above is

necessary but not sufficient to establish the viability of this model. Here we explore in more detail the probable nature of the planetesimal surface environment and the processes acting within it over relevant timescales, note the characteristics that might be expected for volatile distributions that derived from it, and compare these with observation.

Adsorption of ambient gases. Evidence from meteorites, the Moon, and experimental and theoretical studies of regolith formation points to planetesimal regoliths that were thick and dynamically active (Housen *et al.* 1979, Langevin and Maurette 1980), exposed both to a flux of impacting bodies that cratered, heated, and overturned surface materials to various depths, and to solar wind, flare, and photon irradiation once the nebula had cleared. Even before nebular dissipation it appears that this environment would not have been a favorable one for survival of grain-mantle ices and the highly volatile species trapped within them, except perhaps during low-energy accretion of the planetesimal core. It seems more likely that these grain-mantle gases would have been largely mobilized and ejected by impact from the surface and atmosphere of the growing body prior to eruption of core volatiles through the subregolith ice layer.

Gas perfusion into the porous structure of the uppermost regolith and adsorption on receptive grain surfaces would have begun as soon as this erupted atmosphere was emplaced, and continued throughout the blowoff phase and beyond. What kind of noble gas mass distribution would we then expect to see in a sample derived from this regolith at some later time? Two hypotheses for the behavior of adsorbed grain-surface volatiles bear on this question. Suppose first that noble gases, once adsorbed, could still exchange with ambient gases. If the exchange rate in the planetesimal environment was faster than or comparable to the rate of atmospheric evolution, adsorbed isotopic patterns would track those of the ambient phase. For a given grain they would reflect the full degree of atmospheric fractionation attained up to the time of its last exposure. Individual grains in a representative sample of the regolith should then exhibit isotopic signatures ranging from near-solar to fully fractionated, with their mixing ratio depending on the distribution of times at which grains were finally isolated from the atmosphere by deep regolith gardening or consolidation into impact breccias.

Alternatively, we may suppose that noble gases, once adsorbed, do not exchange with the gas phase as ambient partial pressures decrease, but that grains instead "remember" their highest pressure exposure (Yang *et al.* 1982, Yang and Anders 1982a). Here a similar range of isotopic patterns might be anticipated, but now with a mixing ratio controlled by the rate at which fresh grain surfaces were created or exposed by comminution or excavation during and following atmospheric blowoff. One

might expect fractionated noble gases to dominate the adsorbed Q-component in either scenario if the episode of hydrodynamic escape was followed by a relatively long period of active cratering, comminution, and regolith overturn that exhumed a high proportion of older grain surfaces or created many new ones.

Fixation of adsorbed gases. Q-component noble gases in chondrites are both retentively bound, generally with release temperatures above 1000°C in vacuum pyrolysis, and apparently surface-sited since mild oxidation removes little of the carrier material but most of the gases (Yang *et al.* 1982, Wacker *et al.* 1985, Zadnik *et al.* 1985, Wacker and Anders 1986, Wacker 1989, and references therein). Experiments by the Chicago group (data field (d) and references in Fig. 18) show that much of the gas adsorbed from an ambient atmosphere at a given temperature in the laboratory is loosely held and rapidly desorbs under vacuum at the same temperature. Their relatively low k_M values are calculated from the tightly bound residual component. It seems clear that desorption and loss of a substantial fraction of gases adsorbed on regolith grains at ≈ 80 K would likewise occur during the postejction history of this material—in effect requiring higher k_M than shown in Fig. 18 for the Q-carrier planetesimal model—*unless* loosely bound gases were somehow “fixed” by transfer into retentive surficial sites prior to vacuum exposure.

A number of fixation processes have been proposed to account for the high thermal retentivity of trapped noble gases in meteoritic carriers. These include occlusion of physisorbed gases during grain growth, trapping by physisorption in interior micropore structures of meteoritic carbon grains, and diffusion (Fanale and Cannon 1972, Yang *et al.* 1982, Yang and Anders 1982b, Zadnik *et al.* 1985, Wacker and Anders 1986, Wacker 1989). However, it may be that a different mechanism, fixation of loosely bound adsorbed gases into retentive grain-surface sites by impact shock in the regolith, was important in the planetesimal environment.

Laboratory investigations by Bogard *et al.* (1986) and Wiens and Pepin (1988) demonstrate that shock implantation of ambient gases into solid surfaces is both efficient and nonfractionating at shock pressures as low as 20 kbar. Gases so injected are tightly bound against thermal release. Bogard *et al.* (1986) found that even for 20-kbar shock, about 50% of the implanted Xe is held to $T \geq 1000^\circ\text{C}$ under vacuum pyrolysis. Neither set of studies directly addressed the emplacement of surface-adsorbed volatiles, as distinguished from ambient gas phase species. However, it is clear from data obtained by Wiens and Pepin (1988) that organic carbon and nitrogen contaminants adsorbed on grain surfaces prior to shock were efficiently and retentively implanted. Thus it seems likely that shock would have been effective in fixing physisorbed noble gases in a cold, actively cratered planetesimal rego-

lith. In one possible scenario, these gases might first have migrated into carbon grain structure “labyrinths” as suggested by Wacker and Anders (1986) and Wacker (1989), and then been embedded in micropore walls by local concentrations of shock energy.

Comparison with observation: Isotopic distributions in carbonaceous chondrites. Calculated isotopic compositions of noble gases in the fractionated, postblowoff planetesimal atmosphere are in agreement with Q-component compositions in bulk CI chondrites. This requires that most of the gases in meteorites that subsequently derived from the planetesimal regolith were adsorbed and fixed in carrier grains after termination of hydrodynamic escape. But as discussed above it seems likely that signatures of more solar-like compositions should have survived in some population of grains that adsorbed and retained gases from earlier and less fractionated stages of atmospheric evolution. In this context we note several observations from carbonaceous chondrites. A few of these meteorites (e.g., Nawapali, Nogoya Dark, and Pollen among the CMs, and Mokoia and Vigarano among the CV3s) contain large amounts of solar-like Ne with $^{20}\text{Ne}/^{22}\text{Ne} > 11$ (Mazor *et al.* 1970), usually and probably correctly attributed to solar wind irradiation of their parent-body regoliths although direct confirming evidence in the form of solar wind ion tracks is often lacking. But others, notably Alais (CI), Orgueil (CI), and Murray (CM), show large differences in $^{20}\text{Ne}/^{22}\text{Ne}$ in samples with comparable amounts of ^{20}Ne —e.g., from ~ 7 to 10.5 in separate bulk samples of Murray (Black and Pepin 1969), and from ~ 7.5 to 11 in Orgueil (Mazor *et al.* 1970). These variations do not appear to be due to mixing with variable amounts of volume-sited Ne-E, with low $^{20}\text{Ne}/^{22}\text{Ne}$ (Fig. 3), for two reasons: Ne-E tends to be homogeneously distributed in bulk samples (Black and Pepin 1969), and Mazor *et al.* (1970) found that increases in $^{20}\text{Ne}/^{22}\text{Ne}$ in carbonaceous chondrites correlate roughly with increases in $^{36}\text{Ar}/^{38}\text{Ar}$. This kind of isotopic variability could in principle arise either from the presence of variable amounts of a solar-wind component or, equally well, from inhomogeneous mixing of grains that sampled the planetesimal atmosphere at different times in its isotopic evolution from solar to a fully fractionated composition.

Comparison with observation: Distribution of the CI-type noble gas carrier. Noble gases characterized by isotopic and relative elemental abundances remarkably similar to those in the CI carrier discussed here are found in many other types of meteorites ranging from ureilites to ordinary chondrites (e.g., Wieler *et al.* 1990b and references therein). Even the enstatite chondrites, in addition to their distinctly different—and differently sited—“sub-solar” component (Crabb and Anders 1981, 1982), contain a second noble gas component which resembles CI compositions both elementally and (as far as can be determined) isotopically, and is probably located, as are the CI

gases, in a carbonaceous carrier. Thus it seems probable that a common carrier of CI-type gases was widely distributed in the early Solar System and was a constituent of source materials for many meteorite classes.

In this context, an important feature of the model described here is the decoupling of Q-gas carrier grains from any necessarily unique association with the CI meteorites. It is true that the compositional and geological nature of their proposed parent planetesimal(s) has several features in common with what one might anticipate for a CI parent body—e.g., high contents of water and carbonaceous matter supplied by icy mantle materials, and the possibility of subsurface hydrothermal circulation at relatively high temperatures under the cap of a surficial ice layer. Moreover the close spatial association of putative CI-like subsurface matter with the surface carrier-grain reservoir in this planetesimal model suggests that the CIs could well have incorporated, on average, a relatively high abundance of the noble gas carrier—which, in fact, they have. But since the Q-carrier grains are produced on or near the surface, they are also vulnerable to ejection and dispersal through space during the subsequent collisional history of the body.

There is no reason to believe that nature constructed only one of these objects, nor that atmospheres on other bodies with somewhat different physical, chemical, and environmental properties (masses, temperatures, atmospheric mixing ratios, relative abundances of nucleogenic components, energy inputs and the like) followed precisely the same evolutionary track as the prototype planetesimal considered here. It seems more likely that noble gas carrier grains were formed on a distribution of parent bodies, and on each of these were characterized by differing relative and absolute abundances of adsorbed gases, and isotopic compositions ranging from underfractionated to overfractionated with respect to observed Q-gases. Therefore the presence of compositionally near-uniform noble gases in a wide variety of meteorite classes appears to require that compositionally diverse carrier grains from these separate sources were homogenized by ejection and mixing in a collisionally active planetesimal environment. The various meteorite parent bodies would then have acquired their averaged common gas carrier from a dispersed and well-mixed dust reservoir.

VI. PLANETARY ENERGY DEMANDS, EVOLUTIONARY TIMESCALES, AND HYDROGEN AND NOBLE GAS REQUIREMENTS

Model parameters deduced from best compositional matches to planetary volatile distributions also define requirements for the chronology of atmospheric evolution and planetary outgassing relative to the age of the sun, and for the solar EUV energy levels and the inventories

and losses of the principal atmospheric constituent—assumed to be molecular hydrogen—needed to implement the escape episodes. From such information one can assess the model on grounds other than its ability to replicate observed mass distributions, by comparison with observational evidence, other models, and conjectures relating to the timescales for origin and evolution of primary and degassed planetary atmospheres, the evolution of solar activity, and the nature and abundance of potential early sources of hydrogen. Implications of model parameter values in these areas are discussed in this section.

VI.A. Estimates of Initial EUV Energy Deposition

Direct observations of young stellar objects near one solar mass indicate that fine circumstellar dust tends to disappear from most of them somewhere in the ~ 0.1 - to 10-million year stellar age interval populated by both the classical T-Tauri stars and the naked T-Tauri stars that presumably evolved from the CTTS by dissipation of accretion disks (Strom *et al.* 1988, 1989a,b, 1991, Walter *et al.* 1988, Walter and Barry 1990). These observations provide astronomical estimates of the *earliest* time for nebular clearing of both dust and gas to the low levels required for penetration of solar EUV irradiation to planetary distances in the early Solar System, and were one consideration in the choice of an initial time $t_0 = 50$ myr in the present model.

The energy demands of the planetary models in Sections V.A–C are defined by Eq. (11) in terms of the ratio Φ_{EUV}^0 of solar EUV flux at initial time t_0 to the present flux $\phi(t_p)$. Of the variables in Eq. (11), the initial crossover masses m_c^0 determined by isotopic matching are listed in Tables AI–AVI, and $m_1 = 2$ amu for hydrogen. It remains to estimate β^3 , ε , and $\phi_{\oplus}(t_p)$. Plausible estimates are a hydrogen escape level r equal to twice the planetary radius r_s , giving $\beta^3 \equiv (r/r_s)^3 = 8$; a solar EUV heating efficiency $\varepsilon \sim 0.3$ – 0.5 ; and a present-day globally averaged EUV flux $\phi_{\oplus}(t_p)$ at Earth of ~ 0.3 – 0.6 ergs $\text{cm}^{-2} \text{sec}^{-1}$ (Hunten *et al.* 1989, Zahnle and Walker 1982, Roble 1977). The product of these parameter values is close to unity. Note, however, the sensitive dependence on β .

With $\phi_{\oplus}(t_p)\varepsilon\beta^3$ assumed to be 1, required values of Φ_{EUV}^0 were calculated from Eq. (11) for each of the planetary models considered in this paper and are listed in Table VI. They are all below ~ 450 , and therefore point to EUV flux enhancements at $t_0 = 50$ myr that are lower by factors of ~ 2 or more than the measured X-ray enhancements of $\Phi_X^0 \cong 1000$, in accord with the expectation discussed in Section III.B.3. Required η from Eq. (11) is ≤ 780 at 50 myr; t_0 could be increased to as long as ≤ 120 myr without exceeding the value of $\eta \cong 1700$ inferred for the X-ray flux. The conclusion that enough solar EUV energy to drive escape was in fact available rests on direct observa-

TABLE VI

Timescales t , Initial Relative EUV Intensities Φ_{EUV}^0 and Hydrogen Fluxes F_1^0 , and Inventories N_1 of the Dominant Light Constituent (Hydrogen for Planets, Methane for the CI Carrier Parent Body) for Stages of Atmospheric Evolution by Hydrodynamic Escape in the Various Models Discussed in the Text

Model	τ (myr)	t_0	t_{og}	t_v	t_f	Φ_{EUV}^0	F_1^0 (No. $\text{cm}^{-2} \text{sec}^{-1}$)	N_1^0	N_1^{og}	N_1^f	ΣN_1	$\Delta \text{H}_2\text{O}$ (g/g-planet)
Model I: Baseline noble gas planetary models												
Venus I	90	≈ 50	—	—	≥ 346	448	4.78(14)	1.33(30)	—	$\leq 2.68(28)$	1.33(30)	0.0377
Earth I	90	≈ 50	143	—	258	448	2.14(14)	4.63(28)	1.58(29)	9.69(26)	5.49(29)	0.0140
Mars I	90	≈ 50	342	—	372	448	4.52(14)	9.28(29)	1.42(28)	1.40(25)	9.42(29)	0.0636
Model I: Special cases												
Earth Ia ^a	90	≈ 50	75	—	183	211	1.01(14)	6.41(27)	1.54(29)	1.71(27)	2.23(29)	0.0057
Earth Ib ^b	90	≈ 50	143	—	251	226	1.08(14)	2.33(28)	7.71(28)	8.74(26)	2.75(29)	0.0070
Mars Ia ^c	90	≈ 50	342	—	372	448	4.52(14)	9.48(29)	1.42(28)	2.08(25)	9.62(29)	0.0650
Mars Ib ^d	90	≈ 50	342	—	372	448	4.52(14)	1.18(30)	1.42(28)	1.40(25)	1.19(30)	0.0803
Model II: Combined C–N–noble gas planetary models												
Venus II	90	≈ 50	—	205	≥ 306	270	2.89(14)	7.95(29)	—	$\leq 2.21(28)$	7.95(29)	0.0224
Earth II	90	≈ 50	97	205	209	270	1.29(14)	2.12(28)	1.56(29)	1.71(27)	3.06(29)	0.0078
Mars II	90	≈ 50	297	—	327	270	2.73(14)	4.02(29)	1.42(28)	1.65(25)	4.16(29)	0.0281
Planetesimal Model: Carbonaceous chondrite noble gases												
CI Carrier Parent body ^e	≈ 0.01	?	[$t_f - t_{\text{og}} = 0.024$]			—	2.96(12)	—	9.33(23)	8.42(22)	9.33(23)	—

Note. Subscripts and superscripts designate times and inventories at the beginning (0), at outgassing (og), at veneer addition (v), and at the end (f) of the process. ΣN_1 represents the total light constituent inventory needed to implement the escape episodes on each body, and $\Delta \text{H}_2\text{O}$ the amount of accreted water that would be required to supply ΣN_1 . Powers of ten multipliers in parentheses.

^a Variant of the baseline Earth I model in which 40% of the final Xe inventory is derived from outgassing (Section VII.A).

^b Variant of the baseline Earth I model in which escape temperature is assumed to be 3000 K (Section VII.B).

^c Variant of the baseline Mars I model in which a Venus-like “solar” A_s component is added to the CI gases in the initial atmosphere (Section V.B.4).

^d Variant of the baseline Mars I model in which the CI–Xe content of the primary atmosphere is reduced by a factor of 800 (Section VI.C.2).

^e Model in which the atmospheric methane mole fraction $X_1 = 0.9$, $T = 80$ K, and parent body mass $M_p = 8 \times 10^{24}$ g (Section V.D.4).

tions of young solar-type stars at bracketing wavelengths and is thus reasonably firm.

VI.B. The Timing of Evolutionary Stages

Here we wish to calculate the times, relative to the onset of hydrodynamic escape at t_0 , at which major subsequent phases of atmospheric evolution were initiated by outgassing or veneer accretion, and terminated by depletion of the light gaseous constituent. These may be calculated from Eq. (13), which, with $\tau = 90$ myr and m_c^0 from Tables AI–AVI, yields $t_{\text{og}} - t_0$, $t_v - t_0$, and $t_f - t_0$ upon respective substitution, for m_2 , of Table AI–AVI values of m_c^{og} , m_c^v , and m_c^f .

VI.B.1. Planetary Outgassing

Calculated chronologies for the major stages of atmospheric development in each of the planetary models are set out in Table VI. Outgassing times for Earth range from 75 myr (Model Ia, Section VII. A) to 143 myr for Earth I.

A relevant question is whether these rather long delays are compatible with current geophysical and geochemical estimates of evolutionary timescales. One could argue that they are not. Metallic core formation, for instance, is presently viewed as initiating during planetary accretion, and early disruption of a planetary core reservoir for the OG_1 component (Section VII.D.2) would therefore be expected (Stevenson 1981). This could perhaps have led to outgassing of their contents on rather short timescales. However, such an inference requires prompt thermal equilibration and degassing of the core fragments, contrary to Stevenson’s (1981) view (Section VII.A), and rapid rates of subsequent gas transport from the deep interior, for which no firm arguments exist.

On the geochemical side, current interpretations of radiogenic xenon distributions in the terrestrial mantle and atmosphere (e.g., Thomsen 1980, Allègre *et al.* 1987, and references therein) require early outgassing of the bulk of the Earth’s atmosphere, within ~ 100 myr or less. It should be noted, however, that these interpretations are ques-

tionable in the context of the present model, since they presume that all nonradiogenic and radiogenic Xe currently in the atmosphere outgassed from the mantle, contrary to a central assumption made here (Sections II.A, V.B.1, VII.A). They also assume that all radiogenic ^{129}Xe now in the atmosphere–mantle system was generated by decay of live ^{129}I in the mantle, which would not have been the case, as noted in Section V.C.4, if a late accreting E chondrite-like veneer contributed substantial amounts of ^{129}Xe to the atmosphere. There is no rigid constraint on timescales from argon chronology. Terrestrial argon isotope systematics allow most of the present atmospheric inventory of the nonradiogenic isotopes ($^{36,38}\text{Ar}$) to be degassed up to $t_{\text{og}} \sim 500$ myr or even somewhat later (Hamano and Ozima 1978).

Mars degasses substantially later than Earth in these models (Table VI). Isotopic observations potentially bearing on the question of outgassing chronology, from the SNC meteorites, are not incompatible with these longer timescales. Ott and Begemann (1985) and Ott (1988) have pointed out that the nonatmospheric Xe component in the SNCs is characterized by a $^{129}\text{Xe}/^{130}\text{Xe}$ ratio significantly lower than that in the Martian atmosphere. The fact that just the opposite distribution is observed for mantle-derived rocks vs the atmosphere on Earth has been used, as noted above, to argue for separation and outgassing of the terrestrial atmosphere from the mantle within a few half-lives of 17 myr ^{129}I . It is clear from Ott and Begemann's observation that this argument cannot even be made for Mars if nonatmospheric Xe in the SNCs is taken to represent Martian mantle compositions. In the present model, where most of the nonradiogenic atmospheric Xe on all three planets is not outgassed but is instead a remnant of their primary atmospheric Xe, preferential addition of radiogenic ^{129}Xe to a highly depleted residual atmosphere on Mars, as discussed earlier in Section V.C.4, appears to be a credible explanation for this kind of mantle–atmosphere distribution. The long model timescales in Table VI for outgassing of nonradiogenic atmospheric constituents on Mars are therefore not constrained by radiogenic Xe (or Ar) systematics. It is interesting to note, in the context of implied thermal histories for Mars, that degassing of nonradiogenic species, besides taking longer, may also have been inefficient compared to that of Earth (Section VII.D.2).

Outgassing contributions to the massive atmosphere on Venus, in amounts comparable to those degassed from Earth, would have left no signatures detectable with current abundance or isotopic data (Section V.B.2). Therefore the present model yields no information on when, if at all, substantial outgassing might have occurred.

VI.B.2. Veneer Accretion

A veneer of E chondrite-like material, explored in Model II as a possible source of surface carbon and nitro-

gen on Earth and Venus, was assumed in Section V.C.1 to be added to Earth at a time t_v such that veneer nitrogen isotopes were fractionated, in subsequent hydrodynamic escape, from the E chondrite to the terrestrial $^{15}\text{N}/^{14}\text{N}$ ratio. This requirement sets the value of m_c^v in Table AII, and yields $t_v = 205$ myr from Eq. (13). Veneers were assumed to accrete simultaneously on both planets, but as noted previously could have been added over timescales distributed around this nominal value. Bombardment by veneering planetesimals would have occurred in the neighborhood of 4.4 byr ago, essentially at the estimated age of the oldest, most densely cratered lunar crust (Basaltic Volcanism Study Project, 1981, Ch. 8 and 7). There are no obvious constraints from the lunar or planetary cratering record that would rule out this accretion time, or the later times that would result from a choice of >90 myr for τ .

VI.C. Hydrogen Inventories

The equations for hydrodynamic escape, applied to a particular stage in the evolution of a planetary atmosphere, yield parameters that specify the initial atmospheric hydrogen inventories and escape fluxes needed to generate the fractionations occurring during that stage. On all three planets, the total amounts of hydrogen required to implement the loss processes from beginning to end turn out to be very large. Amounts are estimated in this section, and possible sources discussed in the next.

VI.C.1. Atmospheric Hydrogen Inventories, Escape Fluxes, and Total Requirements

Column densities N_1 of molecular hydrogen required to be present in planetary atmospheres initially (N_1^0), at times of outgassing (N_1^{og}), and at the end of escape episodes (N_1^f) were calculated using data in Tables I and AI–AVI and the applicable choice of Eq. (14), (18), or (17) with appropriate values of m_c and α . They are tabulated in Table VI. Amounts of hydrogen escaping to space during the various evolutionary stages are given by Eq. (15) or (19). The total hydrogen abundances ΣN_1 needed to implement all stages of hydrodynamic escape from the three planets are simply equal to the residual inventories N_1^f plus the sum of all losses. These are also listed in Table VI, along with initial escape fluxes F_1^0 calculated from Eq. (9).

Nominal hydrogen surface pressures at t_0 corresponding to calculated N_1^0 column densities vary widely among the different models, ranging from ~ 20 bar (Earth Ia, Section VII.A) up to the kilobar range for Venus I. Atmospheric column densities are sharply lower in the constant inventory model assumed for stage 1 evolution on Earth (Section V.B.1) than in the Venus and Mars Rayleigh models, but calculation of integrated losses to space using Eq. (15) shows that the total amounts of hydrogen in-

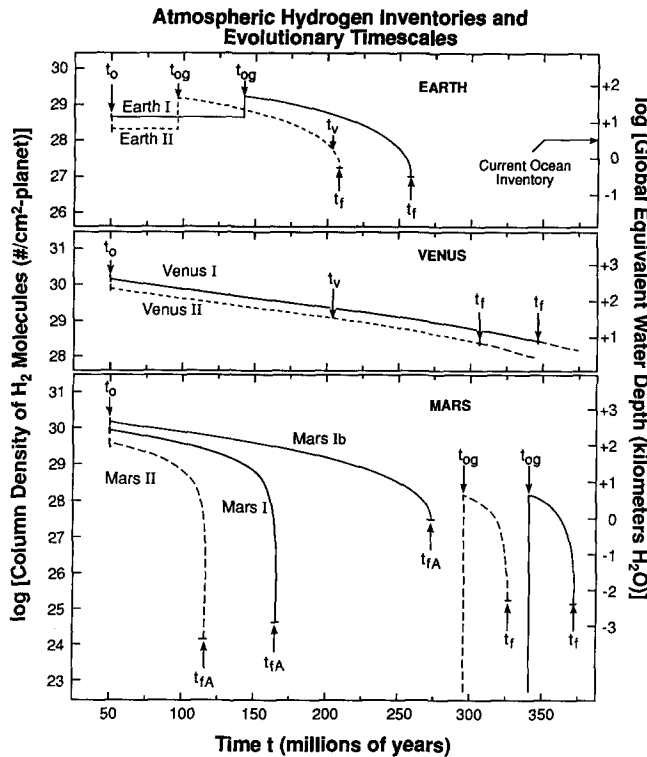


FIG. 19. Required hydrogen column densities and equivalent global water depths vs time in Models I and II of hydrodynamic escape from Earth, Venus, and Mars. The t_0 , t_{fA} , t_{og} , t_v , and t_f designations refer to times of initiation of escape, end of stage 1 evolution of primary atmospheres, planetary outgassing, veneer accretion (Model II), and termination of escape respectively; t_{fA} is coincident with t_{og} on Earth and with t_f on Venus. Data from Table 6. Crossover masses at t_f on Venus are below the masses of atmospheric constituents considered in the models, so escape could continue beyond these times. Outgassing at terrestrial levels would contribute only modestly to final Venus noble gas inventories, and there is no estimate for t_{og} . The major loss of primary noble gases occurs at constant H_2 inventory in both Earth I and II; all other escape episodes assume Rayleigh distillation of H_2 . The alternative Mars Ib model for stage 1 evolution is characterized by higher H_2 pressure at t_{fA} (Section VI.C.2).

involved in the process are not. In the former, the low constant inventory is replenished many times over during escape, whereas in the latter all of the required hydrogen is initially in the atmosphere. In all cases F_1^0 is high, ranging from ~ 1 to $5 \times 10^{14} H_2$ molecules $cm^{-2}sec^{-1}$.

Atmospheric H_2 inventories vs time during escape are plotted for Models I and II in Fig. 19, in units of both column densities and equivalent planetwide water depths. Markers indicate the timing and inventory requirements, taken from Table VI, for major evolutionary stages. Note that the amounts of primary atmospheric H_2 remaining at t_{og} on Earth and Mars are too low to implement the subsequent escape of outgassed species, and so additional H_2 (or H_2O) must be degassed along with the noble gases.

Termination of escape. The final inventories N_1^f given

in Table VI and plotted at t_f in Fig. 19 are the column densities of atmospheric H_2 remaining on the body when hydrodynamic escape ceases (or, on Venus, when $m_c(Ne)$ drops to < 20 amu; however, in this case H_2 loss could continue, to exhaustion, without influencing any of the gases we are tracking here). For Earth and Mars, final crossover masses $m_c^f(Ne)$ calculated from isotopic matching are still above or among the Ne isotopes (Tables AI, AII and AIV–AVI); and on Mars, as pointed out earlier in Section V.B.3, the crossover mass $m_c^{fA}(Xe)$ at the end of stage 1 evolution at t_{fA} is above the Xe range.

One cannot assume that escape simply ended at convenient crossover masses. Physical reasons for terminating it are required. For Earth, however, there is no demonstrable problem. Although the crossover masses $m_c^f(Ne)$ are nominally slightly above 20 amu, differences are small enough to lie within the noise of the model's input data. Changes of 1–2% from adopted values for the diffusion parameter $b(Ne)$ and the solar $^{20}Ne/^{22}Ne$ ratio would yield terrestrial $^{20}Ne/^{22}Ne$ for $m_c^f(Ne) \leq 20$ amu. Uncertainties of this order certainly pertain to the solar Ne composition (Section IV.A.2, Fig. 3), and to $b(Ne)$ as well, particularly if escape occurred at high temperature (Mason and Marrero 1970; Section VII.B). For $m_c^f(Ne) \leq 20$ amu on Earth, as on Venus, subsequent escape history is outside the purview of the model since the noble gas inventories are all frozen.

The required value of $m_c^f(Ne)$ in the Mars models is substantially higher, indicating actual truncation of the process. Events that could have suppressed hydrodynamic outflow include rapid chemical extraction of H_2 from the atmosphere, or addition of other atmospheric components to the extent that hydrogen was no longer the dominant constituent and its escape flux became limited by radiative cooling and diffusion through heavier species (Hunten *et al.* 1989, Zahnle *et al.* 1990a). The amounts of “excess” hydrogen N_1^{fA} and N_1^f on Mars are very small, equivalent to pressures ranging from ≈ 2 to 25 mbar (Table VI, Fig. 19). Surface thermal and magmatic conditions for efficient hydrogen oxidation (e.g., via $H_2 + FeO \rightarrow H_2O + Fe$) might well have been met, and adequate oxidant supplied in FeO-bearing eruptives. Removal of the ~ 20 mbars of N_1^f in Mars II in this way, for instance, would have required reduction of 5 wt% FeO to Fe in ~ 130 m of magma and produced ~ 180 mbars of water vapor.

Degassing of enough CO_2 to produce a substantial atmospheric CO_2/H_2 mixing ratio could have played an important role in truncating blowoff, for two reasons (Zahnle *et al.* 1990a): it is a good infrared radiator and thus tends to quench escape by radiating away available energy; and the H_2 escape flux may become limited by having to diffuse upward through the heavier constituent. For example, if all of the degassed C in the Mars II model entered the atmosphere as CO_2 at t_f , the calculated molar CO_2/H_2 mixing ratio would have been > 2 from data in

Tables VI and AVI. Much smaller contributions of CO_2 could have acted to throttle escape at t_{fA} , when the residual H_2 inventory was only ~ 2 mbar (Fig. 19).

VI.C.2. Impact Erosion on Mars: A Special Case

There are several unsatisfying aspects of the evolutionary patterns shown in Fig. 19 for Martian H_2 . Both models require column densities to fall to extremely low levels (\sim mbar) toward the end of stage 1 at t_{fA} in order to implement the needed Xe fractionations, yet at these levels, as noted just above, the escape process itself could easily have been suppressed prior to t_{fA} by addition of atmospheric "impurities" such as CO_2 . Moreover this fractionated Xe is presumed to be stored in the atmosphere throughout the long (~ 180 myr) hiatus between t_{fA} and t_{og} . During this interval, if its total pressure remained low, the residual atmosphere would have been extremely vulnerable to episodic partial removal of atmospheric mass by impact erosion (Cameron 1983, Watkins and Lewis 1986, Walker 1987, Melosh and Vickery 1988, 1989, Hunten *et al.* 1989). Among the terrestrial planets, small and low-g Mars is most susceptible by far to such losses.

Effects of erosion can be estimated from Melosh and Vickery's (1989) analytic treatment, which assumes that the ejection process is nonfractionating and that Mars was exposed to a time- and size-dependent projectile flux distribution similar to that derived from the lunar cratering record. Ejection efficiency in their formulation depends sensitively on the masses of both the projectile and the impacted atmosphere. For the Mars I and II models, it turns out that during most of the t_0-t_{fA} and $t_{og}-t_f$ evolutionary stages, when pressures are relatively high, only large and correspondingly rare impactors are capable of efficiently removing the atmospheric mass above the plane tangent to the impact point. However, between t_{fA} and t_{og} , ≥ 10 km projectiles can do the job, assuming that total pressures remain in the neighborhood of the <10 -mbar range at t_{fA} shown in Fig. 19. If the lunar cratering flux distribution is taken to apply roughly to this early epoch, these impacted the planet about once every 2×10^5 yr. Partial atmospheric ejection at this rate during the ~ 180 myr prior to outgassing would have completely denuded the planet of residual primary Xe.

An alternative model for Mars. There are model variations for stage 1 evolution that could ameliorate both of these difficulties. It was pointed out in Section V.B.3 that an unbounded number of $[\alpha_0(A), m_c^{fA}(\text{Xe})]$ free parameter combinations can satisfy Martian Xe isotopic constraints, each pair associated with a different initial Xe concentration $C_{130}^i(A_{CI})$ in the primary atmosphere. The values chosen for Mars I and II (Tables AIV, AVI) correspond to the large $C_{130}^i(A_{CI})$ that would have been supplied by accretion of Dreibus and Wänke's (1985, 1987, 1989) 40% CI-

like-component, *on the assumption* that it contained the same loading of noble gas carrier phases that characterize present-day CI meteorites. However, in the context of the planetesimal model for carrier production developed in Section V.D, there is no intrinsic requirement that all CI-like materials necessarily incorporated only this mixing ratio of carrier phases (Section V.D.5), nor even that the carrier which contributed noble gases to the primary Martian atmosphere was physically associated with the oxidized CI-like accretional component at all.

To explore what possibilities might exist if early CI and noble gas carrier materials were decoupled from their contemporary relative abundance, a Mars Ib model was constructed in which the carrier-to-CI mixing ratio was arbitrarily taken to be only 1/800 of its meteoritic value, thus reducing $C_{130}^i(A_{CI})$ and increasing $f_{130}(A)$ in Table AIV by the same factor. Calculated isotope ratios are identical to those given for Mars I in Table IV. Mars Ib data relevant to the abundance and time evolution of atmospheric hydrogen are listed in Table VI and plotted in Fig. 19. Note that the effects of this much lower Xe loading of the initial primary atmosphere are appreciable: H_2 pressures are above ~ 4 bars throughout stage 1 evolution, which now extends ~ 100 myr longer than in Mars I, to $t_{fA} \cong 275$ myr. This more massive atmosphere is correspondingly less susceptible to contamination by CO_2 or other species, and its higher pressure and increased longevity afford a considerably higher degree of protection against large impact-erosion losses. In this case, if the ~ 4 bar pressure at t_{fA} is reduced only by erosion until degassing at t_{og} , ejection of atmospheric mass above the tangent plane requires ≥ 70 km projectiles (Melosh and Vickery 1989). These are relatively uncommon, ~ 1 every 3myr or so if the lunar flux mass distribution applies, and only about 1/4 of the residual atmosphere (and its Xe) is eroded away in the ~ 70 myr interval between t_{fA} and t_{og} .

Postescape erosion and scenarios for the history of Martian CO_2 . A second period of susceptibility to atmospheric impact erosion is that following termination of hydrodynamic escape at $t_f \cong 330-370$ myr (Table VI, Fig. 19), in particular during the next ~ 650 myr until the end of late heavy bombardment about 3.5 byr ago. If we assume, with Melosh and Vickery (1989), that the present ~ 6.5 mbar CO_2 atmosphere is simply an impact-eroded remnant of an earlier, denser atmosphere, their expression for pressure evolution yields a $p(\text{CO}_2)$ approximately a factor of 8 higher—about 50 mbars—at $t_f \cong 330$ myr for Mars II. Available CO_2 in Mars II at t_f , from Table AVI, is $\sim 5.9 \times 10^{-6}$ g/g-Mars, close to 1 bar if all outgassed. We have assumed that because of isotopic constraints (Section V.C.4) most "outgassed" CO_2 was acutely retained in the planet at least until the end of escape at t_f . So one possible interpretation is that $\sim 5\%$ of the available CO_2 was degassed at t_f and impact-eroded to its current

pressure over the next ~ 4.2 byr—with most of the depletion ($>80\%$) occurring in the first 650 myr. To match present atmospheric inventories of noble gases, this erosive loss—which applies to *all* atmospheric species if there is no fractionation in the ejection process—would require a factor of ~ 8 upward scaling of each of the separate C_M^i inventories for the A_{Cl} , OG_I , and OG_{Cl} components in Table AVI. This could be accommodated by \sim eightfold increases in the low accreted abundance of the noble gas carrier assumed for Mars Ib, and in degassing efficiency from an interior reservoir that may well have been gas-rich (Section VII.D.2). Available CO_2 at t_f then rises to ~ 8 bars. These calculations assume that the degassed CO_2 stayed entirely in the gas phase. The actual situation would have been more complicated if partial condensation of CO_2 in regolith–atmosphere–cap exchange (Fanale *et al.* 1982) began earlier than ~ 3.5 byr ago.

This approach would seem to limit early $p(CO_2)$ to ≈ 50 mbars. A climatologically more interesting scenario, in the context of an early greenhouse, is one in which the entire ~ 1 bar of available CO_2 was degassed to the atmosphere at or shortly after t_f . Impact erosion of this higher pressure atmosphere would have been considerably more gentle. A generalization of Melosh and Vickery's (1989) Eq. (6) which allows both starting and ending times for impact losses to be specified yields erosive depletion of CO_2 and other gases by only about 25% between t_f and the end of heavy bombardment. Continuing erosion to the present is not important, and so present conditions on Mars require that $\sim 99\%$ of the surviving ~ 0.75 bar of CO_2 must have been removed as carbonate rock or otherwise segregated in nonatmospheric reservoir(s) during the following ~ 3.5 byr. The important point for a greenhouse is that $p(CO_2)$ could have been substantial for an indefinite (possibly long) period following t_f , depending on the rate at which it was sequestered by precipitation as carbonate.

VI.D. Hydrogen and Noble Gas Sources

Condensation of ambient nebular H_2 in planetary gravitational wells or capture of H_2O -rich planetesimals would appear to be the only ways for the terrestrial planets to acquire initially massive amounts of hydrogen. However, as pointed out in the next section there are several problems with the first hypothesis, among them the inability of nebular capture to supply the required ΣN_1 inventories in Table VI. The second implies accretion of substantial amounts of water, comprising up to a few percent of total planetary masses. Geochemical consequences of providing ΣN_1 as water, for the final FeO contents of planetary mantles and for Fe abundances in planetary source materials, are discussed below in Section VI.E.

VI.D.1. Nebular Capture

In the models discussed in this paper, noble gases in the primary atmospheres on Earth and Venus are taken to be solar in isotopic composition. Thus one possibility for their origin on these planets is direct capture from the nebula. Substantial gravitational condensation of ambient gases requires the growth of protoplanets to appreciable fractions of present masses prior to dissipation of the nebular gas phase (see Section VII.D.2). A difficulty that presently confronts this requirement has to do with the relative timing of nebular dissipation vs planetary growth. Current estimates of timescales for loss of circumstellar dust and gas, from observation (Strom *et al.* 1988, 1989a,b, 1991, Walter *et al.* 1988, Walter and Barry 1990) and theory (Boss *et al.* 1989), are on the order of $\approx 10^7$ yr or less, compared to $\sim 10^8$ yr for planetary growth to full mass in the standard model of planetary accumulation (Wetherill 1986, 1990a).

However, to reiterate a point made earlier, nebular lifetimes inferred from astronomical observation are based solely on evolution of the fine dust component. Measurements of molecular line emissions that could at least set upper limits on the longevity of the dominant gas-phase component in “naked” T-Tauri disks do not yet exist (Strom *et al.* 1991). There is no reason to believe that disappearance of micrometer-size dust from IR detectability, say by accretion into larger grains, would necessarily be coincident with gas loss. Since t_0 in the present model marks the clearing of both nebular dust and gas to low EUV opacity levels, this was one consideration in choosing $t_0 = 5 \times 10^7$ yr, five times longer than the rough upper limit on dust evolution timescales. In 50 myr the standard accumulation model predicts terrestrial planet growth to $\geq 90\%$ of final masses (Wetherill 1986). So if a significant remnant of gas did manage to survive until shortly before this time, large-scale gravitational capture would have occurred. And there are further uncertainties, pertaining to the influence of ambient gas on the dynamics and time-scales of accretion itself. On the one hand, although they have not been well studied, it is not out of the question that gas drag effects during accumulation could have resulted in full planetary growth within $\approx 10^7$ yr (Wetherill 1990a), much more commensurate with estimates of nebular lifetimes and thus with condensation of massive primary atmospheres on Earth and Venus. On the other, it is possible that *loss* of nebular gas was an important trigger for accumulation of \sim Mercury-size planetary embryos into larger bodies (Wetherill 1990b; Section VII.D.2), foreclosing the possibility of significant capture.

It would appear that current observations and modeling cannot firmly rule out a capture origin for primary atmospheres on Earth and Venus. But from the point of view of the model discussed here, this source seems unlikely

for two reasons. First, as seen in Fig. 13a, the derived elemental composition of the primordial atmosphere on Venus—and by assumption on Earth as well, prior to its modification supposedly by partial ejection in a giant impact (Section V.B.4)—has a distinctly nonsolar Ne/Ar ratio. There is presently no reason to assume elemental fractionation in the capture process itself, although it may be that this possibility needs more theoretical attention. Second, and more central for this discussion, is the fact that condensation of enough elementally solar gas to provide the initial atmospheric $C_M^i(A_S)$ noble gas concentrations in Tables AI–AIII cannot supply the required total hydrogen inventories listed as ΣN_1 in Table VI. For example, taking Xe in Earth I for illustration, $C_{130}^i(A_S) = 4.08 \times 10^{-13} \text{ g}^{130}\text{Xe/g-Earth}$ (Table AI). Multiplying by the solar H/ ^{130}Xe ratio of 9.4×10^8 from Table II yields $3.8 \times 10^{-4} \text{ g-H/g-Earth} = 1.3 \times 10^{29} \text{ molecules H}_2/\text{cm}^2\text{-Earth}$, about a factor of 4 below ΣN_1 . This is the smallest shortfall; it exceeds a factor of 10 for other Earth and Venus models.

VI.D.2. Accretion of Icy Planetesimals

At reasonable nebular temperatures and pressures at its radial distance, Mars is too small to have condensed appreciable abundances of ambient gases even in the limiting case of isothermal capture (Section VII.D.2). Therefore, independent of the plausibility of capture as a hydrogen source for Venus and Earth, some other way—e.g., accretion of water—is needed in the present model to supply Mars. For Mars II the 40% CI-like accretional component proposed by Dreibus and Wänke (1985, 1987, 1989) would have provided just about enough hydrogen— $>85\%$ of ΣN_1 —if it carried contemporary CI abundances ($\sim 6 \text{ wt}\% \text{ H}_2\text{O}$ if all present as water, which it mostly is). But other Mars models required more than just this CI water content, and in the absence of nebular capture—or even with it—Earth and Venus clearly need another source.

Required amounts of accreted hydrogen (in units of g-H₂O/g-planet) were calculated from the ΣN_1 column densities in Table VI and are listed there as $\Delta \text{H}_2\text{O}$ for all the planetary models. Inferred water concentrations are comparable to or lower than those in carbonaceous chondrites, and are not intrinsically implausible. But they apply to entire planetary masses, and so if no separate carrier were involved would have to be carried entirely by the dominant accretional material in the Earth and Venus models (“component-A” in Dreibus and Wänke’s terminology). This presents a problem, since concentrations of this magnitude imply abundant structural water in minerals and are inconsistent with Dreibus and Wänke’s geochemical characterization of A-component material as refractory and volatile-poor.

Accretion of a separate water-rich carrier is a plausible alternative. In fact, Wänke’s (1981) geochemical model of Earth’s bulk composition requires just such a carrier, namely $\sim 15\%$ by mass of the same CI-like material (termed “component-B”) that contributed in higher proportion to Mars. Consequences of accreting a 15% mass fraction of CI matter on Earth for Xe isotopic composition in its primary atmosphere are discussed in Section VII.C. It is interesting to note here that a CI water content of 6% in a 15% accretional component, if retained in the putative giant impact event or added afterward, would have supplied 2/3 of the needed hydrogen in Earth I and slightly oversupplied ΣN_1 in all other Earth models. But only a much higher mass fraction ($\sim 35\text{--}60\%$) of this particular material in Venus, which seems unlikely, would satisfy hydrogen requirements there.

For this reason a different water-rich carrier seems to be indicated. It is evident from the $\Delta \text{H}_2\text{O}$ inventories in Table VI that fairly large proportions of comet-like ices, up to $\sim 5\%$ of total accreted planetesimal mass after CI–water contributions to Mars are taken into account, would do the job for all the planetary models as far as ΣN_1 is concerned. For the noble gases, arguments have been made in Section V.B.4 that (1) relative Ne depletion in such ices is likely; (2) this source could have contributed to both Venus and Earth if the fractionated noble gas elemental pattern in the Earth’s atmosphere at t_0 shown in Fig. 13a is a consequence of partial mass-dependent ejection of an initially Venus-like primary atmosphere by giant impact; and (3) addition to Mars of the same mass of planetesimal ices (on a g/g-planet basis) as that accreted by Venus and Earth does not present intractable problems for Martian isotopic evolution (Mars Ia model).

However, this kind of water–noble gas source has potential problems of its own. Cometary ices could have carried other volatiles into primary atmospheres, possibly in large amounts. For instance, material released from Comet Halley, assuming a dust/gas mass ratio of ~ 6 near the upper end of McDonnell *et al.*’s (1986) range and taking all H as H₂O and all H₂O in the gas phase, contains $\sim 0.2 \text{ g-C/g-H}_2\text{O}$ and ≈ 0.02 to $<0.08 \text{ g-N/g-H}_2\text{O}$ (Jessberger *et al.* 1989). Accretion of a carrier of this composition to supply the required initial H₂O inventory of 3.77 wt% in the Venus I model adds $C_{44}^i(A_S) \sim 2.8 \times 10^{-2} \text{ g-CO}_2/\text{g-Venus}$ (for C as CO₂) and $C_{28}^i(A_S) \approx 8$ to $<30 \times 10^{-4} \text{ g-N}_2/\text{g-Venus}$ in the planet. If we assume that all cometary CO₂ and N₂ was in the atmosphere and that escape proceeded as in Venus I (problematic in this case since the initial CO₂/H₂ molar mixing ratio would be ~ 0.3), then data in Table AIII yield, for final inventories, $C_{44}^f(A_S) \sim 3.0 \times 10^{-3}$ and $C_{28}^f(A_S) \approx 6$ to $<22 \times 10^{-5} \text{ g/g-Venus}$. This oversupplies the present-day atmospheric CO₂ inventory by a factor of ~ 30 but does replicate the observed CO₂/N₂ ratio for a Halley N₂ abundance just

above its minimum value. So on this basis alone one could postulate a C–N source resembling Halley except for a factor ~ 30 less fractionated (i.e., lower) C/H ratio (which in Halley, for gas/dust ~ 6 , is ~ 300 times the solar ratio), or that all but a few percent of this C and N was retained in the planet during accretion and throughout its subsequent geologic history. However, there is a carbon isotope constraint which appears to rule out a strictly Halley-like source. Wyckoff *et al.* (1989) report $^{12}\text{C}/^{13}\text{C} = 65 \pm 9$ ($\delta^{13}\text{C} = 370 \pm 190\text{‰}$) in Halley from ground-based spectral measurements, well below the Venus value of 89.3 ± 1.6 . Hydrodynamic escape of carbon as CO_2 or any lighter species, if it occurred, would worsen the disparity by making residual carbon even heavier. Other comets could perhaps satisfy this constraint: average $^{12}\text{C}/^{13}\text{C}$ in four of them is 103 ± 30 (Wyckoff *et al.* 1989), within range of Venus with or without escape fractionation.

Apart from potential isotopic difficulties there is another problem, in the context of the present model, in postulating that C–N-rich comet-like planetesimals could have been the source not only of hydrogen and noble gases in primary atmospheres, but of planetary carbon and nitrogen as well. Accretion from a common planetesimal population would have resulted in compositionally similar primary atmospheres on both Venus and Earth. But the primary C and N abundances required to generate their final inventories on Venus, if initially present in about the same amounts on Earth as well, would presumably have been first partly ejected in the giant impact event and then attenuated to levels far below present-day terrestrial inventories by the severe hydrodynamic losses characterizing stage 1 evolution (Table AI). Thus an additional C and N contribution to Earth, but not to Venus, is probably needed at some point. That such a scenario could have resulted in final inventories as similar, in composition and abundance, as those presently existing on the two planets would be a remarkable coincidence. On the whole, the arguments set out at the end of Section V.B.4 for a late-stage veneer source seem more convincing. Therefore in the following section we assume, for illustration, a hypothetical icy planetesimal source with C/H and N/H ratios low enough (less fractionated, compared to Halley) to avoid substantial carbon and nitrogen contributions to Venus and Earth, and estimate its required water and noble gas composition.

VI.D.3. Composition of a Cometary Source for Hydrogen and Noble Gases on Venus

Noble gas distributions in comets are unknown. As noted earlier, solar isotopic compositions would be expected in condensates from the nebula, and heavier and less volatile species (Xe, Kr, and Ar) could arguably be trapped in approximately solar elemental proportions for

condensation histories at low temperatures. Abundances per gram H_2O might be appreciable (Bar-Nun *et al.* 1985). If they are, incorporation of a few percent of icy cometary matter into an accreting terrestrial planet could potentially have supplied solar-like heavy noble gases to its primary atmosphere, in addition to the hydrogen needed to implement hydrodynamic escape. This kind of source is particularly attractive in that the low Ne/Ar ratio which might be expected in these ices (Sections V.B.4 and V.D.3) would provide a natural explanation for the apparent underabundance of primary neon on Venus. A cometary or “icy planetesimal” carrier of primordial Venus volatiles with just these characteristics has been proposed (Owen 1987, Hunten *et al.* 1988).

To supply the required hydrogen, remove the Ne/Ar “anomaly,” and otherwise replicate the results for Venus I given in Table AIII, the amount of accreted water equivalent to ΣN_1 would have been 3.77×10^{-2} g- H_2O /g-planet, and the elemental composition of this material as follows: $^{130}\text{Xe}/\text{H}_2\text{O} = 7.2 \times 10^{-12}$ g/g, $\text{Xe}/\text{Kr} \cong$ solar, $\text{Ar}/\text{Kr} \cong 75\%$ of solar, and $\text{Ne}/\text{Kr} \cong 0.75\%$ of solar. Compared to known volatile carriers, the inferred ^{130}Xe loading is about the same as bulk CI concentrations (Table II), or about 15 times smaller than the $^{130}\text{Xe}/\text{H}_2\text{O}$ ratio in the CIs. None of these numbers appear intrinsically implausible, but something clearly needs to be known about elemental and isotopic abundances of all these species in “pristine” comets, and a great deal more on Venus, before the possibility of this kind of source can be assessed in a meaningful way.

VI.D.4. Accretion of Solar-Wind-Rich Materials

One potential problem with the compositional characteristics set out in the preceding section for an icy planetesimal source is that there is no experimental or observational evidence that low-temperature occlusion of nebular noble gases on ice can yield approximately unfractionated (i.e., \sim solar) elemental ratios for Xe:Kr:Ar. There is evidence that while clathrated noble gases are characterized by large Ne depletions, they do *not* reflect ambient gas-phase relative abundances for Xe/Ar and Kr/Ar but instead are severely fractionated in favor of the heavier species (Lunine and Stevenson 1985). A purely clathrated component therefore appears unlikely to serve, and one must appeal to low-temperature physical adsorption of noble gases which, as yet, has not been extensively studied in the laboratory.

Noble gases implanted into lunar and meteoritic dust grains by low-energy solar wind irradiation are known to display solar-like elemental abundance ratios, with typical ^{20}Ne loadings in lunar grains of $\approx 10^{-6}$ g/g (e.g., see Pepin *et al.* 1970, Eberhardt *et al.* 1972, Marti *et al.* 1972, Hintenberger *et al.* 1974). Implanted neon (and helium) can

be depleted preferentially by subsequent heating, or lost even at low temperatures by rapid diffusion from certain mineral structures, notably plagioclase (e.g., Frick *et al.* 1988). Accretion of planetesimals containing $\approx 25\text{--}40$ wt% of solar-wind-irradiated material, loaded to lunar levels in Xe, Kr, and Ar but depleted ≈ 100 -fold in ^{20}Ne to a content of $\approx 10^{-8}$ g/g, could account for the absolute noble gas abundances $C_M^i(A_S)$ in Venus's primary atmosphere (Table AIII) and for the elemental composition shown in Fig. 13a within the error bars that currently pertain to it.

This general kind of solar wind source for noble gases on the terrestrial planets has been proposed in various contexts by Wetherill (1981), Donahue *et al.* (1981), and McElroy and Prather (1981). Wetherill's (1981) model specifically addresses the large ^{36}Ar abundance on Venus. He perceived its major difficulty to be that of confining accretion of solar-wind-rich materials largely to just this planet, given the likelihood that gravitational scattering would tend to disperse it throughout the inner Solar System. But it is important to note that in the context of the model discussed here, this is not a problem. Earth is supposed to have acquired a compositionally Venus-like primary atmosphere as well, later fractionated to its Fig. 13a elemental pattern by partial ejection, and the Mars Ib model indicates that Mars can tolerate addition of this A_S component to its CI-dominated primary atmosphere at about the same g/g-planet abundance level as on Venus and Earth (Section V.B.4).

It appears that the possibility of a solar-wind source of this kind for noble gases on Venus and Earth must be taken seriously. It may turn out on compositional grounds to be more plausible than either gravitational capture or icy planetesimal accretion. Moreover Sasaki's (1991) recent arguments for off-disk penetration of an early and intense solar wind flux into a postnebular environment rich in fine collisional dust could imply the existence of a hitherto unconsidered ancient reservoir of abundant and heavily loaded carriers of solar-like noble gases. Its obvious disadvantage compared to accretion of ices, from the point of view taken in this paper, is that the hydrogen supplied by even fully retentive irradiated grains would generally be inadequate (Section VI.D.1 above), and this problem is exacerbated since the diffusive depletion of Ne needed to match the Venus primary inventory would be expected to strip the carrier of most of its implanted hydrogen as well. A separate source of planetary hydrogen or water is again required.

VI.E. Geochemical Consequences of Water Accretion, and Constraints on EUV Flux Histories

Let us assume that the planetary hydrogen inventories needed for hydrodynamic escape, listed as $\Delta\text{H}_2\text{O}$ in Table VI, were accreted as water and then converted to H_2 on

some time scale by chemical reduction on or within the planet. The issue addressed here concerns the geochemical behavior of water and hydrogen during and following accretion, and whether the abundances of reduction products left in the planet at the end of the process are consistent with planetary compositions deduced from geochemical and geophysical modeling. This comparison provides an independent constraint on allowable EUV flux histories, because for a given planet the amounts of water that must be converted to hydrogen and lost are proportional to the parameter α (or α_0) and thus to the mean flux decay time τ (Eqs. (15), (17), (19)).

The redox pathways that would have to be followed by accreted water and hydrogen during the various stages of atmospheric evolution shown in Fig. 19 depend on the type of model. In pure single-stage Rayleigh loss, such as on Venus, all of the necessary H_2 is in the atmosphere at t_0 . Consequently strongly reducing conditions for accreted H_2O must have prevailed during planetary growth, and the product hydrogen simply accumulated in a coaccreting primary atmosphere. In all other models, since they involve either stages of loss at constant inventory followed by Rayleigh escape of degassed hydrogen (Earth I and II) or multiple episodes of Rayleigh escape (Mars I and II), various fractions of the accreted water must have been stored in the planet for later conversion to hydrogen and release to the atmosphere. Conversion of sequestered water to H_2 during the constant inventory loss stage on Earth is assumed to be controlled by buffering reactions on the surface, as discussed in Section V.A.4. Required redox conditions are considerably less stringent in the stage 2 Rayleigh escape episodes driven by outgassed H_2 on Earth and Mars. Here the reduction of incorporated water could have occurred over time in planetary interiors, with the resulting hydrogen accompanying—and plausibly carrying—other degassed species into the atmosphere.

Minimum amounts of water that must be stored in planetary interiors are just the H_2O equivalents of $\Sigma N_1 - N_1^0$ —i.e., the total hydrogen required for hydrodynamic escape minus that in the atmosphere at t_0 —and are readily calculated from data in Table VI. They are listed in Table VII as $[\text{H}_2\text{O}]_{\text{st}}$ in weight percent of the planetary mass, and should be regarded as strict lower limits on actual concentrations since the water would undoubtedly have been incorporated into less than a planet's entire mass, and neither reduction nor outgassing would have been totally efficient. The Earth models have by far the highest demand (≈ 1 wt%) for water storage, too large to be consistent with dissolution of a few tenths weight percent of water in surface basaltic magmas under conditions of high atmospheric H_2O pressure followed by convective transport of this water into interiors (Holloway 1988a,b, Abe and Matsui 1985). Stored abundances of this magnitude

TABLE VII
Comparison of Abundances of Iron Oxide [FeO]_m in Planetary Mantles Deduced from Geochemical–Geophysical Models (GGM) of Planetary Interiors with Those Calculated from the Baseline (I) and C,N-Veneer (II) Atmospheric Evolution Models

Model	τ (myr)	$\Delta\text{H}_2\text{O}$	$[\text{H}_2\text{O}]_{\text{st}}$	m_{CI}	Geochemical–geophysical models ^a			Atmospheric models ^b	
					m_m	$m_c(\text{Fe})$	$[\text{FeO}]_m$	$[\text{FeO}]_m$	$[\text{Fe}]_A$
Venus I	90	3.77	0	0	71.0	25.1	0.2–18.7	21.2	36.8
Earth I	90	1.40	1.29	0 [15]	68.3	25.4	7.6–10.6	8.2 [13.5]	29.8 [35.0]
Mars I	90	6.36	0.10	40	80.5	14.1	15.8–26.8	43.5	56.5
Venus II	90	2.24	0	0	71.0	25.1	0.2–18.7	12.6	32.1
Earth II	90	0.78	0.73	0 [15]	68.3	25.4	7.6–10.6	4.6 [9.8]	27.8 [32.7]
Mars II	90	2.81	0.10	40	80.5	14.1	15.8–26.8	25.9	38.1

Note. $[\text{Fe}]_A$ designates the calculated amounts, in wt %-A, of metallic iron in accreted A-component material. Required planetary hydrogen inventories (ΣN_i) expressed as total accreted water $\Delta\text{H}_2\text{O}$ (Table VI), the amounts of this water $[\text{H}_2\text{O}]_{\text{st}}$ required to be initially stored within planets, and mass fractions m_{CI} of accreted carbonaceous chondrite material in the atmospheric models are also listed. Bracketed values of $[\text{FeO}]_m$ and $[\text{Fe}]_A$ are calculated for the higher (bracketed) m_{CI} mass fraction proposed in Wänke's (1981) GGM for Earth. GGM estimates of mantle mass fractions m_m , core iron contents $m_c(\text{Fe})$, and mantle iron oxide abundances $[\text{FeO}]_m$ are taken from the cited reference.

^a Basaltic Volcanism Study Project (1981, Chap. 4). GGM model estimates from BVSP for m_m and $m_c(\text{Fe})$ are in units of wt %-planet, and $[\text{FeO}]_m$ in wt %-mantle. Tabulated values of m_m and $m_c(\text{Fe})$ are averages for the various models, and $[\text{FeO}]_m$ the ranges.

^b This paper.

would probably be attainable only if impact degassing of water-rich accreted materials was incomplete and bulk water was buried during planetary growth, or if thermal conditions allowed hydration reactions and interior storage of hydrated species.

Mantle Iron Oxide Abundances

Turning first to the effects of water reduction on oxidation state, we assume that the dominant reduction reaction was $\text{H}_2\text{O} + \text{Fe} \rightarrow \text{H}_2 + \text{FeO}$, and compare independent estimates of planetary FeO contents with the sum of FeO amounts produced by reaction of $\Delta\text{H}_2\text{O}$ with Fe and contributed by a CI accretional component (if present). The calculated FeO content of a planetary mantle is then given by

$$[\text{FeO}]_m = \frac{4\Delta\text{H}_2\text{O} + m_{\text{CI}}[\text{FeO}]_{\text{CI}}}{m_m} \text{ g/g-mantle, } (30)$$

where $\Delta\text{H}_2\text{O}$ is in units of g/g-planet, m_m is the planetary mass fraction of mantle + crust, m_{CI} is defined as the planetary mass fraction of CI material, and $[\text{FeO}]_{\text{CI}}$ is the iron oxide content of this material in g/g. $[\text{FeO}]_{\text{CI}} \cong 24$ wt%, taking all Fe in the CIs (18.5 wt%; Anders and Ebihara 1982) as oxidized. It should be kept in mind that this expression leads to overestimates of FeO production if reduced species other than metallic Fe (e.g., C, metallic Si) are available in the accreted material, and to underestimates in cases where a CI component is present and

reduction of sulfates is important (Dreibus and Wänke 1985). We take $\text{FeO} \sim 0$ in the non-CI accretional component (Dreibus and Wänke's reduced component A), and assume for the moment that FeO was not extracted from mantles into planetary cores.

Calculated values of $[\text{FeO}]_m$ from Eq. (30) are listed in Table VII under "Atmospheric models." Ranges of comparison values from geochemical–geophysical planetary modeling (GGM) are taken from the Basaltic Volcanism Study Project (BVSP) (1981, Ch. 4). (Dreibus and Wänke's (1985, 1987, 1989) more recent Mars geochemical model, based on SNC meteorites, gives $[\text{FeO}]_m = 17.9$ wt%, intermediate in the GGM range from BVSP.) The large Venus $[\text{FeO}]_m$ content of 18.7% is from Ringwood and Anderson's (1977) oxidation state model, and is perhaps a rough upper limit for Venus; competing equilibrium condensation models assume low to ~zero FeO (BVSP 1981, Phillips and Malin 1983). Two values of calculated $[\text{FeO}]_m$ are listed in Table VII for the Earth models: the first excludes Wänke's (1981) 15% CI-component, and the second (bracketed) value includes it.

In general, for the choice of $\tau = 90$ myr discussed in Section III.B.3, the calculated abundances of $[\text{FeO}]_m$ in Table VII are not grossly different from estimates deduced from geochemical and geophysical considerations. There is one prominent discrepancy in Model I results: the large $\Delta\text{H}_2\text{O}$ for Mars I drives $[\text{FeO}]_m$ to a level well above the GGM range. This anomaly could be resolved by choosing a smaller τ : reduction from 90 myr to ~42 myr would yield $\Delta\text{H}_2\text{O} = 2.99$ wt% for Mars I, and $[\text{FeO}]_m = 26.8$ wt% at

the upper end of the GGM range. Of course since a particular history for the solar EUV flux—whatever it was—must apply to all the planets, this reduction in τ would also lower $\Delta\text{H}_2\text{O}$ on Earth and Venus by the same factor; however, $[\text{FeO}]_m$ in both planets from Eq. (30) would now fall in the middle of the GGM range if Wänke's (1981) proposed 15 wt% CI contribution to Earth is included. Another possibility, now just affecting Mars, is that the assumption of no FeO extraction from the mantle into the core is incorrect. Ringwood (BVSP 1981, Ch. 4.3.2) has proposed that *all* of the Fe in the Martian core is oxidized. If so, we must subtract the FeO equivalent of the 14.1 wt% core Fe from the numerator of Eq. (30), yielding a comfortable $[\text{FeO}]_m = 21$ wt%.

The lower water demands in Model II lead to $[\text{FeO}]_m$ values which are compatible with GGM ranges on all three planets for $\tau = 90$ myr, again including Wänke's CI component on Earth. But given the uncertainties in τ and in the GGM estimates, this correspondence does not really identify Model II as "preferred" in any firm way.

Accreted Metallic Iron

Similar mass balance criteria can be used to calculate the required metallic iron contents of accretional materials. This provides a test, from the perspective of these atmospheric evolution models, for the assumption in two-component geochemical mixing models that the reduced, metal-rich matter accreted in different proportions into the terrestrial planets was chemically homogeneous (Ringwood 1979, Wänke 1981, Dreibus and Wänke 1985, 1987, 1989). Since the CI-component is fully oxidized, non-CI matter—Dreibus and Wänke's "component-A"—must have provided both the iron in planetary cores (assuming no core FeO) and the iron eventually oxidized to FeO by accreted water. Therefore

$$[\text{Fe}]_A = \frac{m_c(\text{Fe}) + 3.11\Delta\text{H}_2\text{O}}{(1 - m_{\text{CI}})} \text{g/g-A}, \quad (31)$$

where $m_c(\text{Fe})$ represents the abundance of core iron in g-Fe/g-planet and other quantities have their previous definitions and values.

Iron contents of planetary A-component carriers calculated from Eq. (31) are listed in the last column of Table VII. Note that except for Mars I, $[\text{Fe}]_A$ values for the three planets are relatively tightly grouped for both Model I and Model II, either with (bracketed values) or without the 15 wt% CI contribution to Earth. Accounting for the Mars I anomaly by assuming a smaller τ , as above, yields $[\text{Fe}]_A$ for Mars I of 39 wt% and a Model I average for the three planets of 32 [34] wt%; assuming a fully oxidized core gives a Mars I value of 33 wt% and a planetary average of 33 [35] wt%. Mean A-component Fe contents in Model II are 33 [34] wt%, with deviations from the

mean values of $\sim 15\%$ or less in individual planets. All of these calculated metallic iron concentrations are similar, and reasonably close to Ringwood's estimate of 29 wt% for Earth (BVSP 1981, Ch. 4.3.2).

Conclusions

It is encouraging that for values of τ in the range suggested by current astronomical data, chemical reduction of these substantial amounts of accreted water does not lead to final planetary oxidation states which strain the limits of current estimates, nor does it require unreasonable supplies of metallic iron. However, the various uncertainties in these calculations are still too large to precisely define a mean EUV decay time for comparison with observation, or to rule between the two principal evolutionary models discussed here. Nevertheless the results do indicate (1) that Model II, or variants of Model I that require less water—e.g., Earth Ia (Section VII.A) or Earth Ib (Section VII.B) and their Venus and Mars analogues—may be somewhat more geochemically compatible with the present planets; and (2) that τ is probably restricted to values ranging from a factor of 2 or so smaller than 90 myr to less than a factor of 2 larger. It is clear from the present stellar data shown in Fig. 1 that at the moment both of these rough limits on τ are observationally acceptable.

VII. FURTHER CONSIDERATIONS

VII.A. Retention of Xenon in Planetary Interiors

In the evolutionary models developed in this paper, the isotopic compositions of present-day atmospheric xenon inventories are fixed by the fractionations $f_{M/130}(A)$ in escape of primary atmospheres and, for Earth and Venus in Model II, by subsequent additions of small amounts of veneer-derived Xe (Sections V.C.1, 2; Tables AII, AIII). Consequently these compositions could not have been perturbed by substantial later contributions from other, isotopically different sources, specifically from planetary outgassing. Therefore amounts of outgassed solar-composition Xe are necessarily restricted to negligible fractions of current atmospheric abundances—the most crucial assumption of the model as it presently stands. This then leads to a requirement for extreme fractionation in the degassed ratio of Xe to lighter noble gases—i.e., for a highly Xe-specific partitioning process operating in the bodies of the terrestrial planets. In this section we reexamine the initial assumption, and point to one possible mechanism, which can be tested experimentally, for preferential Xe retention.

Although no Xe is outgassed in the models discussed earlier, it is possible to lift this restriction to a certain extent by taking a somewhat different approach to setting its final composition. On Earth, for example, rather than

choosing a parameter pair [$m_c^0(\text{Xe})$, $\alpha(\text{A})$] whose fractionation factors directly generate the nonradiogenic terrestrial composition from primary atmospheric Xe (Section V.B.1), one could instead assume ab initio that nonradiogenic terrestrial Xe is really some mixture of fractionated primary solar Xe and unfractionated, degassed solar Xe. Then, with x representing the proportion of outgassed Xe in the present-day inventory, $[^{M'}\text{Xe}/^{130}\text{Xe}]_{\oplus} = [1 - x]f_{M'/130}(\text{A})[^{M'}\text{Xe}/^{130}\text{Xe}]_{\odot} + x[^{M'}\text{Xe}/^{130}\text{Xe}]_{\odot}$, and one seeks values of [$m_c^0(\text{Xe})$, $\alpha(\text{A})$] whose fractionation factors $f_{M'/130}(\text{A})$ satisfy this equation for a given x . Solutions exist, within the uncertainties in $[^{M'}\text{Xe}/^{130}\text{Xe}]_{\oplus}$, for x up to ~ 0.4 .

A model of this type, designated Earth Ia, has been constructed for $x = 0.4$. It is characterized by a lower initial crossover mass $m_c^0(\text{Xe})$ (163 amu cf. 343 amu) and larger $\alpha(\text{A})$ (44.52 cf. 13.13) compared to Earth I. It yields final isotopic compositions for all noble gases that fall, with one exception, within the error bars of the terrestrial isotope ratios given in Table III. The exception is a calculated $^{21}\text{Ne}/^{22}\text{Ne}$ ratio about 4.6% lower than observed, suggesting, as in Earth II, postescape degassing of $^{21}\text{Ne}_n$ (Section V.B.4, Fig. 10). Other data for Earth Ia are given in Table VI, where it is seen that evolutionary timescales are somewhat compressed and water requirements are significantly lower than in Earth I. Similar variants of Mars I yield similar results in that they demand less water and can accommodate some Xe degassing without seriously perturbing final compositions.

Mixed atmospheric Xe inventories, however, even with the maximum degassed contributions allowed by isotope systematics, do not do much to relax the requirement that most of the Xe expected to accompany the lighter degassed noble gases must still be sequestered in planetary interiors. The amount of outgassed ^{84}Kr required in Earth I, for example, is $C_{84}^i(\text{OG}_1) \cong 1.6 \times 10^{-12}$ g/g from Table AI. Assuming an adsorbed interior reservoir for the OG_1 component (Section VII.D.2) and an adsorbed Xe/Kr ratio $\sim 8 \times$ solar from laboratory data (Fig. 13b), then the corresponding ^{130}Xe abundance in the source is $\sim 1.8 \times 10^{-13}$ g/g, about $30 \times$ higher than 40% of the present atmospheric inventory. So $>95\%$ of this Xe must somehow have been retained within the Earth while Kr and lighter species were degassing. This extreme fractionation requires that Xe from the interior source reservoir behaved as a highly compatible element in geochemical partitioning while the lighter noble gases did not.

A model for origin of degassed planetary noble gases by adsorption on protoplanetary cores is developed in Section VII.D.2 below. Results suggest a terrestrial core mass in the neighborhood of 5–10% M_{\oplus} . Stevenson (1981) has described a model of terrestrial metallic core formation in which iron, migrating downward during planetary growth, collects in an unstable layer around this compara-

tively cold accretional core before eventually penetrating, fracturing, and displacing it. If this overturn occurred when the Earth was largely accreted and core pressures high, Xe—but not lighter noble gases (Stevenson 1985)—in the primordial core material could have metallized and preferentially partitioned into the iron (Stevenson 1985, Goettel *et al.* 1989). Stevenson (1981) considers it more likely that the instability developed when the protoEarth was still small and interior pressures relatively low. He points out, however, that fragments of the disrupted gas-rich core, floating as “rockbergs” on the new metallic core, would take longer than the accretion time of the Earth to thermally equilibrate. Outgassing of the rockbergs, on this equilibration timescale, could then still have occurred at high enough hydrostatic pressure (~ 1.3 megabars; Goettel *et al.* 1989) for Xe to metallize and incorporate into surrounding iron at the core–mantle interface.

Stevenson’s picture of core formation provides a natural connection between the primary source of outgassed volatiles in the present model and a plausible mechanism for sequestering its Xe. Thus one could propose that the Xe missing from the degassed component was retained in the iron cores of Earth (and Venus) in just this way. However, interior hydrostatic pressures of ~ 1.3 megabars required for Xe transition to a metallic state could not have been reached at any stage in the accumulation of Mars. To account for the atmospheric deficit there, we must suppose that pressure-induced effects actually begin to influence the geochemical partitioning of Xe well before it metallizes, leading to preferentially high solubilities in (presumably) siderophile phases at pressures not exceeding a few hundred kilobars. Such behavior could occur (Stevenson 1985) and is perhaps not unlikely (K. Goettel, personal communication) on theoretical grounds. These suggestions currently lack experimental confirmation. We do know that preferential incorporation of ambient gas-phase Xe into silicates, relative to lighter noble gases, does *not* occur under nonequilibrium shock conditions, at shock pressures up to ~ 600 kbar (Bogard *et al.* 1986, Wiens and Pepin 1988). *Equilibrium* partitioning behavior is amenable to experimental investigation, at least up to 100 kbar or so, since pressures on this order are accessible in experimental petrology laboratories.

VII.B. Effects of Escape at Higher Temperatures

The planetary atmospheric temperatures T listed in Table I and used throughout these model calculations are roughly equal to gray-body temperatures at present heliocentric distances and solar luminosity. They could well have been either somewhat lower, under early conditions of $\sim 30\%$ reduction in luminosity, or dramatically higher, perhaps up to ~ 2000 – 4000 K at low altitudes on Earth, in

cases where primary atmospheres with large gas or dust opacities were heated from below by high rates of accretional energy deposition (Hayashi *et al.* 1979, Mizuno *et al.* 1982, Mizuno and Wetherill 1984, Nakazawa *et al.* 1985, Hayashi *et al.* 1985, Abe and Matsui 1985, Matsui and Abe 1986, Sasaki and Nakazawa 1990). This “thermal blanketing” effect would have been important in primary atmospheres if accretion rates beyond $t_0 = 50$ myr were in the range deduced from Wetherill’s (1986) planetary growth curves. Although temperatures substantially above gray-body are therefore likely, no attempt was made in the present model to estimate what particular values, within the broad range of possibilities noted above, might actually have pertained during hydrodynamic escape. This inattention to a central parameter in the analytic formalism is justified because, as shown in this section, the principal isotopic and inventory results derived from the model are almost independent of assumed temperature. Given this insensitivity, the only other potential problem with very high temperatures is the increasing uncertainty, up to $\sim 10\text{--}20\%$, in experimental determination of diffusion parameters (Mason and Marrero 1970).

Diffusion parameter values, given in Table I for the indicated temperatures, typically vary as $b \propto T^{-0.75}$ for the noble gases, N_2 , and CO_2 (Mason and Marrero 1970, Zahnle and Kasting 1986). Equations for isotopic fractionation $f_{M/M}$ of a single element do not involve T since values of b are essentially the same for all isotopes and we are dealing with isotope ratios. However, a very small temperature dependence does enter into model calculations of simultaneous isotopic fractionation across a suite of elements, because the typical exponent of ~ 0.75 varies somewhat from element to element. The largest difference among the noble gases is for $b(\text{Xe}) \propto T^{0.712}$ compared to $b(\text{Kr}) \propto T^{0.76}$. Therefore determination of $m_c(\text{Kr})$ from a known value of $m_c(\text{Xe})$ utilizing Eq. (10) or (11) yields $(m_c^0(\text{Kr}) - m_1)/(m_c^0(\text{Xe}) - m_1) = b(\text{Xe})/b(\text{Kr}) \propto T^{-0.05}$. All other elemental pairs are even less sensitive. Required hydrogen fluxes F_1 and inventories N_1 calculated from Eqs. (9), (14), and (18), and energy enhancements Φ_{EUV}^0 from Eq. (11), are more (but not greatly) dependent on temperature since the terms Ab , Cb , and b/B in these expressions are all approximately proportional to $T^{0.75}/T \propto T^{-0.25}$.

The minor effects of even an extreme temperature change from the 270 K assumed for Earth are illustrated by results of a variant of the Earth I model, Earth Ib, in which T is taken to be 3000 K rather than 270 K. All the diffusion parameters listed in Table I are therefore a factor ~ 6 larger. Best-fit isotope ratios derived from Earth Ib are listed in Table IV. They are by and large indistinguishable from Earth I results, although the Kr composition, identical for both Kr-1 and Kr-2, is a slightly rougher match to

the terrestrial pattern, and, interestingly, the lower $^{21}\text{Ne}/^{22}\text{Ne}$ ratio now suggests the same $\sim 4\text{--}5\%$ postescape augmentation by degassed $^{21}\text{N}_n$ implied by all Earth models other than Earth I (Sections V.B.4, VII.A).

Timescale, energy, and hydrogen flux and inventory requirements for Earth Ib are given in Table VI. Evolutionary timescales are essentially unchanged from Earth I; the remaining parameters are smaller by just about the factor ~ 2 expected from their $\sim T^{-0.25}$ temperature dependencies. Therefore the demand for accretional water is correspondingly eased, both here and in the high-temperature Mars and Venus analogues of the Earth Ib model. Overall, aside from this potentially important water reduction (Section VI.E), we may conclude that model perturbations introduced by even order-of-magnitude temperature increases from the Table I values are not significant.

VII.C. Limits on Carbonaceous Chondrite Accretion by Earth

The Dreibus and Wänke (1985, 1987, 1989) two-component geochemical model discussed in Sections II.B.3 and V.B.3 and elsewhere represents an extension to Mars of earlier and similar efforts by Ringwood (1977, 1979) and Wänke (1981) to account for the chemical composition of Earth. The same two components are involved, but in Wänke’s terrestrial model, unlike that for Mars, they are proposed to accrete inhomogeneously and in different proportions. Most of the Earth’s mass ($\sim 85\%$) is assembled largely or completely from chemically reduced type-A planetesimals, with the remaining $\sim 15\%$ dominated by accretion of the oxidized, CI-like component B during later stages of planetary growth. This model clearly seems to require a substantial contribution of impact-degassed CI volatiles to the Earth’s atmosphere, but in the context of the terrestrial model described in Section V.B.1 there is no obvious signature of their presence at any stage of atmospheric evolution. The question is whether these two modeling approaches are necessarily incompatible.

It is evident, from the discussion of isotopic constraints in Section VII.A above, that the composition of nonradiogenic terrestrial Xe prohibits addition to Earth of even a tiny fraction of the amounts of isotopically distinctive CI-Xe that would have been present in a 15% mass fraction loaded to contemporary CI meteorite abundances, at any stage following establishment of the residual Xe composition by dissipation of the bulk of the primary atmosphere. We turn, therefore, to the possibility of earlier accretion of CI planetesimals, at times prior to or immediately following t_0 when the full prescape complement of primary solar Xe was present on the planet. Here the mixing ratio of an additional component would have been lowest, and its chances to elude detection by isotopic perturbation highest.

The solar Xe concentration initially in the primary atmosphere is $C_{130}^i(A_S) \cong 4.1 \times 10^{-13}$ g/g-Earth in the Earth I model (Table AI). To this we propose to add the Xe carried in 15% of an Earth-mass of CI meteorite material with the Xe content listed in Table II. It cannot be done. The added CI component would have supplied $>1 \times 10^{-12}$ g- ^{130}Xe /g-Earth, more than tripling the initial Xe abundance and imprinting an unmistakably CI-like isotopic signature on the mixed reservoir. Variations of the Earth I model in which $C_{130}^i(A_{CI})$ is allowed to be nonzero show that an initial CI-Xe/solar-Xe mixing ratio of $\sim 10\%$ or more perturbs the final calculated compositions of terrestrial Xe and/or Kr beyond their error bounds. The lower $C_{130}^i(A_S)$ in the Earth II model (Table AII) makes it even more vulnerable. Results of these Earth model calculations with nonzero $C_{130}^i(A_{CI})$ limit the accreted mass fraction of material carrying the Xe content of present-day CI meteorites to $\approx 0.07\%$, a factor ≈ 200 below the Wänke (1981) model requirement.

This large discrepancy could be resolved in a straightforward way if the very substantial amounts of oxidized B-component (~ 1.4 Mars masses) accreted by Earth to satisfy geochemical demands contained, on average, a much smaller proportion of the noble gas carrier phase than do contemporary CI meteorites. This kind of fractionation in the carrier phase/"CI" ratio, which does not appear improbable in the context of the Section V.D model for carrier production, was assumed for entirely different reasons in constructing the Mars Ib model discussed in Section VI.C.2. There, for illustration, the carrier abundance was arbitrarily taken to be $800\times$ lower than CI levels; here a depletion factor of ≥ 200 would be needed to avoid significant isotopic distortion of the present-day terrestrial Xe pattern.

VII.D. Models for Origin of Outgassed Planetary Components by Adsorption

As noted earlier, the decline in solar-normalized noble gas abundance ratios from Kr to Ne in planetary atmospheres and meteorites shown in Fig. 6 is qualitatively similar to many of the adsorption fractionation patterns seen in the laboratory and in terrestrial sedimentary rocks. This has led to a widespread belief that adsorption has played a central role in establishing these ratios. Atmospheric Xe, however, is anomalously low in this regard, and the failure of atmospheric Xe/Kr on Earth (and Mars) to follow the steeply inclined trend defined by Ne/Kr and Ar/Kr triggered a long and unsuccessful search of the terrestrial sedimentary column for the presumably adsorbed "missing" Xe (see Pepin 1989a).

In the present model the relative abundances of the secondary, isotopically solar OG_1 component outgassed from the interiors of the two planets again display this

characteristic ratio pattern for Ne, Ar, and Kr (Fig. 13b). Origin of the interior source reservoirs by adsorption from solar-composition ambient gases is therefore an attractive possibility. Atmospheric Xe can now be excluded from consideration because it does not derive from the outgassed component. As discussed earlier, the key assumption of the model is that Xe is not significantly degassed from interior reservoirs—most of the atmospheric Xe on Earth and Mars is taken to be a relict from primary planetary atmospheres and is thus decoupled from the lighter secondary gases. However, interior (I) components incorporated into preplanetary or protoplanetary material by adsorption from the nebula would certainly have included I-Xe. Figure 13b, where Xe/Kr is plotted as the mean of fractionations observed in laboratory adsorption experiments, is an estimate of the relative elemental abundance pattern that might have characterized adsorbed I-gases. Note that the Ne/Kr and Ar/Kr ratios derived separately from the Earth and Mars models are identical, implying a common process. Two models of adsorption environments are considered here, one on free-floating preplanetary dust in the open nebula and the other on accreting protoplanetary core materials, and each is assessed against available adsorption data.

VII.D.1. Adsorption on Preplanetary Nebular Dust

To obtain approximate lower limits for the required adsorption partition coefficients k_M in this case, let us assume I-component adsorption on nebular dust comprising a full 100% of the final planetary mass, in amounts equal to twice the outgassed abundance ($C_M^i(OG_1)$) of species M (allowing for 50% degassing efficiency). For Earth, choosing ^{36}Ar as the reference species, k_{36} must then be $2C_{36}^i(OG_1)/5.7 \times 10^{-6} p_n$ g/g-atm, where the denominator is the partial pressure of ^{36}Ar in a nebula of total pressure p_n (Table V). With $C_{36}^i(OG_1) \cong 6.1 \times 10^{-11}$ g/g-Earth (Tables AI, AII) and p_n taken to be 10^{-6} atm, $k_{36} \cong 21$ g/g-atm. This and the remaining k_M , readily calculated from the data used to construct Fig. 13b, are plotted in the upper part of Fig. 20. They exceed the highest measured values (data field (a), from Fanale and Cannon's (1972) physical adsorption experiment at very low (113 K) temperature) by factors >500 . Corresponding data for outgassed Ar on Mars yield $k_{36} \cong 0.7$ g/g-atm with $p_7 \cong 3 \times 10^{-7}$ atm, considerably smaller but still a factor >10 above data field (a). However, one cannot definitely rule out even the Earth values as implausibly high, since the laboratory experiments do not replicate nebular conditions of long adsorption times and possible burial of saturated surfaces by fresh material during grain growth, both of which could increase adsorption efficiency. Nevertheless they are large enough to make it worthwhile to explore an alternative model.

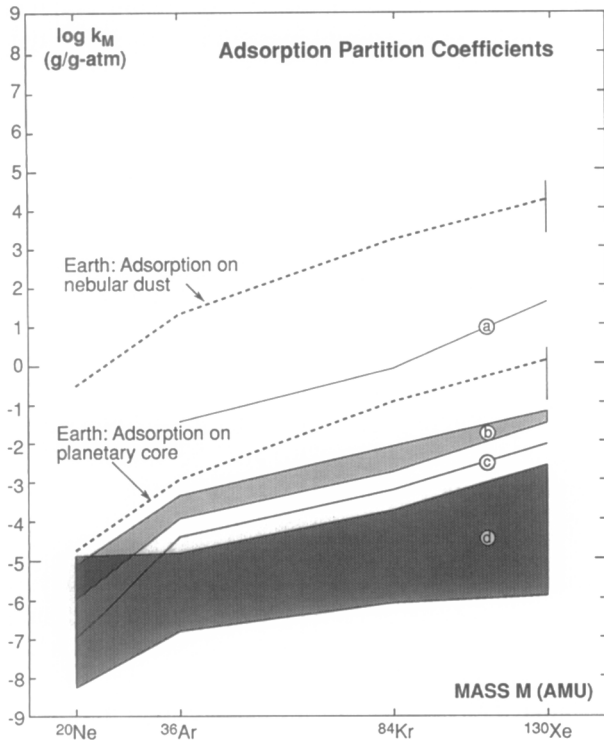


FIG. 20. Gas \rightarrow solid partition coefficients k_M required to account for abundances of outgassed noble gases on Earth, by adsorption of interior (I-component) noble gases on free-floating nebular dust (Section VII.D.1) compared to adsorption on accreting protoplanetary core surface materials (Section VII.D.2). The ^{36}Ar partition coefficient k_{36} is taken to be 10^{-3} for core adsorption, and degassing of the interior reservoir is assumed to be 50% efficient in both cases. References for the laboratory data fields (a)–(d) are listed in the legend to Fig. 18.

VII.D.2. Adsorption on Protoplanetary Cores

Terrestrial planet cores, growing through sizes of a few lunar masses (M_{moon}) in the presence of nebular gas at temperatures and pressures estimated from astronomical observations and from accretion disk models, would have captured tenuous atmospheres by condensation of ambient gases in their gravitational wells. The coefficients k_{36} required for adsorption of I-component Ar on accreting core-surface dust could then be significantly smaller than the values above, despite the fact that in this case adsorption occurred on only a fraction of final planetary masses, if atmospheric pressures p_s at core surfaces were much higher than p_n .

Formalism. Computation of I–Ar adsorption in this environment is set up in the following way. Suppose that at a particular time in core growth the core mass is M and the surface pressure is $p_s(M)$. A small increment of mass ΔM is then accreted to the core surface in the next time increment Δt and exposed to p_s . The adsorbed Ar abundance ΔA_{36} on this mass increment is

$$\Delta A_{36} = k_{36}[5.7 \times 10^{-6} p_s(M)] \Delta M \text{ grams} \quad (32)$$

and total adsorbed Ar when the core has grown to a “final” mass $M_c = \Sigma(\Delta M)$ is $A_{36} = \Sigma(\Delta A_{36})$. The objective of the calculation is to determine the value of k_{36} which for a given M_c yields $A_{36} = 2C_{36}^i(\text{OG})M_p$, where M_p is the final planetary mass and the right side is therefore just twice the mass of degassed ^{36}Ar (again assuming an outgassing efficiency $e(\text{OG})$ of 50%). To do this, however, we need to estimate p_s as a function of core mass M .

The p, T structure of atmospheres developing during planetary growth has been investigated by several workers, under assumptions of ambient nebular gas capture and various levels of grain opacity in the resulting atmospheres (Hayashi *et al.* 1979, Mizuno *et al.* 1982, Mizuno and Wetherill 1984, Nakazawa *et al.* 1985, Sasaki and Nakazawa 1990), or of water-vapor atmospheres formed by degassing of impacting planetesimals (Abe and Matsui 1985, Matsui and Abe 1986). Here we use the approach of Hayashi *et al.* (1979), which assumes nebular water content and low dust opacity in the atmosphere, and further assume that M is always small enough ($M/M_\oplus < 0.2$) that condensed atmospheres are relatively thin and in radiative equilibrium. Then for small M/M_\oplus , Hayashi *et al.*'s expressions for hydrostatic equilibrium and radiative temperature gradient yield an approximation of their Eq. (12) for the dependence of core-surface temperature on pressure:

$$T_s \equiv \left[\frac{3LCp_s^2}{32\pi\sigma GM} + T_f^4 \right]^{1/4}. \quad (33)$$

In deriving Eq. (33) we have taken the $\text{H}_2 + \text{H}_2\text{O}$ opacity κ to be proportional to pressure ($\kappa = C_p$), and assumed that in Hayashi *et al.*'s Eq. (12) the photospheric temperature T_p may be replaced by T_f , and that $p_p \ll p_s$. The effect of these latter two assumptions is small when either term in the brackets of Eq. (33) dominates; when they are comparable, calculated T_s for a given p_s is slightly high. T_f is the core-surface temperature for the case of negligible atmospheric opacity and is given by $T_f^4 = T_n^4 + GMM/4\pi r_s^3\sigma$ (Hayashi *et al.* 1979) where T_n is the nebular temperature, \dot{M} the core accretion rate, and r_s the core radius. L is the core-surface luminosity, given by $L = [1 + (2\theta)^{-1}]hGMM/r_s$, where h is the fraction of accretional energy radiated from the surface and the Safronov number θ is taken to be 4 (Abe and Matsui 1985). G and σ have their usual definitions and values. With r_s expressed in terms of M and core density ρ_c , and numerical values substituted, Eq. (33) becomes

$$T_s \equiv [954Ch\rho_c^{1/3}\dot{M}M^{-1/3}p_s^2 + T_f^4]^{1/4}. \quad (34)$$

A second expression approximately relating T_s and p_s to M may be derived by assuming that the temperature of this radiative atmosphere falls to T_n and the pressure to p' at some radial distance r' , and remains isothermal at T_n from r' out to the Hill sphere radius $r_H = R(M/3M_\odot)^{1/3}$ where R is the heliocentric distance of the core. This approximation is not a good one for the zoned radiative-convective atmospheres surrounding higher mass ($M/M_\oplus > 0.2$) objects, but it serves well enough for the tenuous atmospheres considered here. Straightforward combination and integration of the equations for hydrostatic $[GM/r^2 = -(kT/p\mu m_1)dp/dr]$ and radiative $[dT/dp = T/4p]$ equilibrium then yields $r_s/r' = 1 - [4kr_s(T_s - T_n)/(GM\mu m_1)]$, $p'/p_n = \exp\{[GM\mu m_1/kT_n r'] [1 - (r_s/r_H)]\}$, and $p_s/p' = (T_s/T_n)^4$. Combining these to eliminate r' and p' gives

$$\frac{p_s}{p_n} = \exp \left[\left(\frac{GM\mu m_1}{kT_n r_s} \right) \left(1 - \frac{r_s}{r_H} \right) \right] \times \left(\frac{T_s}{T_n} \right)^4 \exp \left[\left(\frac{-4(T_s - T_n)}{T_n} \right) \left(1 - \frac{r_s}{r_H} \right) \right], \quad (35)$$

where μ is the mean molecular weight of the atmosphere and m_1 is the hydrogen atom mass. The first exponential term in Eq. (35) is just Hunten's (1979) expression for p_s/p_n resulting from *isothermal* capture at temperature T_n , modified slightly by inclusion of a finite Hill sphere radius r_H . The remaining terms combine to reduce the p_s calculated for isothermal capture when $T_s > T_n$.

Parameters. Aside from p_s , T_s , and M , Eqs. (34) and (35) involve the quantities μ , T_n , p_n , ρ_c , h , \dot{M} , and C . The following values are adopted for "reference" core-adsorption models for Earth, Venus, and Mars; effects of different choices for the more critical of these parameters are explored below. For a solar composition atmosphere, $\mu = 2.30$ (Section V.D.3). T_n is estimated from Beckwith *et al.*'s (1990) observational survey of circumstellar disks around young stellar objects (ages ranging from $\sim 10^5$ to $\sim 10^7$ years) in Taurus-Auriga. The implied mean temperature at 1 AU of the 68 detected disks with known IR flux densities is ~ 150 K, and $T \propto R^{-0.59}$, yielding $T_n \sim 180$, 150, and 120 K at the radial positions of Venus, Earth, and Mars, respectively. We assume that at 1 AU, $p_n \equiv 1 \times 10^{-6}$ atm; the radial pressure dependence $p_n \propto R^{-13/4}$ derivable from Beckwith *et al.*'s (1990) data then gives $p_n \sim 2.9 \times 10^{-6}$ atm for Venus and 2.5×10^{-7} atm for Mars. Core densities ρ_c are assumed equal to the uncompressed densities of the present planets: 4.03 and 3.95 g/cm³ for Earth and Venus respectively (Kaula 1990) and ~ 3.7 g/cm³ for Mars—the model is relatively insensitive to $\pm 10\%$ variation in these values. The partition factor h between the rates of accretional energy input and surface-radiated energy is quite uncertain. It is set to 0.50,

crudely reflecting the possibilities of both substantial buried heat and radiant energy loss from material lofted to high altitudes by impact (Kaula 1979).

We consider two different core accretion rates $\dot{M}(M)$: "fast" rates (to $\sim 10 M_{\text{moon}}$ in ~ 1 myr for Earth) calculated from the slopes of Wetherill's (1986) planetary growth curves for the terrestrial planets; and, for comparison, "slow" rates (to $\sim 10 M_{\text{moon}}$ in ~ 9 myr for Earth) taken from Kaula's (1979) rederivation of Safronov's (1972) accumulation rate. Finally, the hydrogen and water vapor opacity κ , for which the proportionality $\kappa \equiv C\rho$ was assumed in deriving Eq. (33), is treated as follows: best-fit values of C were estimated separately for temperatures ranging from 150 to 1000 K from the κ - ρ - T plot given in Fig. 2 of Hayashi *et al.* (1979), and the value of C most appropriate to the p - T range over which the bulk of ^{36}Ar adsorption occurs was then used in Eq. (34).

Results. For a given M , Eqs. (34) and (35) may now be iteratively solved for $T_s(M)$ and $p_s(M)$, and the resulting value of $p_s(M)$ substituted into Eq. (32). ΔM is set equal to $M_c/100$ for each step of the summation, and Δt for each step is then $\Delta M/\dot{M}(M)$; thus total accretion time t to final core mass M_c is $\Sigma \Delta t = \Sigma \Delta M/\dot{M}(M)$. Results of the computations are shown in Figs. 21 and 22. The numbers (1) and (2) in Fig. 21 designate $T_s(M)$ and $p_s(M)$ vs M_c curves derived for Earth using the Wetherill (1986) and Kaula (1979) accretion rates respectively; (3) refers to a more recent core accumulation rate by Wetherill (1990a,b) and is discussed below. Solid curves represent calculated values, and the dashed curves the trends that T_s and p_s would follow for zero atmospheric opacity throughout growth (i.e., for $T_s \equiv T_f$). Below $M_c \sim 3M_{\text{moon}}$ the captured atmospheres are so tenuous that $T_s \equiv T_f$. Above this mass opacity begins to dominate. Solid circles define an Earth core reference model which uses Wetherill's (1986) accretion rate, and in which k_{36} is taken to be 10^{-3} .

Values of k_{36} vs the corresponding core masses M_c required for adsorption of amounts of I - ^{36}Ar equal to twice the outgassed inventories $C_{36}(\text{OG}_1)$ on Earth and Mars are given by the solid curves in Fig. 22. The solid circle defines the $k_{36} = 10^{-3}$ reference model for Earth: the required core mass is $6.24 M_{\text{moon}}$ (about $0.077 M_\oplus$), and $T_s \equiv 520$ K and $p_s \equiv 1.8$ atm from Fig. 21. The full set of calculated k_M values for this choice of k_{36} is plotted in Fig. 20. As noted earlier in Section V.B.2, there is currently no way to decide whether outgassed I-gases have contributed to the Venus atmosphere. The long-dashed curve in Fig. 22 represents k_{36} vs M_c for a Venus core assumed to have adsorbed the same abundance of I - ^{36}Ar per g -planet as Earth. The short-dashed Venus curve denotes required core sizes for the extreme case where *all* of the abundant atmospheric ^{36}Ar ($>70 \times$ Earth's inventory on a g/g -planet basis) derives from 50% degassing

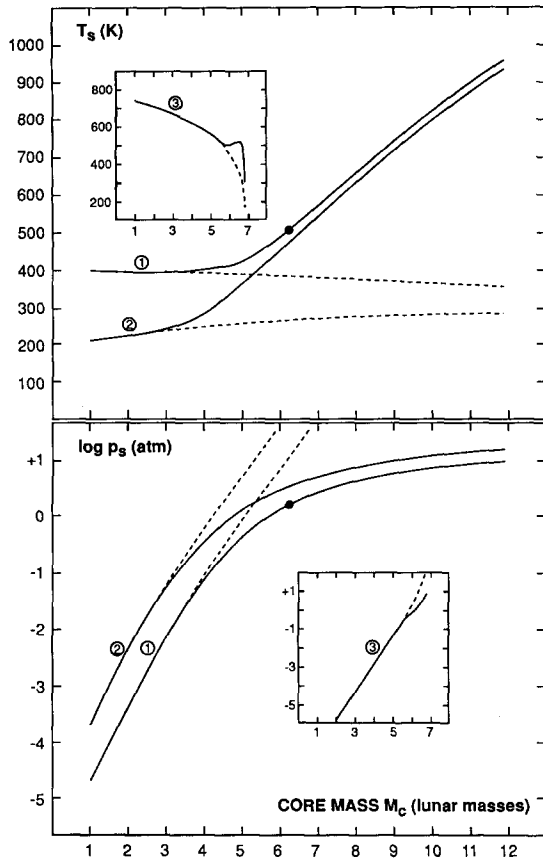


FIG. 21. Surface temperature and pressure vs core mass on an accreting protoEarth core surrounded by a gravitationally captured solar-composition atmosphere. Curves (1), (2), and (3) represent results for core accretion at different rates (see text, Section VII.D.2). Dashed curves show calculated surface T, p conditions for zero atmospheric opacity. Solid circles identify an Earth core reference model with $k_{36} = 10^{-3}$ and other parameter values specified in the text.

of adsorbed I–Ar. In this case, for $k_{36} = 10^{-3}$, M_c would have to be $>12 M_{\text{moon}}$, or $\sim 20\%$ of the final planetary mass.

Figure 23 shows the consequences, for calculated Earth core masses, of separately altering individual parameter values adopted for the Earth reference model (represented as before by the solid circles) while keeping the others fixed. The substantial variations in nebular temperature and pressure in panels (a) and (b) are accommodated by core masses that differ from the reference mass by factors <2 . Note that this relative insensitivity to ambient p, T conditions reduces the importance of the tacit assumption that growth of protoplanetary cores occurred at precisely the heliocentric distances of the present-day planets—an assumption *not* in accord with the standard model of planetary accumulation (Wetherill 1986, 1990a).

It is informative to consider a case, based on a nebular model, in which both these parameters depart from the

nebular conditions inferred from Beckwith *et al.*'s (1990) observational data. If we suppose that terrestrial planet cores grew during a late stage of disk evolution in which the solar accretion rate was $\sim 10^{-7} M_{\odot}/\text{year}$ (a value suggested by Beckwith *et al.* to account for observed disk luminosities), then Wood and Morfill's (1988) solar nebula model yields (T_n, p_n) combinations of (280 K, 2.1×10^{-6} atm) for Venus, (170 K, 1.0×10^{-6} atm) for Earth, and (90 K, 3.9×10^{-7} atm) for Mars. For the latter two these produce only modest changes in the k_{36} vs M_c curves shown in Fig. 22: for a given k_{36} , the required M_c is only slightly smaller for Mars and slightly larger for Earth. But the combination of significantly higher T_n and lower p_n reduces adsorption efficiency on the Venus core to the extent that M_c is $\sim 50\%$ larger at $k_{36} = 10^{-3}$ than the reference model (long-dashed curve) value.

Figure 23c indicates that a doubling of M_c could accommodate outgassing efficiencies $e(\text{OG}) \sim 50$ times lower than the nominal reference value of 50%. Such inefficient core degassing seems unlikely for Earth, but perhaps not for Mars or Venus. Panel (d) indicates that M_c is not very sensitive to the choice of the energy partition coefficient h , and thus to core-surface luminosity, over its possible range from 1 to 0. However, that is not the case for substantial increases in atmospheric opacity due to the

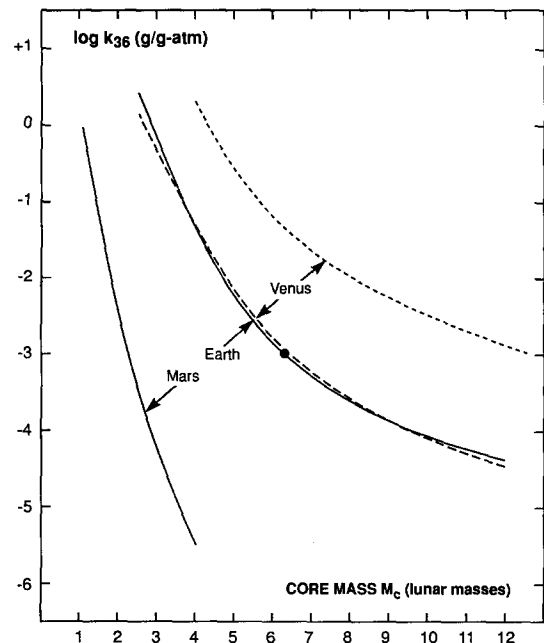


FIG. 22. Protoplanetary core masses M_c vs values of k_{36} for ^{36}Ar adsorption on core surface materials required to account for abundances of outgassed Ar on Earth and Mars, assuming 50% degassing efficiencies from core reservoirs. The dashed curves for Venus, where in the present model outgassing has contributed only modestly if at all to present-day atmospheric inventories (Section V.B.2), are discussed in Section VII.D.2. The solid circle is the Earth core reference model.

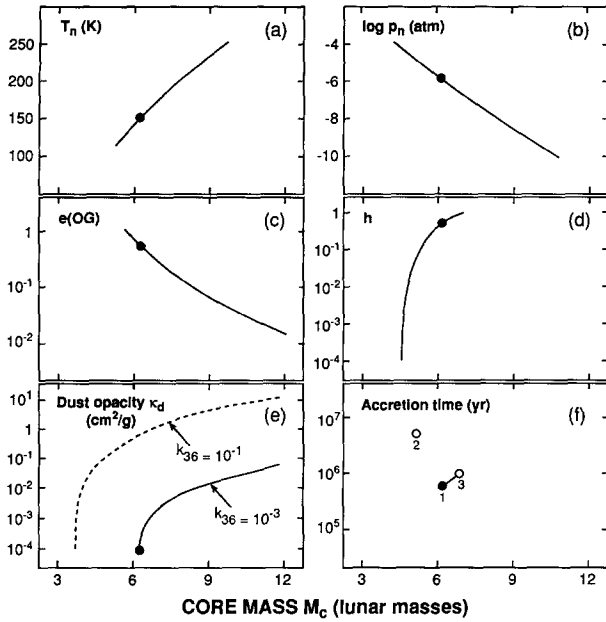


FIG. 23. Effects on the required core mass for Earth of separately varying individual model parameters around the values adopted for the reference model (solid circles). Panels (a) and (b) show sensitivities of M_c to ambient nebular temperatures and pressures at the Hill sphere radius; (c) and (d) to assumed degassing efficiency $e(\text{OG})$ and the impact energy partitioning factor h ; (e) to atmospheric dust opacity κ_d ; and (f) to accretion time, where the numbers refer as in Fig. 21 to the three differing core accretion rates discussed in the text.

presence of dust (Mizuno *et al.* 1980, Mizuno and Wetherill 1984, Sasaki and Nakazawa 1990) or water vapor (Abe and Matsui 1985, Matsui and Abe 1986) above the low levels assumed by Hayashi *et al.* (1979). This is illustrated for dust opacity κ_d in panel (e). The reference model takes $\kappa_d = 10^{-4} \text{ cm}^2/\text{g}$ after Hayashi *et al.*, and with $k_{36} = 10^{-3}$ it cannot accommodate a κ_d much higher than $\sim 10^{-1}$. Higher k_{36} would be needed to permit $\kappa_d \geq 1$ —the maximum value considered by Mizuno *et al.* (1980) and Mizuno and Wetherill (1984)—for relatively small M_c , as illustrated by the dashed curve for $k_{36} = 10^{-1}$. So the reference core adsorption models defined here presume relatively dust-free (and dry) atmospheres.

Adsorption on Wetherill's (1990b) "planetary embryos." As shown in Fig. 23f, the effect on M_c of the roughly order-of-magnitude average difference between the slow Kaula (1979) accretion rate (2) and the faster Wetherill (1986) rate (1) is not dramatic—again a reflection of relative insensitivity to core luminosity. This is also true for the results of Wetherill's (1990b) most recent modeling of planetary accumulation, represented by (3) in panel (f), in which ~ 20 planetary embryos grow very rapidly—in $\sim 10^4$ – 10^5 years—from an initial population of ~ 10 km planetesimals, and then more slowly to masses

of $\sim 5 \times 10^{26} \text{ g}$ ($6.8 M_{\text{moon}}$) within about 10^6 yr. The fact that this new version of Wetherill's standard accumulation model leads to similar results for I-component adsorption is remarkable, since core accretion rates \dot{M} and thus the profiles of surface temperature and pressure vs core mass are distinctly different. An illustration is shown in the insets to Fig. 21, for a case where a protoEarth embryo is assumed to grow to 90% of its final mass M_f in 10^5 years and asymptotically approach M_f at 10^6 years (expressed by $M = M_f(1 - e^{-\beta t})$ and $\dot{M} = \beta(M_f - M)$ with $M_f = 5 \times 10^{26} \text{ g}$ and $\beta = 2.3 \times 10^{-5}/\text{year}$). The T_s and p_s dependences on M_c shown in the insets are derived from Eqs. (34) and (35) using this \dot{M} and reference values for the remaining parameters. Summation of Eq. (32) to a final (now specified) core mass $M_f = M_c = 6.8 M_{\text{moon}}$ actually generates $\sim 50\%$ more adsorbed I–Ar than the earlier reference model for Earth (so point 3 in Fig. 23f is for an outgassing efficiency $e(\text{OG}) \cong 1/3$ rather than $1/2$), despite the fact that the very high \dot{M} characterizing early core growth keeps its surface hot enough to prevent appreciable atmospheric condensation until M_c approaches $6 M_{\text{moon}}$. Here almost all of the I-component is adsorbed in the low \dot{M} period between 10^5 and 10^6 yr. Consequently its distribution is more sharply peaked toward the core surface; 90% is contained in the outer $\sim 1/8$ of the core mass, compared to the outer $\sim 1/4$ in the reference model.

Some distribution of final planetary embryo sizes around the $\sim 6.8 M_{\text{moon}}$ average at $\sim 10^6$ yr exists in the Wetherill (1990b) accretion model. An embryo for Earth a factor of ~ 2 larger would enable sufficient I-gas adsorption for unfavorable parameter values in Fig. 23 (although not for unfavorable parameter combinations). The model raises some interesting possibilities for the I-component content of Mars. Whether the low surface abundance of Martian noble gases is due to major losses of degassed atmospheric species to space, inefficient degassing, or an intrinsically low initial endowment of volatiles is presently unclear (Fanale *et al.* 1991). The smallest embryo that could adsorb an amount of ^{36}Ar just equal to the outgassed abundance on Mars, requiring $e(\text{OG}) = 1$, is about $2.2 M_{\text{moon}}$ or $\sim 1/3$ the average embryo mass. A slightly larger core ($\sim 2.7 M_{\text{moon}}$) yields $e(\text{OG}) \cong 1/6$. But if it somehow happened that the embryo destined for Mars grew to the average mass of the distribution, $\sim 6.8 M_{\text{moon}}$, and thus managed to accrete only another $\sim 30\%$ of mass in becoming the final planet, then the calculated outgassing efficiency is $\sim 4 \times 10^{-4}$ and in this case either the Martian interior is much more volatile-rich than its surface reservoirs, or losses of degassed species have been large.

VII.D.3. Conclusions

The k_M values plotted for the Earth core model in Fig. 20, for the moderate core mass given by setting $k_{36} =$

10^{-3} , are lower than those shown for nebular adsorption by factors of $\sim 2 \times 10^4$. (The $\sim 20 \times$ smaller values given by Pepin (1990a) in a preliminary version of this model are for a larger Earth core ($\sim 9 M_{\text{moon}}$), and moreover assume isothermal atmospheric capture, given by the first bracketed term of Eq. (35), which overestimates the surface pressure p_s .) Although they still fall above most of the laboratory data fields, they do not appear unreasonably large, and so the core model seems the more plausible of the two in the context of adsorption data currently on hand.

Further assessment of the viability of either of these models, and of adsorption in general as a mechanism of noble gas incorporation into preplanetary or protoplanetary materials, will require new experimental approaches. A central question, noted earlier, is the relevance of the present data to adsorption in nebular or core-accretion environments which differ in important chemical and physical respects from the laboratory conditions under which they were obtained. The most obvious need, in both models, is for measurement of adsorption of noble gases from a solar-like, hydrogen-dominated gas phase in which they are only trace constituents. Such measurements should be extended to helium, which is not included in the current data base. There is clear evidence for the presence of solar-like and presumably primordial He within the Earth and in meteorites, and it is possible that this component could derive from adsorption on protoplanetary cores and on meteorite parent bodies (Section V.D)—perhaps by diffusion and trapping in grain pore labyrinths (Wacker *et al.* 1985, Wacker 1989)—at temperatures well above the low adsorption temperature usually assumed for it. Moreover it is important to note that most of the experimental values refer to adsorption on carbonaceous substrates, and data are needed for the more common silicate minerals that would be expected to dominate in the nebular dust and core-accretion regimes. One interesting question along these lines for a protoplanetary core accreting by energetic impacts is whether condensates of impact-vaporized materials in this kind of H_2 -rich environment might resemble the hydrogenated amorphous carbon (a-C:H), silicon (a-Si:H), or hybrid (a-C:Si:H) films that have been produced experimentally by low-pressure vapor deposition and are now under intensive study in industrial laboratories (for example see DeVries 1987 and references therein). Some of these unusual “alloys” appear to grow with extremely high vacancy concentrations (Bar-Yam and Moustakas 1989). Such condensation films, if they were able to form in a natural accretional environment under kinetically rapid conditions, could conceivably be characterized by very large gas/solid distribution coefficients.

Adsorption and occlusion of gases within growing protoplanetary cores would appear to be a natural conse-

quence of Wetherill's (1990b) new early-stage model of planetary accumulation, at decreasing rates and in the presence of nebular gas, to embryo masses of $\sim 5 \times 10^{26}$ g in $\sim 10^6$ years. His speculation that dissipation of nebular gas at about this time may have initiated the next stage of accretion, to essentially final planetary masses by “giant impact” merger of these embryos, has a number of implications for atmospheric evolution if it turns out to be correct. Core adsorption would be naturally truncated at $\sim 10^6$ years or shortly thereafter, but at levels that appear large enough to supply outgassed species on Earth and Mars if distribution coefficients for Ar adsorption on the total mass of accreting core materials approached or exceeded $\sim 10^{-4}$ – 10^{-3} . However, capture of increasingly more massive and opaque solar-like atmospheres from the nebula as planetary growth continued beyond the core mass range considered here would not occur. Therefore, although the planets were extensively melted during the giant impact stage (Wetherill 1990a), and atmospheres accumulating from impact-degassed planetesimal volatiles (e.g., Abe and Matsui 1985, Matsui and Abe 1986, Tyburczy *et al.* 1986) were probable, solar-composition atmospheric sources of high enough Ne partial pressure to drive significant dissolution of Ne into molten surface materials (Mizuno *et al.* 1980, Mizuno and Wetherill 1984, Sasaki and Nakazawa 1990) might not have been present throughout later stages of planetary growth.

VIII. SUMMARY

The model described in this paper attempts to synthesize approaches taken in previous efforts to understand the origin of volatile distributions in planetary atmospheres and meteorites, and to place them in a context more fully integrated into ideas about the nature of the Solar System's early astrophysical environment and how that environment might have evolved with time. The hypothesis of hydrodynamic escape of massive primary atmospheres clearly places the basic planetary model in Donahue and Pollack's (1983) “gas-rich” class. But direct conceptual antecedents of the adsorbed components in planetary and planetesimal interiors are found in earlier gas-poor “grain-accretion” theories, and the meteoritic source invoked for carbon and nitrogen on Earth and Venus is obviously just a restricted and specific version of previous “vener” scenarios. So the model involves a combination of familiar primordial components and theories, and processes of adsorption and escape that are likewise well known although the hydrodynamic loss mechanism is a relatively new development.

It differs from most earlier approaches, however, in three respects. (1) The full ranges of observed isotopic variations, from primordial to contemporary compositions on and within present-day planetary and meteoritic

reservoirs, are taken into account and attributed to a single fractionating process operating to varying degrees under individual planetary or planetesimal rather than nebular conditions. Final isotopic distributions therefore can be (and are) specific to a particular body. (2) Primordial volatiles are processed in defined astrophysical environments with characteristics that relate directly to, and can be assessed from, the observational astronomical record of conditions and processes in pre-main-sequence stars and their accretion disks. (3) The chronology for the various stages of planetary atmospheric evolution (t_0 , t_{fA} , t_{og} , t_v , and t_f) is tied directly to timescales for evolution of surface activity on the young sun, via expressions for the time dependence of the solar EUV flux driving hydrodynamic escape from planets.

The present models are basically attempts to solve inversion problems by modeling back from volatile inventories observed in terrestrial planet atmospheres and meteorites. But there is a forward-modeling aspect as well, because something is presumed to be known about initial compositions. The processes in between can be regarded in a mathematical sense as operators that map one mass distribution into another. Thus the objective has been to identify astrophysically credible processes, here adsorption and hydrodynamic escape, express them analytically as operator equations, and seek and assess those subsets of solutions that fractionate primordial into contemporary compositions.

These evolutionary models are operationally presented as exercises in forward modeling, in which process operators act on assumed primary mass distributions. But the overriding criterion is replication of present-day inventories, and primary compositions are subject to this constraint. Models of this kind, with a strong backward modeling flavor, characteristically do not yield unique inversion solutions. This one is no different. The "solar" isotopic compositions taken to characterize noble gases in the early nebula, in solar-like primordial atmospheres, and in interior planetary and planetesimal reservoirs are not the only ones that could serve—as demonstrated, for example, by the ability of the model to accommodate different initial Kr compositions. However, these "solar" compositions are subject to constraints which bound their allowed ranges, and it is encouraging that the particular suite of isotope ratios used here, based on direct observation and fossil records of solar wind composition and thus arguably our best measure of solar and nebular distributions, leads to generally acceptable results.

A much more fundamental assumption underlying the basic model is that concerning the geochemical behavior of xenon in planetary interiors. There is no obvious way to generate observed Xe compositions on Earth and Mars if outgassed Kr and lighter noble gases were accompanied by more than a small fraction of their associated Xe.

Consequently the model demands that most of this Xe be retained within the solid planets, presumably by preferential partitioning into iron-rich mineral phases under conditions of high pressure. The small size of Mars dictates that this behavior must occur at pressures not exceeding a few hundred kilobars. Thus the model, at least in its present form, will stand or fall on the results of laboratory investigations of Xe partitioning in this pressure range.

It is clear that the planetary models, with appropriate choices for parameters that directly control fractionation during hydrodynamic loss, are able to generate generally acceptable matches to observed isotope distributions, and yield reasonable elemental fractionation patterns for the noble gas adsorption process. This capability does not depend sensitively, if at all, on assumptions about the mode of hydrogen escape (constant-inventory vs Rayleigh loss), the precise way in which the magnitude of the hydrogen escape flux declined with time (exponential vs power law decay), or, for exponential decline, the value of the mean decay constant τ . Similar statements apply to the more speculative planetesimal model for meteorite noble gas evolution. In this sense the models are robust. But this also means that the criterion of best fit to observation, in and of itself, has little or no selective power for what on other grounds might be preferred choices for these particular parameters. There are ancillary considerations, however, that do have this power to some degree. Arguments based on hydrogen and energy requirements, the consequences of water reduction for the present oxidation states of the terrestrial planets, and the observational record of surface activity evolution on solar-type pre-main-sequence stars, together point to a restricted class of acceptable histories for early solar EUV radiation and hydrogen escape fluxes from planets. These are characterized by EUV intensities that initially were a few hundred times above present solar levels, declined as short time constant exponentials (departing by relatively small factors from $\tau \sim 90$ myr) or as small-exponent power laws (s probably $\approx 5/6$ or less), and drove atmospheric evolution by hydrodynamic escape during the first ~ 400 myr or less of planetary lifetimes.

Although matches to present-day isotopic compositions are generally satisfactory, several anomalies are evident in the Fig. 10 comparisons of observed light-element planetary ratios with those derived from the model. Low calculated values for $^{21}\text{Ne}/^{22}\text{Ne}$ and $^{15}\text{N}/^{14}\text{N}$ on Earth and Mars respectively are straightforwardly interpreted as reflecting later augmentation by terrestrial outgassing of a nucleogenic crustal $^{21}\text{Ne}_n$ component and preferential loss of Martian ^{14}N to space, both occurring after the epochs of hydrodynamic escape had ended. The hypothesis that hydrodynamic overfractionation of $^{20}\text{Ne}/^{22}\text{Ne}$ on Mars was compensated by postescape addition of solar wind species is more speculative but not intrinsically unreasonable.

able, given the susceptibility of the tenuous Martian atmosphere to such alteration and the strengths of potential IDP or direct capture sources.

Monoisotopic species such as $^{21}\text{Ne}_n$ are wild cards in the sense that the evolution of isotopic systems to which they contribute is not controlled solely by fractionation processes. Two additional cases of largely or purely monoisotopic perturbation appear in the heavy gases Kr and Xe: at ^{86}Kr , where the excesses in meteorites shown in Figs. 5 and 11 are attributed to nucleogenetic H- ^{86}Kr components; and at ^{129}Xe , where the effects of different proportions of radiogenic ^{129}Xe in the Martian atmosphere and interior are strikingly demonstrated by comparison of $^{129}\text{Xe}/^{130}\text{Xe}$ ratios in Figs. 8 and 14. This distribution on Mars, implying early and extreme surface concentration of the planetary ^{129}I inventory and efficient separation of its daughter from nonradiogenic atmospheric Xe during atmospheric loss, seems at least qualitatively consistent with the expected behavior of iodine compounds in the escape model environment.

Turning from isotopic to elemental abundance distributions, one sees from Fig. 13 that primordial atmospheric reservoirs display planet-to-planet variations in noble gas ratios, but interior reservoir compositions are uniform on the two planets where products of outgassing are detectable. Origin of interior sources for secondary atmospheres by adsorption of gravitationally condensed nebular gases on protoplanetary cores appears to account reasonably well for both the isotopic and the elemental characteristics of outgassed species on Earth and Mars. Remnant gases from this source could also explain the traces of solar-like He and Ne still degassing from Earth (*if* He adsorbs efficiently enough on core materials, an issue not yet addressed in laboratory experiments).

Deductions of origin from the elemental signatures in primary atmospheres are more problematic. Mars is the clearest case; there the assumption of the carbonaceous chondrite pattern shown in Fig. 13a follows directly from the isotopic evidence of Fig. 8 for derivation of Martian Xe from CI-Xe, and from the need for a substantial CI-like component in geochemical models of bulk composition. On Venus and Earth, elemental compositions derived from the model appear to be related by mass fractionation. This suggests as one possibility that both atmospheres were originally characterized by the more solar-like Venus distribution and the Earth pattern resulted from later fractionation, prior to the beginning of hydrodynamic escape, by partial ejection in a giant impact event. Principal candidates for isotopically solar, Venus-like atmospheric sources are gravitational capture and accretion of icy planetesimals. Of these, at the moment, ices appear more attractive in view of (1) current estimates of shorter timescales for nebular dissipation than for planetary growth to masses large enough for substantial cap-

ture; (2) their potential ability to supply adequate hydrogen and noble gases simultaneously; and (3) evidence that occlusion of noble gases in ices discriminates against Ne and could therefore account for the Ne depletion on Venus. But nebular capture cannot be ruled out, and an icy source has problems of its own. There is a danger of oversupplying the planets with carbon and nitrogen, and as yet no experimental confirmation that low-temperature adsorption on ices can yield the roughly solar Ar : Kr : Xe ratios that characterize Venus's primary atmosphere (while there is evidence that clathration does not).

The general argument for derivation of surficial carbon and nitrogen on Venus and Earth from late accretion of C-N-rich veneers is based on the compositionally similar inventories of these elements on the two bodies, in contrast to evidence for markedly dissimilar planetary histories of magmatism, tectonic activity, and outgassing. Origin from infall of chemically uniform materials from a common external source therefore appears more straightforward than degassing from internal sources. A specific modeling argument for this hypothesis is that it appears to work reasonably well in accounting for isotopic and elemental ratios. Compositional demands on the veneering material are met by a known meteorite class, the E chondrites, for which an inner solar system provenance has been suggested on other grounds. One apparent problem with this source is that it might easily oversupply radiogenic ^{129}Xe to Earth. On Mars, surface carbon and nitrogen could have been emplaced by degassing of a CI accretional component, in amounts greatly exceeding present-day atmospheric abundances. There is no particular difficulty in attributing the underabundances of N_2 and CO_2 in the contemporary Martian atmosphere to long-term nitrogen escape and incorporation into mineral phases, and sequestering of most of the initial carbon dioxide inventory in carbonate reservoirs. However, quantification of this C-N outgassing hypothesis involves arguments within the error bars of current noble gas data, and so at the moment is more an illustrative example than a serious modeling exercise.

The analytically simple escape-adsorption model for production of fractionated, surface-sited noble gases in planetesimal surface grains does a remarkably good job of replicating most of the Q-component isotope ratios observed in meteorite carrier phases. Required elemental fractionations in adsorption fall within the data field yielded by laboratory studies of the process in artificial and natural samples. These two results follow directly from application to the planetesimal regime of postulates or deductions from the planetary models—that noble gases outgassed from the interior reservoir were isotopically solar, and, as on Venus, were elementally solar-like in Xe : Kr : Ar but depleted in Ne. But neither of these successes should obscure the fact that several of the

model assumptions are more speculative, notably those relating to the identity and production of the dominant atmospheric constituent (methane or some other species), the mixing ratios of noble gases with this constituent, and the energetics and timescale of hydrodynamic blowoff. The questions of where in the solar system and when in nebular history the Q-component was generated are open, as are the issues of how many parent bodies were involved and how their carrier materials might have been ejected and thoroughly mixed prior to incorporation into meteorites. Nevertheless, despite all these uncertainties, the basic planetesimal model appears promising.

Finally, it is useful to summarize the experimental and observational tests that can be applied to the model. Most crucial to the planetary models is laboratory assessment of the high-pressure partitioning behavior of Xe relative to that of the lighter noble gases. Experimental demonstration that low-temperature adsorption of noble gases on accreting ices can reflect gas-phase relative abundances for Xe, Kr, and Ar, while discriminating against

Ne, would support the icy carrier hypothesis for the origin of noble gases in primary atmospheres on Venus, Earth, and in planetesimal interiors. Observation of significant departures from ambient heavy noble gas ratios, however, would force a reevaluation of how well such elementally fractionated compositions could serve, and different approaches to the nature of the carrier if they failed. At the moment it appears that purely clathrated noble gases are not feasible sources, although there is room to accommodate some variation from solar composition in view of the large uncertainties in measured abundances of Xe, Kr, and to a lesser extent Ar, on Venus. The precise composition of the present-day Venus atmosphere is a key observational test, and not primarily because of this need for more accurate determination of elemental abundances or because the Venus model is poorly constrained by the isotopic information we currently have for Ne and Ar. The most central issue is the completely unknown compositions of Kr and Xe, for which the model makes specific predictions.

APPENDIX

TABLE AI

Earth I Model: Partial Spreadsheet Output, Assuming Initial Kr Composition = Solar Kr-1 (Table III)

	Mass M (amu)						Isotopes M'/M						
	130 (Xe)	84 (Kr)	44 (CO ₂)	36 (Ar)	28 (N ₂)	20 (Ne)	$\frac{124\text{Xe}}{130\text{Xe}}$	$\frac{78\text{Kr}}{84\text{Kr}}$	$\frac{13\text{C}^{16}\text{O}_2}{12\text{C}^{16}\text{O}_2}$	$\frac{36\text{Ar}}{38\text{Ar}}$	$\frac{15\text{N}^{14}\text{N}}{14\text{N}_2}$	$\frac{20\text{Ne}}{22\text{Ne}}$	$\frac{21\text{Ne}}{22\text{Ne}}$
Hydrodynamic escape fractionation factors													
$f_{M, f_{M'/M}(A)_C^a$	3.429(-02)	8.557(-03)	1.268(-03)	1.256(-03)	7.623(-04)	7.883(-04)	0.79300	0.76410	1.04299	0.90173	1.04961	0.86623	0.93071
$f_{M, f_{M'/M}(OG)_R^b$	1	9.526(-01)	5.246(-01)	5.206(-01)	2.355(-01)	2.595(-01)	1	0.97048	1.03287	0.92584	1.15066	0.71533	0.87203
Initial volatile inventories ^c													
$C_M^i, C_{M'/M}^i(A_s)$	4.08(-13)	1.18(-11)	7.22(-07)	4.54(-09)	4.76(-08)	0	2.947(-2)	6.359(-3)	?	5.80	?	13.7	3.27(-2)
$C_M^i, C_{M'/M}^i(OG)_i$	-0	1.64(-12)	8.03(-09)	6.06(-11)	5.29(-10)	3.85(-11)	2.947(-2)	6.359(-3)	?	5.80	?	13.7	3.27(-2)
Residual volatile inventories ^c													
$C_M^f, C_{M'/M}^f(A_s)$	1.40(-14)	9.63(-14)	4.80(-10)	2.97(-12)	8.55(-12)	0	2.337(-2)	4.716(-3)	—	4.842	—	8.489	2.654(-2)
$C_M^f, C_{M'/M}^f(OG)_i$	-0	1.56(-12)	4.21(-09)	3.15(-11)	1.25(-10)	1.00(-11)	—	6.172(-3)	—	5.370	—	9.800	2.852(-2)
$C_M^f, C_{M'/M}^f(\text{calculated})^d$	1.40(-14)	1.66(-12)	4.69(-09)	3.45(-11)	1.33(-10)	1.00(-11)	2.337(-2)	6.087(-3)	—	5.320	—	9.800	2.852(-2)
$C_M^f, C_{M'/M}^f(\text{Earth})^e$	1.40(-14)	1.66(-12)	3.7(-05)	3.45(-11)	9.1(-07)	1.00(-11)	2.337(-2)	6.087(-3)	111.6(-4)	5.320	7.353(-3)	9.800	2.899(-2)

Note. Subscript C designates escape at constant hydrogen inventory, R designates Rayleigh escape. Powers of ten multipliers in parentheses.

^a $\alpha [A] = 13.13334, m_1 = 2. (m_2^0, m_2^A) = 343.0, 123.9$ (Xe); 303.3, 109.7 (Kr); 322.9, 116.7 (CO₂); 263.2, 95.4 (Ar); 281.0, 101.7 (N₂); 190.1, 69.3 (Ne).

^b $\alpha_{\text{OG}} = 1.37395, m_1 = 2. (m_2^0, m_2^A) = 109.7, 31.8$ (Kr); 116.7, 33.7 (CO₂); 95.4, 27.8 (Ar); 101.7, 29.6 (N₂); 69.3, 20.6 (Ne).

^c Units are g/g-Earth for C_M^i and $C_{M'/M}^i$, atom/atom for C_M^f and $C_{M'/M}^f$.

^d $C_M^f, C_{M'/M}^f(\text{calculated}) = \Sigma C_M^f, C_{M'/M}^f(A_s + OG)_i$.

^e Tables II, III.

TABLE AII

Earth II Model: Partial Spreadsheet Output, Assuming Initial Kr Composition = Solar Kr-1 (Table III)

	Mass M (amu)						Isotopes M'/M						
	130 (Xe)	84 (Kr)	44 (CO ₂)	36 (Ar)	28 (N ₂)	20 (Ne)	$\frac{124\text{Xe}}{130\text{Xe}}$	$\frac{78\text{Kr}}{84\text{Kr}}$	$\frac{13\text{C}^{16}\text{O}_2}{12\text{C}^{16}\text{O}_2}$	$\frac{36\text{Ar}}{38\text{Ar}}$	$\frac{15\text{N}^{14}\text{N}}{14\text{N}_2}$	$\frac{20\text{Ne}}{22\text{Ne}}$	$\frac{21\text{Ne}}{22\text{Ne}}$
Hydrodynamic escape fractionation factors													
$f_{M, f_{M'/M}(A)_C^a$	2.375(-01)	5.091(-02)	6.070(-03)	6.007(-03)	3.443(-03)	3.575(-03)	0.77710	0.74104	1.04800	0.89117	1.05542	0.85217	0.92313
$f_{M, f_{M'/M}(OG)_R^b$	1	9.520(-01)	5.164(-01)	5.124(-01)	2.298(-01)	2.492(-01)	1	0.97008	1.03424	0.92299	1.12426	0.71704	0.85305
$f_{M, f_{M'/M}(V)_R^c$	1	1	1	1	9.005(-01)	9.210(-01)	1	1	1	1	1.03302	0.92166	0.96714

TABLE AII—Continued
Earth II Model: Partial Spreadsheet Output, Assuming Initial Kr Composition = Solar Kr-1 (Table III)

	Mass M (amu)						Isotopes M'/M						
	130 (Xe)	84 (Kr)	44 (CO ₂)	36 (Ar)	28 (N ₂)	20 (Ne)	$\frac{124\text{Xe}}{130\text{Xe}}$	$\frac{78\text{Kr}}{84\text{Kr}}$	$\frac{13\text{C}^{16}\text{O}_2}{12\text{C}^{16}\text{O}_2}$	$\frac{36\text{Ar}}{38\text{Ar}}$	$\frac{15\text{N}^{14}\text{N}}{14\text{N}_2}$	$\frac{20\text{Ne}}{22\text{Ne}}$	$\frac{21\text{Ne}}{22\text{Ne}}$
	Initial volatile inventories ^d												
$C_M^j, C_{M'/M}^j(A_S)$	5.52(-14)	1.76(-12)	1.08(-07)	6.13(-10)	7.10(-09)	0	2.947(-2)	6.359(-3)	?	5.80	?	13.7	3.27(-2)
$C_M^j, C_{M'/M}^j(\text{OG}_1)$	~0	1.65(-12)	8.08(-09)	6.22(-11)	5.32(-10)	4.00(-11)	2.947(-2)	6.359(-3)	?	5.80	?	13.7	3.27(-2)
$C_M^j, C_{M'/M}^j(V)$	8.99(-16)	6.56(-15)	3.38(-05)	7.24(-13)	1.10(-06)	4.39(-14)	2.97(-2)	6.34(-3)	111.4(-4)	5.46	7.118(-3)	6.7	?
	Residual volatile inventories ^d												
$C_M^f, C_{M'/M}^f(A_S)$	1.31(-14)	8.53(-14)	3.39(-10)	1.89(-12)	5.62(-12)	0	2.290(-2)	4.571(-3)	—	4.771	—	8.371	2.575(-2)
$C_M^f, C_{M'/M}^f(\text{OG}_1)$	~0	1.57(-12)	4.17(-09)	3.19(-11)	1.22(-10)	9.96(-12)	—	6.169(-3)	—	5.353	—	9.823	2.789(-2)
$C_M^f, C_{M'/M}^f(V)$	8.99(-16)	6.56(-15)	3.38(-05)	7.24(-13)	9.91(-07)	4.04(-14)	2.97(-2)	6.34(-3)	111.4(-4)	5.46	7.353(-3)	6.175	—
$C_M^f, C_{M'/M}^f(\text{calculated})^e$	1.40(-14)	1.66(-12)	3.38(-05)	3.45(-11)	9.91(-07)	1.00(-11)	2.334(-2)	6.087(-3)	111.4(-4)	5.320	7.353(-3)	9.800	2.789(-2)
$C_M^f, C_{M'/M}^f(\text{Earth})^f$	1.40(-14)	1.66(-12)	3.7(-05)	3.45(-11)	9.1(-07)	1.00(-11)	2.337(-2)	6.087(-3)	111.6(-4)	5.320	7.353(-3)	9.800	2.899(-2)

Note. Subscript C designates escape at constant hydrogen inventory, R designates Rayleigh escape. Powers of ten multipliers in parentheses.

^a $\alpha [A] = 17.32863, m_1 = 2. (m_C^0, m_C^A) = 208.0, 123.9 \text{ (Xe)}; 184.0, 109.7 \text{ (Kr)}; 195.9, 116.7 \text{ (CO}_2\text{)}; 159.8, 95.4 \text{ (Ar)}; 170.5, 101.7 \text{ (N}_2\text{)}; 115.7, 69.3 \text{ (Ne)}$.

^b $\alpha_0[\text{OG}] = 1.38875, m_1 = 2. (m_C^0, m_C^S) = 109.7, 33.0 \text{ (Kr)}; 116.7, 35.0 \text{ (CO}_2\text{)}; 95.4, 28.9 \text{ (Ar)}; 101.7, 30.7 \text{ (N}_2\text{)}; 115.7, 69.3, 21.4 \text{ (Ne)}$.

^c $\alpha_0[V] = 1.38875, m_1 = 2. (m_C^0, m_C^S) = 36.5, 35.0 \text{ (CO}_2\text{)}; 30.0, 28.9 \text{ (Ar)}; 32.0, 30.7 \text{ (N}_2\text{)}; 22.2, 21.4 \text{ (Ne)}$.

^d Units are g/g-Earth for C_M^j and $C_{M'/M}^j$, atom/atom for $C_{M'/M}^f$ and $C_{M'/M}^f$.

^e $C_M^f, C_{M'/M}^f(\text{calculated}) = \Sigma C_M^f, C_{M'/M}^f(A_S + \text{OG}_1 + V)$.

^f Tables II, III.

TABLE AIII
Venus I and Venus II Models: Partial Spreadsheet Outputs, Assuming Initial Kr Compositions = Solar Kr-1 (Table III)

	Mass M (amu)						Isotopes M'/M						
	130 (Xe)	84 (Kr)	44 (CO ₂)	36 (Ar)	28 (N ₂)	20 (Ne)	$\frac{124\text{Xe}}{130\text{Xe}}$	$\frac{78\text{Kr}}{84\text{Kr}}$	$\frac{13\text{C}^{16}\text{O}_2}{12\text{C}^{16}\text{O}_2}$	$\frac{36\text{Ar}}{38\text{Ar}}$	$\frac{15\text{N}^{14}\text{N}}{14\text{N}_2}$	$\frac{20\text{Ne}}{22\text{Ne}}$	$\frac{21\text{Ne}}{22\text{Ne}}$
	Hydrodynamic escape fractionation factors (Venus I)												
$f_M, f_{M'/M}(A)_R^a$	3.272(-01)	2.402(-01)	1.103(-01)	1.091(-01)	7.263(-02)	7.484(-02)	0.95661	0.92710	1.02795	0.93537	1.05103	0.87313	0.93677
	Initial volatile inventories (Venus I) ^b												
$C_M^j, C_{M'/M}^j(A_S)$	2.71(-13)	1.96(-11)	4.80(-06)	2.30(-08)	3.16(-07)	3.88(-09)	2.947(-2)	6.359(-3)	?	5.80	?	13.7	3.27(-2)
	Residual volatile inventories (Venus I) ^b												
$C_M^f, C_{M'/M}^f(A_S)$	8.87(-14)	4.71(-12)	5.29(-07)	2.51(-09)	2.30(-08)	2.90(-10)	2.819(-2)	5.896(-3)	—	5.43	—	11.96	3.06(-2)
$C_M^f, C_{M'/M}^f(\text{calculated})^c$	8.87(-14)	4.71(-12)	5.29(-07)	2.51(-09)	2.30(-08)	2.90(-10)	2.819(-2)	5.896(-3)	—	5.43	—	11.96	3.06(-2)
$C_M^f, C_{M'/M}^f(\text{Venus})^d$	8.9(-14)	4.7(-12)	9.55(-05)	2.51(-09)	2.20(-06)	2.9(-10)	?	?	112(-4)	5.56	7.3(-3)	11.8	?
	Hydrodynamic escape fractionation factors (Venus II)												
$f_M, f_{M'/M}(A)_R^e$	4.955(-01)	3.730(-01)	1.758(-01)	1.740(-01)	1.157(-01)	1.192(-01)	0.96077	0.93133	1.02766	0.93604	1.05174	0.87205	0.93634
$f_M, f_{M'/M}(V)_R^f$	1	9.998(-01)	7.514(-01)	7.465(-01)	5.600(-01)	5.732(-01)	1	0.99505	1.01700	0.96025	1.03915	0.90366	0.95316
	Initial volatile inventories (Venus II) ^b												
$C_M^j, C_{M'/M}^j(A_S)$	1.73(-13)	1.26(-11)	3.09(-06)	1.44(-08)	2.03(-07)	2.43(-09)	2.947(-2)	6.359(-3)	?	5.80	?	13.7	3.27(-2)
$C_M^j, C_{M'/M}^j(V)$	3.36(-15)	2.48(-14)	1.26(-04)	2.70(-12)	4.10(-06)	1.64(-13)	2.97(-2)	6.34(-3)	111.4(-4)	5.46	7.118(-3)	6.7	?
	Residual volatile inventories (Venus II) ^b												
$C_M^f, C_{M'/M}^f(A_S)$	8.56(-14)	4.69(-12)	5.43(-07)	2.51(-09)	2.35(-08)	2.90(-10)	2.831(-2)	5.922(-3)	—	5.43	—	11.95	3.06(-2)
$C_M^f, C_{M'/M}^f(V)$	3.36(-15)	2.48(-14)	9.48(-05)	2.02(-12)	2.29(-06)	9.39(-14)	2.97(-2)	6.31(-3)	113.3(-4)	5.24	7.397(-3)	6.05	—
$C_M^f, C_{M'/M}^f(\text{calculated})^g$	8.90(-14)	4.72(-12)	9.52(-05)	2.51(-09)	2.31(-06)	2.90(-10)	2.837(-2)	5.924(-3)	113.3(-4)	5.43	7.397(-3)	11.94	3.06(-2)
$C_M^f, C_{M'/M}^f(\text{Venus})^d$	8.9(-14)	4.7(-12)	9.55(-05)	2.51(-09)	2.20(-06)	2.9(-10)	?	?	112.(-4)	5.56	7.3(-3)	11.8	?

Note. Subscript R designates Rayleigh escape. Powers of ten multipliers in parentheses.

^a $\alpha_0[A] = 1.01800, m_1 = 2. (m_C^0, m_C^A) = 879.1, \approx 33.0 \text{ (Xe)}; 779.0, \approx 29.4 \text{ (Kr)}; 823.7, \approx 31.0 \text{ (CO}_2\text{)}; 673.2, \approx 25.7 \text{ (Ar)}; 713.3, \approx 27.1 \text{ (N}_2\text{)}; 483.4, \approx 19.0 \text{ (Ne)}$.

^b Units are g/g-Venus for C_M^j and $C_{M'/M}^j$, atom/atom for $C_{M'/M}^f$ and $C_{M'/M}^f$.

^c $C_M^f, C_{M'/M}^f(\text{calculated}) = C_M^f, C_{M'/M}^f(A_S)$.

^d Tables II, III.

^e $\alpha_0[A] = 1.03250, m_1 = 2. (m_C^0, m_C^A) = 531.9, \approx 33.0 \text{ (Xe)}; 471.4, \approx 29.4 \text{ (Kr)}; 498.4, \approx 31.0 \text{ (CO}_2\text{)}; 407.5, \approx 25.7 \text{ (Ar)}; 431.7, \approx 27.1 \text{ (N}_2\text{)}; 292.8, \approx 19.0 \text{ (Ne)}$.

^f $\alpha_0[V] = 1.03250, m_1 = 2. (m_C^0, m_C^S) = 85.4, \approx 29.4 \text{ (Kr)}; 90.2, \approx 31.0 \text{ (CO}_2\text{)}; 74.1, \approx 25.7 \text{ (Ar)}; 78.4, \approx 27.1 \text{ (N}_2\text{)}; 53.7, \approx 19.0 \text{ (Ne)}$.

^g $C_M^f, C_{M'/M}^f(\text{calculated}) = \Sigma C_M^f, C_{M'/M}^f(A_S + V)$.

TABLE AIV
Mars I Model: Partial Spreadsheet Output, Assuming Initial Kr Composition = Solar Kr-1 (Table III)

	Mass M (amu)						Isotopes M'/M						
	130 (Xe)	84 (Kr)	44 (CO ₂)	36 (Ar)	28 (N ₂)	20 (Ne)	$\frac{124\text{Xe}}{130\text{Xe}}$	$\frac{78\text{Kr}}{84\text{Kr}}$	$\frac{13\text{C}^{16}\text{O}_2}{12\text{C}^{16}\text{O}_2}$	$\frac{36\text{Ar}}{38\text{Ar}}$	$\frac{15\text{N}^{14}\text{N}}{14\text{N}_2}$	$\frac{20\text{Ne}}{22\text{Ne}}$	$\frac{21\text{Ne}}{22\text{Ne}}$
	Hydrodynamic escape fractionation factors												
$f_M, f_{M'/M}(\text{A})_R^a$	7.428(-05)	3.093(-05)	1.044(-05)	1.032(-05)	7.807(-06)	7.986(-06)	0.86951	0.85713	1.02460	0.94237	1.02848	0.91975	0.95903
$f_M, f_{M'/M}(\text{OG})_R^b$	1	1	3.842(-01)	3.591(-01)	7.035(-02)	8.034(-02)	1	1	1.15264	0.70682	1.17842	0.61322	0.78308
$f_M, f_{M'/M}(\text{SW})$	1	1	1	1	1	1	1	1	1	1	1	1	1
	Initial volatile inventories ^c												
$C_M^i, C_{M'/M}^i(\text{A}_{\text{Cl}})$	2.80(-12)	1.43(-11)	?	5.00(-10)	?	1.16(-10)	2.851(-2)	5.962(-3)	111.2(-4)	5.30	7.662(-3)	8.9	?
$C_M^i, C_{M'/M}^i(\text{OG}_1)$	~0	1.72(-14)	8.42(-11)	5.93(-13)	5.55(-12)	3.06(-13)	2.947(-2)	6.359(-3)	?	5.80	?	13.7	3.27(-2)
$C_M^i, C_{M'/M}^i(\text{SW})$	9.92(-21)	7.18(-19)	1.76(-13)	1.10(-15)	1.16(-14)	1.92(-14)	2.947(-2)	6.359(-3)	?	5.80	?	13.7	3.27(-2)
	Residual volatile inventories ^c												
$C_M^f, C_{M'/M}^f(\text{A}_{\text{Cl}})$	2.08(-16)	4.42(-16)	?	1.85(-15)	?	7.42(-17)	2.479(-2)	5.110(-3)	131.3(-4)	3.53	9.286(-3)	5.020	—
$C_M^f, C_{M'/M}^f(\text{OG}_1)$	~0	1.72(-14)	3.24(-11)	2.13(-13)	3.90(-13)	2.45(-14)	—	6.359(-3)	—	4.10	—	8.401	2.58(-2)
$C_M^f, C_{M'/M}^f(\text{SW})$	9.92(-21)	7.18(-19)	1.76(-13)	1.10(-15)	1.16(-14)	1.92(-14)	2.947(-2)	6.359(-3)	—	5.80	—	13.7	3.27(-2)
$C_M^f, C_{M'/M}^f(\text{calculated})^d$	2.08(-16)	1.76(-14)	3.26(-11)	2.16(-13)	4.02(-13)	4.38(-14)	2.479(-2)	6.328(-3)	131.3(-4)	4.10	9.286(-3)	10.10	2.82(-2)
$C_M^f, C_{M'/M}^f(\text{Mars})^e$	2.08(-16)	1.76(-14)	4.08(-08)	2.16(-13)	7.3 (-10)	4.38(-14)	2.45 (-2)	6.37 (-3)	<118(-4)	4.1	11.9 (-3)	10.1	?

Note. Subscript R designates Rayleigh escape. Powers of ten multipliers in parentheses.

^a $\alpha_0[\text{A}] = 1.38439, m_1 = 2. (m_1^0, m_1^{\text{A}}) = 1734.3, 483.0 (\text{Xe}); 1573.2, 438.3 (\text{Kr}); 1663.3, 463.3 (\text{CO}_2); 1362.3, 379.7 (\text{Ar}); 1439.5, 401.1 (\text{N}_2); 967.2, 270.0 (\text{Ne}).$

^b $\alpha_0[\text{OG}] = 3.52985, m_1 = 2. (m_1^0, m_1^{\text{OG}}) = 66.7, 48.4 (\text{CO}_2); 55.0, 40.0 (\text{Ar}); 58.0, 42.2 (\text{N}_2); 39.6, 29.0 (\text{Ne}).$

^c Units are g/g-Mars for C_M^i and $C_{M'/M}^i$, atom/atom for $C_{M'/M}^f$ and $C_{M'/M}^f$.

^d $C_M^f, C_{M'/M}^f(\text{calculated}) = \Sigma C_M^i, C_{M'/M}^i(\text{A}_{\text{Cl}} + \text{OG}_1 + \text{SW})$

^e Tables II, III.

TABLE AV
Mars Ia Model: Partial Spreadsheet Output, Assuming Initial Kr Composition = Solar Kr-1 (Table III)

	Mass M (amu)						Isotopes M'/M						
	130 (Xe)	84 (Kr)	44 (CO ₂)	36 (Ar)	28 (N ₂)	20 (Ne)	$\frac{124\text{Xe}}{130\text{Xe}}$	$\frac{78\text{Kr}}{84\text{Kr}}$	$\frac{13\text{C}^{16}\text{O}_2}{12\text{C}^{16}\text{O}_2}$	$\frac{36\text{Ar}}{38\text{Ar}}$	$\frac{15\text{N}^{14}\text{N}}{14\text{N}_2}$	$\frac{20\text{Ne}}{22\text{Ne}}$	$\frac{21\text{Ne}}{22\text{Ne}}$
	Hydrodynamic escape fractionation factors												
$f_M, f_{M'/M}(\text{A})_R^a$	6.771(-05)	2.612(-05)	8.016(-06)	7.916(-06)	5.845(-06)	5.991(-06)	0.85895	0.84566	1.02678	0.93749	1.03101	0.91305	0.95553
$f_M, f_{M'/M}(\text{OG})_R^b$	1	1	3.993(-01)	3.748(-01)	8.097(-02)	9.173(-02)	1	1	1.14285	0.72170	1.16686	0.63149	0.79466
$f_M, f_{M'/M}(\text{SW})$	1	1	1	1	1	1	1	1	1	1	1	1	1
	Initial volatile inventories ^c												
$C_M^i, C_{M'/M}^i(\text{A}_3)$	2.71(-13)	1.96(-11)	1.20(-06)	2.30(-08)	7.90(-08)	3.88(-09)	2.947(-2)	6.359(-3)	?	5.80	?	13.7	3.27(-2)
$C_M^i, C_{M'/M}^i(\text{A}_{\text{Cl}})$	2.80(-12)	1.43(-11)	?	5.00(-10)	?	1.16(-10)	2.851(-2)	5.962(-3)	111.2(-4)	5.30	7.662(-3)	8.9	?
$C_M^i, C_{M'/M}^i(\text{OG}_1)$	~0	1.67(-14)	8.18(-11)	3.87(-13)	5.39(-12)	2.60(-13)	2.947(-2)	6.359(-3)	?	5.80	?	13.7	3.27(-2)
$C_M^i, C_{M'/M}^i(\text{SW})$	9.17(-21)	6.63(-19)	1.62(-13)	1.02(-15)	1.07(-14)	1.77(-14)	2.947(-2)	6.359(-3)	?	5.80	?	13.7	3.27(-2)
	Residual volatile inventories ^c												
$C_M^f, C_{M'/M}^f(\text{A}_3)$	1.84(-17)	5.13(-16)	3.84(-12)	6.84(-14)	3.74(-14)	2.14(-15)	2.531(-2)	5.378(-3)	—	3.92	—	7.899	2.48(-2)
$C_M^f, C_{M'/M}^f(\text{A}_{\text{Cl}})$	1.90(-16)	3.73(-16)	?	1.48(-15)	?	6.35(-17)	2.449(-2)	5.042(-3)	130.5(-4)	3.59	9.218	5.132	—
$C_M^f, C_{M'/M}^f(\text{OG}_1)$	~0	1.67(-14)	3.27(-11)	1.45(-13)	4.36(-13)	2.39(-14)	—	6.359(-3)	—	4.19	—	8.651	2.60(-2)
$C_M^f, C_{M'/M}^f(\text{SW})$	9.17(-21)	6.63(-19)	1.62(-13)	1.02(-15)	1.07(-14)	1.77(-14)	2.947(-2)	6.359(-3)	—	5.80	—	13.7	3.27(-2)
$C_M^f, C_{M'/M}^f(\text{calculated})^d$	2.08(-16)	1.76(-14)	3.67(-11)	2.16(-13)	4.84(-13)	4.38(-14)	2.456(-2)	6.303(-3)	130.5(-4)	4.10	9.218(-3)	10.10	2.79(-2)
$C_M^f, C_{M'/M}^f(\text{Mars})^e$	2.08(-16)	1.76(-14)	4.08(-08)	2.16(-13)	7.3 (-10)	4.38(-14)	2.45 (-2)	6.37 (-3)	<118(-4)	4.1	11.9 (-3)	10.1	?

Note. Subscript R designates Rayleigh escape. Powers of ten multipliers in parentheses.

^a $\alpha_0[\text{A}] = 1.35515, m_1 = 2. (m_1^0, m_1^{\text{A}}) = 1734.3, 456.0 (\text{Xe}); 1573.2, 413.8 (\text{Kr}); 1663.3, 437.4 (\text{CO}_2); 1362.3, 358.5 (\text{Ar}); 1439.5, 378.7 (\text{N}_2); 967.2, 254.9 (\text{Ne}).$

^b $\alpha_0[\text{OG}] = 3.52985, m_1 = 2. (m_1^0, m_1^{\text{OG}}) = 66.7, 48.4 (\text{CO}_2); 55.0, 40.0 (\text{Ar}); 58.0, 42.2 (\text{N}_2); 39.6, 29.0 (\text{Ne}).$

^c Units are g/g-Mars for C_M^i and $C_{M'/M}^i$, atom/atom for $C_{M'/M}^f$ and $C_{M'/M}^f$.

^d $C_M^f, C_{M'/M}^f(\text{calculated}) = \Sigma C_M^i, C_{M'/M}^i(\text{A}_3 + \text{A}_{\text{Cl}} + \text{OG}_1 + \text{SW}).$

^e Tables II, III.

TABLE AVI
Mars II Model: Partial Spreadsheet Output, Assuming Initial Kr Composition = Solar Kr-2 (Table III)

	Mass <i>M</i> (amu)					Isotopes <i>M</i> / <i>M</i>							
	130 (Xe)	84 (Kr)	44 (CO ₂)	36 (Ar)	28 (N ₂)	20 (Ne)	¹²⁴ Xe ¹³⁰ Xe	⁷⁸ Kr ⁸⁴ Kr	¹³ C ¹⁶ O ₂ ¹² C ¹⁶ O ₂	³⁶ Ar ³⁸ Ar	¹⁵ N ¹⁴ N ¹⁴ N ₂	²⁰ Ne ²² Ne	²¹ Ne ²² Ne
	Hydrodynamic escape fractionation factors												
<i>f</i> _M , <i>f</i> _M / <i>M</i> (A) _R ^a	7.428(-05)	3.089(-05)	1.040(-05)	1.028(-05)	7.778(-06)	7.957(-06)	0.86931	0.85691	1.02464	0.94228	1.02853	0.91962	0.95897
<i>f</i> _M , <i>f</i> _M / <i>M</i> (OG) _R ^b	1	1	1 ^c	3.655(-01)	7.459(-02)	8.490(-02)	1	1	1 ^c	0.71298	1.17359	0.62076	0.78789
<i>f</i> _M , <i>f</i> _M / <i>M</i> (SW)	1	1	1	1	1	1	1	1	1	1	1	1	1
	Initial volatile inventories ^d												
<i>C</i> _M ⁱ , <i>C</i> _M ⁱ / <i>M</i> (A _{CI})	2.80(-12)	1.43(-11)	?	5.00(-10)	?	1.16(-10)	2.851(-2)	5.962(-3)	111.2(-4)	5.30	7.662(-3)	8.9	?
<i>C</i> _M ⁱ , <i>C</i> _M ⁱ / <i>M</i> (OG _I)	-0	1.56(-14)	7.64(-11)	5.28(-13)	5.03(-12)	2.68(-13)	2.947(-2)	6.470(-3)	?	5.80	?	13.7	3.27(-2)
<i>C</i> _M ⁱ , <i>C</i> _M ⁱ / <i>M</i> (OG _{CI})	-0	1.56(-15)	5.94(-06)	5.46(-14)	6.60(-08)	1.26(-14)	2.851(-2)	5.962(-3)	111.2(-4)	5.30	7.662(-3)	8.9	?
<i>C</i> _M ⁱ , <i>C</i> _M ⁱ / <i>M</i> (SW)	1.03(-20)	7.45(-19)	1.82(-13)	1.14(-15)	1.20(-14)	1.99(-14)	2.947(-2)	6.470(-3)	?	5.80	?	13.7	3.27(-2)
	Residual volatile inventories ^d												
<i>C</i> _M ^f , <i>C</i> _M ^f / <i>M</i> (A _{CI})	2.08(-16)	4.41(-16)	?	1.88(-15)	?	7.81(-17)	2.478(-2)	5.109(-3)	—	3.56	—	5.081	—
<i>C</i> _M ^f , <i>C</i> _M ^f / <i>M</i> (OG _I)	-0	1.56(-14)	7.64(-11)	1.93(-13)	3.75(-13)	2.27(-14)	—	6.470(-3)	—	4.14	—	8.504	2.58(-2)
<i>C</i> _M ^f , <i>C</i> _M ^f / <i>M</i> (OG _{CI})	-0	1.56(-15)	5.94(-06)	2.00(-14)	4.92(-09)	1.07(-15)	—	5.962(-3)	111.2(-4)	3.78	8.992(-3)	5.525	—
<i>C</i> _M ^f , <i>C</i> _M ^f / <i>M</i> (SW)	1.03(-20)	7.45(-19)	1.82(-13)	1.14(-15)	1.20(-14)	1.99(-14)	2.947(-2)	6.470(-3)	—	5.80	—	13.7	3.27(-2)
<i>C</i> _M ^f , <i>C</i> _M ^f / <i>M</i> (calculated) ^e	2.08(-16)	1.76(-14)	5.94(-06)	2.16(-13)	4.92(-09)	4.38(-14)	2.478(-2)	6.391(-3)	111.2(-4)	4.10	8.992(-3)	10.10	2.82(-2)
<i>C</i> _M ^f , <i>C</i> _M ^f / <i>M</i> (Mars) ^f	2.08(-16)	1.76(-14)	4.08(-08)	2.16(-13)	7.3(-10)	4.38(-14)	2.45(-2)	6.37(-3)	<118(-4)	4.1	11.9(-3)	10.1	?

Note. Subscript R designates Rayleigh escape. Powers of ten multipliers in parentheses.
^a α₀[A] = 1.92901, m₁ = 2. (m₂⁰, m₂^A) = 1048.5, 506.0 (Xe); 951.2, 459.1 (Kr); 1005.6, 485.3 (CO₂); 823.8, 397.8 (Ar); 870.4, 420.2 (N₂); 585.1, 282.8 (Ne).
^b α₀[OG] = 3.52923, m₁ = 2. (m₂⁰, m₂^A) = 66.7, 48.4 (CO₂); 55.0, 40.0 (Ar); 58.0, 42.2 (N₂); 39.6, 29.0 (Ne).
^c CO₂ outgassing assumed to be delayed until t ≥ t_f; if not, f₄₄(OG)_R = 3.904(-01) and f_{45/44}(OG)_R = 1.14855.
^d Units are g/g-Mars for C_Mⁱ and C_M^f, atom/atom for C_Mⁱ/*M* and C_M^f/*M*.
^e C_M^f, C_M^f/*M* (calculated) = Σ C_Mⁱ, C_Mⁱ/*M*(A_{CI} + OG_I + OG_{CI} + SW).
^f Tables II, III.

ACKNOWLEDGMENTS

I am particularly indebted to D. M. Hunten for advice and encouragement during preparation of this paper, and for many specific comments and suggestions. Spirited discussions of the subject with K. Zahnle, J. Pollack, and J. Kasting were instrumental in refining a number of these ideas, and in several instances modifying them. Two anonymous reviewers provided helpful comments and suggestions. Special thanks are due to K. Zahnle for his comprehensive informal review of the original version of the manuscript. The work was supported by Grant NAG 9-60 from the NASA Planetary Materials and Geochemistry Program. Additional sabbatical year support through Grant NAGW-1371 from the NASA Planetary Atmospheres Program is gratefully acknowledged.

REFERENCES

ABE, Y., AND T. MATSUI 1985. The formation of an impact-generated H₂O atmosphere and its implications for the early thermal history of the Earth. *Proc. Lunar Planet. Sci. Conf. 15th; J. Geophys. Res.* **90**, C545-C559.
 ALAERTS, L., R. S. LEWIS, AND E. ANDERS 1979. Isotopic anomalies of noble gases in meteorites and their origins. IV. C3 (Ormans) carbonaceous chondrites. *Geochim. Cosmochim. Acta* **43**, 1421-1432.
 ALAERTS, L., R. S. LEWIS, J. MATSUDA, AND E. ANDERS 1980. Isotopic anomalies of noble gases in meteorites and their origins VI. Presolar components in the Murchison C2 chondrite. *Geochim. Cosmochim. Acta* **44**, 189-209.
 ALLAMANDOLA, L. J. 1984. In *Galactic and Extragalactic Infrared Spectroscopy* (M. F. Kessler and J. P. Phillips, Eds.) pp. 5-35. Reidel, Dordrecht.

ALLAMANDOLA, L. J., AND S. A. SANDFORD 1988. Interstellar grain chemistry and organic molecules. In *Carbon in the Galaxy: Studies from Earth and Space* (J. C. Tarter, S. Chang, and D. J. DeFrees, Eds.), NASA Conf. Pub. 3061, pp. 113-146.
 ALLÈGRE, C. J., T. STAUDACHER, AND P. SARDA 1987. Rare gas systematics: Formation of the atmosphere, evolution and structure of the Earth's mantle. *Earth Planet. Sci. Lett.* **81**, 127-150.
 ANDERS, E. 1987. Local and exotic components of primitive meteorites, and their origin. *Philos. Trans. R. Soc. Lond. Ser. A* **323**, 287-304.
 ANDERS, E. 1988. In *Meteorites and the Early Solar System* (J. Kerridge and M. Matthews, Eds.), pp. 927-955. Univ. Arizona Press, Tucson.
 ANDERS, E., AND M. EBIHARA 1982. Solar-system abundances of the elements. *Geochim. Cosmochim. Acta* **46**, 2363-2380.
 ANDERS, E., AND N. GREVESSE 1989. Abundances of the elements: Meteoritic and solar. *Geochim. Cosmochim. Acta* **53**, 197-214.
 BAR-NUN, A., G. HERMAN, D. LAUFER, AND M. L. RAPPAPORT 1985. Trapping and release of gases by water ice and implications for icy bodies. *Icarus* **63**, 317-332.
 BAR-YAM, Y., AND T. D. MOUSTAKAS 1989. Defect-induced stabilization of diamond films. *Nature* **342**, 786-787.
 BASALTIC VOLCANISM STUDY PROJECT 1981. *Basaltic Volcanism on the Terrestrial Planets*, Pergamon Press, New York.
 BASFORD, J. R., J. C. DRAGON, R. O. PEPIN, M. R. COSCIO, JR., AND V. R. MURTHY 1973. Krypton and xenon in lunar fines. *Proc. Lunar Sci. Conf. 4th; Geochim. Cosmochim. Acta Suppl.* **4**, 1915-1955.
 BECKER, R. H., AND R. O. PEPIN 1984a. The case for a Martian origin of the shergottites: Nitrogen and noble gases in EETA 79001. *Earth Planet. Sci. Lett.* **69**, 225-242.

- BECKER, R. H., AND R. O. PEPIN 1984b. Solar composition noble gases in the Washington County iron meteorite. *Earth Planet. Sci. Lett.* **70**, 1–10.
- BECKER, R. H., AND R. O. PEPIN 1986. Mars, Earth, and SNC meteorites: The noble gas–nitrogen connection. *Terra Cognita* **6**, 102.
- BECKER, R. H., AND R. O. PEPIN 1989. Long-term changes in solar wind elemental and isotopic ratios: A comparison of two lunar ilmenites of different antiquities. *Geochim. Cosmochim. Acta* **53**, 1135–1146.
- BECKER, R. H., AND R. O. PEPIN 1991. Composition of solar wind noble gases released by surface oxidation of a metal separate from the Weston meteorite. *Earth Planet. Sci. Lett.*, in press.
- BECKER, R. H., R. O. PEPIN, R. S. RAJAN, AND E. R. RAMBALDI 1986a. Light noble gases in Weston metal grain surfaces. *Meteoritics* **21**, 331–332.
- BECKER, R. H., R. S. RAJAN, AND E. R. RAMBALDI 1986b. In *Workshop on Past and Present Solar Radiation: The Record in Meteoritic and Lunar Regolith Material* (R. Pepin and D. McKay, Eds.), LPI Tech. Report 86-02, pp. 12–13. Lunar and Planetary Institute, Houston.
- BECKWITH, S. V. W., A. I. SARGENT, R. S. CHINI, AND R. GÜSTEN 1990. A survey for circumstellar disks around young stellar objects. *Astron. J.* **99**, 924–945.
- BENKERT, J.-P., H. BAUR, A. PEDRONI, R. WIELER, AND P. SIGNER 1988. Solar He, Ne and Ar in regolith minerals: All are mixtures of two components. *Lunar Planet. Sci. XIX*, 59–60.
- BENZ, W., AND A. G. W. CAMERON 1991. In *Origin of the Earth* (H. E. Newsom and J. H. Jones, Eds.), pp. 61–67. Oxford Univ. Press, New York.
- BERNATOWICZ, T. J., AND A. J. FAHEY 1986. Xe isotopic fractionation in a cathodeless glow discharge. *Geochim. Cosmochim. Acta* **50**, 445–452.
- BERNATOWICZ, T. J., AND F. A. PODOSEK 1986. Adsorption and isotopic fractionation of Xe. *Geochim. Cosmochim. Acta* **50**, 1503–1507.
- BERNATOWICZ, T. J., AND B. E. HAGEE 1987. Isotopic fractionation of Kr and Xe implanted in solids at very low energies. *Geochim. Cosmochim. Acta* **51**, 1599–1611.
- BERNATOWICZ, T. J., F. A. PODOSEK, M. HONDA, AND F. E. KRAMER 1984. The atmospheric inventory of xenon and noble gases in shales: The plastic bag experiment. *J. Geophys. Res.* **89**, 4597–4611.
- BERNATOWICZ, T. J., B. M. KENNEDY, AND F. A. PODOSEK 1985. Xe in glacial ice and the atmospheric inventory of noble gases. *Geochim. Cosmochim. Acta* **49**, 2561–2564.
- BLACK, D. C. 1971. Trapped neon–argon isotopic correlations in gas-rich meteorites and carbonaceous chondrites. *Geochim. Cosmochim. Acta* **35**, 230–234.
- BLACK, D. C. 1972. On the origins of trapped helium, neon and argon isotopic variations in meteorites I. Gas-rich meteorites, lunar soil and breccia. *Geochim. Cosmochim. Acta* **36**, 347–375.
- BLACK, D. C., AND R. O. PEPIN 1969. Trapped neon in meteorites II. *Earth Planet. Sci. Lett.* **6**, 395–405.
- BOCHSLER, P., AND J. GEISS 1977. Elemental abundances in the solar wind. *Trans. Int. Astron. Union B XVI*, 120–123.
- BOCHSLER, P., J. GEISS, AND S. KUNZ 1986. Abundances of carbon, oxygen, and neon in the solar wind during the period from August 1978 to June 1982. *Solar Phys.* **103**, 177–201.
- BOGARD, D. D., AND P. JOHNSON 1983. Martian gases in an Antarctic meteorite? *Science* **221**, 651–654.
- BOGARD, D. D., F. HÖRZ, AND P. H. JOHNSON 1986. Shock-implanted noble gases: An experimental study with implications for the origin of Martian gases in shergottite meteorites. *Proc. Lunar Planet. Sci. Conf. 17th; J. Geophys. Res.* **91**, E99–E114.
- BOGARD, D. D., W. C. HIRSCH, AND L. E. NYQUIST 1974. Noble gases in Apollo 17 fines: Mass fractionation effects in trapped Xe and Kr. *Proc. Lunar Sci. Conf. 5th; Geochim. Cosmochim. Acta Suppl.* **5**, 1975–2003.
- BOSS, A. P., G. E. MORFILL, AND W. M. TSCHARNUTER 1989. In *Origin and Evolution of Planetary and Satellite Atmospheres* (S. Atreya, J. Pollack, and M. Matthews, Eds.) pp. 35–72. Univ. Arizona Press, Tucson.
- BROWNLEE, D. E. 1985. Cosmic dust: Collection and research. *Annu. Rev. Earth Planet. Sci.* **13**, 147–173.
- CAMERON, A. G. W. (1982). In *Essays in Nuclear Astrophysics* (C. Barnes, D. Clayton, and D. Schramm, Eds.), pp. 23–43. Cambridge University Press, Cambridge.
- CAMERON, A. G. W. 1983. Origin of the atmospheres of the terrestrial planets. *Icarus* **56**, 195–201.
- CAMERON, A. G. W., AND W. BENZ 1988. In *Abstracts of the Conference on the Origin of the Earth, Oakland, CA*, pp. 11–12. Lunar and Planetary Institute, Houston.
- CANALAS, R., E. ALEXANDER, AND O. MANUEL 1968. Terrestrial abundance of noble gases. *J. Geophys. Res.* **73**, 3331–3334.
- CANUTO, V. M., J. S. LEVINE, T. R. AUGUSTSSON, AND C. L. IMHOFF 1982. UV radiation from the young Sun and oxygen and ozone levels in the prebiological palaeoatmosphere. *Nature* **296**, 816–820.
- CLAYTON, R. N., AND M. H. THIEMENS 1980. In *The Ancient Sun: Fossil Record in the Earth, Moon and Meteorites* (R. Pepin, J. Eddy, and R. Merrill, Eds.), pp. 463–473. Pergamon Press, New York.
- CLAYTON, R. N., T. K. MAYEDA, AND A. E. RUBIN 1984. In *Proc. Lunar Planet. Sci. Conf. 15th; J. Geophys. Res.* **89**(Suppl.), C245–C249.
- CRABB, J., AND E. ANDERS 1981. Noble gases in E-chondrites. *Geochim. Cosmochim. Acta* **45**, 2443–2464.
- CRABB, J., AND E. ANDERS 1982. On the siting of noble gases in E-chondrites. *Geochim. Cosmochim. Acta* **46**, 2351–2361.
- DEINES, P., AND F. E. WICKMAN 1985. The stable carbon isotopes in enstatite chondrites and Cumberland Falls. *Geochim. Cosmochim. Acta* **49**, 89–95.
- DEVRIES, R. C. 1987. Synthesis of diamond under metastable conditions. *Annu. Rev. Mater. Sci.* **17**, 161–187.
- DONAHUE, T. M. 1986. Fractionation of noble gases by thermal escape from accreting planetesimals. *Icarus* **66**, 195–210.
- DONAHUE, T. M., AND J. B. POLLACK 1983. In *Venus* (D. Hunten, L. Colin, T. Donahue, and V. Moroz, Eds.), pp. 1003–1036. Univ. Of Arizona Press, Tucson.
- DONAHUE, T. M., J. H. HOFFMAN, AND R. R. HODGES, JR. 1981. Kryptonite and xenon in the atmosphere of Venus. *Geophys. Res. Lett.* **8**, 513–516.
- DREIBUS, G., AND H. WÄNKE 1985. Mars, a volatile-rich planet. *Meteoritics* **20**, 367–381.
- DREIBUS, G., AND H. WÄNKE 1987. Volatiles on Earth and Mars: A comparison. *Icarus* **71**, 225–240.
- DREIBUS, G., AND H. WÄNKE 1989. In *Origin and Evolution of Planetary and Satellite Atmospheres* (S. Atreya, J. Pollack, and M. Matthews, Eds.), pp. 268–288. Univ. Arizona Press, Tucson.
- DUSHMAN, S. 1962. *Scientific Foundations of Vacuum Technique* (J. Lafferty, Ed.). Wiley, New York.
- DZICZKANIEC, M., G. LUMPKIN, K. DONOHOE, AND S. CHANG 1981. Plasma synthesis of carbonaceous material with noble gas tracers. *Lunar Planet. Sci.* **XII**, 246–248.

- EBERHARDT, P., O. EUGSTER, AND J. GEISS 1965. A redetermination of the isotopic composition of atmospheric neon. *Z. Naturforsch. A Astrophys. Phys. Chem.* **21**, 623–624.
- EBERHARDT, P., J. GEISS, H. GRAF, N. GRÖGLER, M. D. MENDIA, M. MÖRGELI, H. SCHWALLER, A. STETTLER, U. KRÄHENBÜHL, AND H. R. VON GUNTEN 1972. Trapped solar wind noble gases in Apollo 12 lunar fines 12001 and Apollo 11 breccia 10046. *Proc. Lunar Sci. Conf. 3rd; Geochim. Cosmochim. Acta Suppl.* **3**, 1821–1856.
- EUGSTER, O., P. EBERHARDT, AND J. GEISS 1967. The isotopic composition of krypton in unequilibrated and gas rich chondrites. *Earth Planet. Sci. Lett.* **2**, 385–393.
- FANALE, F. P. 1976. Martian volatiles: Their degassing history and geochemical fate. *Icarus* **28**, 179–202.
- FANALE, F. P., AND W. A. CANNON 1971. Physical adsorption of rare gas on terrigenous sediments. *Earth Planet. Sci. Lett.* **11**, 362–368.
- FANALE, F. P., AND W. A. CANNON 1972. Origin of planetary primordial rare gas: The possible role of adsorption. *Geochim. Cosmochim. Acta* **36**, 319–328.
- FANALE, F. P., AND B. M. JAKOSKY 1982. Regolith–atmosphere exchange of water and carbon dioxide on Mars: Effects on atmospheric history and climate change. *Planet. Space Sci.* **30**, 819–831.
- FANALE, F. P., J. R. SALVAIL, W. B. BANERDT, AND R. S. SAUNDERS 1982. Mars: The regolith–atmosphere–cap system and climate change. *Icarus* **50**, 381–407.
- FANALE, F. P., J. B. POLLACK, M. H. CARR, R. O. PEPIN, AND S. E. POSTAWKO 1991. In *Mars* (H. H. Kieffer and B. Jakosky, Eds.). Univ. Arizona Press, Tucson, in press.
- FEIGELSON, E. D., AND G. A. KRISS 1989. Soft X-ray observations of pre-main-sequence stars in the Chamaeleon dark cloud. *Astrophys. J.* **338**, 262–276.
- FELDMAN, W. C., J. R. ASBRIDGE, S. J. BAME, AND J. T. GOSLING 1977. In *The Solar Output and its Variation* (O. R. White, Ed.), pp. 351–382. Colorado Associated Univ. Press, Boulder.
- FREDRIKSSON, K., AND J. F. KERRIDGE 1988. Carbonates and sulfates in CI chondrites: Formation by aqueous activity on the parent body. *Meteoritics* **23**, 35–44.
- FRICK, U., AND R. O. PEPIN 1981. Study of solar wind gases in a young lunar soil. *Lunar Planet. Sci. XII*, 303–305.
- FRICK, U., R. MACK, AND S. CHANG 1979. Noble gas trapping and fractionation during synthesis of carbonaceous matter. *Proc. Lunar Planet. Sci. Conf. 10th; Geochim. Cosmochim. Acta Suppl.* **11**, 1961–1973.
- FRICK, U., R. H. BECKER, AND R. O. PEPIN 1988. In *Proceedings of the 18th Lunar and Planetary Science Conference*, pp. 87–120. Cambridge University Press, Cambridge, and Lunar and Planetary Institute, Houston.
- GEISS, J. 1982. Processes affecting abundances in the solar wind. *Space Sci. Rev.* **33**, 201–217.
- GEISS, J., AND P. BOCHSLER 1982. Nitrogen isotopes in the solar system. *Geochim. Cosmochim. Acta* **46**, 529–548.
- GEISS, J., AND P. BOCHSLER 1985. In *Proceedings of the International Conference on Isotope Ratios in the Solar System, Paris 1984*. CNES, Paris.
- GOETTEL, K. A., J. H. EGGERT, I. F. SILVERA, AND W. C. MOSS 1989. Optical evidence for the metallization of xenon at 132(5) GPa. *Phys. Rev. Lett.* **62**, 665–668.
- GRADY, M. M., I. P. WRIGHT, L. P. CARR, AND C. T. PILLINGER 1986. Compositional differences in enstatite chondrites based on carbon and nitrogen stable isotope measurements. *Geochim. Cosmochim. Acta* **50**, 2799–2813.
- GREENBERG, J. M. 1978. In *Cosmic Dust* (J. McDonnell, Ed.), pp. 187–294. Wiley, New York.
- GREENBERG, J. M. 1982. In *Submillimeter Wave Astronomy* (J. Beckman and J. Phillips, Eds.), pp. 261–306. Cambridge Univ. Press, Cambridge.
- GREENBERG, R., J. F. WACKER, W. K. HARTMANN, AND C. R. CHAPMAN 1978. Planetesimals to planets: Numerical simulation of collisional evolution. *Icarus* **35**, 1–26.
- GROS, J., H. TAKAHASHI, J. HERTOGEN, J. W. MORGAN, AND E. ANDERS 1976. Composition of the projectiles that bombarded the lunar highlands. *Proc. Lunar Sci. Conf. 7th; Geochim. Cosmochim. Acta Suppl.* **7**, 2403–2425.
- GROSS, S. H. 1974. The atmospheres of Titan and the Galilean satellites. *J. Atmos. Sci.* **31**, 1413–1420.
- HAMANO, Y., AND M. OZIMA 1978. In *Terrestrial Rare Gases* (E. C. Alexander, Jr. and M. Ozima, Eds.), pp. 155–171. Japan Scientific Societies Press, Tokyo.
- HARTMANN, W. K. 1976. Planet formation: Compositional mixing and lunar compositional anomalies. *Icarus* **27**, 553–559.
- HAYASHI, C., K. NAKAZAWA, AND H. MIZUNO 1979. Earth's melting due to the blanketing effect of the primordial dense atmosphere. *Earth Planet. Sci. Lett.* **43**, 22–28.
- HAYASHI, C., K. NAKAZAWA, AND Y. NAKAGAWA 1985. In *Protostars and Planets II* (D. Black and M. Matthews, Eds.), pp. 1100–1153. Univ. Arizona Press, Tucson.
- HEYMANN, D., M. DZICZKANIEC, AND R. PALMA 1976. Limits for the accretion time of the earth from cosmogenic ^{21}Ne produced in planetesimals. *Proc. Lunar Sci. Conf. 7th, Geochim. Cosmochim. Acta Suppl.* **7**, 3411–3419.
- HINTENBERGER, H., E. VILCSEK, AND H. WÄNKE 1965. Über die Isotopenzusammensetzung und über den Sitz der leichten Uredelgase in Steinmeteoriten. *Z. Naturforsch. A Astrophys. Phys. Phys. Chem.* **20**, 939–945.
- HINTENBERGER, H., H. W. WEBER, AND L. SCHULTZ 1974. Solar, spallogenic, and radiogenic rare gases in Apollo 17 soils and breccias. *Proc. Lunar Sci. Conf. 5th; Geochim. Cosmochim. Acta Suppl.* **5**, 2005–2022.
- HOFFMAN, J. H., R. R. HODGES, JR., T. M. DONAHUE, AND M. B. McELROY 1980. Composition of the Venus lower atmosphere from the Pioneer Venus mass spectrometer. *J. Geophys. Res.* **85**, 7882–7890.
- HOLLOWAY, J. R. 1988a. Planetary atmospheres during accretion: The effect of C–O–H–S equilibria. *Lunar Planet. Sci. XIX*, 499–500.
- HOLLOWAY, J. R. 1988b. Distribution of H_2O between early atmospheres and magma oceans. *EOS: Trans. Am. Geophys. Union* **69**, 388.
- HONDA, M., J. H. REYNOLDS, E. ROEDDER, AND S. EPSTEIN 1987. Noble gases in diamonds: Occurrences of solarlike helium and neon. *J. Geophys. Res.* **92**, 12,507–12,521.
- HONDA, M., I. McDOUGALL, D. B. PATTERSON, A. DOULGERIS, AND D. A. CLAGUE 1991. Possible solar noble-gas component in Hawaiian basalts. *Nature* **349**, 149–151.
- HOUSEN, K. R., L. L. WILKENING, C. R. CHAPMAN, AND R. GREENBERG 1979. Asteroidal regoliths. *Icarus* **39**, 317–351.
- HUDSON, B., G. J. FLYNN, P. FRAUNDORF, C. M. HOHENBERG, AND J. SHIRCK 1981. Noble gases in stratospheric dust particles: Proof of extraterrestrial origin. *Science* **211**, 383–386.
- HUNTEN, D. M. 1979. Capture of Phobos and Deimos by protoatmospheric drag. *Icarus* **37**, 113–123.
- HUNTEN, D. M., R. O. PEPIN, AND J. C. G. WALKER 1987. Mass fractionation in hydrodynamic escape. *Icarus* **69**, 532–549.

- HUNTEN, D. M., R. O. PEPIN, AND T. C. OWEN 1988. In *Meteorites and the Early Solar System* (J. Kerridge and M. Matthews, Eds.), pp. 565–591. Univ. Arizona Press, Tucson.
- HUNTEN, D. M., T. M. DONAHUE, J. F. KASTING, AND J. C. G. WALKER 1989. In *Origin and Evolution of Planetary and Satellite Atmospheres* (S. Atreya, J. Pollack, and M. Matthews, Eds.), pp. 386–422. Univ. Arizona Press, Tucson.
- HUSS, G. R. 1987. The role of presolar dust in the formation of the solar system. Ph.D. thesis, University of Minnesota, Minneapolis.
- HUSS, G. R., AND E. C. ALEXANDER, JR. 1987. On the pre-solar origin of "normal planetary" noble gases. *Proc. Lunar Planet. Sci. Conf. 17th; J. Geophys. Res.* **92**, Suppl., E710–E716.
- ISOTOMIN, V. G., K. V. GRECHNEV, AND V. A. KOCHNEV 1980. In *23rd COSPAR Meeting, Budapest*; also Preprint D-298, Space Res. Inst., USSR Acad. Sci.
- JESSBERGER, E. K., J. KISSEL, AND J. RAHE 1989. In *Origin and Evolution of Planetary and Satellite Atmospheres* (S. Atreya, J. Pollack, and M. Matthews, Eds.), pp. 167–191. Univ. Arizona Press, Tucson.
- JUNGCK, M. H. A., AND P. EBERHARDT 1979. Neon-E in Orgueil density separates. *Meteoritics* **14**, 439–440.
- JUNK, G., AND H. J. SVEC 1958. The absolute abundance of the nitrogen isotopes in the atmosphere and compressed gas from various sources. *Geochim. Cosmochim. Acta* **14**, 234–243.
- KALLEMEYN, G. W., AND J. T. WASSON 1986. Compositions of enstatite (EH3, EH4,5 and EL6) chondrites: Implications regarding their formation. *Geochim. Cosmochim. Acta* **50**, 2153–2164.
- KAULA, W. M. 1979. Thermal evolution of Earth and Moon growing by planetesimal impacts. *J. Geophys. Res.* **84**, 999–1008.
- KAULA, W. M. 1990. Venus: A contrast in evolution to Earth. *Science* **247**, 1191–1196.
- KERRIDGE, J. F. 1980. In *The Ancient Sun: Fossil Record in the Earth, Moon and Meteorites* (R. Pepin, J. Eddy, and R. Merrill, Eds.), pp. 475–489. Pergamon Press, New York.
- KERRIDGE, J. F. 1982. Whence so much ^{15}N ? *Nature* **295**, 643–644.
- KERRIDGE, J. F. 1985. Carbon, hydrogen and nitrogen in carbonaceous chondrites: Abundances and isotopic compositions in bulk samples. *Geochim. Cosmochim. Acta* **49**, 1707–1714.
- KRUMMENACHER, D., C. M. MERRIHUE, R. O. PEPIN, AND J. H. REYNOLDS 1962. Meteoritic krypton and barium versus the general isotopic anomalies in xenon. *Geochim. Cosmochim. Acta* **26**, 231–249.
- KUNG, C.-C., AND R. N. CLAYTON 1978. Nitrogen abundances and isotopic compositions in stony meteorites. *Earth Planet. Sci. Lett.* **38**, 421–435.
- KYSER, T. K., AND W. RISON 1982. Systematics of rare gas isotopes in basic lavas and ultramafic xenoliths. *J. Geophys. Res.* **87**, 5611–5630.
- LANGVIN, Y., AND M. MAURETTE 1980. A model for small body regolith evolution: The critical parameters. *Lunar Planet. Sci.* **XI**, 602–604.
- LEWIS, R. S., B. SRINIVASAN, AND E. ANDERS 1975. Host phase of a strange xenon component in Allende. *Science* **190**, 1251–1262.
- LEWIS, R. S., L. ALAERTS, AND E. ANDERS 1979. Isotopic anomalies in the Orgueil meteorite: Neon-E, s-process Xe, and CCFXe. *Lunar Planet. Sci.* **X**, pp. 728–730.
- LUNINE, J. I., AND D. J. STEVENSON 1985. Thermodynamics of clathrate hydrate at low and high pressures with application to the outer solar system. *Astrophys. J. Suppl. Series* **58**, 493–531.
- MARTI, K. 1980. In *The Ancient Sun: Fossil Record in the Earth, Moon and Meteorites* (R. Pepin, J. Eddy, and R. Merrill, Eds.), pp. 423–429. Pergamon Press, New York.
- MARTI, K., L. L. WILKENING, AND H. E. SUESS 1972. Solar rare gases and the abundances of the elements. *Astrophys. J.* **173**, 445–450.
- MASON, E. A., AND T. R. MARRERO 1970. The diffusion of atoms and molecules. *Advan. At. Mol. Phys.* **6**, 155–232.
- MATSUDA, J., R. S. LEWIS, H. TAKAHASHI, AND E. ANDERS 1980. Isotopic anomalies of noble gases in meteorites and their origins-VII. C3V carbonaceous chondrites. *Geochim. Cosmochim. Acta* **44**, 1861–1874.
- MATSUI, T., AND Y. ABE 1986. Evolution of an impact-induced atmosphere and magma ocean on the accreting Earth. *Nature* **319**, 303–305.
- MAZOR, E., D. HEYMANN, AND E. ANDERS 1970. Noble gases in carbonaceous chondrites. *Geochim. Cosmochim. Acta* **34**, 781–820.
- MCDONNELL, J. A. M., J. KISSEL, E. GRÜN, R. J. L. GRARD, Y. LANGVIN, R. E. OLEARCYK, C. H. PERRY, AND J. C. ZARNECKI 1986. In *20th ESLAB Symposium on the Exploration of Halley's Comet* (B. Battrock, E. J. Rolfe, and R. Reinhard, Eds.), ESA SP-250, Vol. 2, pp. 25–38.
- MCELROY, M. B., T. Y. KONG, AND Y. L. YUNG 1977. Photochemistry and evolution of Mars' atmosphere: A Viking perspective. *J. Geophys. Res.* **82**, 4379–4388.
- MCELROY, M. B., AND M. J. PRATHER 1981. Noble gases in the terrestrial planets. *Nature* **293**, 535–539.
- MELOSH, H. J., AND A. M. VICKERY 1988. Atmospheric erosion by high speed impact ejecta. *EOS: Trans. Am. Geophys. Union* **69**, 338.
- MELOSH, H. J., AND A. M. VICKERY 1989. Impact erosion of the primordial atmosphere of Mars. *Nature* **338**, 487–489.
- MEWALDT, R. A., J. D. SPALDING, AND E. C. STONE 1984. A high-resolution study of the isotopes of solar flare nuclei. *Astrophys. J.* **280**, 892–901.
- MIZUNO, H., AND G. W. WETHERILL 1984. Grain abundance in the primordial atmosphere of the Earth. *Icarus* **59**, 74–86.
- MIZUNO, H., K. NAKAZAWA, AND C. HAYASHI 1980. Dissolution of the primordial rare gases into the molten Earth's material. *Earth Planet. Sci. Lett.* **50**, 202–210.
- MIZUNO, H., K. NAKAZAWA, AND C. HAYASHI 1982. Gas capture and rare gas retention by accreting planets in the solar nebula. *Planet. Space Sci.* **30**, 765–771.
- MUSSELWHITE, D. S., M. J. DRAKE, AND T. D. SWINDLE 1991. Early outgassing of the Earth and Mars: Inferences from the geochemical behavior of iodine and xenon. *Nature*, in press.
- NAKAZAWA, K., H. MIZUNO, M. SEKIYA, AND C. HAYASHI 1985. Structure of the primordial atmosphere surrounding the early-Earth. *J. Geomag. Geoelectr.* **37**, 781–799.
- NIEMEYER, S., AND A. ZAIKOWSKI 1980. I-Xe age and trapped Xe components of the Murray (C-2) chondrite. *Earth Planet. Sci. Lett.* **48**, 335–347.
- NIEMEYER, S., AND K. MARTI 1981. Noble gas trapping by laboratory carbon condensates. *Proc. Lunar Planet. Sci. Conf. 12th; Geochim. Cosmochim. Acta Suppl.* **16**, 1177–1188.
- NIER, A. O. 1950. A redetermination of the relative abundances of the isotopes of carbon, nitrogen, oxygen, argon and potassium. *Phys. Rev.* **77**, 789–793.
- NIER, A. O., AND M. B. MCELROY 1977. Composition and structure of Mars' upper atmosphere: Results from the neutral mass spectrometers on Viking 1 and 2. *J. Geophys. Res.* **82**, 4341–4349.
- OTT, U. 1988. Noble gases in SNC meteorites: Shergotty, Nakhla, Chassigny. *Geochim. Cosmochim. Acta* **52**, 1937–1948.

- OTT, U., AND F. BEGEMANN 1985. Are all the "martian" meteorites from Mars? *Nature* **317**, 509–512.
- OWEN, T. 1986. In *Workshop on the Evolution of the Martian Atmosphere* (M. Carr, P. James, C. Leovy, and R. Pepin, Eds.), LPI Tech. Report 86-07, pp. 31–32. Lunar and Planetary Institute, Houston.
- OWEN, T. 1987. In *Mars: Evolution of its Climate and Atmosphere* (V. Baker, M. Carr, F. Fanale, R. Greeley, R. Haberle, C. Leovy, and T. Maxwell, Eds.), LPI Tech. Report 87-01, p. 91. Lunar and Planetary Institute, Houston.
- OWEN, T., K. BIEMANN, D. R. RUSHNECK, J. E. BILLER, D. W. HOWARTH, AND A. L. LAFLEUR 1977. The composition of the atmosphere at the surface of Mars. *J. Geophys. Res.* **82**, 4635–4639.
- OZIMA, M., AND K. NAKAZAWA 1980. Origin of rare gases in the Earth. *Nature* **284**, 313–316.
- OZIMA, M., AND F. A. PODOSEK 1983. *Noble Gas Geochemistry*. Cambridge Univ. Press, Cambridge.
- OZIMA, M., AND S. ZASHU 1987. Solar-type Ne in Zaire cubic diamonds. *Geochim. Cosmochim. Acta* **52**, 19–25.
- OZIMA, M., AND G. IGARASHI 1989. In *Origin and Evolution of Planetary and Satellite Atmospheres* (S. Atreya, J. Pollack, and M. Matthews, Eds.), pp. 306–327. Univ. Arizona Press, Tucson.
- PEPIN, R. O. 1967. Trapped neon in meteorites. *Earth Planet. Sci. Lett.* **2**, 13–18.
- PEPIN, R. O. 1980. In *The Ancient Sun: Fossil Record in the Earth, Moon and Meteorites* (R. Pepin, J. Eddy, and R. Merrill, Eds.), pp. 411–421. Pergamon Press, New York.
- PEPIN, R. O. 1985. Evidence of martian origins. *Nature* **317**, 473–475.
- PEPIN, R. O. 1986. In *Mars: Evolution of its Climate and Atmosphere* (V. Baker, M. Carr, F. Fanale, R. Greeley, R. Haberle, C. Leovy, and T. Maxwell, Eds.), LPI Tech. Report 87-01, pp. 99–101. Lunar and Planetary Institute, Houston.
- PEPIN, R. O. 1987. Volatile inventories of the terrestrial planets. *Rev. Geophys.* **25**, 293–296.
- PEPIN, R. O. 1989a. In *Origin and Evolution of Planetary and Satellite Atmospheres* (S. Atreya, J. Pollack, and M. Matthews, Eds.), pp. 291–305. Univ. Arizona Press, Tucson.
- PEPIN, R. O. 1989b. In *The Formation and Evolution of Planetary Systems* (H. A. Weaver and L. Danly, Eds.), pp. 55–74. Cambridge University Press, Cambridge, England.
- PEPIN, R. O. 1990a. Adsorption of nebular gases on protoplanetary cores. *Lunar Planet. Sci. XXI*, 940–941.
- PEPIN, R. O. 1990b. A model for noble gas fractionation on a carbonaceous chondrite parent body. *Meteoritics* **25**, 397–398.
- PEPIN, R. O., AND D. PHINNEY 1978. Components of xenon in the solar system. Unpublished preprint.
- PEPIN, R. O., AND M. H. CARR 1991. In *Mars* (H. H. Kieffer and B. Jakosky, Eds.). Univ. Arizona Press, Tucson, in press.
- PEPIN, R. O., L. E. NYQUIST, D. PHINNEY, AND D. C. BLACK 1970. Rare gases in Apollo 11 lunar material. *Proc. Apollo 11 Lunar Sci Conf.; Geochim. Cosmochim. Acta Suppl.* **1**, 1435–1454.
- PHILLIPS, R. J., AND M. C. MALIN 1983. In *Venus* (D. Hunten, L. Colin, T. Donahue, and V. Moroz, Eds.), pp. 159–214. Univ. Arizona Press, Tucson.
- PHINNEY, D. 1972. ³⁶Ar, Kr, and Xe in terrestrial materials. *Earth Planet. Sci. Lett.* **16**, 413–420.
- PODOSEK, F. A., J. C. HUNEKE, D. S. BURNETT, AND G. J. WASSERBURG 1971. Isotopic composition of xenon and krypton in the lunar soil and in the solar wind. *Earth Planet. Sci. Lett.* **10**, 199–216.
- PODOSEK, F. A., M. HONDA, AND M. OZIMA 1980. Sedimentary noble gases. *Geochim. Cosmochim. Acta* **44**, 1875–1884.
- PODOSEK, F. A., T. J. BERNATOWICZ, AND F. E. KRAMER 1981. Adsorption of xenon and krypton on shales. *Geochim. Cosmochim. Acta* **45**, 2401–2415.
- PRINN, R. G., AND B. FEGLEY, JR. 1989. In *Origin and Evolution of Planetary and Satellite Atmospheres* (S. Atreya, J. Pollack, and M. Matthews, Eds.), pp. 78–136. Univ. Arizona Press, Tucson.
- RAY, J., AND D. HEYMANN 1980. In *The Ancient Sun: Fossil Record in the Earth, Moon and Meteorites* (R. Pepin, J. Eddy, and R. Merrill, Eds.), pp. 491–512. Pergamon Press, New York.
- RINGWOOD, A. E. 1977. *Composition and Origin of the Earth*. Publication No. 1299, Res. School of Earth Sciences, Australian National Univ., Canberra.
- RINGWOOD, A. E. 1979. *On the Origin of the Earth and Moon*. Springer Verlag, New York.
- RINGWOOD, A. E., AND D. L. ANDERSON 1977. Earth and Venus: A comparative study. *Icarus* **30**, 243–253.
- RISON, W. 1980. Isotopic studies of the rare gases in igneous rocks: Implications for the mantle and atmosphere. Ph.D. thesis, University of California, Berkeley.
- ROBLE, R. G. 1977. In *The Solar Output and its Variations* (O. White, Ed.), pp. 8–13. Colorado Assoc. Univ. Press, Boulder.
- RUBEY, W. W. 1951. Geologic history of sea water. *Bull. Geo. Soc. Amer.* **62**, 1111–1147.
- SAFRONOV, V. S. 1972. Evolution of the protoplanetary cloud and formation of the earth and planets. *NASA Tech. Transl. TTF-677*.
- SARDA, P., T. STAUDACHER, AND C. J. ALLÈGRE 1988. Neon isotopes in submarine basalts. *Earth Planet. Sci. Lett.* **91**, 73–88.
- SASAKI, S. 1991. Off-disk penetration of ancient solar wind. *Icarus* **91**, 29–38.
- SASAKI, S., AND K. NAKAZAWA 1986. In *Abstracts for the Japan-U.S. Seminar on Terrestrial Rare Gases* (J. Reynolds, Ed.), pp. 68–71. Dept. of Physics, Univ. California, Berkeley.
- SASAKI, S., AND K. NAKAZAWA 1988. Origin of isotopic fractionation of terrestrial Xe: Hydrodynamic fractionation during escape of the primordial H₂-He atmosphere. *Earth Planet. Sci. Lett.* **89**, 323–334.
- SASAKI, S., AND K. NAKAZAWA 1990. Did a primary solar-type atmosphere exist around the proto-Earth? *Icarus* **85**, 21–42.
- SCHELHAAS, N., U. OTT, AND F. BEGEMANN 1985. Trapped noble gases in some type 3 chondrites. *Meteoritics* **20**, 753.
- SCHWARZ, H. P., J. HOEFS, AND D. WELTE 1969. In *Handbook of Geochemistry*, Vol. II/1, pp. 6-B-1–6-O-3. Springer-Verlag, Berlin.
- SIGNER, P., AND H. E. SUESS 1963. In *Earth Science and Meteoritics* (J. Geiss and E. Goldberg, Eds.), pp. 241–272. North-Holland Publishing Co., Amsterdam.
- SIMON, T., G. HERBIG, AND A. M. BOESGAARD 1985. The evolution of chromospheric activity and the spin-down of solar-type stars. *Astrophys. J.* **293**, 551–574.
- SRINIVASAN, B., J. GROS, AND E. ANDERS 1977. Noble gases in separated meteoritic minerals: Murchison (C2), Ornans (C3), Karoonda (C5), and Abee (E4). *J. Geophys. Res.* **82**, 762–778.
- STEVENSON, D. J. 1981. Models of the Earth's core. *Science* **214**, 611–619.
- STEVENSON, D. J. 1985. Partitioning of noble gases at extreme pressures within planets. *Lunar Planet. Sci. XVI*, 821–822.
- STROM, K. M., S. E. STROM, S. EDWARDS, S. CABRIT, AND M. F. SKRUTSKIE 1989a. Circumstellar material associated with solar-type pre-main sequence stars: A possible constraint on the timescales for planet-building. *Astron. J.* **97**, 1451–1470.
- STROM, S. E., K. M. STROM, AND S. EDWARDS 1988. In *NATO Ad-*

- vanced Study Institute: *Galactic and Extragalactic Star Formation* (R. Pudritz and M. Fich, Eds.), pp. 53. Reidel, Dordrecht.
- STROM, S. E., S. EDWARDS, AND K. M. STROM 1989b. In *The Formation and Evolution of Planetary Systems* (H. A. Weaver and L. Danly, Eds.), pp. 91–109. Cambridge University Press, Cambridge, England.
- STROM, S. E., S. EDWARDS, AND M. F. SKRUTSKIE 1991. In *Protostars and Planets III* (E. H. Levy and J. Lunine, Eds.). Univ. Arizona Press, Tucson, in press.
- SWINDLE, T. D., M. W. CAFFEE, AND C. M. HOHENBERG 1986. Xenon and other noble gases in shergottites. *Geochim. Cosmochim. Acta* **50**, 1001–1015.
- TIELENS, A. G. G. M., AND L. J. ALLAMANDOLA 1987a. In *Physical Processes in Interstellar Clouds* (G. E. Morfill and M. Scholer, Eds.), pp. 333–376. Reidel, Dordrecht.
- TIELENS, A. G. G. M., AND L. J. ALLAMANDOLA 1987b. In *Interstellar Processes* (D. J. Hollenbach and H. A. Thronson, Jr., Eds.), pp. 397–469. Reidel, Dordrecht.
- THOMSEN, L. 1980. ^{129}Xe on the outgassing of the atmosphere. *J. Geophys. Res.* **85**, 4374–4378.
- TYBURCZY, J. A., B. FRISCH, AND T. J. AHRENS 1986. Shock-induced volatile loss from a carbonaceous chondrite: Implications for planetary accretion. *Earth Planet. Sci. Lett.* **80**, 201–207.
- VON STEIGER, R., AND J. GEISS 1989. Supply of fractionated gases to the corona. *Astron. Astrophys.* **225**, 222–238.
- VON ZAHN, U., S. KUMAR, H. NIEMANN, AND R. PRINN 1983. In *Venus* (D. Hunten, L. Colin, T. Donahue, and V. Moroz, Eds.), pp. 299–430. Univ. Arizona Press, Tucson.
- WACKER, J. F. 1989. Laboratory simulation of meteoritic noble gases. III. Sorption of neon, argon, krypton and xenon on carbon: Elemental fractionation. *Geochim. Cosmochim. Acta* **53**, 1421–1433.
- WACKER, J. F., AND E. ANDERS 1986. In *Abstracts for the Japan–U.S. Seminar on Terrestrial Rare Gases* (J. Reynolds, Ed.), pp. 89–92. Dept. of Physics, Univ. California, Berkeley.
- WACKER, J. F., M. G. ZADNIK, AND E. ANDERS 1985. Laboratory simulation of meteoritic noble gases. I. Sorption of xenon on carbon: Trapping experiments. *Geochim. Cosmochim. Acta* **49**, 1035–1048.
- WALKER, J. C. G. 1977. *Evolution of the Atmosphere*. Macmillan, New York.
- WALKER, J. C. G. 1987. Impact erosion of planetary atmospheres. *Icarus* **68**, 87–98.
- WALTER, F. M. 1986. X-ray sources in regions of star formation. I. The naked T Tauri stars. *Astrophys. J.* **306**, 573–586.
- WALTER, F. M., AND D. C. BARRY 1990. Pre- and main sequence evolution of solar activity (preprint).
- WALTER, F. M., A. BROWN, R. D. MATHIEU, P. C. MYERS, AND F. J. VRBA 1988. X-ray sources in regions of star formation. III. Naked T Tauri stars associated with the Taurus-Auriga complex. *Astron. J.* **96**, 297–325.
- WÄNKE, H. 1965. Der Sonnenwind als Quelle der Uredelgase in Steinmeteoriten. *Z. Naturforsch. A. Astrophys. Phys. Phys. Chem.* **20**, 946–949.
- WÄNKE, H. 1981. Constitution of terrestrial planets. *Phil. Trans. Royal Soc. Lond. Ser. A* **303**, 287–302.
- WATKINS, G. H., AND J. S. LEWIS 1986. In *Workshop on the Evolution of the Martian Atmosphere* (M. Carr, P. James, C. Leovy, and R. Pepin, Eds.), LPI Tech. Report 86-07, pp. 46–47. Lunar and Planetary Institute, Houston.
- WEIDENSCHILLING, S. 1988. In *Meteorites and the Early Solar System* (J. Kerridge and M. Matthews, Eds.), pp. 348–371. Univ. Arizona Press, Tucson.
- WETHERILL, G. W. 1954. Variations in the isotopic abundances of neon and argon extracted from radioactive minerals. *Phys. Rev.* **96**, 679–683.
- WETHERILL, G. W. 1981. Solar wind origin of ^{36}Ar on Venus. *Icarus* **46**, 70–80.
- WETHERILL, G. W. 1986. In *Origin of the Moon* (W. Hartmann, R. Phillips, and G. Taylor, Eds.), pp. 519–550. Lunar and Planetary Institute, Houston.
- WETHERILL, G. W. 1988. In *Mercury* (F. Vilas, C. R. Chapman, and M. S. Matthews, Eds.), pp. 670–691. Univ. Arizona Press, Tucson.
- WETHERILL, G. W. 1990a. Formation of the Earth. *Annu. Rev. Earth Planet. Sci.* **18**, 205–256.
- WETHERILL, G. W. 1990b. In *Abstracts for the International Workshop on Meteorite Impact on the early Earth*, LPI Contr. No. 746, pp. 54–55. Lunar and Planetary Institute, Houston.
- WIELER, R., H. BAUR, AND P. SIGNER 1986. Noble gases from solar energetic particles revealed by closed system stepwise etching of lunar soil minerals. *Geochim. Cosmochim. Acta* **50**, 1997–2017.
- WIELER, R., H. BAUR, P. SIGNER, R. S. LEWIS, AND E. ANDERS 1989. Planetary noble gases in “Phase Q” of Allende: Direct determination by closed system etching. *Lunar Planet. Sci.* **XX**, 1201–1202.
- WIELER, R., H. BAUR, P. SIGNER, AND R. S. LEWIS 1990a. Noble gases in “Phase Q”. Further studies on the Allende and Murchison meteorites. *Meteoritics* **25**, 420.
- WIELER, R., E. ANDERS, H. BAUR, R. S. LEWIS, AND P. SIGNER 1990b. Noble gases in “Phase Q”: Closed system etching of an Allende residue, submitted for publication.
- WIENS, R. C. 1988. Noble gases released by vacuum crushing of EETA 79001 glass. *Earth Planet. Sci. Lett.* **25**, 55–65.
- WIENS, R. C., AND R. O. PEPIN 1988. Laboratory shock emplacement of noble gases, nitrogen, and carbon dioxide into basalt, and implications for trapped gases in shergottite EETA 79001. *Geochim. Cosmochim. Acta* **52**, 295–307.
- WIENS, R. C., R. H. BECKER, AND R. O. PEPIN 1986. The case for Martian origin of the shergottites. II. Trapped and indigenous gas components in EETA 79001 glass. *Earth Planet. Sci. Lett.* **77**, 149–158.
- WOOD, J. A., AND G. E. MORFILL 1988. In *Meteorites and the Early Solar System* (J. Kerridge and M. Matthews, Eds.), pp. 329–347. Univ. Arizona Press, Tucson.
- WYCKOFF, S., E. LINDHOLM, P. A. WEHINGER, B. A. PETERSON, J.-M. ZUCCONI, AND M. C. FESTOU 1989. The $^{12}\text{C}/^{13}\text{C}$ abundance ratio in comet Halley. *Astrophys. J.* **339**, 488–500.
- YANG, J., AND E. ANDERS 1982a. Sorption of noble gases by solids, with reference to meteorites. II. Chromite and carbon. *Geochim. Cosmochim. Acta* **46**, 861–875.
- YANG, J., AND E. ANDERS 1982b. Sorption of noble gases by solids, with reference to meteorites. III. Sulfides, spinels, and other substances; on the origin of planetary gases. *Geochim. Cosmochim. Acta* **46**, 877–892.
- YANG, J., R. S. LEWIS, AND E. ANDERS 1982. Sorption of noble gases by solids, with reference to meteorites. I. Magnetite and carbon. *Geochim. Cosmochim. Acta* **46**, 841–860.
- YUNG, Y. L., D. F. STROBEL, T. Y. KONG, AND M. B. MCELROY 1977. Photochemistry of nitrogen in the Martian atmosphere. *Icarus* **30**, 26–41.
- ZADNIK, M. G., J. F. WACKER, AND R. S. LEWIS 1985. Laboratory simulation of meteoritic noble gases. II. Sorption of xenon on carbon: Etching and heating experiments. *Geochim. Cosmochim. Acta* **49**, 1049–1059.

- ZAHNLE, K. J., AND J. C. G. WALKER 1982. The evolution of solar ultraviolet luminosity. *Rev. Geophys. Space Phys.* **20**, 280-292.
- ZAHNLE, K. J., AND J. F. KASTING 1986. Mass fractionation during transonic hydrodynamic escape and implications for loss of water from Venus and Mars. *Icarus* **68**, 462-480.
- ZAHNLE, K. J., J. F. KASTING, AND J. B. POLLACK 1990a. Mass fractionation of noble gases in diffusion-limited hydrodynamic hydrogen escape. *Icarus* **84**, 502-527.
- ZAHNLE, K. J., J. B. POLLACK, AND J. F. KASTING 1990b. Xenon fractionation in porous planetesimals. *Geochim. Cosmochim. Acta* **54**, 2577-2586.